Alma Mater Studiorum – Università di Bologna

DOTTORATO DI RICERCA IN

INGEGNERIA CHIMICA, DELL'AMBIENTE E DELLA SICUREZZA

Ciclo XXV

Settore Concorsuale di afferenza: 09D2

Settore Scientifico disciplinare: ING-IND/24

PROPRIETÀ TERMODINAMICHE E MECCANICHE DI

SISTEMI POLIMERO-SOLVENTE

Presentata da: *Ing. Giovanni Cocchi*

Coordinatore Dottorato   **Relatore**

Prof.ssa Serena Bandini   *Prof. Ferruccio Doghieri*

                                                                    Correlatore

                                              Ing. Maria Grazia De Angelis

PROPRIETÀ TERMODINAMICHE E MECCANICHE DI SISTEMI POLIMERO-SOLVENTE

THERMODYNAMIC AND MECHANICAL PROPERTIES OF POLYMER-SOLVENT SYSTEMS

Ing. Giovanni Cocchi

Table of contents

1.

Acknowledgments

Introduction

At the most fundamental levels, both mechanical and thermodynamic properties of materials arise from the very same causes, since they are nothing more than a consequence of molecular and supramolecular level details, such as molecular size, shape, configuration and intramolecular and intermolecular attractions, repulsions and bonding. These details are neither mechanical, nor thermodynamic, at least in a classical sense, since they arise from phenomena that can be described by quantum mechanics and by statistical mechanics. These two disciplines provide the conceptual framework for describing molecules by themselves (even if the jump that is required for connecting the simple, "closed form" , description of hydrogen atoms, to the description of a many atoms molecule is really huge!) and for explaining the macroscopic properties that arise when many molecules are set together. But for the common engineering perspective, mechanical properties and thermodynamic behavior of materials are not the two sides of the same coin: they are seen as two different kind of properties. Indeed, this view is somewhat supported by design experience: a structural designer need to know what is the strength of concrete, not its enthalpy, as well as computing the efficiency of a power steam cycle requires an accurate representation of enthalpy and entropy functions of the working fluid, not its modulus, if a modulus can be defined at all! Cleary the design process of the boiler and of the turbine will call for an evaluation of viscosity of the working fluid at its pressure and temperature, but again this will be considered independently from its enthalpy or from its entropy.

At the same time, it is a matter of fact that mechanics and thermodynamics are two disciplines strongly bonded together, also from the point of view of their historical development. Both disciplines were dealing with the concept of energy and work since their foundation and they were developed in such a way that those concepts share the same definitions and the same meaning. In the framework of continuum (field) theories the relationship between mechanics and thermodynamics is even stronger, since they are both expressed in local terms and the set of conservation laws can be closed only providing constitutive laws, that should satisfy local thermodynamic constraints: It is not conceivable a theoretically sound theory of continuum mechanics that has not passed the scrutiny of thermodynamic. Many of the most powerful methods of mechanics, such as Hamiltonian formulation and the principle of virtual work, are inherently based on a view of the mechanics that begins with the concepts of energy and work. Finally the mechanics of materials and the thermodynamic of materials, that are the theories that most closely deal with the description, the modeling and the prediction of the properties of materials, should be able to be formulated using an unified view, because, as previously said, both mechanical and thermodynamic properties of materials should be considered to arise from the very same causes, since they are nothing more than a consequence of molecular and supramolecular level details. In fact many models that provide a physical picture of polymer – solvent systems, such as those based on the idea that molecules lay in a disordered lattice, in which the number of possible configuration can be estimated quite easily, can be used as a common starting point for thermodynamic models, as well as for mechanical models, such as those that deals with elasticity and viscoelasticity.

Beside the relationships that can be recognized between part of the most common successful theories of mechanical and thermodynamic properties, there are several problems, that arise in polymer science and technology, in which the relationship between mechanical and thermodynamic properties can't be neglected and should be properly addressed. First of all, it can be observed that in sorption and diffusion of low molecular weight species in polymers,

especially below the glass transition temperature, the system departs from the free stress state and a stress field is developed. This influence the sorption kinetic, that can be significantly different from the one predicted by constitutive laws that neglects such effects, such as Fick's law. Moreover stresses will affect the processing of the polymer, its use and its final state. In same case this is even beneficial, but in other cases can be deeply detrimental and thus it is necessary to develop theoretical and experimental tools that can be used for characterization and modeling of those processes.

A short and not exhaustive list of processes or applications in which stresses in polymer-solvent systems plays a role or need to be controlled can be the following:

1. Controlled Drug Release
2. Coating
3. Permeation/Membrane Separation
4. Sensing Devices
5. Production of Polymeric Foams through Thermoplastic Expansion

The case in which the stress state plays the most detrimental role is the case of coating: virtually all kinds of major coating defects can be related to the stresses that arise when the adhesion to substrate frustrates the shrinkage that the coating material will undergo upon drying or curing. On the other side, sensing devices based on micro-cantilever coated by polymer that swell upon contact with solvent species base their working principle in the mechanical answer of the material upon sorption.

Between these extremes, there are many other cases in which the coupling between mechanical and thermodynamic properties still plays a role in the process.

In the present work theoretical and experimental methods have been applied to the characterization of phase equilibria and pseudoequilibria, mass transport properties and kinetic and mechanical properties of system made by one or more low molecular weight species and a polymer.

Chapter number 1 and 2 deal with Equations of State. First of all, Equations of State have been applied to modeling mixture and pure substances volumetric properties and phase equilibria that were relevant to biomedical applications. It must be said that for systems in which the stress state is the hydrostatic one (in which all the three principal stress are equal to pressure), the thermodynamic description of the volumetric behavior of the fluid that is provided by the Equation of State is also the mechanical one! Since the system considered are made of species that will form hydrogen bonds, the modeling effort has been quite challenging and has prompted the choice of advanced models, like the Perturbed Chain Statistical Associating Fluid Theory. I was given the opportunity to learn the application of this model directly from the research group of Professor Gabriele Sadowski at the Technical University of Dortmund.

Chapter 3 reports the results of the considerable amount of time that has been devoted to experimental measurement of vapor and liquid solubility and sorption kinetic in glassy and rubbery polymers, like Matrimid 5218 and PDMS. The sorption of one of the best solvent of Matrimid 5218 in the polymer itself was extensively characterized, with the aim of crossing the boundary between glassy and rubbery region not by acting on the thermal modes of the polymer chain segment, but through solvent induced plasticization. Intriguing kinetic data were obtained as well, for vapors and liquids. Pure and mixed liquid solubility in PDMS were characterized with aim of understanding if PDMS membrane could be used for separation process in the food and aroma industry and particularly to the deacidification of olive oils.

Chapter 4 deals with modeling of the pseudo equilibrium sorption isotherms that had been collected for several vapors in the glassy Matrimid 5218. This task

has been achieved in the framework of the Non Equilibrium Thermodynamic of Glassy Phase theory of Professor Giulio Cesare Sarti and Professor Ferruccio Doghieri. Not only this theory is undoubtedly successful in providing a theoretically sound thermodynamic picture of the sorption of low molecular weight species in glassy polymer, but can be naturally conjugated with a simple rheological description of the swelling process that came along with sorption. Matrimid 5218, due to its really high glass transition temperature lacked the proper PVT data required for applying the above mentioned model and especially its rheological part, but with some engineering ingenuity, it was possible to overcame these obstacles.

The kinetics of the sorption of some vapors and liquids in Matrimid 5218 were modeled too and the results are presented in Chapter 5. The phenomenological model of Berens and Hopfenberg was applied and it was defined a procedure to use some of the tools of the Non Equilibrium Thermodynamic of Glassy Phase to reduce the number of the adjustable parameters of the model. Then, after a brief review of the works of Long and Richman, the more recent and physically sound model of Carlà and Doghieri, was applied to model non Fickian sorption. It must be said that the model that has been applied is completely consistent with the Non Equilibrium Thermodynamic of Glassy Phase approach and relies on the very same rheological assumption. It is found that the viscosity of the glassy matrix deeply affect the sorption kinetic, controlling rate of the volume relaxation effects. Moreover, it was found out that in integral sorption steps with really high activity jumps, such as in liquid sorption, the plasticization effect of the low molecular weight penetrant has to be explicitly taken into account and viscosity should be allowed to depend on penetrant concentration.

Chapter 6 present the results of the synthesis and characterization, in term of double bond conversion and gas permeability, of glassy crosslinked acrylate polymers that were prepared in collaboration with Dr. Ben Richter of the 3M corporate research laboratories of Saint. Paul and with Professor Alon McCormick of the University of Minnesota. The samples were cured by means

of exposition to an electron beam, in order to promote the formation of radical species without using any initiator. The effect of the radiation dose has been determined, especially for what concerns the relationship between radiation doses and gas permeability and ideal selectivity.

Lastly Chapter 7 discusses some features of the manufacturing process of polymeric foams, especially for what concerns expanded polystyrenes. The results of some mechanical characterizations that were performed on pentane loaded polystyrenes are also presented. The experiments had been performed at the Technical University of Dortmund, under the supervision of Professor Gabriele Sadowski.

2. Modeling of Phase Equilibria With an Equation of State Approach

2.1. Introduction

Let us consider a closed system, spatially homogeneous, made by a single component and by a single phase. According to the classical theories of mechanics and electromagnetism, there are several kind of work that the system can exchange with the surrounding environment. All the kinds of work are means of exchanging energy and thus, from the point of view of energy balance, they can be even lumped into a single term, but listing each contribution separately can provide some insight on the physical processes behind them. Since the system is not considered to be isolated, it can exchange energy with the surrounding environment in the form of heat. Again this contribution is nothing but one more mean of exchanging energy, but consolidated experimental evidence, collected and analyzed starting from the very beginning of thermodynamic discipline, support the view that heat and work plays different roles[1-5]. It is a matter of fact that heat can't be completely transformed into work and that it is not possible to create any kind of process that brings heat from a cold source to a hot one, without supplying some kind of work to the system. The first statement is due to Lord Kelvin and Max Planck and is usually stated saying that it is not possible to build a device that have the only effect of producing work from heat supplied by a single source. The second

statement is due to Rudolf Clausius and is usually stated saying that it is not possible to build a device that has the only effect of transferring heat from a colder body to a hotter body. These two statements have been frequently adopted as the operational statement of the second law of thermodynamics and can be proven equivalent. Albeit their usefulness when dealing with power cycles and refrigeration, they are not well suitable for exploiting an analysis of the constitutive laws or of the models for mechanical and thermodynamic properties of materials. In the framework of rational thermodynamics, it is a well established practice to introduce an extensive variable, function of the state of the system, here yet to be defined, named Entropy, that obeys an additional balance equations that is very special: the change of entropy with time is always required to be greater or at least equal than the sole contribution from the Entropy flux that is exchanged with the surrounding environment. This means that there is an entropy generation term that has to be always equal or greater than zero. Second Law can be obeyed only by those processes, that we will call thermodynamically admissible, in which the generation of Entropy is strictly non negative[4, 5].

2.1
$$\frac{dS}{dt} \geq \dot{\Phi}$$

If we restrict our analysis to a closed system of fixed volume that exchanges only heat, the energy balance, that in mathematical form is the statement of the First Law of thermodynamic, is strikingly simple:

2.2
$$\frac{dU}{dt} = \dot{Q}$$

Since both First and Second Laws have to be satisfied, one can think to write them together, by means of the introduction of a Lagrange multiplier, say β. Thus for every process:

2.3
$$\frac{dU}{dt} - \beta\frac{dS}{dt} \le \beta\dot{\Phi} + \dot{Q}$$

Entropy, as a function of state, can be thought to be function of the internal energy and of the volume of the system, at least for some kind of ideal material, thus we can expand the time derivative of entropy , taking into account that volume is fixed.

2.4
$$\frac{dU}{dt} - \beta\frac{\partial S}{\partial U}\frac{dU}{dt} \le \beta\dot{\Phi} + \dot{Q}$$

Since we have no experimental evidence that $\frac{dU}{dt}$ is not free to have any value in the real set and neither we have theoretical arguments for the same request, we have to assume that $\frac{dU}{dt}$ can take any value. It is easy to recognize that if this is the case, it is straightforward to find cases in which the inequality can be violated, unless the Lagrange multipier is equal to the inverse of the derivative of entropy respect to internal energy $\beta = \left(\frac{\partial S}{\partial U}\right)^{-1}$.

The residual inequality is then: $0 \le \beta\dot{\Phi} + \dot{Q}$. Again since we can think that heat flux can be somewhat controlled also by the environment that surrounds the system, it is possible that an action outside the system causes the failure to comply with the inequality inside the system. This again should be not possible if we want that the inequality of Second Law holds for every process that can take place in nature and thus we should have that $\dot{\Phi} = \frac{\dot{Q}}{\beta}$.

With the trick of considering a system that can exchange only heat, we have found a way to show that entropy flux is inded proportional to the heat flux. Moreover a system that exchange only heat with the surrounding environment is the homologous of many different kind of devices used in the empirical science of thermometry and by comparison with the several thermometric scales that have been defined, especially with those based on measuring the

properties of some gaseous species that fill ampoules of fixed volume and for which the relationship between pressure, empirical temperature and volume is known to be simple, i.e. the so called ideal gas, it is possible to recognize that the Lagrange multiplier is function of the empirical temperature $\beta = \left(\dfrac{\partial S}{\partial U}\right)^{-1} = f(\vartheta)$, for every empirical temperature scale. Since the Lagrange multipier β is equal to the inverse of the derivative of entropy respect to internal energy, it can be defined to be itself the measure of the absolute temperature of any body.

$$2.5 \qquad\qquad \frac{dS}{dt} \geq \frac{\dot{Q}}{T}$$

This formulation of Second Law that exploits the link between heat exchanges and entropy generation can be used to analyze the Clausius statement and the statement by Planck and Kelvin and their equivalency can be proven. As well, we have the conceptual instruments for analyzing systems that exchange heat and work of any kind. A comprehensive list of the kind of work that are recognizable from mechanic and electromagnetism theory will comprise for sure the work associated to change in volume, the work that has to be exerted for impressing a change in the shape of the system, the work required for changing the extension of the surface of the system, as well as the work required by an electric field for polarizing a polarizable medium and the work required by a magnetic field to magnetize a magnetic medium. All these kind of work are related to a specific property of the system that can be changed. Changing volume or shape means that the system will appear deformed respect to configuration that it had before, as well as creating new surface or changing the ordering of its polarizable constituent by means of application of an electric field. This strongly suggest that work and deformation are indeed correlated.

Let us consider a closed system, spatially homogenous and made by a single phase, that initially has volume V_0. The control volume of the system is bounded by a control surface on which can act the forces exerted by the surrounding environment. For example let us assume that in each point of the control surface is applied a force, which has a normal component that in every differential area element dA is equal to $d\overline{F}_S * \hat{n} = PdA$, where the scalar P is the pressure or the normal stress acting on the boundary of the system. If this force has a non zero component in any direction that is not parallel to the vectors normal to the control surface, we will also have a tangential component, that for a given direction $\hat{t}$ in the tangent plane is equal to $d\overline{F}_S * \hat{t} = \tau_{\hat{n},t} dA$, where $\tau_{\hat{n},t}$ is the shear stress acting on the boundary of the system, in the direction $\hat{t}$, normal to the direction $\hat{n}$. Let us assume that on the system acts also a field of conservative forces per unit of volumes: $d\overline{F}_V = f'''\rho dV$, such as gravity or an electric field.

If the system is actually a *rigid body* the effect of the forces acting locally on the boundary of the control volume is to change the kinetic and potential energy of the *rigid body* that we are considering: $\dfrac{dK}{dt} + \dfrac{d\Psi}{dt} = \int \overline{v} * d\overline{F}_S$. In the case of a less ideal kind of body, one that will be *deformed* by the action of the external, surface forces, only a fraction of their power will be spent changing the potential and the kinetic energy of the system and the other fraction will have the only effect of changing the relative position of the material particles of the body_$\dfrac{dK}{dt} + \dfrac{d\Psi}{dt} = \int \overline{v} * d\overline{F}_S - \dot{W}_{DEF}$. Subtracting this mechanical energy balance equation to the total energy balance equation $\dfrac{dU}{dt} + \dfrac{dK}{dt} + \dfrac{d\Psi}{dt} = \int \overline{v} * d\overline{F}_S + \dot{Q}$, we obtain the so called thermal energy balance, that is the relevant one when looking for the most intimate and non trivial relationships between mechanics and thermodynamics. $\dfrac{dU}{dt} = \dot{Q} + \dot{W}_{DEF}$. In this discussion it will be proven useful

to introduce an extensive variable, function of the state of the system like internal energy and entropy, known as Helmolhtz Free Energy, defined as $A = U - TS$.

It is easy to show that the work (actually the power) of a force field acting on the surface of the system with uniform normal stress and that change the volume of the system, is equal to $-P\dfrac{dV}{dt}$. If this is the only work done on the system, the thermal energy balance and the entropy balance can be coupled to give a free energy balance:

2.6
$$\frac{dA}{dt} + S\frac{dT}{dt} + P\frac{dV}{dt} \leq 0$$

The free energy should be a function of the state of the system, that we can guess to be identified by its temperature, its volume and the pressure. Applying the chain rule for the derivative $\dfrac{dA}{dt}$, the inequality, that should hold for every admissible process, became:

2.7
$$\left[\left(\frac{\partial A}{\partial T}\right)\bigg|_{V,P} + S\right]\frac{dT}{dt} + \left[\left(\frac{\partial A}{\partial V}\right)\bigg|_{T,P} + P\right]\frac{dV}{dt} + \left(\frac{\partial A}{\partial P}\right)\bigg|_{V,T}\frac{dP}{dt} \leq 0$$

It is required that this inequality holds for every process. It is not possible to provide any reasonable theoretical bound for $\dfrac{dT}{dt}, \dfrac{dV}{dt}$ and $\dfrac{dP}{dt}$. Moreover, since the change on temperature, pressure or volume could be even separately controlled from the environment outside the body, the inequality 1.8 should be decomposed in three separate inequalities, one for each term, that should hold by themselves. Therefore the terms inside the brackets should be equated to zero and the following useful relationship can be proven[4]:

2.8
$$S = -\left(\frac{\partial A}{\partial T}\right)\bigg|_{V,P} \; ; P = -\left(\frac{\partial A}{\partial V}\right)\bigg|_{T,P} \; ; \left(\frac{\partial A}{\partial P}\right)\bigg|_{T,V} = 0$$

The latter one is especially important since it means that Helmholtz Free Energy is not a function of the pressure of the system. It is then possible to write simply $A = A(V,T)$ and the thermodynamic derivatives can be written as $S = -\left(\frac{\partial A}{\partial T}\right)\bigg|_{V}$ and $P = -\left(\frac{\partial A}{\partial V}\right)\bigg|_{T}$. Moreover the second one say that the pressure is itself a function of the state of system, so we can say that: $P = f(T,V)$. Since it has been assumed that the state of the system is independent from the rate of deformation $\frac{dV}{dt}$, thus under isothermal conditions the pressure (and the free energy) depends only on the volume of the system and have the same value if the system is deformed slowly or really quickly or even if it is kept at rest. This is indeed the case of elastic materials.

For the sake of generality, we could say that the pressure $P_{eq} = f(T,V)$ is the value that holds for $\frac{dV}{dt} = 0$, and that in general $P = f\left(T,V,\frac{dV}{dt}\right)$, so that $P_{eq} = f(T,V,0)$. Expanding $f\left(T,V,\frac{dV}{dt}\right)$ as a Taylor- series near $\frac{dV}{dt} = 0$, we can see that $P \approx P_{eq}$ provided that $\frac{dV}{dt}$ is small enough. In fact near $\frac{dV}{dt} = 0$ we have that $P = P_{eq} + \frac{\partial f(T,V,0)}{\partial \frac{dV}{dt}}\frac{dV}{dt} + ...$

On the base of this discussion about the value of pressure outside equilibrium, it is then necessary to check if the Helmholtz Free Energy also is a function of the rate of deformation $\frac{dV}{dt}$. Applying again the chain rule for the derivative $\frac{dA}{dt}$, the inequality, that should hold for every admissible process, became:

$$2.9 \qquad \left[\left(\frac{\partial A}{\partial T}\right)\bigg|_{V,\frac{dV}{dt}} + S\right]\frac{dT}{dt} + \left[\left(\frac{\partial A}{\partial V}\right)\bigg|_{T,\frac{dV}{dt}} + P\right]\frac{dV}{dt} + \left(\frac{\partial A}{\partial \frac{dV}{dt}}\right)\bigg|_{T,V}\frac{dV}{dt} \leq 0$$

It is again straightforward to obtain the relationship between entropy and free energy and the indication that since $\left(\dfrac{\partial A}{\partial \frac{dV}{dt}}\right)\bigg|_{T,V}$ should be always zero, the free energy is not a function of the deformation rate. But the residual inequality $\left[\left(\dfrac{\partial A}{\partial V}\right)\bigg|_{T,\frac{dV}{dt}} + P\right]\dfrac{dV}{dt} \leq 0$ can't be treated in the same way, since with the choice $P = f\left(T,V,\dfrac{dV}{dt}\right)$ the argument of the brackets is not independent from the time derivative $\dfrac{dV}{dt}$. From Second Law, we can say that if $\left[\left(\dfrac{\partial A}{\partial V}\right)\bigg|_{T,\frac{dV}{dt}} + P\right]$ is positive, the process should be isochoric or compressive, while if $\left[\left(\dfrac{\partial A}{\partial V}\right)\bigg|_{T,\frac{dV}{dt}} + P\right]$ is negative, an expansion is allowed. Close to equilibrium, where $\dfrac{dV}{dt}$ goes to zero, if $\left[\left(\dfrac{\partial A}{\partial V}\right)\bigg|_{T,\frac{dV}{dt}} + P\right]$ is a continuous function, as it should be granted without extraordinary wisdom, we recover the result that[4]:

$$2.10 \qquad P_{eq} = -\left(\frac{\partial A}{\partial V}\right)\bigg|_{T}$$

Thus free energy is a potential for entropy even outside equilibrium and at equilibrium is a potential for pressure. The equilibrium

relationship $P_{eq} = -\left(\dfrac{\partial A}{\partial V}\right)\bigg|_T = f(V,T)$ is known as the Volumetric Equation of State.

A more extensive presentation of this approach and on how this procedure can be applied to more general systems can be found in the thermodynamic book written by Astarita[4], in which it is possible to find some interesting observations on the thermodynamic description of relaxation phenomena in polymers.

Since Helmholtz Free Energy is not a function of pressure, even outside equilibrium, if for a given Volume and Temperature the system is not in equilibrium, the pressure value that can be computed by $P_{eq} = -\left(\dfrac{\partial A}{\partial V}\right)\bigg|_T = f(V,T)$ will be the hypothetical pressure at which that Volume and Temperature will be those of equilibrium. This observation will be useful to properly identify and calculate the driving force of volume relaxation that takes place during the sorption of low molecular weight species in glassy polymers, as modeled in chapter 5.

Let us consider now a system that acts like a spring, that under the influence of an external force applied at its ends it can be elongated without changing its volume (isochoric transformation), like happens in the case of a rubber band. The volume of the system will be changed only by the pressure and will not be affected by the force acting on the spring, but at the same time it is not possible to neglect that the free energy of the system is affected also by elongation. Thus we have to assume that the free energy depends on temperature, volume and elongation. The total deformation work (power) is $-P\dfrac{dV}{dt} + \bar{f} * \bar{l}$. Let us assume that the pressure is always the equilibrium value, so that we can neglect the effect of $\dfrac{dV}{dt}$ on the value of the pressure itself.

The free energy inequality, that must be obeyed in order to comply with the Second Law, can be exploited in the following form:

2.11
$$\left[\left(\frac{\partial A}{\partial T}\right)\bigg|_{V,\bar{l}} + S\right]\frac{dT}{dt} + \left[\left(\frac{\partial A}{\partial V}\right)\bigg|_{T,\bar{l}} + P\right]\frac{dV}{dt} + \left[\left(\frac{\partial A}{\partial \bar{l}}\right)\bigg|_{T,V} - \bar{f}\right]*\frac{d\bar{l}}{dt} \leq 0$$

With the same derivation shown before, it is possible to prove that the inequality can be satisfied only if the free energy is assumed to be a potential for the force that acts on the spring: $\bar{f} = \left(\frac{\partial A}{\partial \bar{l}}\right)\bigg|_{T,V}$.

This force is indeed and equilibrium property, since it does not depend on elongation rate, but simply on the value of the elongation and we could even recognize that there should exist an Elongation Equation of State such that $\bar{f} = g(T,V,\bar{l})$.

From the discussion of the conditions that must hold in order to guarantee that the inequality provided by Second Law is satisfied for every process, many interesting results can be obtained:

- Entropy is the isochoric derivative of the Helmholtz Free Energy respect to temperature
- Even in non equilibrium, Helmholtz Free Energy does not depend on Pressure, nor it depends on deformation rate
- At equilibrium, Pressure is equal in moduls and opposite in sign to the isothermal derivative of Helmholtz Free Energy respect to volume
- A similar result can be extended to all the elastic forces, even when the deformation is done under isochoric constraint, so that we can say that if there is a stress state under which the system can rest in equilibrium, the stress tensor must be equal in modulus and opposite in sign to the isothermal derivative of Helmholtz Free Energy respect to a measure of the strain: $\overline{\overline{\sigma}} = -\frac{\partial A}{\partial \overline{\overline{B}}}$ [6]

- At equilibrium, Pressure is function of Temperature and Volume alone. The function that represent this relationship is named Equation of State. If an expression for Helmholtz free energy is available from some molecular or mechanical statistical theory, then the equation of state can be explicitly derived as $P_{eq} = -\left(\dfrac{\partial A}{\partial V}\right)\bigg|_{T} = f(V,T)$ [4, 7].

2.2. Constrained Systems and Single Component Phase Equilibria

It is useful to exploit the consequence of Second Law on the evolution of systems that required to obey some constrains. The first example could be a closed homogeneous single component system, that is held a fixed volume V and that can exchange heat with the surrounding environment in such a way that its temperature T is fixed in time. The energy balance for this system is: $\dfrac{dU}{dt} = \dot{Q}$, while the Second Law is embodied by the usual inequality $\dfrac{dS}{dt} \geq \dfrac{\dot{Q}}{T}$, so it is possible to eliminate the heat power from these two equations, to give:

$$\frac{dA}{dt} \leq 0$$

Since Helmholtz free energy is only allowed to decrease during the approach of the equilibrium condition, it should be minimum at equilibrium. Thus the equilibrium condition for a system held at fixed volume and temperature is that Helmholtz Free Energy is minimum $A \rightarrow A_{\min}$ [1].

Repeating this reasoning for a closed system that is held at fixed temperature T and pressure P, it is possible to find out that under that constraints the function $G = U + PV - TS$, known as the Gibbs Free Energy, obeys the evolution

condition $\dfrac{dG}{dt} \leq 0$ and thus at equilibrium Gibbs Free Energy should be minimum $G \rightarrow G_{\min}$[1].

Finally it is useful to derive the criterion that rules the equilibrium between two phase of a single component closed system. Let us assume that pressure and temperature in the two phases are the same, so that thermal and mechanical equilibrium is granted. This system is constrained at fixed pressure and temperature, so its evolution should comply with the condition $\dfrac{dG}{dt} \leq 0$, that descend directly from the Second Law of thermodyamics. At any time, the system will contain a given mass fraction of phase I, say ω^I, and a complementary fraction of phase II, say ω^{II}, such that $\omega^I + \omega^{II} = 1$. Each phase will have its own free energy content, say $m^I \hat{G}^I$ and $m^{II} \hat{G}^{II}$, so that $G = m^I \hat{G}^I + m^{II} \hat{G}^{II}$, thus $\dfrac{d\hat{G}}{dt} = \left(\hat{G}^I - \hat{G}^{II} \right) \dfrac{d\omega^I}{dt} \leq 0$. The latter inequality means that if the Gibbs Free Energy of phase I is higher than the one of phase II, its mass fraction in the system will decrease. The opposite will happen if the Gibbs Free Energy of phase II would be higher. At equilibrium the Gibbs Free Energy of phase I should be equal to the Gibbs Free Energy of phase II: the phase equilibrium criterion is $\hat{G}^I = \hat{G}^{II}$[1].

2.3.   Equations of State for a Single Component System

According to the arguments and the findings presented in the introduction, under equilibrium conditions the state of an homogenous, single phase and single component system shall be represented by its pressure, temperature and volume. But it is straightforward to list and count the number of the equations representing equilibrium conditions and the number of the variables for each phase and found out that the degrees of freedom are only two, not three. In fact,

for a system made by N_P phases, there are $N_P - 1$ relations like $T^i = T^j$ that represent the thermal equilibrium criterion, there are $N_P - 1$ relations like $P^i = P^j$ for mechanical equilibrium, as well as there are $N_P - 1$ relations like $G^i = G^j$ that represent the thermodynamic phase equilibrium criterion. Then equilibrium is attained if the system obeys to $3(N_P - 1)$ constraints. Since Gibbs Free Energy is function of Pressure and Temperature in each phase, in general there are $2N_P$ variables, thus the number of degrees of freedom is equal to $N_F = 3 - N_P$[1]. Thus for a single phase, single component system, there are two degrees of freedom, which means that the state of the system is specified only if pressure and temperature, or if volume and temperature, or if volume and pressure are specified. For a two phase system, there is only one degree of freedom: thus if two phase are coexisting the state of the system is univocally identified by its pressure, or by its temperature or by its volume. Finally in a single component, three phase system there are no degrees of freedom: this is the reason behind the fact that the triple point (coexistence of Solid, Liquid and Vapor phases) of a pure substance can be assumed as a reference point in thermometric scales.

For a single component, single phase system, once that volume and temperature are specified, the Equation of State can be used for calculating the equilibrium pressure of the system. The equation of state can be applied for a gas or vapor phase or for a liquid phase as well, for representing its volumetric behavior. If the two phases are supposed to coexist, the equation of state should be applied to both phases simultaneously and the equality of Gibbs Free Energy will assure that the pressure that is being calculated is the equilibrium pressure of a system in which the coexistence of the two phases is allowed. If the system, at a given volume and temperature, could only be made by liquid, the Gibbs free energy of the vapor phase will be always greater than that of liquid. The opposite will happen if the system should be gaseous only. It is important to note that at fixed temperature and pressure, Equation of State can

have multiple roots, corresponding to different values of volume (or density) of the system. For instance this happens when two (or more phases) coexists: for each phase there should be a root of the equation of state. In fact, in the region of pressure and temperature in which coexistence of vapor and liquid is possible, there should be a root for the specific volume of the liquid and a separate, different root for the specific volume of the vapor (clearly at the critical point the two physical roots became one)[1, 7]. But beside these roots, there could be other roots that don't represent stable phases and that in same case could even be only a consequence of the mathematical form of the specific Equation of State.

Mathematical complexity is the price that has to be paid for obtaining a good representation of the properties of real substances. For example, the Ideal Gas Equation of State is the simplest and most empirical form of equation of state and has only one root, that represents the density of a gas, but its theoretical importance cannot be understated, since it can be made rigorous in terms of statistic theory of a gas made by hard particle, can be extended to quantum particles and is used as a reference term for many others advanced equation of state. Moreover from an engineering point of view is good enough for representing the volumetric properties of air and of many other simple gaseous species at ambient temperature and pressure.

2.12
$$\hat{V} = \frac{MRT}{P}$$

The Van der Waals Equation of State, that has been proposed for the first time in 1873 and is an historical milestone in thermodynamic, can describe the volumetric behavior of liquid and vapors and can be written as a third order polynomial in term of compressibility. Actually the Van der Waals Equation of State does not works well in representing the specific volume of the liquid phase, but it was the first Equation of State that was able to predict the vapor liquid phase change. Many other Equations of State that have been

successfully applied to hydrocarbons systems, such as Peng Robinson EoS (1976)[1, 7, 8] and Redlich Kwong Soave EoS (1972)[1, 7, 9], share the same mathematical form: they can be written in the form of a third order polynomial of the compressibility and hence they are collectively known as Cubic Equation of State. It is straightforward to recognize that at fixed pressure and temperature, there could be up to three roots of the Cubic Equations of State. Two roots could even be complex, and it is clear that complex roots does not have a physical meaning in the representation of the volumetric property of fluid phase. With the values of the coefficients of the polynomial that are encountered when dealing with real substances, it is common to find three real roots. Checking the corresponding value of the Gibbs Free Energy provide a criteria for phase equilibria and phase stability. From such analysis it is clear that one root can describe a gaseous phase, one root represent a liquid phase, while the last root lies refers to an unstable condition, that is doubtfully accessible by a real system.

The general form of the Cubic Equations of State is:

2.13 $$Z^3 + \alpha Z^2 + \beta Z + \gamma = 0$$

where Z is the compressibility factor, defined as $Z = \dfrac{P\hat{V}}{MRT}$, and the coefficients α, β and γ are, for example, defined according to the following matrix[1]:

	Van der Waals	Redlich Kwong Soave	Peng Robinson
α	$\left[-1 - \left(bP/RT\right)\right]$	-1	$\left[-1 + \left(bP/RT\right)\right]$
β	$\left[aP/(RT)^2\right]$	$\left[\left(aP/(RT)^2\right) - \left(bP/RT\right) - \left(bP/RT\right)^2\right]$	$\left[\left(aP/(RT)^2\right) - 2\left(bP/RT\right) - 3\left(bP/RT\right)^2\right]$
γ	$-\left[\left(aP/(RT)^2\right)\left(bP/RT\right)\right]$	$-\left[\left(aP/(RT)^2\right)\left(bP/RT\right)\right]$	$\left[-\left(aP/(RT)^2\right)\left(bP/RT\right) + \left(bP/RT\right)^2 + \left(bP/RT\right)^3\right]$

the three coefficients α, β and γ are function of two parameters, namely a and b, that are characteristic of every real substance. The parameter a is

usually recognized to be related to the interactions between molecules and it is sometimes called the *attraction parameter* or even the *force parameter*, while parameter b is related to the volume occupied by the molecules.

In 1976 Sanchez and Lacombe[10] proposed an Equation of State based on a rigorous mechanical statistics approach based on the physical picture that the molecule of a fluid (liquid or vapor) can be regarded as lying randomly on the sites of a compressible lattice. The lattice fluid approach, albeit disregarding compressibility, has been previously proven successful in the theory of polymeric solutions, by Flory and Huggins[11-13]. The Sanchez Lacombe Equation of State successfully describe the volumetric properties of polymers (rubber and melts), as well as, the properties of low molecular weight substances, such as alkanes, aromatics, carbon dioxide and several oxygenated species. The representation of alcohols is hampered by the lack of a way to take into account hydrogen bonding effects and, for the same reason, modeling liquid water density is seriously flawed. Despite these drawbacks, the Sanchez Lacombe Equation of State can be applied to many system of industrial and scientific relevance, has been extended in order to provide a description of the thermodynamic of non equilibrium glassy phases[14] and provide a good tradeoff between accuracy and complexity of the calculations. The Sanchez Lacombe Equation of State is written in term of reduced Pressure, Temperature and Density and albeit is not in the form of a third order polynomial, it can have three real roots, with the same physical meaning discussed in the case of the Cubic Equations of State.

The Sanchez Lacombe Equation of State is usually written as:

2.14
$$\tilde{\rho}^2 + \tilde{P} + \tilde{T}\left[\ln(1-\tilde{\rho}) + \tilde{\rho}\left(1 - \frac{1}{r}\right)\right] = 0$$

where $\tilde{\rho}$, $\tilde{P}$ and $\tilde{T}$ are, respectively, the reduced density, pressure and temperature, while r is the number of segment (known as *mers)* connecting the sites of the lattice occupied by each molecule of the fluid. The reduced variable are defined according as: $\tilde{\rho} = \dfrac{\rho}{\rho *}$, $\tilde{P} = \dfrac{P}{P *}$ and $\tilde{T} = \dfrac{T}{T *}$. In the theory of Sanchez Lacombe $\rho *$ is the characteristic density of the fluid, that correspond to its close packing limit. In the paper of Sanchez and Lacombe published in 1976[10] it was stated that *as a first approximation $\rho *$ is equal to the crystal density*. In the subsequent paper from the same authors that was published in 1978[15], specifically dealing with polymer solutions, a more careful analysis of this important point is provided and it is clearly stated that their theory is intended to describe a fluid, disordered state and not a crystalline, ordered state. In fact it is argued that the value of $\rho *$ of many common hydrocarbon is around 10 % lower that the density of their crystal state, in strong analogy with the fact that the packing fraction of hard spheres in an hexagonal or face centered cubic lattice is 0.74 and the random packing fraction is 0.637. From the mathematical point of view, it is straightforward to observe that if a fluid could be denser than its close packing limit, we should have $\rho > \rho *$ and thus $\tilde{\rho} > 1$ and the Equation of State would be solved by evaluating the natural logarithm of a negative number: again we find a situation in which, even if an algebraic solution could be found in the field of complex numbers, there is no way to assign a physical meaning to that result. The characteristic temperature $T *$ can be promptly transformed in a characteristic energy $\varepsilon * = \dfrac{T *}{R}$, that has been shown to be proportional to the depth of the effective potential energy well that acts between each mer pair[15]. In this picture $r\varepsilon *$ is the total interaction energy of a single molecule and should be considered as the amount of energy required to bring one mole of the fluid, initially at equilibrium in the closed packed state, to the state of a vapor of negligible density. With similar reasoning it is possible to show that in the framework of Sanchez Lacombe Lattice Fluid Theory, the characteristic pressure $P *$ is equal to the density of cohesive

energy of the fluid in the close packed state, thus it is equal to the ratio between the vaporization energy $r\varepsilon*$ and the volume occupied by the same chain in the close packed state $rv*$ [15].

A more recent equation of state that has gained a lot of popularity and that has been found to be able to deal with systems that usually pose a significant challenge to the above mentioned models, is the so called Statistical Associating Fluid Theory Equation of State[16-19]. Actually this name refers more to a *class of models* that share the same underlying physical picture (the fluid is depicted as made by chains of spherical segments) and use the same perturbation approach, than to a single equation of state. The version developed by Huang and Radosz is the most commonly used. Complex fluids, hydrogen bonding species and the so called asymmetric mixtures, in which one component is much different from the other in term of size, shape, molecular interactions and critical point can be modeled with Statistical Associating Fluid Theory Equation of State with good to excellent results. Unlucky it has been shown that for certain substances and in certain temperature regions, there are multiple volume roots and that these roots can be more than three. One of these roots can be even beyond the theoretical close packing limit of the model[20, 21]. All these mathematical artifacts hamper the use of such Equation of State in a fully automated fashion, as it should be required for application in process simulators, where the benefit of a model that can deal so proficiently with complex mixtures would be very appreciated by the chemical plant designer community. It is interesting to note that the Perturbed Chain Statistical Associating Fluid Theory Equation of State, developed by Gross and Sadowsky from the original Statistical Associating Fluid Theory Equation of State, has been shown the be usually as good as the original model, and sometimes even better, in dealing with many complex systems and seems to be not affected by the abnormal multiplicity of the volume roots[22-24].

Both Statistical Associating Fluid Theory and Perturbed Chain Statistical Associating Fluid Theory have been extended in order to provide a description of the thermodynamic of non equilibrium glassy phases[25, 26].

According to their perturbative approach, the equations of state of these kind can be formally written in term of compressibility factor expressed as a sum of contribution due to the various interaction mechanism between the single chains that represent the fluid. As said before, the fluid is assumed to be made by chains of sphere, permanently bonded together and each sphere can bear several kind of interaction sites, that can be used for describing association and hydrogen bonding phenomena. For instance, it is customary to write the Perturbed Chain Statistical Associating Fluid Theory Equation of State as[22, 23]:

2.15 $$Z = 1 + Z^{hc} + Z^{disp} + Z^{assoc}$$

where $Z = 1$ would have been the expression for an ideal gas, Z^{hc} is the contribution of the hard chain, Z^{disp} is the contribution of the dispersive interaction and Z^{assoc} is the term that introduce the effect of association and hydrogen bonding. The molecular parameters, characteristic of each real substance, that are required for computing Z^{hc} and Z^{disp} are function of three parameters, that are known as the temperature-independent segment diameter σ, the depth of the potential ε, and the number of segments in a chain m. Beside these three parameters that are specific of each substance, the model requires 42 numerical constants, that should be universal and hold true for any chainlike molecule. The values of these constants were retrieved by Gross and Sadowski[22] by means of an optimization procedure based on a Levenberg-Marquardt algorithm, used to regress the vapor pressures and liquid, vapor, and supercritical volumes of a series of normal alkane. The normal alkane series started with methane, that was assumed to be a single segment spherical molecule ($m = 1$). The association contribution Z^{assoc} requires the definition of an association scheme, that dictates how many interaction sites are present into

each molecules and how many different *kind* of association sites are available[23]. In fact the association phenomena are addressed assuming that associating molecule i exhibit one or more association sites (i.e. $A_i, B_i, ...$) giving rise to short-range attractions, that can be idealized by a square-well potential acting between the association sites. The depth of this square-well potential is $\varepsilon^{A_i B_j}$ and the temporary bonding can take place only if the sites get closer than the characteristic width $r^{A_i B_j}$, that is assumed to correspond to an effective volume $k^{A_i B_j}$. Thus, modelling of pure components that give raise to self association, such as water molecules, requires two more parameters namely the association energy $\varepsilon^{A_i B_j}$ and the association volume $k^{A_i B_j}$.

All the equations of state, in order to describe the volumetric behavior of a specific substance, require that the values of some parameters specific of the given substance is provided. Some of these parameters are physical constants, such as the molecular weight or can be deduced by the application of the corresponding principle by means of the value of the coordinates of the critical point[1]. Sometimes the corresponding state principle can be adopted in a modified form, using also the acentric factor, proposed by Pitzer, for correlate the properties of non spherical molecules. The corresponding state approach is commonly used for Cubic Equations of State and their parameters are directly correlated to macroscopic property of the fluid. The more advanced theories, such as Sanchez Lacombe Equation of State and Statistical Associating Fluid Theory Equation of State are formulated in terms of parameters that have a clear meaning in term of microscopic or molecular property of the fluid. In both cases the parameters should be retrieved from the available experimental data.

The critical point of a fluid can be defined, somewhat empirically, as the highest temperature at which a liquid can exist: this definition relies on the fact that in a Pressure Volume plot, the isotherm curves, in order to have more than one root for the volume, with increasing volume the pressure exhibit a local minimum

followed by a local maximum, that gives the characteristic region of coexistence. The isotherm of the critical temperature is the very last isotherm to exhibit such behavior, with maximum and minimum lumped together in a single extreme value. The pressure in that point is the critical pressure and specific volume is the critical volume. Mathematically the critical point is defined by the following requirements[1]:

2.16
$$\left(\frac{\partial P}{\partial \hat{V}}\right)_{Tc} = 0 \quad \text{and} \quad \left(\frac{\partial^2 P}{\partial \hat{V}^2}\right)_{Tc} = 0$$

For the Van der Waals Equation of State the applications of these two equalities gives the value of the critical pressure as $P_c = \frac{a}{27b^2}$, the critical volume as $\tilde{V}_c = 3b$ and the critical temperature as $T_c = \frac{8a}{9R\tilde{V}_c}$, thus the compressibility factor at the critical point is $Z_c = \frac{3}{8} = 0.375$ for every fluid[1]. This suggest that the volumetric properties of the substances could be predicted by means of a universal correlation such as $Z = Z\left(\frac{T}{T_c}, \frac{P}{P_c}\right)$, that embodies the principle of corresponding states. The value of the parameters a and b of the Van der Waals Equation of State can be calculated explicitly as $a = \frac{27R^2T_c^2}{64P_c}$ and $b = \frac{RT_c}{64P_c}$ [1].

For many fluid of industrial interest the experimental value of the compressibility at critical point is slightly lower, ranging from 0.23 to 0.31, although not perfect, the agreement seems to be really good, due to the simplicity of the van der waals Equation of State. An improvement of the principle of corresponding states can be made by using Z_c as a sort of parameters that give the departure from the idealized behavior predicted by the Van der Waals Equation of State:

$Z = Z\left(\dfrac{T}{T_c}, \dfrac{P}{P_c}, Z_c\right)$, or using the acentric factor ω: $Z = Z\left(\dfrac{T}{T_c}, \dfrac{P}{P_c}, \omega\right)$. The parameters of the Cubic Equations of States can be directly calculated by means of this approach. For example, for the Peng Robinson Equation of State:

$$a = 0.45724\frac{R^2 T_c^{\,2}}{P_c}\alpha(T) \text{ and } b = 0.07780\frac{RT_c}{P_c}, \text{ where } \alpha(T) = \left[1 + k\left(1 - \sqrt{\frac{T}{T_c}}\right)\right]^2 \text{ with}$$

$k = 0.37464 + 1 - 5422\omega + 0.26992\omega^2$ [1, 27]. Despite the length of the algebraic calculations, the parameters of the Cubic Equations of State can be retrieved by critical point data alone or at list adding the single vapor pressure data that is required for estimating the value of the acentric factor. Another approach that can be used for estimating the characteristic parameter of these Equation of State is the regression of a set of phase equilibria data, such as vapor pressure and saturated liquid and vapor densities. While seldom performed in the case of low molecular weight species, it could be possible to estimate the characteristic parameters from single phase volumetric data alone, usually in the form of the volume or the density of the system for a range of temperature measured at fixed pressure (PVT data).

Applying the definition of the critical point to the Sanchez Lacombe Equation of State it is possible to calculate explicitly the critical density, temperature and pressure. The critical reduced density can be shown to be equal to $\tilde{\rho}_c = \dfrac{1}{1 + \sqrt{r}}$ and the critical reduced temperature is equal to $\tilde{T}_c = \dfrac{2r}{\left(1 + \sqrt{r}\right)^2}$, thus by substitution in the Equation of State it is possible to find the reduced critical pressure $\tilde{P}_c = \dfrac{2r}{\left(1 + \sqrt{r}\right)^2}\left[r\ln\left(1 + \dfrac{1}{\sqrt{r}}\right) + 0.5 - \sqrt{r}\right]$ [10]. In the Sanchez Lacombe Equation of State the critical point is explicitly a function of the length of the chain of the molecule and critical temperature increases with r, while the critical

pressure decreases and goes to zero for a chain of infinite length. This behavior is qualitatively the same that is exhibited by the homologous series of normal alkanes. The critical compressibility factor is itself a function of r, and for $r = 1$ is equal to 0.386, while goes to 1/3 for a chain of infinite length[10]. Thus the prediction of the critical conditions is even poorer than that of van der Waals Equation of State. Due to this features, the Sanchez Lacombe Equation of State does not, in general, obey a simple form of corresponding state principle, thus it is not possible to develop simple relationship, like those exploited for the Cubic Equations of State, for estimating the characteristic parameters. The approach that is usually followed, for low molecular weight species, is to regress a set of vapor pressure and saturated liquid densities data. According to Sanchez and Lacombe 1978[15], the characteristic parameters of low molecular weight substances could be estimated also by means of one value of the heat of vaporization, one value of the vapor pressure and the corresponding liquid specific volume, all at the same temperature. In the case of macromolecules, for which it is acceptable to put $r \rightarrow +\infty$, the equation of state is simplified a bit and the characteristic parameters can be retrieved by means of regression on PVT data[15]:

2.17
$$\tilde{\rho}^2 + \tilde{P} + \tilde{T}\left[\ln(1 - \tilde{\rho}) + \tilde{\rho}\right] = 0$$

More recently, in 2000 Gauter and Heidemann[28] have proposed a parametrization of the parameters of the Sanchez Lacombe Equation of State that enables to directly retrieve them from the critical coordinates and from the acentric factor, but the critical compressibility factor remains still too high respect to the range of values of the real fluids. This will lead to a poor prediction of the liquid phase specific volumes, that is avoided when regressing the characteristic parameters directly on the saturated liquid data.

Similar procedures applies to the equations of state that belongs to the class of the Statistical Associating Fluid Theory Equation of State, but some other

approach have been proposed. For instance Gross and Sadowski obtained the parameters of polyethylene by extrapolation from the low molecular weight alkane parameters[22], while in later works[24] it was suggested that the characteristic parameters of polymeric species could be obtained by fitting simultaneously PVT or liquid density data and binary phase equilibrium data. Even if it is then necessary to estimate a fourth parameter (the binary interaction parameter between the polymer and a low molecular weight substance), the procedure, albeit pragmatic, was found to be robust enough to provide parameters that performed well even for mixtures different from the one used for optimization. The same authors suggested that when the paucity of the data set can hamper the effort of regressing four free parameters, it seems reasonable to assume that the temperature independent segment diameter is equal to 4.1 Å[24].

Finally it is necessary to observe that since glassy polymers are outside equilibrium, it is not correct to regress PVT data obtained below the glass transition temperature. There are cases in which there are no available PVT data in the rubbery region, this is especially true for polymer that have really high glass transition. In some case this obstacle could be overcome by means of using some PVT data of a solution containing the polymer of interest, along with some binary equilibrium data, as done by Hesse and Sadowski for the polyimide Matrimid and P84[29]. Another type of approach that has been recently introduced in literature by Pricl[30, 31] and Minelli et al.[32] is to run Molecular Dynamics simulations of the polymer at high temperature and obtain *synthetic* PVT from which estimating the characteristic parameters for the equation of state. This multiscale approach is particularly ingenious, since the characteristic parameters of Equation of State are retrieved from the results of a calculations based on fundamental properties, such as the molecular structure and the interaction potential. It must be noted that Equation of State are always less computationally intensive than any kind of Molecular Dynamics, so they can be used for performing calculations that are still beyond the capability of Molecular

Dynamics, such as phase equilibria calculation. Therefore this approach takes the best from both methodologies.

2.4. *Fugacity and Gibbs Free Energy*

Models like Sanchez Lacombe Equations of State and Statistical Associating Fluid Theory Equation of State that are based on a well defined, yet somewhat idealized, description of the fluid at a molecular level, have been developed by their authors by means of the method of statistical mechanics. Therefore an expression for the Gibbs Free Energy or for the Helhlmoltz Free Energy of the system is directly available for calculations. Many other Equations of State are based on a more empirical approach and an explicit expression for the Gibbs or the Helmholtz Free Energy is lacking.

Since $P = -\dfrac{\partial \widetilde{A}}{\partial \widetilde{V}}$ and $\widetilde{S} = -\dfrac{\partial \widetilde{A}}{\partial T}$, the differential form of $\widetilde{A} = \widetilde{A}(T,V)$ is $d\widetilde{A} = -Pd\widetilde{V} - \widetilde{S}dT$ and since $G = A + PV$, the differential form for $\widetilde{G} = \widetilde{G}(T,P)$ is $d\widetilde{G} = \widetilde{V}dP - \widetilde{S}dT$, under isotherm condition, the change in Gibbs Free Energy upon a pressure change $P_1 \rightarrow P_2$ is $\widetilde{G}(T,P_2) - \widetilde{G}(T,P_1) = \int_{P_1}^{P_2} \widetilde{V}dP$. If the fluid is an ideal gas, the integral $\int_{P_1}^{P_2} \widetilde{V}dP$ becames $\int_{P_1}^{P_2} \dfrac{RT}{P} dP$ and since all fluid behave like ideal gases when $P \rightarrow 0$, the value of the Gibbs Free Energy of a real gas can be evaluated starting from its ideal gas value, provided that their volumetric behavior is known, for instance by means of an Equation of State, using the formula: $\widetilde{G}(T,P) = \int_{0}^{P}\left(\widetilde{V} - \dfrac{RT}{P}\right)dP + \widetilde{G}^{IG}(T,P)$ Helmholtz Free Energy can be calculated as $\widetilde{A}(T,\widetilde{V}) = \int_{0}^{P}\left(\widetilde{V} - \dfrac{RT}{P}\right)dP - P\widetilde{V} + \widetilde{A}^{IG}(T,\widetilde{V})$. These formulas can be used for calculating the Free Energies using an Equation of State that provide the description of the volumetric behavior of the fluid. Many calculations, such

as phase equilibria, can be performed without the need to evaluate the actual value of the free energy, but simply its departure from the ideal gas value. In that case it is commonly used the thermodynamic function known as the fugacity, defined as

2.18
$$f = P \exp\left(\frac{\tilde{G}(T,P) - \tilde{G}^{IG}(T,P)}{RT}\right) = P \exp\left(\frac{\int_0^P \left(\tilde{V} - \frac{RT}{P}\right)dP}{RT}\right)$$

or in term of compressibility factor

2.19
$$f = P \exp\left(\frac{\int_{+\infty}^{\frac{ZRT}{P}} \left(\frac{RT}{\tilde{V}} - P\right)d\tilde{V}}{RT} - \ln Z + (Z-1)\right)$$

When using an equation of state, the fugacity of a vapor can be calculate by using, in the evaluation of the above integral, the specific volume or compressibility root that correspond to a vapor state, while the fugacity of a liquid can be calculated by using the root that correspond to the liquid state[1].

With the van der Waals Equation of State the fugacity can be readily evaluated as:

2.20
$$\ln\left(\frac{f}{P}\right) = (Z-1) - \ln(Z-B) - \frac{A}{Z}$$

and for Peng Robinson Equation of State:

2.21
$$\ln\left(\frac{f}{P}\right) = (Z-1) - \ln(Z-B) - \frac{A}{2\sqrt{2}B}\ln\left[\frac{Z + \left(1+\sqrt{2}\right)B}{Z + \left(1-\sqrt{2}\right)B}\right].$$

2.5.   System made by several chemical species: thermodynamic function and equations of state

Many of the above mentioned considerations can be plainly extended to the case of homogenous single phase systems with more than one chemical species. In that case composition plays a major role as a descriptor of the state of the system itself and some kind of composition measure should be introduced in the set of variable that define the state of the system. Regarding to extensive properties, the most straightforward choice is to define the composition of the system in term of number of the moles of each species $(n_1 \quad ... \quad n_i \quad ... \quad n_{Nc})$ or as the amount in mass term of each species $(m_1 \quad ... \quad m_i \quad ... \quad m_{Nc})$. For intensive properties, such as specific enthalpy or specific entropy, when they are expressed on a mass basis, the composition of the system is completely specified once that the mass fraction of $Nc-1$ species are given, like $(\omega_1 \quad ... \quad \omega_i \quad ... \quad \omega_{Nc-1})$, on the other hand, when the intensive properties are expressed on a molar basis, the molar fraction of $Nc-1$ species should be provided, like $(x_1 \quad ... \quad x_i \quad ... \quad x_{Nc-1})$. In same cases it is useful to work on a volume base and the composition of the system can be specified by providing Nc density of the single species, defined as $\rho_i = \dfrac{m_i}{V}$, thus the state of the system will include the following array of densities: $(\rho_1 \quad ... \quad \rho_i \quad ... \quad \rho_{Nc})$. Any general rule for calculating the property of the mixture from the properties of the single constituents should encompass the mixing effects. This can be exploited by means of theory of the partial molar properties[1, 7]. Let us say that $\tilde{\theta}$ is a generic property, on a molar basis, of a multicomponent system, it follows that $\tilde{\theta} = \tilde{\theta}(T, P, x_1 \quad ... \quad x_i \quad ... \quad x_{Nc-1})$, if the system contains globally N moles of molecules, then the total amount of θ in the system is $\theta = N\tilde{\theta}$. The problem of writing explicitly $\tilde{\theta}$ as a sum of contribution from the single species can be overcome by introducing the partial molar thermodynamic property $\bar{\theta}_i$,

defined as $\bar{\theta}_i = \left(\dfrac{\partial \theta}{\partial n_i} \right)_{T,P,n_{j \neq i}}$. The partial molar thermodynamic property $\bar{\theta}_i$ is a

function of Pressure, Temperature and composition of the system $\bar{\theta}_i = \bar{\theta}_i(T, P, x_1 \quad ... \quad x_i \quad ... \quad x_{Nc-1})$ and not equal to the corresponding pure component property. It can be proved by construction that $\tilde{\theta} = \sum_{i=1}^{Nc} x_i \bar{\theta}_i$. The array of variables that define the state of the system for the Gibbs Free Energy and the Helmholtz Free Energy, as well as the other properties of the multicomponent system, should include the above mentioned composition variables:

2.22 $$ G = G(T, P, n_1 \quad ... \quad n_i \quad ... \quad n_{Nc}) $$

2.23 $$ A = A(T, P, n_1 \quad ... \quad n_i \quad ... \quad n_{Nc}) $$

The same happens for the corresponding specific free energies, in term of mole and mass basis:

2.24 $\tilde{G} = \tilde{G}(T, P, x_1 \quad ... \quad x_i \quad ... \quad x_{Nc-1})$ and $\hat{G} = \hat{G}(T, P, \omega_1 \quad ... \quad \omega_i \quad ... \quad \omega_{Nc-1})$

2.25 $\tilde{A} = \tilde{A}(T, V, x_1 \quad ... \quad x_i \quad ... \quad x_{Nc-1})$ and $\hat{A} = \hat{A}(T, V, \omega_1 \quad ... \quad \omega_i \quad ... \quad \omega_{Nc-1})$

The Helmholtz Free Energy for unit of volume of the system is:

2.26 $$ \breve{A} = \breve{A}(T, \rho_1 \quad ... \quad \rho_i \quad ... \quad \rho_{Nc}). $$

All this functional dependence can be shown to be compliant with the prescriptions that arise from the inspection of the Second Law Inequality, in a similar fashion to the procedure that was explicitly followed in the case of the single component system.   The partial molar Gibbs Free Energy

$\overline{G}_i = \left(\dfrac{\partial G}{\partial n_i} \right)_{T,P,n_{j\neq i}}$ plays a prominent role in the following phase equilibria

computations and is usually named as the chemical potential of the component i and historically has been indicated with the symbol μ_i. Clearly $\mu_i = \mu_i(T,P,x_1 \ ... \ x_i \ ... \ x_{Nc-1})$. It can be shown that

$\mu_i = \left(\dfrac{\partial G}{\partial n_i} \right)_{T,P,n_{j\neq i}} = \left(\dfrac{\partial A}{\partial n_i} \right)_{T,V,n_{j\neq i}}$, but it should be noted that the last partial

derivative is not the partial molar Helmholtz free energy. The chemical potential on a mass basis is readily calculated as $\mu_i^{m} = \left(\dfrac{\partial \breve{A}}{\partial \rho_i} \right)_{T,\rho_{j\neq i}}$. It should be noted

that, from the inspection of the Second Law inequality, the functional relationship between entropy and Helmholtz free energy can be explicity exploited as:

2.27
$$S = -\left(\frac{\partial A}{\partial T} \right)_{V,n_{j\neq i}} \text{ or } \tilde{S} = -\left(\frac{\partial \tilde{A}}{\partial T} \right)_{V,x_{j\neq i}} \text{ or } \hat{S} = -\left(\frac{\partial \hat{A}}{\partial T} \right)_{V,\omega_{j\neq i}}$$

and on a volume basis

2.28
$$\breve{S} = -\left(\frac{\partial \breve{A}}{\partial T} \right)_{\rho_{j\neq i}} .$$

Finally it is possible to affirm that at equilibrium, Pressure is function of Temperature, Volume and composition. The function that represent this relationship is the Equation of State. And like the case of the pure component, if an expression for Helmholtz free energy is available from some molecular or mechanical statistical theory, then the equation of state can be explicitly derived

as $P_{eq} = -\left(\dfrac{\partial A}{\partial V}\right)_{T,n_{j\neq i}} = f(V,T,n_1 \quad ... \quad n_i \quad ... \quad n_{Nc})$ .or in term of intensive

properties $P_{eq} = -\left(\dfrac{\partial \tilde{A}}{\partial \tilde{V}}\right)_{T,x_{j\neq i}} = f(\tilde{V},T,x_1 \quad ... \quad x_i \quad ... \quad x_{Nc})$. When the Helmholtz

free energy on a volume basis is used, the relationship between equilibrium pressure and Helmholtz free energy is[6]:

$$2.29 \qquad P_{eq} = \sum_{i=1}^{Nc} \rho_i \left(\frac{\partial \breve{A}}{\partial \rho_i}\right)_{T,\rho_{j\neq i}} - \breve{A}$$

or in term of chemical potential on a mass basis:

$$2.30 \qquad P_{eq} = \sum_{i=1}^{Nc} \rho_i \mu_i^m - \breve{A} \,.$$

It is straightforward to recognize that the Equation of State for a multicomponent system could be written explicitly in term of the densities of the single species of the system:

$$2.31 \qquad P_{eq} = f(T,\rho_1 \quad ... \quad \rho_i \quad ... \quad \rho_{Nc})$$

2.6. Equations of State for Multicomponent Systems: Mixing Rules

The Equations of State developed for providing a description of the volumetric behavior of pure fluids can be extended to the case of multicomponent mixtures. Generally speaking, the characteristic parameters of the mixture can be obtained in a purely predictive way by those of the pure fluids, by means of appropriate mixing rules. Frequently happens that the prediction of the Equation

of State for the mixture is not as good as was the prediction of the properties of the pure fluids and it is necessary to introduce a correction to the value of some of the characteristic parameters. This is usually done by means of the use of binary interaction parameters. The value of that parameters is generally obtained by means of regression of binary mixtures data, for each pair of components of the system, even if the mixture contains more than two substances. Sometimes, due to lack of pertinent binary data for one pair of substance, the competent binary interaction parameters can be found only by regression of the complete mixture data. Clearly if this is the case, the model acts only as a regression or correlation tool.

It must be emphasized that in many cases in the literature it is possible to find several set of different mixing rules for the same equation of state and their choice retains a certain level of empiricism[1, 7, 27].

The first example of mixing rules that can be considered is that of the mixing rules commonly used for calculating the mixture characteristic coefficients a_{mix} and b_{mix} for the Peng Robinson Equation of State:

2.32
$$a_{mix} = \sum_{i=1}^{Nc} \sum_{j=1}^{Nc} x_i x_j a_{ij}$$

2.33
$$b_{mix} = \sum_{i=1}^{Nc} x_i b_i$$

The coefficient b_i is the characteristic parameter of the pure substance i, while the coefficient a_{ij} is calcolate for every pair of substance i and j according to the combining rule $a_{ij} = \sqrt{a_i a_j}\left(1 - k_{ij}\right)$, where a_i and a_j are the characteristic parameters of the pure substances and k_{ij} are the above mentioned binary

interaction parameters. From the definition of the combining rule, since there is no physical reason to assume that $k_{ij} \neq k_{ji}$, the matrix of the a_{ij} is symmetrical. These mixing rules are known as the van der Waals one fluid mixing rules[1, 27], due to the fact that the mixture is being described by the same equation of state of the pure fluids, but the characteristic parameters a_{mix} and b_{mix} are effectively composition dependent. In particular a_{mix} is a quadratic form in x_i and b_{mix} is a linear form in the same variable.

The Sanchez Lacombe Equation of State provide another interesting example of mixing rules. In fact there are at least three different set of mixing rules that have been proposed for this equation of state[33]. The first set of mixing rules acts directly on the characteristic density and on the characteristic pressure of the system:

$$2.34 \qquad \frac{1}{\rho^*} = \sum_{i=1}^{Nc} \frac{\omega_i}{\rho^*_i}$$

$$2.35 \qquad P^* = \rho^{*2} \sum_{i=1}^{Nc} \sum_{j=1}^{Nc} \frac{\omega_i}{\rho^*_i} \frac{\omega_j}{\rho^*_j} \Delta P^*_{ij}$$

with the combining rule

$$2.36 \qquad \Delta P^*_{ij} = \sqrt{P^*_i \, P^*_j} \left(1 - ki_j\right).$$

Another set of mixing rule for Sanchez Lacombe Equation of State acts directly on the characteristic volume of the lattice v^* and on the characteristic energy ε^*:

$$2.37 \qquad v^* = \sum_{i=1}^{Nc} \phi_i v^*_i$$

2.38
$$\varepsilon^* = \sum_{i=1}^{Nc} \sum_{j=1}^{Nc} \phi_i \phi_j \varepsilon^*_{ij}$$

with the combining rule $\varepsilon^*_{ij} = \sqrt{\varepsilon^*_i \varepsilon^*_j}\left(1 - ki_j\right)$. The variable ϕ_i represent the volume fraction of the component i in the lattice. Finally more recently has been proposed that the following mixing rules set is the most versatile and accurate:

2.39
$$v^* = \sum_{i=1}^{Nc} \sum_{j=1}^{Nc} \phi_i \phi_j v^*_{ij}$$

2.40
$$v^* \varepsilon^* = \sum_{i=1}^{Nc} \sum_{j=1}^{Nc} \phi_i \phi_j \varepsilon^*_{ij} v^*_{ij}$$

with the combining rule $\varepsilon^*_{ij} = \sqrt{\varepsilon^*_i \varepsilon^*_j}\left(1 - ki_j\right)$ and $v^*_{ij} = 0.5\left(v^*_i + v^*_j\right)\left(1 - \eta_{ij}\right)$, where η_{ij} is a binary interaction coefficient that acts directly on the specific volume of the site cells in the mixture lattice. This latter mixing rules are more flexible, but the price that has to be paid is increase of the number of the free parameters. While this could be a strength for a correlation tool, it is usually regarded as a shortcoming if the model is going to be used as a predictive or semi-predictive tool. It is interesting to point out that the mixing rule for the characteristic energy or for the characteristic pressure, that since its relationship with the cohesive energy density it is still a measure of the energy of the intermolecular interactions, is a quadratic form in the composition variable in all the three cases, while the mixing rule for the characteristic density or for the characteristic site volume is a linear form in the first two sets, while it has quadratic order in the latter case.

The Equations of State belonging to the class of the Statistical Associating Fluid Theory Equations of State require mixing rules for both the dispersion and the association contribution. The characteristic parameters for the dispersion

contribution for mixtures are calculated according to the so-called one fluid theory, parametrizing the dispersive Helmholtz energy of an hypothetical single-component fluid with respect to the characteristic parameters of the pure components by means of the following mixing rules[22]:

2.41
$$\sigma_{ij} = \frac{\sigma_i + \sigma_j}{2}$$
$$\varepsilon_{ij} = \sqrt{\varepsilon_i \varepsilon_j}\left(1 - k_{ij}\right)$$

In the case of mixtures of associating compounds, that give rise to self association as well as to cross association (temporary bonding between sites on molecules of different species) it is necessary to adopt a set of mixing rules also for the characteristic parameters of the association contribution[23]:

2.42
$$\varepsilon^{A_iB_j} = \frac{\left(\varepsilon^{A_iB_i} + \varepsilon^{A_jB_j}\right)}{2}$$

2.43
$$k^{A_iB_j} = \sqrt{k^{A_iB_i} k^{A_jB_j}}\left(\frac{\sqrt{\sigma_{ii}\sigma_{jj}}}{\frac{1}{2}\left(\sigma_{ii} + \sigma_{jj}\right)}\right)^3$$

According to these equations, the values of the characteristic parameters of the association term are completely defined by the values of the pure components, without using any correction parameters.

It is possible to observe that in the case of the van der Waals one fluid mixing rules for Cubic Equations of State as well as in the case of the Sanchez Lacombe, the mixing rules for the characteristic parameters that are more closely related to the interaction energy between the molecules of the fluid are quadratic form in the composition variable and that their combining rule is based on the geometric average of the pure fluid characteristic parameter. On the

other hand, for the parameters that are related to the volume of the molecules (or of the sites of the lattice) there is no combining or the combing rule is based on a simple average. This observations extends to the mixing rules that are commonly adopted in the equations of state that belongs to the class of Statistical Associating Fluid Theory.

It is interesting to observe that from statistical mechanics it is known that the second virial coefficient B, that in the virial series expansion is the first correction term to the ideal gas equation of state, is a quadratic function of the composition variables[1]:

2.44
$$Z = 1 + \frac{B}{\tilde{V}} + \frac{C}{\tilde{V}^2} + ...$$

2.45
$$B = \sum_{i=1}^{Nc} \sum_{j=1}^{Nc} x_i x_j B_{ij}$$

Therefore it is a reasonable to expect that also the mixing rules of more empirical models comply to such quadratic composition dependence, at least for the interaction characteristic parameter. This can be checked by expanding the compressibility calculated from the model in series respect to $\frac{1}{\tilde{V}}$ and comparing the second term of the series with those of the virial equation of state. For instance it can be shown that for Cubic Equations of State $B = b - \frac{a}{RT}$.

It is a matter of fact that quadratic mixing rules are quite always sufficient for the correlation of phase equilibria. On the other hand several authors have been felt compelled to introduce a composition dependent binary interaction parameter, in order to model more complex systems. Any choice like this will make the

mixing rule a non quadratic form. For example Panagiotopoulos and Reid in 1986 proposed to use the following combining rule[27, 34]:

2.46
$$a_{ij} = \sqrt{a_i a_j}\left[\left(1-k_{ij}\right)+\left(k_{ij}-k_{ji}\right)x_i\right] \quad with \quad k_{ij} \neq k_{ji}$$

Similar combining rules have been proposed also by Adachi and Sugie[27, 35] in 1986 and also a general form of non quadratic mixing rule have been proposed, in the form $ki_j = \delta_i x_i + \delta_j x_j$ [27]. These kind of mixing rules have been found appropriate for modeling several binary systems, including some system with supercritical components. In anyway, it must be observed that these kind of non quadratic mixing rules, due their asymmetrical mathematical form, suffer from the so called Michelsen-Kistenmacher syndrome[27, 36-38]. These pathological behavior arises when there is a lack of invariancy respect to the fictious subdivision of a component in two or more components with the same pure fluid parameters. In fact if a mixture is made by a fraction ω_A of component A and a fraction $\omega_B = 1 - \omega_A$ of component B, or if the mixture is made by a fraction $\omega_{A1} = 0.3\omega_A$ of a fictious component with the same property of A, by a fraction $\omega_{A2} = 0.7\omega_A$ of a fictious component again with the same property of A and by a fraction $\omega_B = 1 - \omega_{A1} - \omega_{A2}$ of component B, any physical property like density or compressibility to be evaluated by means of an Equation of State should be the same in both cases. With a non quadratic mixing rule this is not going to happen and the calculated property of the system that contains the two fictious components, albeit the total fraction of species that behave like component A is the same, will be different from that of the original system. It has been argued that due to this pathological behavior the non quadratic mixing rules perform poorly when dealing with ternary systems in which there are two components with very similar characteristic parameters, for instance as could be the case for a ternary system containing cyclohexane and benzene.

A different approach to the problem of defining efficient mixing rules has been undertaken by Huron and Vidal[36, 39] in 1979 and subsequently by Wong and Sandler[1, 37, 40] in 1992 is the one of combining the Equation of State with a model for the Gibbs Free Energy or for the excess Gibbs Free Energy. In fact Equations of State are a really powerful tool for predicting volumetric properties on a wide range of pressure and temperature, especially for pure fluids, but have several shortcomings in taking into account the effect of mixture composition. This is particularly true in the case of those mixtures in which local composition effects and non randomness effects can be significant, such as when there is hydrogen bonding or any form of clustering. On the other hand, there are several semi empirical models, like UNIFAC, UNIQUAC, Wilson and so on, that provide an accurate description of the Excess Gibbs Free Energy of those systems, but those models fail to take into account pressure effects and, to a less extent, even temperature effects. These shortcomings are due to the fact that these models does not provide a representation of the volumetric behavior of the fluid mixture. The main idea behind this approach is that since $\left(\dfrac{\partial A}{\partial P}\right) = 0$, the Helmholtz Free Energy at low, ambient pressure, at which those Gibbs Free Energy Models are defined, is equal to the Helmholtz Free Energy at infinite pressure, provided that composition and temperature are held fixed. But at low pressure $A \approx G$ and at infinite pressure the excess Helmholtz free energy of many kind of Equations of State like the Cubic Equations of State reduces to a really simple form, explicit in term of the mixture characteristic parameters. Then these mixture characteristic parameters can be promptly calculated by equating the expression of the infinite pressure excess Helmholtz free energy from the Equation of State to the excess Gibbs Free Energy from the Gibbs Free Energy Models that work well at low pressure. It should be noted that the Wong Sandler treatment provides a set of mixing rules that complies with the theoretical requirement, from statistical mechanics, that the second virial coefficient be a quadratic form of composition.

2.7. *Phase Equilibria in multicomponent system*

Let us consider two separate phases, spatially homogenous and made of several chemical species, that are brought in contact together. For the sake of simplicity let us assume also that the two phases were already at the same temperature and pressure, thus thermal and mechanical equilibria will be immediately attained, with any further need to exploit the energy balance as well as the momentum balance. The substances in the two phases can be in different aggregation states, such as a liquid and vapor or solid and a liquid, but in the case of the condensed phases they could be both solid or both liquid and simply be immiscible (i.e. when brought to contact it will still be possible to recognize, on a macroscopic scale, two different kind of domains, separate by boundary surfaces). This for instance is what happens with water and oil, but it is the same that happens when a polymer sheet is exposed to a vapor or is immersed in a liquid that is not going to act as a solvent for it. This system is constrained at fixed pressure and temperature and the overall amount of each component is fixed, even if it could change the relative amount of each species in the two phases. Again from Second Law, we can say that its evolution should comply with the condition $\dfrac{dG}{dt} \leq 0$, just as we said in the case of the single component system. At any time, the system will be contain a given mass fraction of component i in the phase I, say $\omega_i^{\,I}$, and a corresponding fraction of the same component i in the phase II, say $\omega_i^{\,II}$. Each phase will have its own free energy content, say $m^I \hat{G}^I = \sum\limits_{i=1}^{Nc} m_i^{\,I} \mu_i^{\,m,I}$ and $m^{II} \hat{G}^{II} = \sum\limits_{i=1}^{Nc} m_i^{\,II} \mu_i^{\,m,II}$, so that

$G = m^I \hat{G}^I + m^{II} \hat{G}^{II}$, thus $\dfrac{d\hat{G}}{dt} = \sum\limits_{i=1}^{Nc} \left(\mu_i^{\,m,I} - \mu_i^{\,m,II} \right) \dfrac{dm_i^{\,I}}{dt} \leq 0$. At equilibrium the chemical potential of the species in the phase I should be equal to the chemical potential of the species in phase II: the phase equilibrium criterion is the well known criterion of the equality of the chemical potential[1, 7]:

2.47
$$\mu_i^{m,I} = \mu_i^{m,II} \quad \forall i$$

The equilibrium criterion give Nc equations that have to be solved simultaneously.

When using Equations of State models like Sanchez Lacombe and Statistical Associating Fluid Theory, for which an explicit expression for the Gibbs or Helmholtz Free Energy is available, the chemical potential can be evaluated directly by analytical or numerical differentiation. It should be noted that when the chemical potential is evaluated using an approach based on equations of state, for each phase the density roots of the equation of state should be find (and used in the calculation for providing the value of the density of the system) and when there are multiple roots, only the one corresponding to the aggregation state that is stable at the given pressure and temperature conditions should be used.

It should be noted that the phase equilibrium criterion of the equality of chemical potentials, can be transformed in the criterion of the equality of the fugacity, that is more useful for Equations of State like the Cubic Equations of State, for which an expression for fugacity is promptly available, just like in the case of the pure substances

2.48
$$f_i^I = f_i^{II} \quad \forall i$$

The fugacity f_i for a multicomponent system is defined as:

2.49
$$f_i = x_i P \exp\left(\frac{\mu_i - \mu^{IG}_i}{RT} \right)$$

Depending upon the aim of the calculation, there are several way to calculate the vapor liquid equilibria. For example for a binary system at fixed pressure

and temperature it is possible to solve the equality of the chemical potentials, that form a system of two equations in two variables, in order to obtain the composition of the vapor and of the liquid that are in equilibrium with each other. If the pressure is kept fixed it is possible to calculate the dew point temperature for each vapor composition or the bubble temperature for each liquid composition or If the temperature is kept fixed, analogous calculations can be performed looking for the dew point pressure and the bubble point pressure. In both cases there is always a system of two equations in two variables. Despite their direct application to process simulation and design, these three methods can also be used for drawing the vapor liquid equilibrium diagram for a binary mixture, either at fixed pressure or temperature. Another kind of vapor liquid equilibria calculation that is commonly used in process simulation is the so called flash calculation, in which the vapor liquid equilibrium is calculated when a liquid is partly vaporized or vapor is partly condensed. In this case, along with the criterion of the equality of the chemical potentials, it is necessary to solve simultaneously the N_C equations of the mass (or mole) balances. The same kind of calculations can be run when dealing with liquid liquid equilibria and usually a great emphasis is placed on the calculation of the temperatures at which the liquid system starts to form two immiscible phases. These temperature are generally known as Lower and Upper Consolute Temperature[7]. Like in the case of vapor liquid equilibria there are several well known phase diagram morphology, that relates to specific kinds of phase behavior, also in the case of liquid liquid equilibria some classification scheme has been proposed in literature, especially regarding the shape and the extension of the region in which the liquids are immiscible. Sometimes the temperature at which phase separation starts to happen is named cloud point temperature, due to the change in bulk optical properties that usually accompanies liquid phase separation. In the case of binary liquid liquid equilibria, the above considerations about the number of variables and the number of the equations that have to be solved can be assumed to hold. In the case of ternary liquid liquid system, some more specific consideration can be required, especially noting that even at fixed

pressure and temperature, the system of the chemical potential equalities is undetermined, since it is made by three equations in four variables. When the final goal of the computations is simply to draw the liquid liquid isothermal and isobaric diagram and not to calculate an actual phase splitting (that will require the simultaneous solution of the mass balance equations, like in the case of the flash calculations), with a little empiricism it is possible to operate simply parametrizing the liquidus curves respect to the mass (or mole) fraction of one of the component in one of the phases. In this way the system is made by three equations in three unknowns and it is solvable. Varying the mass (or mole) fraction of the component selected as parameter it is then possible to draw the complete diagram[41, 42].

In vapor liquid equilibria or in liquid liquid equilibria it can happen that one of two phases is made predominantly by a single component that due to some internal constraint is not going to be present in the other phase, so that its mass or mole fraction (or its density) in the other phase will be always null or negligible. In this cases the phase equilibria computation can be called a solubility calculation. For instance this can be the case of a polymer, that have negligible vapor pressure and thus in vapor liquid equilibria it will never be found in the vapor phase, or it could be the case, in liquid liquid equilibria, of a crosslinked rubber, that due to its internal, mechanical constraint, it will never dissolve in the solvent that forms the second liquid phase.

Solubility calculations are somewhat simple than the complete phase equilibria and will be addressed with dedicated algorithm.

2.8.   Concluding remarks

The Equations of State are well defined thermodynamic tools that describe the equilibrium volumetric properties of mixtures and of pure substances. Moreover,

Equations of State can be used for calculating phase equilibria in single and multicomponent systems. A brief review of the most commonly used Equations of State have been performed, along with a discussion of the procedure commonly used for retrieving pure components characteristic parameters and of the mixing and combining rules that are used for estimating the characteristic parameters of mixtures.

3. Equation of State Models of Water-1,4-Dioxane and Polylactides for TIPS Preparation of Scaffolds: Pure Component Properties, Binary VLE and Ternary LLE

3.1.   Introduction

Tissue engineering approach is driving a change of perspective in modern medicine and surgery, providing a way to aid healing, biofactors (cells, genes and proteins) delivery and tissue regeneration and striving to reduce the need of tissue grafting, organ transplantation and use of synthetic implants. The concept behind this approach is to provide porous synthetic, yet degradable and fully biocompatible, scaffolds that can act as a extracellular matrix able to fill surgical resection cavities, support and coordinate three-dimensional cells growth and formation of desired tissue[43]. This can be achieved providing cells with appropriate spatial, mechanical and chemical stimuli, assuring enough mechanical strength to bear the loads, provide size and shape stability, transmit to the cells the mechanical input required to drive tissue formation, permit the necessary transport of gases, nutrients, proteins, cells and waste products. Moreover scaffold could be medicated or cells seeded, in order to deliver biofactors in a controlled way and should be biocompatible: they should promote adherence, cell proliferation and differentiation and should not trigger

acute and chronic inflammatory response. Thus porous scaffolds should ideally have a controlled topology and pore size distribution, to achieve the proper trade-off between mass transport properties, mechanical properties and biological performance. It has been reported that large pore size, with a hierarchical pore size distribution and open cellular structure are the features needed for ensuring cell seeding, tissue growth and neovascularization in the *in vivo* applications. Clearly mass transport and mechanical strength are influenced in opposite way by porosity. Lastly scaffold should be biodegradable, ideally showing an *in vivo* degradation kinetic that mirrors the rate of tissue generation and /or biofactor delivery[43, 44]. Poly(L-Lactic Acid) or PLLA , Poly(D-Lactic Acid) or PDLA and their copolymers are suitable for fabrication of porous scaffolds that exhibit outstanding biodegradability and biocompatibility properties[45, 46]. Among the several methods that are listed in literature to be suitable for porous scaffold preparation, phase separation methods such as Thermally Induced Phase Separation (TIPS) are reported to be suitable to produce scaffold with pore diameter compatible with tissue growth, tailored adjusting thermodynamic and kinetic parameters of the process. Moreover TIPS techniques have already been commercially used for microporous membrane preparation for filtration and for fabrication of PLA 3D scaffolds[46, 47].

In order to develop a physically sound model of the complete TIPS process, that is an effort that will remain outside the scope of this thesis, it is necessary to identify a thermodynamic model that can be used successfully in predicting the liquid-liquid phase equilibria of the actual ternary system. Although there is a long lasting tradition of modelling ternary LLE of mixture containing macromolecular species by means of Gibbs Free Energy models like Flory Huggins and its extensions, the Equation of State models have been successfully applied to similar systems. In this chapter it will be shown the results of the calculations performed with the Sanchez Lacombe Equation of State and the Perturbed Chain Statistical Associating Fluid Theory Equation of State. Modelling of the ternary LLE requires, as a preliminary and necessary step, that the characteristic parameters of the pure components are retrieved by

fitting some pure substance properties or from the literature, as well as comparing the results of the model with the available data for at least one of the pair of substances. The characteristic parameters of the pure polymers will be retrieved by regression of the available PVT data, while the characteristic parameters for water and 1,4 dioxane can be found in the literature, with the relevant exception of the 1,4 dioxane PC-SAFT parameters, that had been retrieved in this work, by means of regression of vapour pressure and saturated liquid density data. Mixtures made by water and 1,4 dioxane are used in several analytical chemistry procedures, as well as in industrial processes, therefore this mixture have already received some attention in the past and several sets of binary thermodynamic data can be found in literature. For the purpose of this work, the relevant sets of data for the binary mixture water – 1,4 dioxane are the Gibbs Free Energy of mixing measured by Goates[48] in 1958, the Vapor Liquid Equilibria that can be found in DECHEMA[49], the 1,4 dioxane vapour pressure data reported by Vinson et al.[50] in 1963 and the mixture density data reported by Nayak et al.[51] in 2004 and by Papanastaslou et al.[52] in 1992. It must be observed that mixture of water and dioxane does not show miscibility gap in liquid phase at ambient temperature and pressure, so it is possible to tune the model, retrieving the required binary interaction coefficient, by correlating the VLE of the mixture, that exhibit a pretty evident azeotrope. It is certainly remarkable to note that, as shown in Mannella et al.[53] in 2010, many activity coefficients models wrongly predict a miscibility gap between water and dioxane at ambient temperature and pressure. De Witte[47, 54], who modelled the ternary LLE of the Water – 1,4 Dioxane - PLA mixtures with the Flory Higgins model, addressed a similar issue by introducing composition dependence energetic interaction parameter. Actually water and 1,4-dioxane liquid mixtures have been shown to be characterized by formation of clusters with composition and structure that strongly depends on dioxane molar fraction. According to Takamuku et al.[55] at $x_{dioxane} < 0.1$ the network of hydrogen bonded water molecules is predominant, while at $x_{dioxane} > 0.3$ the inherent structure of the pure 1,4.dioxane is predominant, with water taking part into the structure by

hydrogen bonding. Finally at $15 \leq x_{dioxane} \leq 0.2$ neither water and 1,4-dioxane structures are predominant and small clusters of one or two dioxane molecules with water molecules are formed. Some vapour liquid equilibria data and some liquid liquid equilibria, in the form of solubility isotherms, can be found for this pair of substance, but that data are mainly referred to conditions in which the polylactides are glassy and thus these data are intrinsically pseudo equilibrium data and cannot be directly used for validating the model for the liquid liquid equilibria, although they can still provide a useful estimate of the order if magnitude of the solubility of water in the polylactides, that is rather low. 1,4 Dioxane is known to be a solvent for polylactides, but it was not possible to find any relevant thermodynamic data, that could be suitable for the purpose of retrieving the binary interaction parameter.

3.2.   The properties of polylactides

As stated in the previous introduction, polylactides or poly lactic acid can be prepared by synthesis yielding two different chiral forms, named L and D, that exhibit different behaviour, especially concerning the possibility to form crystalline phases.
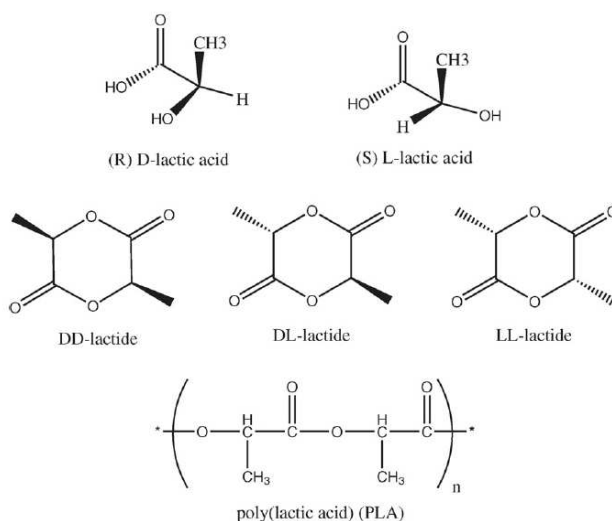
Fig. 3.1   Molecular structures of PLA and of its precursors.

Polymer	Commericial Name	Mw	Mn	Mw/Mn	Tg[K]	Tm [K]	Cristalline fraction %	Ref.
P-L-LA	Resomer® R L206	120000	60000	2	324	442	70	46
P-L-LA	Resomer® R L210	380000	130000	2.77	338	444	70	46
P-D-LA	Resomer® R 206	105000	50000	2.1	323	-	-	46
P-D-LA	Resomer® R 208	250000	136000	1.85	325	-	-	46
PLA	NatureWorks® PLA3001D		660000	-	-	444.6	-	56[56]
PLA	Lacea® H-100E	110000	39000	2.8	337	441	-	57[57]

Tab. 3.1 Melting Temperature and Glass Transition Temperature from several different sources.

Generally speaking PLLA, or copolymer with an high fraction of L monomeric units can form crystalline phases and thus the polymer will be semicristalline, while PDLA or copolymers in which the D form is the most abundant will be amorphous. In the literature the amorphous PDLA is sometimes referred to as simply PLA. The current opinion in literature is that the semicristalline PLLA is best suited for the preparation of scaffolds, due to the fact that the crystallites dispersed in the amorphous matrix will improve its mechanical properties. Crystallization processes will also play a relevant role in the TIPS process, directing influencing the actual phase separation, that in reality would be dictated not only by the liquid liquid equilibria of the mixture, but also by the solid liquid equilibria. Moreover the formation and growth of the crystallites in the polymer rich phase will influence the kinetic of the TIPS process, as well as its final morphology. Also it must be considered, when regressing the PVT data with an Equation of State model, that this model cannot provide an adequate representation of ordered phases and thus they should not be applied at temperature below the melting temperature. Even if the system is amorphous, as in the case of PDLA, a similar attention is to be paid at avoiding to use the Equation of State at temperatures below glass transition temperature, since Equation of State cannot represent the volumetric behavior of the glassy phase.

3.3. Pure Polymers Parameters for Sanchez Lacombe Equation of State

The characteristic parameters of the polylactides PDLA and PLLA have been retrieved by from linear least square regression of PVT data in a temperature range in which the polymer is rubbery and non crystalline. The PVT data are in the form of specific volume (or density) at fixed pressure and as a function of the temperature. Thus the data are represented in the form of isobaric curves, in the specific volume – temperature plane. For retrieving the characteristic parameters of the amorphous PLA was used a set of PVT kindly provided by Professor Mensitieri of the Università di Napoli Federico II, in the framework of an Italian national research project on the production of scaffolds, in which our research group was involved. The PVT data of PLLA were retrieved from Zoller et al. compilation[58]. The Sanchez Lacombe Equation of State was implemented in a Matlab® code and was solved, for each pressure and temperature for which an experimental point was available, looking for the density root that refers to the high density phase. Actually, since macromolecular species have a really high molecular mass M, it was assumed that $r \rightarrow +\infty$. A non linear least square optimization algorithm, from the function library of Matlab® was used for retrieving the polymer characteristic parameters, by minimization of the following objective function:

3.1
$$OF = \sum_{i}^{Np} \left(\frac{\hat{V}_i^{SL-LF} - \hat{V}_i^{Exp}}{\hat{V}_i^{Exp}} \right)^2$$

The termination tolerances for the function value and for the argument array values were set equal to 10^{-16}. The calculation was found to be pretty insensitive to the initial guess values.
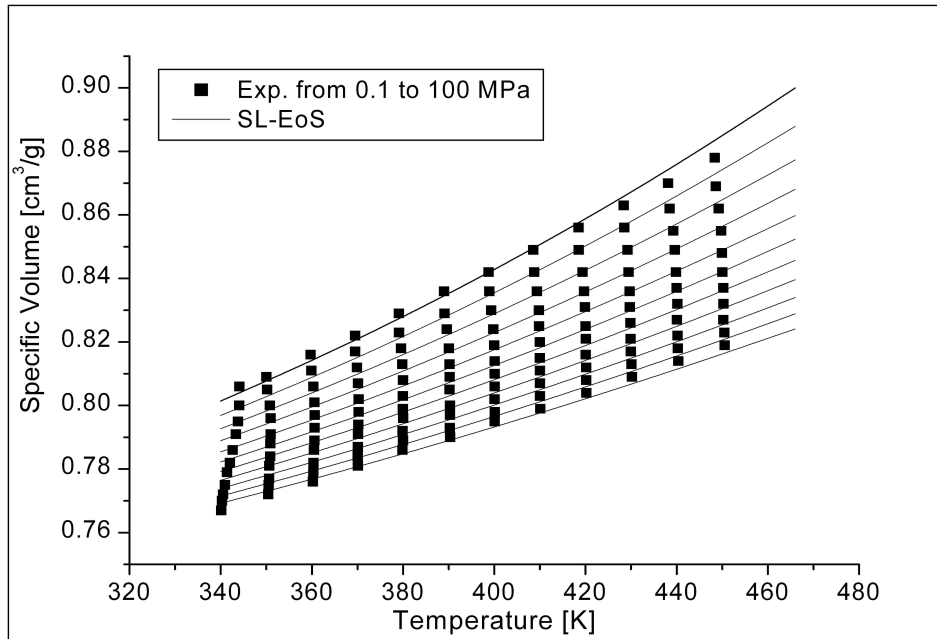
Fig. 3.2   PVT data of amorphous PLA, courtesy of Prof. Mensitieri. Università di Napoli Federico II and the results of the Sanchez Lacombe Equation of State calculations. Isobars ranging from 0.1 to 100 MPa., in the temperature range 340 K – 450 K.

In the case of the amorphous P-(D) LA the regression procedure gave good results, providing an adequate representation of the thermal expansion of the polymer and of its isothermal compressibility. There are some discrepancies between experimental and calculated densities in the 340 K – 360 K range for the highest pressures isobars, but that conditions are really close to glass transition temperature, where the validity of the assumptions on which the Equations of State are based, is more questionable. The characteristic parameters of P-(D) LA for the Sanchez Lacombe Equation of State that have been obtained through the above mentioned regression procedure are listed in the following Table:

T* [K]	P* [MPa]	ρ* [kg/L]
594.1	531.8	1.383

Tab. 3.2   PDLA characteristic parameters for the Sanchez Lacombe Equation of State.

This values will be adopted for the liquid liquid equilibria calculations. At first it could be attempted to consider these parameters adequate for representing the volumetric behavior also of the PLLA, in the temperature region in which there is no crystalline phase and then the polymer can be regarded as amorphous. In fact, at first it could be possible to think that the differences between the two chiral forms of the lactides are not enough, to produce a significant effect on the configurations of the polymeric chains and thus on their volumetric behavior. Although this approach may seem reasonable, several differences between the behavior of mixtures containing PDLA and PLLA have been reported and even concerning their pure substance volumetric behavior, some differences can be recognized. Therefore a separate set of characteristic parameters for PLLA was retrieved by means of the above mentioned procedure.
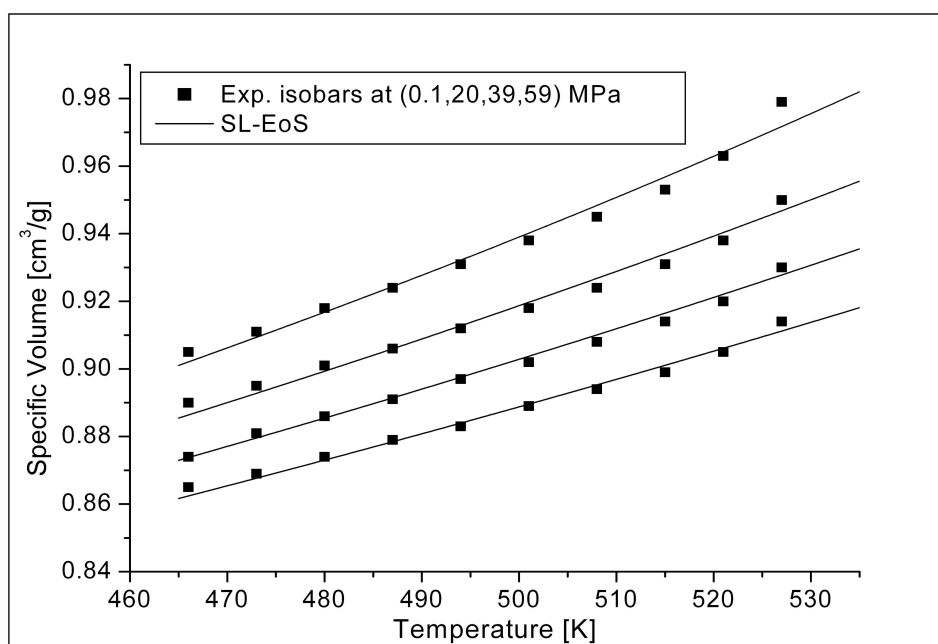
Fig. 3.3   PVT data of PLLA, from Zoller et al.[58], in a temperature range above the melting temperature, and the results of the Sanchez Lacombe Equation of State calculations. Isobars ranging from 0.1 to 59 MPa., in the temperature range 465 K – 525 K.

Also in this case the regression procedure gave really good results and no significant deviation between calculated and experimental values can be

detected. The characteristic parameters of PLLA for the Sanchez Lacombe Equation of State are listed in the following table:

T* [K]	P* [MPa]	ρ* [kg/L]
580.9	866.9	1.396

Tab. 3.3   PLLA characteristic parameters for the Sanchez Lacombe Equation of State.

While the characteristic pressure of PLLA is pretty different from the characteristic pressure of PDLA, the values of characteristic temperature and density of the two polymers are quite close each other.

3.4.   *Water -1,4 Dioxane and PLA mixture modeling with Sanchez Lacombe Equation of State*

The characteristic parameters of the Sanchez Lacombe Equation of State for water and 1,4 dioxane were available in the literature and are listed in the table below:

Substance	T* [K]	P* [MPa]	ρ* [kg/L]	Ref.
Water	670	2400	1.050	58[59]
1,4 – Dioxane	518.4	535	1.162	59[60]

Tab. 3.4   Water and 1,4 Dioxane characteristic parameters for the Sanchez Lacombe Equation of State

In order to perform the phase equilibria calculations required for comparing the predictions of the Sanchez Lacombe Equation of State with the available Vapor Liquid Equilibria experimental data that can be found in DECHEMA, an algorithm for bubble pressure calculations was implanted in Matlab®. This code

was validated against several dataset of Vapor Liquid Equilibria of simpler mixtures, such as the pairs hexane - octane and the pentane – hydrogen sulphide and was found to perform correctly. This code provided the base for developing all the other codes that were used for phase equilibria. The equality of chemical potentials was obtained through minimization of their squared difference, through the already mentioned non linear least square algorithm. For the sake of generality (with the ultimate goal of being able to use other thermodynamic models or modified versions of the Sanchez Lacombe Equation of State, for which could be difficult to write an explicit form of the chemical potential) the chemical potentials were evaluated numerically as derivatives respect to density of the single component of the Helmholtz Free Energy for unit of volume. The subroutine that evaluates the chemical potential works in a fully vectorized way, such that the code can be used for system with more than two species, without any relevant modifications. At each iteration, before evaluating the chemical potentials, the volumetric Equation of State is solved by Newton's method or by bisection algorithm (the choice is made automatically by the code if the Newton's method fails to find a suitable root with the internally provided guess). If multiple roots arises, only the one pertinent to the phase for which the evaluation is performed is retained.

It was found out that the Sanchez Lacombe Equation of State was unable to represent correctly the Vapor Liquid Equilibria of the Water – 1,4 Dioxane system at fixed temperatures. Moreover for some liquid phase compositions the algorithm was not able to converge to any solution of the phase equilibria problem. This difficulties were not removed even if the value of the binary interaction parameter was systematically varied. Experimentally it is found that liquid dioxane and water are completely miscible, so no miscibility gap should be predicted. Therefore it was decided to inspect directly the shape of the Gibbs Free Energy of Mixing function of the liquid mixture, in order to ascertain if a change in concavity was taking place. In fact it is well known that phase stability criteria[1] requires that a single phase is stable (and thus the species are

miscible) only if $\left(\dfrac{\partial^2 \; \Delta G_{mix}\big/RT}{\partial \omega_1^{\;2}} \right)_{T,P} > 0$ for every composition, while if for a given

range of composition $\left(\dfrac{\partial^2 \; \Delta G_{mix}\big/RT}{\partial \omega_1^{\;2}} \right)_{T,P} < 0$, then there will be a miscibility gap:

mixtures of composition comprised in the interval in which the curvature is negative are not stable and will form two separate liquid phases. Goates[48] reported a set of data of Excess Free Energy for the water – 1,4 dioxane mixture at 298 K, obtained through the experimental measurement of heats of mixing and freezing point. The heats of mixing were measured through a calorimetric device, while the freezing points determinations were made by cooling curves of mixtures of known composition. Partial molar enthalpy were calculated from the heat of mixing data, activity coefficients were obtained by the freezing data and reported to 298 K by means of the above mentioned partial molar enthalpy. In this way it was possible to estimate the Gibbs Free Energy of the mixture, that is found to have positive curvature, as it is expected for a system that does not exhibit miscibility gap. The Gibbs Free Energy of Mixing of the mixture, based on the experimental data of Goates is plotted in Fig. 3.4, along with the values calculated with the Sanchez Lacombe Equation of State model. It is easy to recognize that even with pretty high (or low) values of the binary interaction coefficient $k_{w.diox}$, there is a huge region in which the curvature is negative and thus the model will wrongly predict the coexistence of two liquid phases. Mannella et al.[53] have shown that this very same incorrect behaviour is predicted by several sophisticate activity coefficient models.
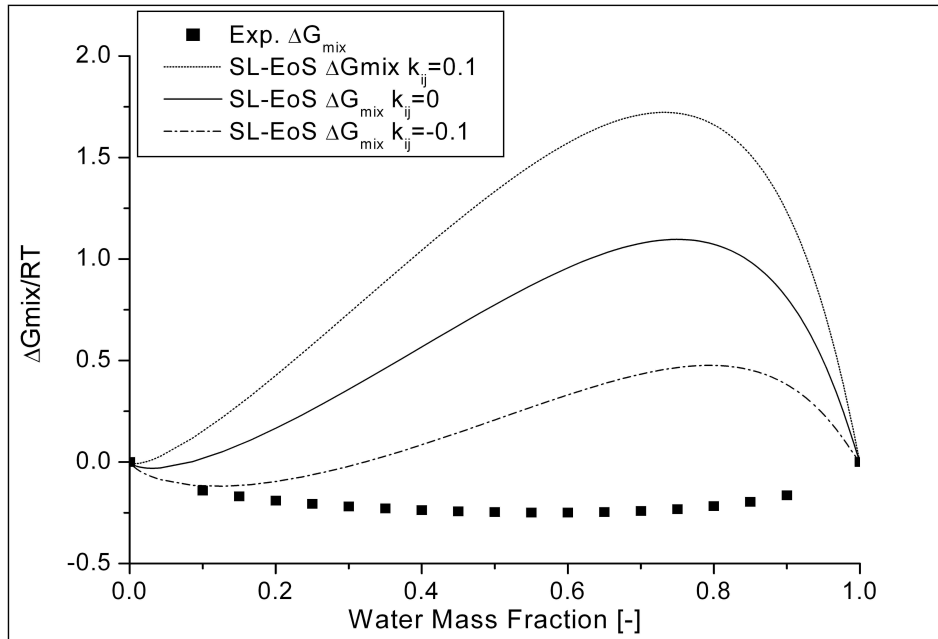
Fig. 3.4 Gibbs Free Energy of Mixing for the Water 1,4 Dioxane liquid mixture at 298K and 1 bar: comparison between the data reported by Goates[48] on the basis of calorimetric and freezing point measures and the Sanchez Lacombe Equation of State predictions.

For this multicomponent calculations, the mixing rules adopted for the Sanchez Lacombe Equation of State are those based on the characteristic pressure, with the combining rule $\Delta P *_{ij} = \sqrt{P *_i P *_j} \left(1 - ki_j\right)$. Thus the binary interaction coefficient acts directly on the value of the mixture characteristic pressure, as a term that proportionally increases or decreases its value, independently from the actual composition of the mixture. In the present case, this is not enough to provide a correct representation of the Gibbs Free Energy of Mixing, at least with the available characteristic parameters of the pure substances, that their widespread use in the literature should qualify them as reliable. It was decided to try to adopt a Non Quadratic Mixing Rule[27], modifying the combining rule in the following way: $\left(1 - k_{w.diox}\right) = 1 + \alpha_{w,diox} + \beta_{w,diox} x_w + \gamma_{w,diox} x_w^2$ were x_w is the water molar fraction. Through non linear least square regression, the best fit of the Gibbs Free Energy of Mixing was obtained with $\alpha_{w,diox} = 0.1026$; $\beta_{w,diox} = 0.1774$; $\gamma_{w,diox} = -0.0456$. The result is shown in Fig. 3.5.
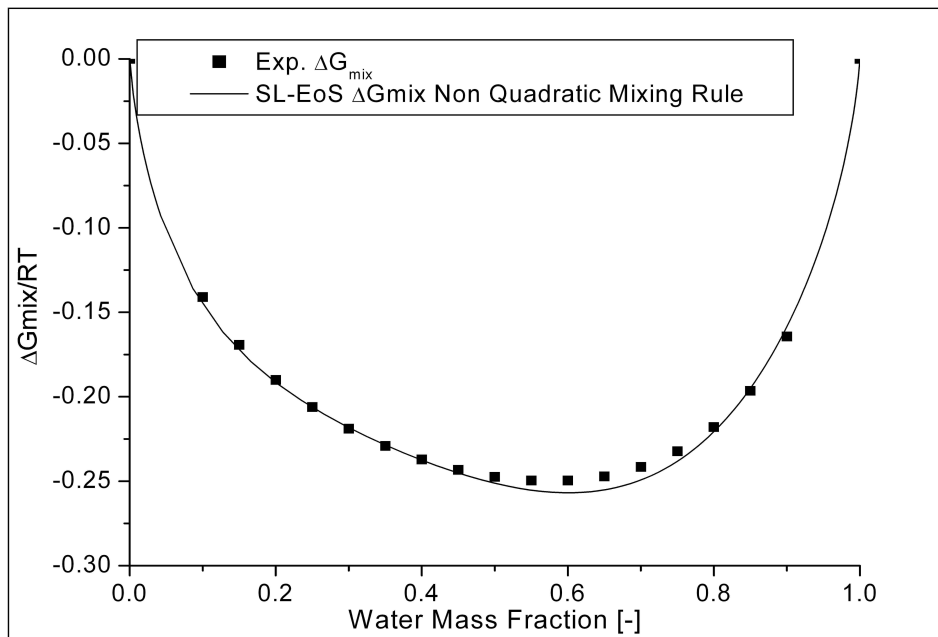
Fig. 3.5   Gibbs Free Energy of Mixing for the Water 1,4 Dioxane liquid mixture at 298K and 1 bar.

The Vapor Liquid Equilibria produced results that compared favorably with the experimental data reported in DECHEMA[49] for Vapor Liquid Equilibria at 308 K and 328 K. the azeotropic behavior and the proper number of phases seems to be predicted. A slight correction to the coefficient $\alpha_{w,diox}$ provided better results. The $\alpha_{w,diox}$ was set to $\alpha_{w,diox} = 0.1001$. Results are shown in Fig. 3.6.
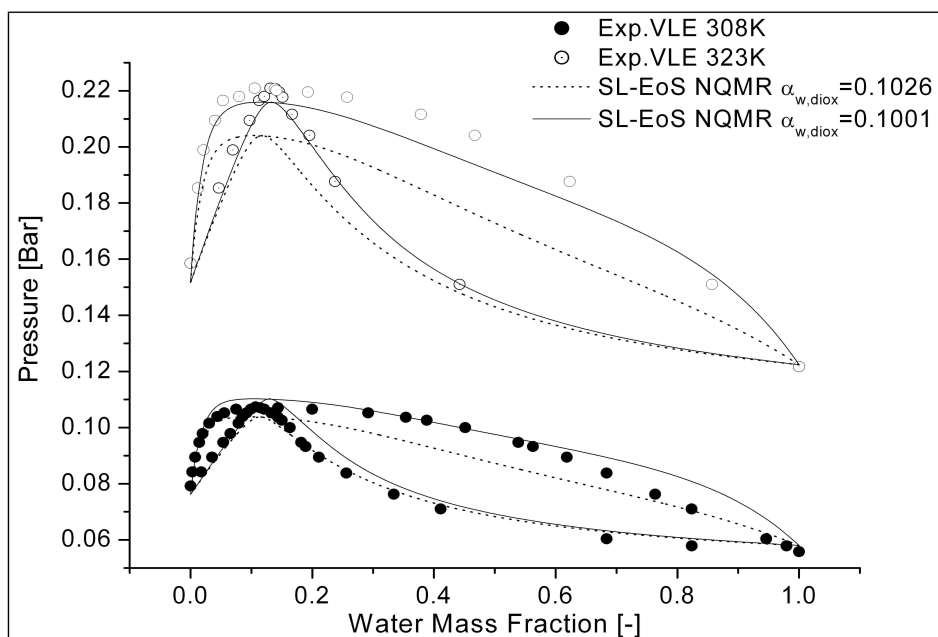
Fig. 3.6   Experimental Vapor Liquid Equilibria[49] for the water-1,4 dioxane system and their comparison with the results of the calculations done with the Sanchez Lacombe Equation of State with Non Quadratic Mixing Rules.

Prediction of the Liquid Liquid Equilibria of the system water- 1,4 dioxane and PLA was then attempted, trying to fit a set of cloud point data provided by Professor Brucato of the Università di Palermo, in the framework of an Italian national research project on the production of scaffolds, in which our research group was involved. The data are in the form of cloud point temperature as a function of the mass fraction of polymer in the liquid mixture, for a given ratio between water and 1,4 dioxane. Data for a water 1,4 dioxane ratio equal 13/87 and for a water 1,4 dioxane ratio equal to 14.5/85.5 were made available to us. Only the data for a water 1,4 dioxane ratio equal to 14.5/85.5 were modelled, setting $k_{w,PLA} = -0.069$ and $k_{diox,PLA} = -0.07$. It was not possible to fit the cloud point data for the water 1,4 dioxane ratio equal to 113/87, unless changing again the values of the binary interaction parameters. The results, in the form of the ternary Liquid Liquid Equilibria diagram at the temperature corresponding to cloud point data, are shown in Fig. 3.7. It is quite obvious that modelling this ternary equilibria with Sanchez Lacombe Equation of State can have only the limiting scope of correlating existing data and that due to the extensive tuning of

the model that has to be done, any extrapolation should be regarded as of dubious reliability.
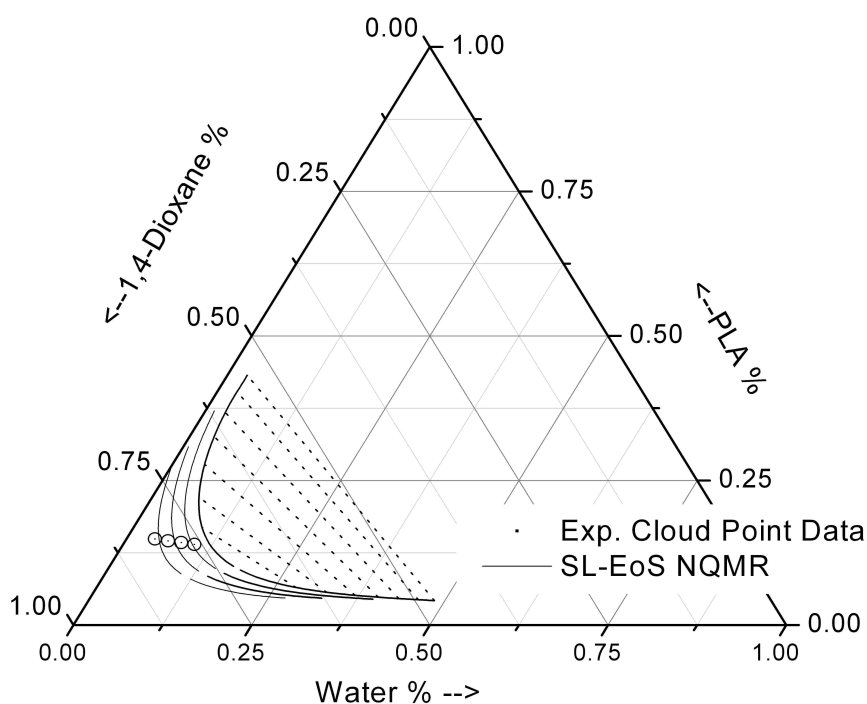
Fig. 3.7   Liquid Liquid Equilibria for the water- 1,4 dioxane and PLA system at 317.75 K, 321.85 K, 325.75 K and 329.75 K, corresponding to the cloud point temperatures of liquid mixture with water 1,4 dioxane ratio equal to 14.5/85.5 and respectively, 4,6,8 and 10 % of PLA.

These results seems to suggest that the physical picture of the intermolecular interactions provided by the Sanchez Lacombe Equation of State is plainly inadequate for representing the behavior of the present mixture. In fact it was already cited that exist physicochemical evidences that water promotes induced association in the mixture, while 1,4 dioxane itself will not self associate, if pure. The Sanchez Lacombe Equation of State is not able to deal with that, as well as with any association phenomena. Its quite successfully use for representing pure substance properties of species like water or methanol is due to the fact that a proper choice of the parameters will force the model to fit the data, not due to an actual capability of modeling association. In fact, the quality of the predictions of the liquid water saturated density could be challenged.

3.5.   Pure Polymers Parameters for Perturbed Chain Statistical Associating Fluid Theory Equation of State

The Perturbed Chain Statistical Associating Fluid Theory Equation of State, developed by Gross and Sadowski[22-24], is a model that have been successfully applied in modelling phase equilibria of system that usually deeply challenge the capability of simpler model, such as associating and polar fluids like water containing systems, polymer-solvent systems even with association, carboxylic acids, alcohols and ethers and biological solutions[29, 61-63]. The possibility to use this model was granted during a visit to the Chemical and Biochemical Engineering faculty of the Technical University of Dortmund, in collaboration with the research group of the Professor Sadowski.

Parameters had been retrieved by means of an automatic regression procedure. Reasonably good agreement can be reached between PC-SAFT predictions and PDLA data, even if there is some shortcomings in the representation of the isothermal compressibility of the fluid. In the case of PLLA only the isobars at pressure lower than 200 atm $P < 200\ atm$ were fitted in an adequate way. At pressure higher that 200 atm the predicted isobars were substantially lower than the experimental data. In anyway since this shortcoming in description of compressibility effects at high pressure should not hinder the performance of the model in the TIPS applications, that are usually restricted to low temperature and atmospheric pressures.

The results of the regression procedure are shown in Fig. 3.8 and Fig. 3.9 and Tab. 3.5 lists the parameters that have been obtained.
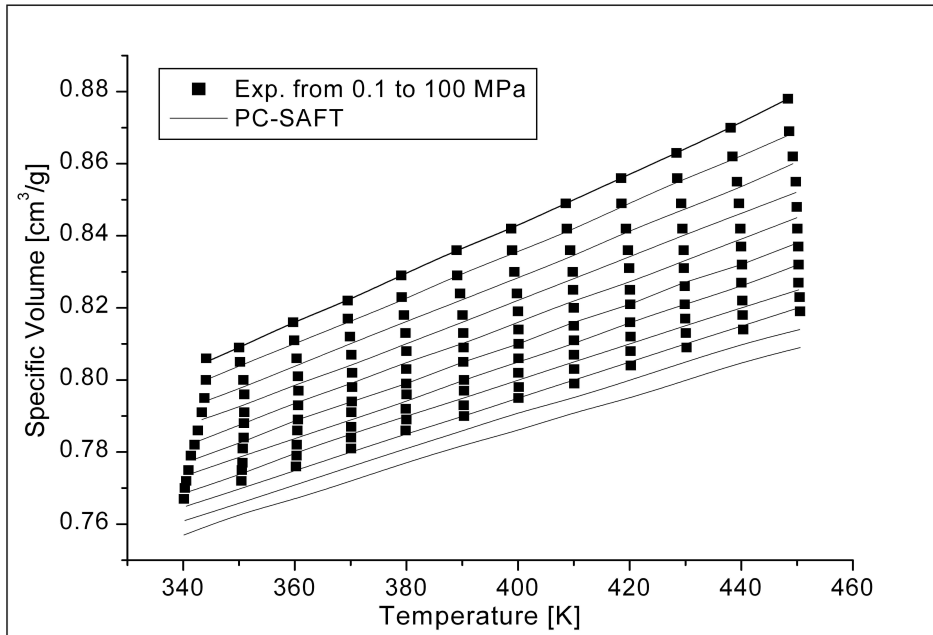
Fig. 3.8   PVT data of amorphous PLA, courtesy of Prof. Mensitieri. Università di Napoli Federico II and the results of the Perturbed Chain Statistical Association Fluid Theory Equation of State calculations. Isobars ranging from 0.1 to 100 MPa., in the temperature range 340 K – 450 K.
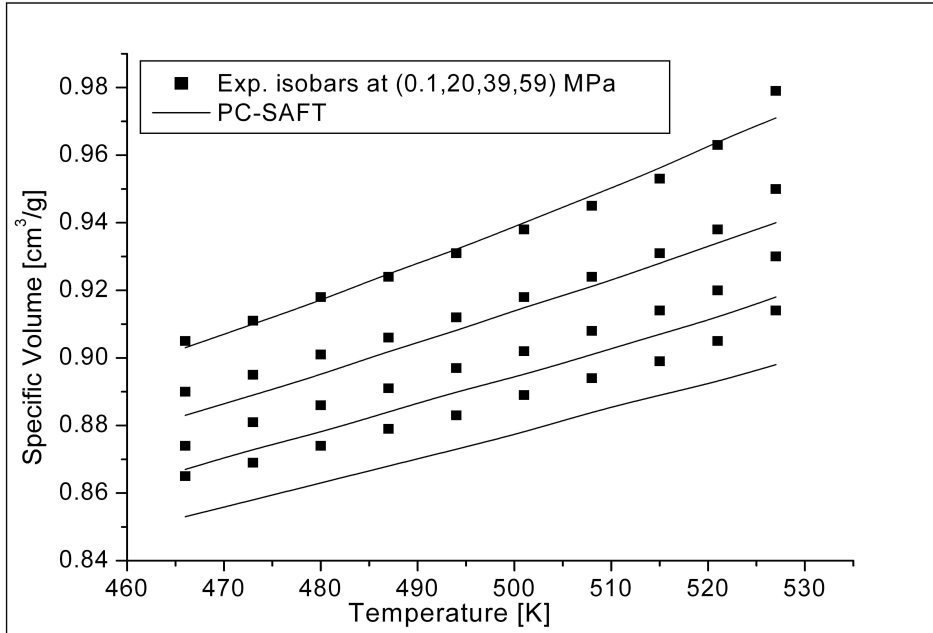

Fig. 3.9   PVT data of PLLA, from Zoller et al.[58], in a temperature range above the melting temperature, and the results of the Perturbed Chain Statistical Association Fluid Theory Equation of State calculations. Isobars ranging from 0.1 to 59 MPa., in the temperature range 465 K – 525 K.

PDLA Parameters			Units
Segment Number	m/M	0.0369972	[mol/g]
Segment Diameter	σ	3.0694	[Å]
Dispersion Energy	ε	222.6695	[K]

PLLA Parameters			Units
Segment Number	m/M	0.060134	[mol/g]
Segment Diameter	σ	2.5879	[Å]
Dispersion Energy	ε	192.879	[K]

Tab. 3.5   PDLA and PLLA characteristic parameters for the Perturbed Chain Statistical Association Fluid Theory Equation of State.

3.6.   Water -1,4 Dioxane pure substance and mixture modelling with Perturbed Chain Statistical Associating Fluid Theory Equation of State

Modeling the thermodynamic properties of the liquid water has been proven to be a hard challenge for many equation of state models, albeit successfully for others species, due to its peculiar hydrogen bonding. Gross and Sadowski have shown that PC-SAFT equation of state can accomplish this task with a 2 site association scheme, known as 2B scheme[23]. With the characteristic parameters of Gross and Sadowski the model is predicting very well both the vapour pressure of water and its condensed phase density, although with some deviation at low temperature, where the density anomaly of water takes place. Since biological applications are usually characterized by the need of an accurate representation of water properties and are restricted to the low temperature regime, Cameretti has later developed an approach to PC-SAFT modelling of water that overcomes the abovementioned low temperature difficulties in density modelling[61, 62]. According to Cameretti it is possible to

model the behaviour of liquid water at low temperature introducing a temperature dependent segment diameter:

3.2
$$\sigma^* = \sigma + t_1 \exp(t_2 T) + t_3 \exp(t_4 T)$$

Since TIPS processing of PLA – water-dioxane solutions take place at low temperature the set of characteristic parameters suggested by Cameretti will be used in this work and are listed in Tab. 3.6.

Water Parameters	Ref. 61, 62		Units
Segment Number	m/M	0.06687	[mol/g]
Segment Diameter	σ	2.7927	[Å]
	t_1	10.11	[Å]
	t_2	-0.01775	$[K^{-1}]$
	t_3	-1.417	[Å]
	t_4	-0.01146	$[K^{-1}]$
Dispersion Energy	ε	353.9449	[K]
Association Sites	N	2	[-]
Association Energy	$\varepsilon^{A_i B_j}$	2425.6714	[K]
Association Volume	$k^{A_i B_j}$	0.45090	[-]

Tab. 3.6 Water characteristic parameters for the Perturbed Chain Statistical Association Fluid Theory Equation of State.

Characteristic parameters of 1,4-dioxane have been obtained in this work by fitting simultaneously vapour pressure and density data several dataset available in literature[50-52].It has been assumed that dioxane's properties can be adequately modelled with PC-SAFT without association terms, taking into account only the dispersive perturbation to the plain hard chain term.

As shown in Fig. 3.10 and Fig. 3.11, the model performs adequately, predicting very well both density and vapour pressure, suggesting that the assumptions that had been done on the nature of the interaction between dioxane's molecules is physically sound. The characteristic parameters are listed in Tab. 3.7.
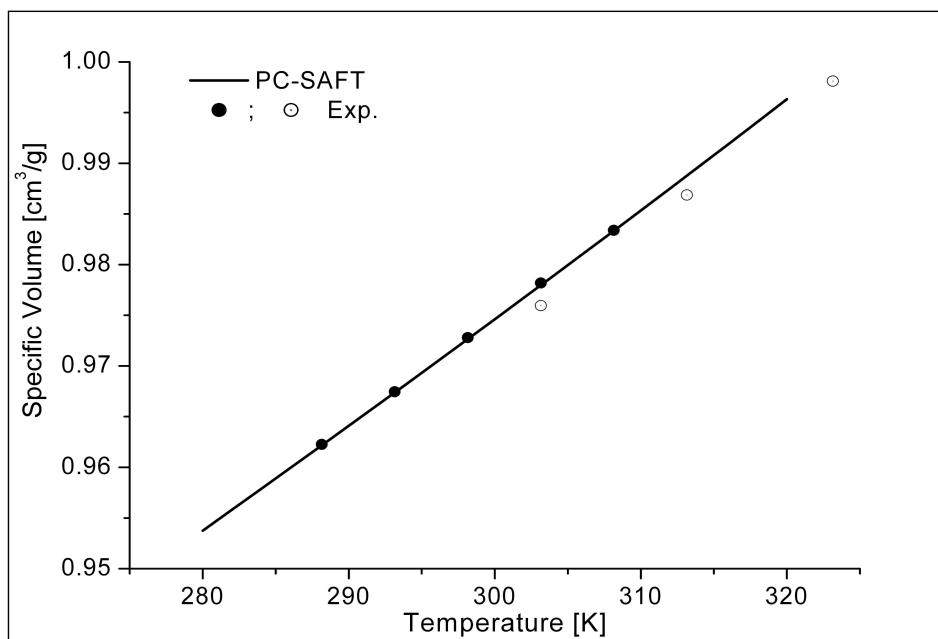
Fig. 3.10   Liquid density of 1,4 dioxane: experimental data from Papanastaslou et al.[52] (filled circles) and from Nayak et al.[51] (hollow circles) and comparison with the predictions of the Perturbed Chain Statistical Association Fluid Theory Equation of State.

1,4Dioxane Parameters			Units
Segment Number	m/M	0.032953	[mol/g]
Segment Diameter	σ	3.4006	[Å]
Dispersion Energy	ε	279.5928	[K]

Tab. 3.7   1,4 dioxane characteristic parameters for the Perturbed Chain Statistical Association Fluid Theory Equation of State.
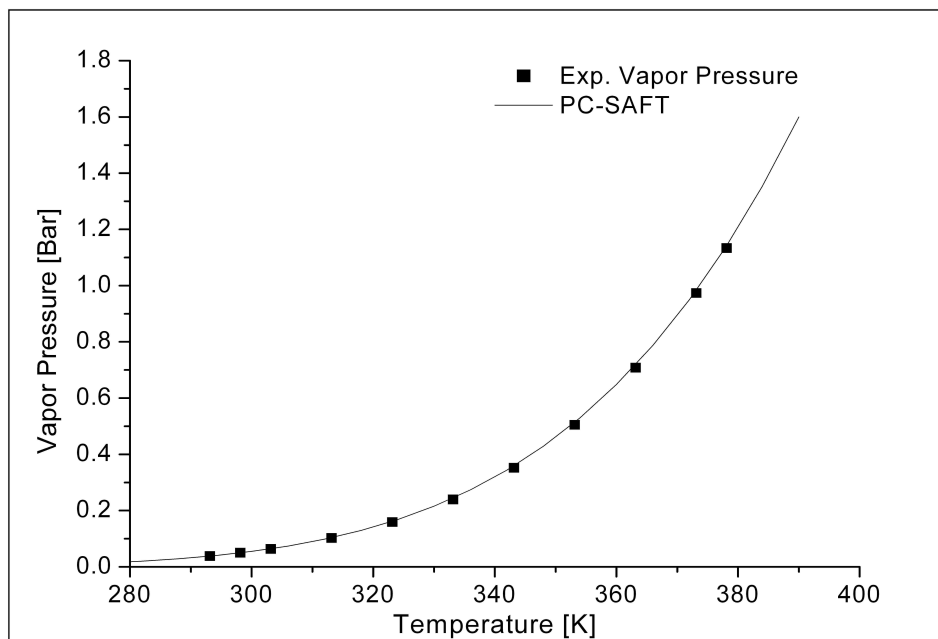
Fig. 3.11 Vapor Pressure of 1,4 Dioxane: experimental data[50] and comparison with the predictions of the Perturbed Chain Statistical Association Fluid Theory Equation of State.

Before attempting to model Vapor Liquid Equilibria of the Water – 1,4 Dioxane mixture, it is necessary to draw some considerations about the above mentioned induced association phenomena in polar mixtures. Associating components show self association under pure conditions, such as hydrogen bonding in water, while polar components does not give rise to temporary bonding by themselves. A mixture of polar and associating components will be characterized by self association of the associating components and by cross association between them and the polar species. The polar components hitherto manifest a behaviour, the aforementioned cross association, that is induced by the presence of the associating species in the mixture and has no parallel in the behaviour that the polar species manifests under pure component conditions. This fact pose a serious challenge to the application of the mixing rules suggested by Wolbach and Sandler, since there are no association energies $\varepsilon^{A_i B_j}$ and association volumes $k^{A_i B_j}$ that can be retrieved by analysis of the pure component behaviour. Guessing any value for those parameters will wrongly introduce self association, unless $\varepsilon^{A_i B_j} = 0$. This

problem could be overcome treating the association characteristic parameters of the mixture as fitting parameters, but this choice, although feasible, will boost the number of the adjustable parameters, deeply hindering the predictive capabilities of the model. A different approach, proposed by Kleiner[63], can be exploited assuming that the association energy parameter of the polar component is equally zero: $\varepsilon^{A_i B_j} = 0$ and that the effective volume of bonding is equal to the one of the associating component, considering this parameter as independent from the nature of the interaction itself. With this choice it is possible to see that no self association is introduced in the description of the interaction of the polar component, while induced association in taken into account, mimicking a "donor-acceptor" scheme. This approach has been proven to be physically sound in the work of Kleiner[63]. It was previously mentioned that there are experimental molecular structure data that suggest that water induced association takes place in the water 1,4 dioxane mixture, such that the energetic interaction between the molecules promote, at least in a certain composition range, the formation of water 1,4 dioxane clusters[55]. Thus this molecular picture suggest that interaction between water and dioxane takes place in such a way that is beyond the descriptive capabilities of the dispersion term alone, substantiating the hypothesis of an induced association mechanism. This is coherent with the fact that pure dioxane is described very well with dispersive interaction alone.

Adopting this induced association scheme, Perturbed Chain Associating Fluid Theory Equation of State can predict very well the Vapor Liquid Equilibria of the water – 1,4 dioxane mixtures, in the full range of compositions. The azeotropic behaviour, as well as the other features of the Vapor Liquid isothermal diagrams are well represented. Only a slight correction, that is obtained setting the binary interaction coefficient $k_{w.diox}$ equal to -0.061 is required. It must be observed that this slight correction affects only the dispersion term: the induced association scheme does not require any additional tuning. The results are shown in Fig. 3.12.
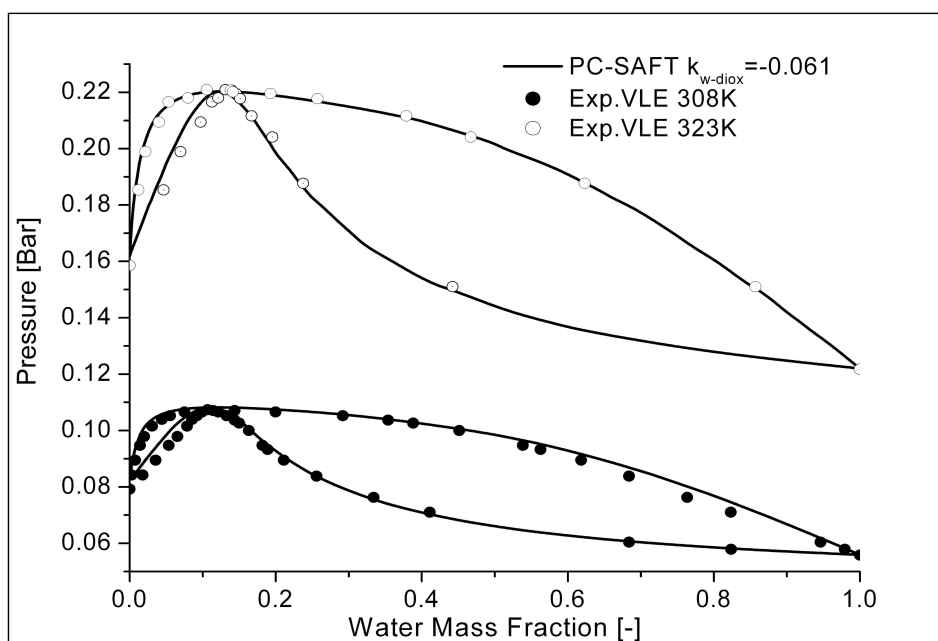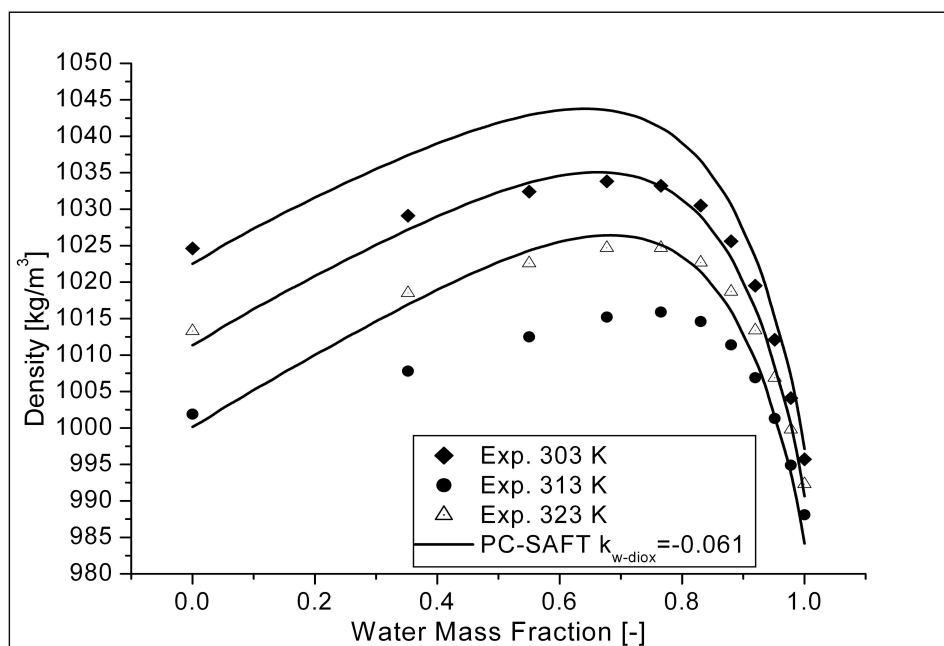
Fig. 3.12   Experimental Vapor Liquid Equilibria[49] for the Water-1,4 Dioxane system and their comparison with the results of the calculations done with the Perturbed Chain Statistical Association Fluid Theory Equation of State with the induced association scheme.

Comparison with liquid density data of the mixture[51] is less favourable, as the model overestimates the density of the mixture, although the qualitative shape of the curves resemble those of the experimental data and the maximum seems to take place at a composition close to the experimental one. The results of the calculation, as well as the corresponding experimental data are shown in Fig. 3.13. Adjusting the value of $k_{w,d}$ in order to fit the liquid mixture density data leads to a poor prediction of VLE, thus due to the higher confidence on the comparison with VLE, the value $k_{w,d} = -0.06$ $k_{w.diox} = -0.061$ was retained. The overprediction of the liquid mixture density could be blamed to a tendency of the induced association scheme to overestimate the strength of the induced association bonding, since the association characteristic energy is estimated directly from the value of the water, in a asymmetric donor-acceptor scheme.
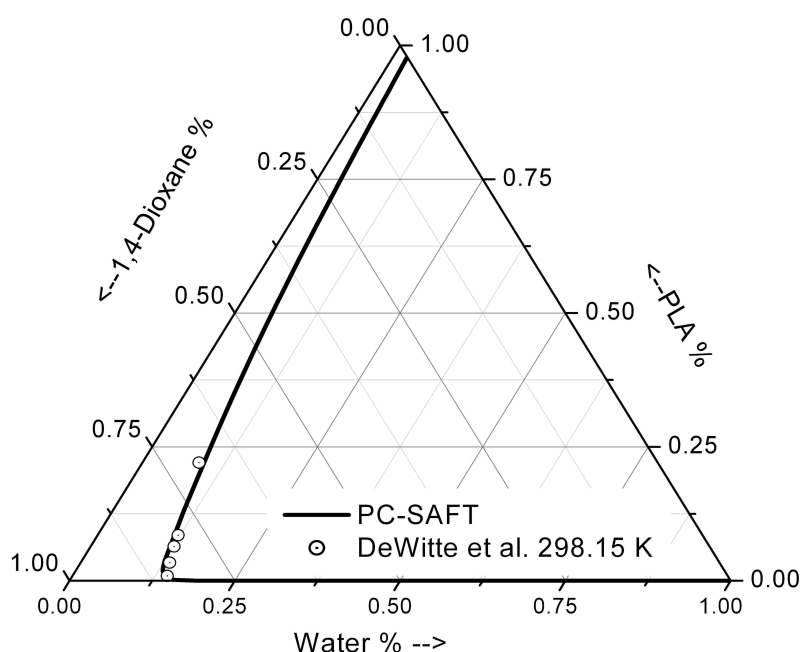
Fig. 3.13   Experimental Liquid Mixture Density[51] for the Water-1,4 Dioxane system and their comparison with the results of the calculations done with the Perturbed Chain Statistical Association Fluid Theory Equation of State with the induced association scheme.

3.7. Modeling of water – 1,4 dioxane - PDLA and water – 1,4 dioxane – PLLA ternary liquid liquid equilibria with the Perturbed Chian Statistical Associating Fluid Theory Equation of State

Corroborated by the ability of the model to provide a suitable representation of the thermodynamic properties of the water – 1,4 dioxane mixture, it was possible to proceed with the modeling of liquid liquid equilibria of the ternary mixtures that containing the macromolecular component. In fact, since the polylactides are completely soluble in the 1,4 dioxane, the role of water, that acts as anti solvent, should be dictated not only by its direct interactions with the polymer, but also by its ability to form clusters with 1,4 dioxane and thus a proper representation of that phenomena is necessary. In fact it could be speculated that   the antisolvent effect takes place not only because water and

polylactides have poor compatibility, as shown by the pure water solubility in PDLA, that according to the data reported in the literature[64] is in the range 0.005 ÷ 0.01 g/g$_{pol}$, but also because the 1,4 dioxane molecules that are clustered with water molecules are not anymore available for solvating the polymer. The model was found able to reproduce successfully the above mentioned cloud point data made available to us by Professor Brucato, but was also able to reproduce others set of cloud point data available in the literature, such as those of those of Witte et al.[54] and to model the ternary liquid liquid equilibria at fixed pressure and temperature diagram from Witte et al.[54] and of Tanaka et al.[65]. The results of this calculations are shown in the following Fig. 3.14, Fig. 3.15, Fig. 3.16 and Fig. 3.17. In the case PDLA it was required to set $k_{w,PLA} = -0.0935$ and $k_{diox,PLA} = -0.029$, while for the PLLA the binary interactions parameter were set equal to $k_{w,PLLA} = -0.078$ and $k_{diox,PLA} = -0.125$. The calculations were found to be independent from the actual value of the polymer molecular mass.

Fig. 3.14 Experimental Liquid Liquid equilibria[54] of the water-1,4 dioxane - PDLA system and their comparison with the results of the calculations done with the Perturbed Chain Statistical Association Fluid Theory Equation of State with the induced association scheme.
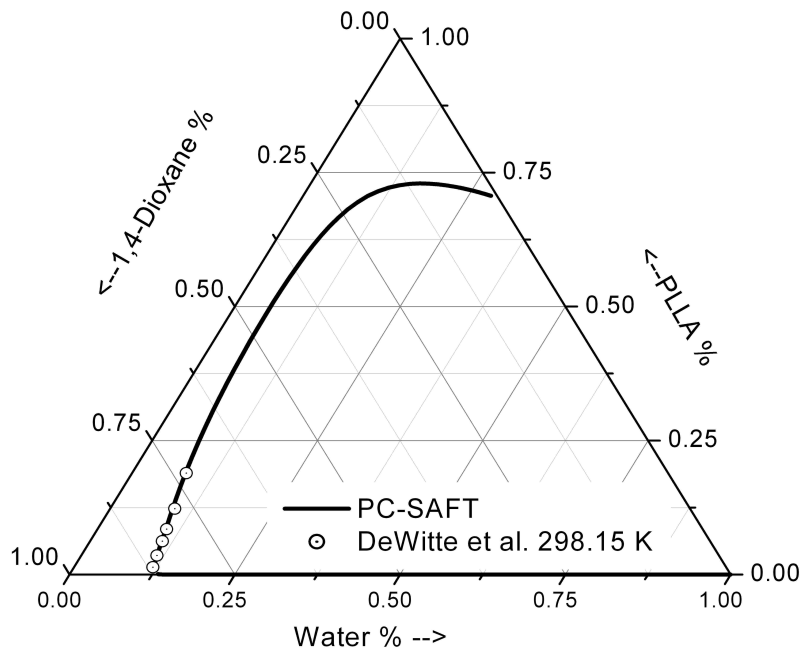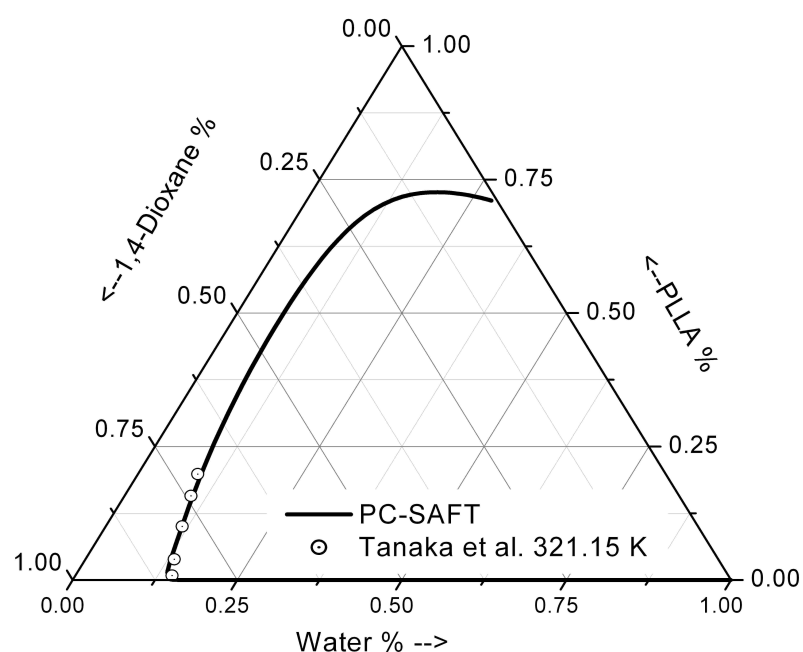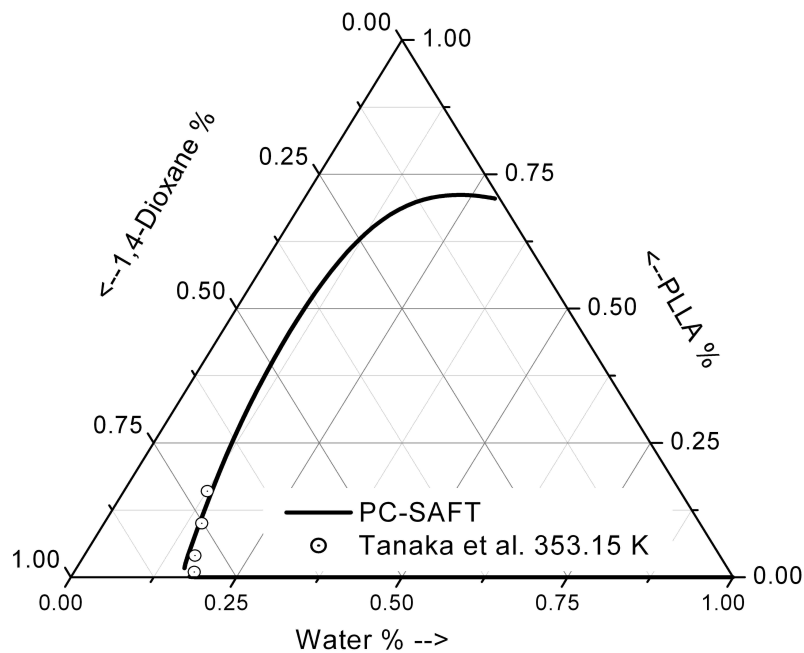
Fig. 3.15 Experimental Liquid Liquid equilibria[54] of the water-1,4 dioxane - PLLA system and their comparison with the results of the calculations done with the Perturbed Chain Statistical Association Fluid Theory Equation of State with the induced association scheme.

Fig. 3.16 Experimental Liquid Liquid equilibria[65] of the water-1,4 dioxane - PLLA system and their comparison with the results of the calculations done with the Perturbed Chain Statistical Association Fluid Theory Equation of State with the induced association scheme.

Fig. 3.17 Experimental Liquid Liquid equilibria[65] of the water-1,4 dioxane - PLLA system and their comparison with the results of the calculations done with the Perturbed Chain Statistical Association Fluid Theory Equation of State with the induced association scheme.

The calculations are in really good agreement with the available experimental data of the ternary system. The only remark is that the prediction of the liquid water solubility in pure PLLA, that is the value that can be read on the PLLA axis of the ternary diagram, seems to be quite high respect to the values that can be found experimentally, even if they are measured on a glassy, semicrystalline polymer. In fact, liquid sorption experiments conducted on a sample of semicrystalline PLLA at 308K suggest that liquid water solubility in PLLA is around 0.011 g/g_{pol}.

3.8.   Concluding Remarks

The Sanchez Lacombe Equation of State has been found to be unable, per se, to provide an adequate representation of the binary system water- 1,4 dioxane, while application of a non standard, non quadratic mixing rule has made

possible to deal with this challenging system. Application to the ternary system is possible, but of doubtful efficacy and with a notable loss of extrapolation capability.

Perturbed Chain Statistical Associating Fluid Theory Equation of State, albeit some lack of quality in the representation of the high pressure behavior of the pure polymers, have been shown to be a powerful and flexible thermodynamic tool, adequate for addressing the issue of challenging systems, like those that exhibit solvent- antisolvent effects on the macromolecular component.

4. Experimental Characterization of Vapors and Liquids Sorption in Glassy and Rubbery Polymers

4.1. Introduction

The sorption and the desorption of low molecular weight species, in the liquid or in the vapor form, in a polymer, plays a major role in many industrial process and applications, as well as in the field of drug delivery, in the development of sensors and in the drying of paint and coatings. Actually this list is quite arbitrary and not exhaustive of all the possible situations that are encountered in practice. In the above mentioned examples, it is always required to know, or at least to estimate, how much of the penetrant species will get inside the polymer phase and how much time will be required before equilibrium (or pseudo equilibrium) conditions will be attained. For example, a membrane separation device can be used for recovering an high valued component from a stream in which the component is mixed with many others only if the permeability of the desired component in the polymer of the membrane is higher than the permeability of the other species[66]. Permeability of a low molecular weight component is given by its diffusivity and its solubility in the polymer that makes the membrane. In the case of drug delivery, the solubility of the molecule that exerts the pharmacological activity in the polymeric matrix that forms the pellet

that will be ingested by the patient, will dictate the maximum loading of the pellet itself. On the other hand, diffusivity will dictate the drug release rate and, ultimately, its concentration in blood and thus, along with its half life time, the effective pharmacological activity[67]. Finally, in the case of the drying of a polymeric coating, solubility and diffusivity of the solvent in the polymer will dictate the drying time, and will affect the appearance of coating defects. In fact, most of the defects arise due to the development of internal stresses, upon frustrated shrinkage, during the drying process[68-71].

In this chapter, data concerning vapor and liquid solubility in glassy and rubbery polymers will be presented and discussed. The polymer – penetrant pairs considered for sorption in glasses are of interest for applications like gas and vapor separation, organic solvent nanofiltration[72], polymer processing and sensor development. The polymer – penetrant pairs considered for sorption in rubbers are relevant to membrane separation process for aroma and nutriceuticals recovery, as well as for food processing[73-76].

The question about how much of the penetrant component will be taken up by the polymer is answered by the thermodynamic. For the given activity value of the penetrant, its solubility in the polymer phase arise from the phase equilibria conditions or, if the polymer phase is glassy, from pseudo equilibrium considerations. The equilibrium is attained between the components of the liquid or of the vapor phase outside the polymer and the same low molecular weight species that in the polymer phase form a mixture with the polymer itself. Since polymers are commonly used and characterized in the form of dense phases, in which the low molecular weight species can diffuse, the question about how much time is required, is answered by the kinetic of the diffusion process itself.

For pure vapor sorption, it is customary to represent the solubility as a function of the pressure of the penetrant, or as a function of its thermodynamic activity, that can be regarded as the ratio between the actual pressure and the vapor

pressure of the component, at the same temperature. The data measured at various pressures (or activities) and at fixed temperature will be collected in the same set, known as a sorption isotherm. The solubility of the pure liquid can complete that set, providing the value at unit activity. In the case in which the penetrant can actually behave like a solvent for the macromolecular component, the solubility of the liquid cannot be measured. For mixtures of liquids it is useful to represent the solubility data, at fixed temperature, as a function of the composition of the external liquid phase.

It is useful to recall the fact that the kinetic of diffusion in simple systems can be modeled by means of the so called Fick's law[6, 77]. This law provide a constitutive equation for the mass flux, that is regarded to be simply proportional to the concentration gradient of the diffusing component itself, in close analogy to Fourier's law for heat flux. In terms of concentration, the mass conservation equation in local form, for a plane sheet of thickness 2δ, is a parabolic partial differential equation, that along with its initial and boundary conditions, can be written as:

4.1
$$\begin{cases} \dfrac{\partial C}{\partial t} = D\dfrac{\partial^2 C}{\partial x^2} \\ C(x,0) = C_0 \quad \forall x \\ C(\delta,t) = C_i \quad \forall t \geq 0 \\ \left.\dfrac{\partial C(t)}{\partial x}\right|_{x=0} = 0 \quad \forall t \geq 0 \end{cases}$$

The problem has been stated assuming that at $t < 0$ the concentration of the penetrant is equal to the initial value C_0, that at the beginning of the sorption experiment the concentration at the boundary is suddenly rose to the value C_i , that will then held constant, and that the middle plane of the slab is a symmetry plane and thus the mirror condition $\dfrac{\partial C}{\partial x}$ can be applied. It is useful to note that the very same formulation can be used to describe diffusion process in a

supported film of thickness δ, if the support is not permeable to the penetrant. The solution of this initial and boundary conditions problem is the function $C(x,t)$ that satisfy the partial differential equation of the local mass balance. The solution describe the evolution of the concentration profile inside a system that obeys the assumptions of the Fick's law. Unfortunately, the actual concentration profile is not a property that can be directly characterized in the commonly performed sorption experiments, since rather complicate apparatus are required and suitable choices of the penetrant polymer pair need to be selected, as done, for example in the work published by Long and Richmann[78, 79]. The property that usually is directly or indirectly measured is the mass uptake in the polymer sample. The sorption experiment is considered finished when the mass uptake $M(t)$ is no longer changing with time. That steady state value is usually indicated as M_∞ and it is customary to express the mass uptake in a relative form, as $\dfrac{M(t)}{M_\infty}$. The mass uptake $M(t)$ can be readily obtained by integrating the concentration $C(x,t)$ respect to the spatial variable: $M(t) = 2A\int_0^\delta C(x,t)dx$. The solution $C(x,t)$ is available in the literature and can be obtained through the standard methods of the variable separation and is in the form of a series of exponential and trigonometric terms. The integrated form of the series can be written as[77]:

4.2
$$\frac{M(t)}{M_\infty} = \left[1 - \sum_{n=0}^{+\infty} \frac{8}{(2n+1)^2 \pi^2} \exp\left(-\frac{(2n+1)^2 \pi^2 tD}{\delta_2} \right) \right]$$

The mass uptake that is calculated from this formula is proportional to $\sqrt{t}$, for small value of t, then at larger value of the time variable a constant value is reached, as shown in the Fig. 4.1. Whenever the experimental mass uptake was found to follow the same behavior, the system was defined as Fickian and the diffusivity D of the penetrant-polymer pair was retrieved by means of regression on the experimental data.
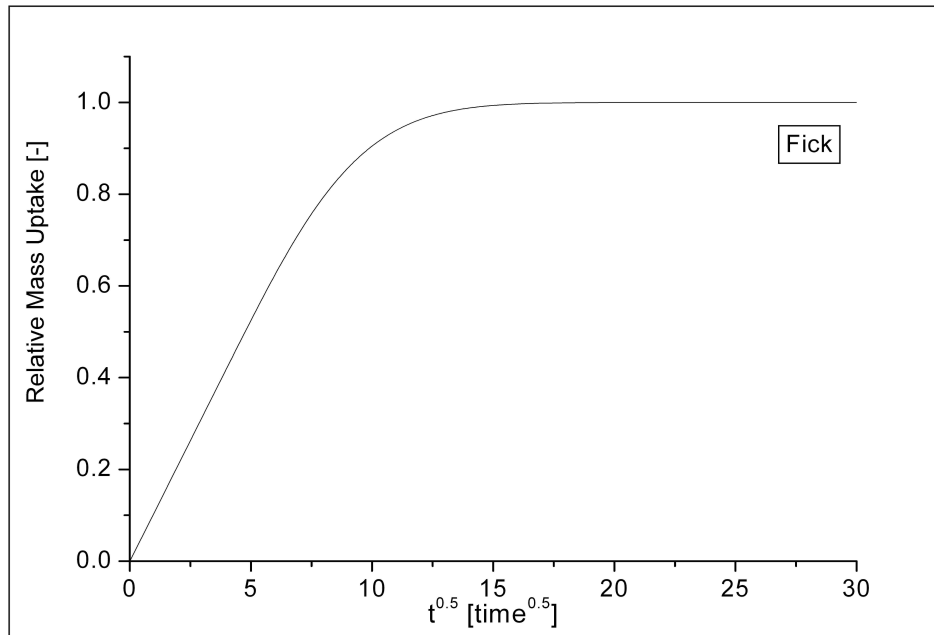
Fig. 4.1   Mass sorption kinetic as calculated by the Fickian Model.

For both of the above mentioned factor, namely solubility and sorption kinetic, it is necessary to mention the differences that arise between the behavior that is commonly observed when the polymer is a rubber or a melt, and the peculiar behavior of polymeric glasses.

In fact, rubbers or polymeric melts are condensed phases that behave, at least respect to their volumetric properties, just like a liquid. It is commonly accepted that, upon changes of pressure and temperature (and composition as well), rubbers or melts will experience a change in volume that can be described by a volumetric equation of state. That, as already noted, applies only to equilibrium states. Rubbers and melts can be regarded as equilibrium phases, even if the huge molecular weight of their chains could certainly slow the kinetic of the equilibration processes, respect to those observed in low molecular weight liquids[80].

The shape of sorption isotherms of low molecular weight penetrants in rubber is characterized by a positive curvature, with upward concavity, as shown in Fig.

4.2, while it is usually expected that the sorption kinetic is well represent by the Fickian kinetic, previously shown in Fig. 4.1.
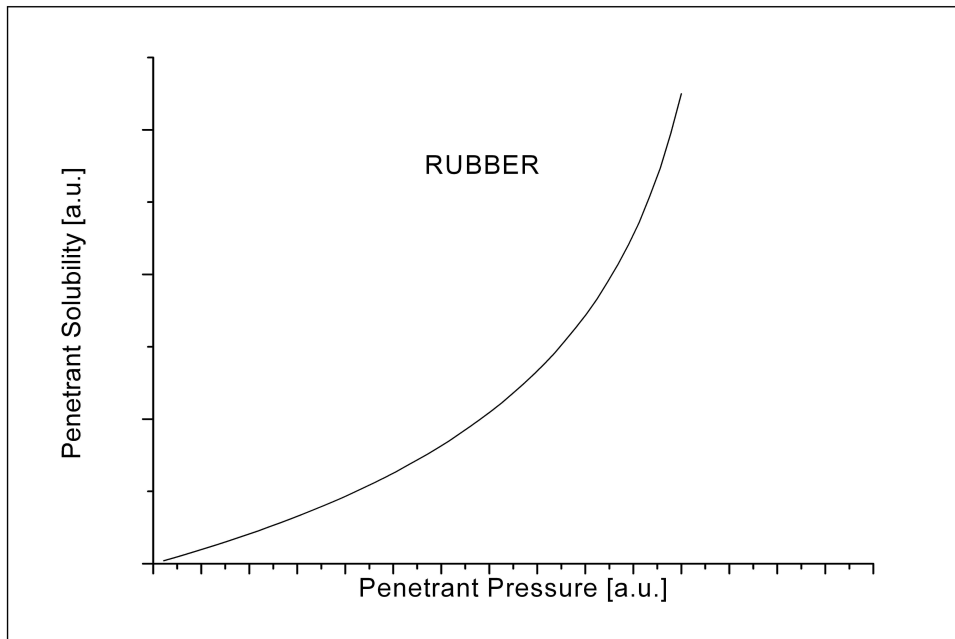
Fig. 4.2   Characteristic sorption isotherm of low molecular weight species in rubbers.

Glassy polymers are non equilibrium phases in which the evolution toward the equilibrium condition is hampered by the really slow kinetic of the molecular motions. It is a matter of fact that a temperature exists, known as glass transition temperature, below which the departure from equilibrium begins and the glassy behavior start to be evident. Below glass transition temperature the polymer exhibit elastic behavior, with elastic modulus even some order of magnitude higher than that of rubbers, it is usually regarded as a tough material and can be brittle. The glassy phase is amorphous, not ordered and the above mentioned rise of high elastic modulus is to be regarded as the effect of the kinetic hindrance of the relative motions between chains. It is commonly stated that below glass transition temperature only local motions of the chains' segments are allowed and no motion of the center of mass of the chain is allowed: self diffusivity of the macromolecular species is close to zero, under glassy conditions. One of the most relevant property of the glassy phases is that

their density is lower than the equilibrium value: there is an excess free volume, that is due to the fact that the chains are not able, due to the above mentioned kinetic constraints, to pack in the configurations that satisfy the minimum condition for the Gibbs Free Energy[80]. Since the glassy state in a non equilibrium state that is retained only due to the really slow kinetic of the equilibration process, the system could still evolve with time, even if it could not be able to reach, in a time compatible with experimental observation, the equilibrium itself. It is a matter of fact that the properties of some glassy polymers change along time in a measurable way: this phenomena are regarded as physical ageing and are commonly believed to affect directly the volumetric properties of the system. Thermal treatment, such as high temperature annealing, could accelerate that phenomena, eventually bringing the system toward a different non equilibrium conditions, that could be regarded as more prone to evolve. Similar results, obtained through prolonged storage of the sample under a controlled atmosphere (i.e. in CO2 at high pressure) or in liquids had been reported in literature[81-87]. Above glass transition temperature, the system behaves like a rubber or a melt. The glass transition temperature is affected by pressure, presence of other species (especially low molecular weight species that can act as plasticizer) and by the cooling rate at which the polymer is cooled from the temperature at which it was originally held as a rubber.

The shape of the sorption isotherms of low molecular weight penetrants in glassy polymers is characterized by a downward concavity, as shown in Fig. 4.3. It is commonly assumed that this behavior can be somewhat explained by the assumption that the total sorption is a sum of two different contribution: the first, known as Henry contribution, accounts for a solubility term proportional to the penetrant's pressure, as it happens for many gases in liquid and solid equilibrium phases, while the second contribution, known as the Langmuir contribution, is thought to be related to the adsorption of the penetrant molecules inside the excess free volume, that is present in the glassy state. This empiric interpretation is at the base of the so called Dual Mode model[88],

that albeit non predictive, has been shown to be a reliable correlation tool for sorption in polymeric glasses. Since glassy state is a non equilibrium state, solubility and sorption isotherms can be influenced also by the history of the sample and by the specific operating conditions. For instance it is well kwon that cycles of sorption and desorption could lead to isteresis effects and that annealing and other thermal pre-treatments can exert a deep influence as well. Regarding to the mass uptake kinetic, there are many possible behaviors that arise due to the specific pair of polymer and penetrant, as well as due to the characteristic of the sorption experiment. In fact, the behavior could be completely described by the Fickian kinetic, such as for many light gases in glassy polymers. But if the penetrant exerts a significant swelling or even plasticizing action on the glassy matrix, different behavior could arise and deviations to the Fickian kinetic could be observed. For example, after an initial Fickian sorption, in which the mass uptake is proportional to $\sqrt{t}$, relaxation process could take place and the mass uptake could start to drift slowly toward an higher value. In other cases, a sigmoidal shape of the kinetic could be observed. In some case the mass uptake could be straight proportional with time. In fact, an empirical way to classify sorption kinetics is to look at the value of the exponent of the curve t^n to which the mass uptake is proportional. The actual sorption kinetic depends to a great extent on the ratio between the characteristic time of the relaxation processes (the time required for the local rearrangements of the chains) and the characteristic time of the diffusion process. When relaxation processes take much longer than diffusion, or when relaxation processes are much quicker than diffusion, the usual Fickian behavior could be observed, at least in the initial portion of the mass uptake curve. When the relaxation characteristic time and the diffusion characteristic time are quite similar or separated by only few orders of magnitude, both processes take place simultaneously and great deviation to the Fickian behavior could be observed at all the stages of the sorption process. It should be noted that the amplitude of the activity jump that is applied to the sample plays a relevant role in determining the kinetic of the sorption process. An extensive

introduction and to some extent classification of this phenomena could be found in the works by Sanopoulou[89-91] and Petropoulos[92].
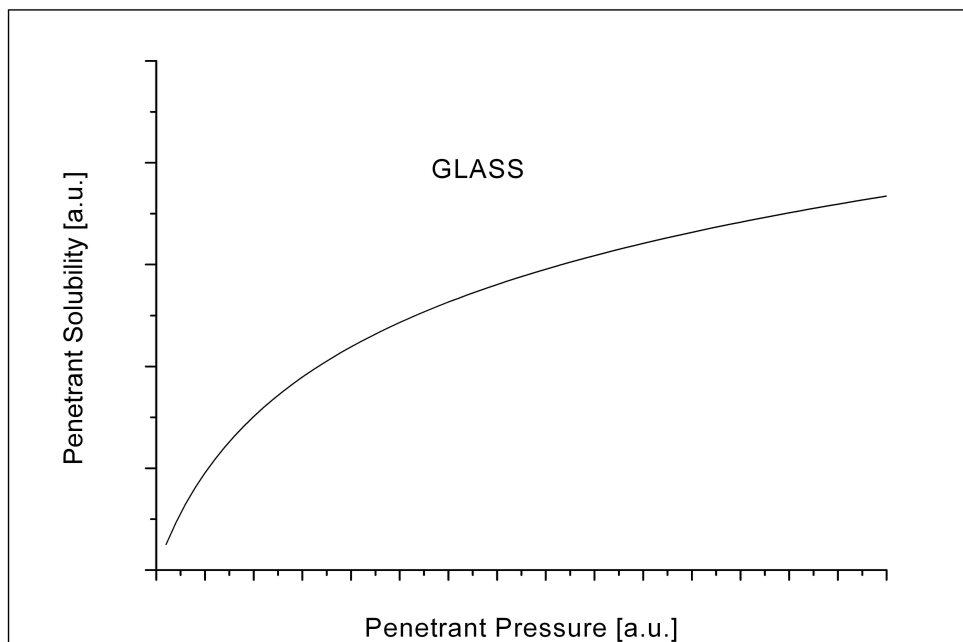

Fig. 4.3   Characteristic sorption isotherm of low molecular weight species in glasses, without plasticization effects.

It is interesting to note that, when the penetrant is a solvent for the polymer itself, or at least has a large plasticizing effect, it is possible that, along with sorption process, the glass transition process takes place. If this is the case, it is possible to have sorption isotherms, known as sigmoidal isotherms, that exhibit a marked change in curvature, or that the increase in mobility of the polymer chains that is promoted by the solvent itself deeply affect the kinetic of the sorption process.

4.2.   Quartz Spring Apparatus

The Quartz Spring Apparatus[93] is a gravimetric device that can operate sorption measurements of vapors in dense polymer films, at pressure below the

atmospheric value. The sample is hanged to the quartz spring, along with a metallic reference and are kept inside a glass column that is connected to a system of pipes and vessels that can be used to vaporize the penetrant and to control its pressure, in order to expose the sample to the desired vapor activity. The glass column is surrounded by a water jacket that provide the necessary temperature control. The water is circulated by means of a magnetic pump and its temperature is adjusted by means of a thermostatic bath. With this setup the temperature can range from 5 °C to 50°C. The glass column and the ancillary vessels can be completely evacuated by means of a vacuum pump. Upon exposure of the sample to the vapor, its weight will start to increase, due to the sorption process that is taking place. The elongation of the spring is continuously monitored and registered in digital form by means of a CCD camera and the weight change of the sample is then collected for all the phases of the vapor sorption experiment. The metallic reference is of known size and it provides the conversion factor between pixels and millimeters, required for estimating the weight from the elongation, by means of the spring constant. Quite high activity values can be reached, but care must be taken to avoid condensation on cold spot and excessive weight gain, since it could happen that the weight of the sample exceeds the maximum load of the spring. The lay out of the apparatus is shown in Fig. 4.4.
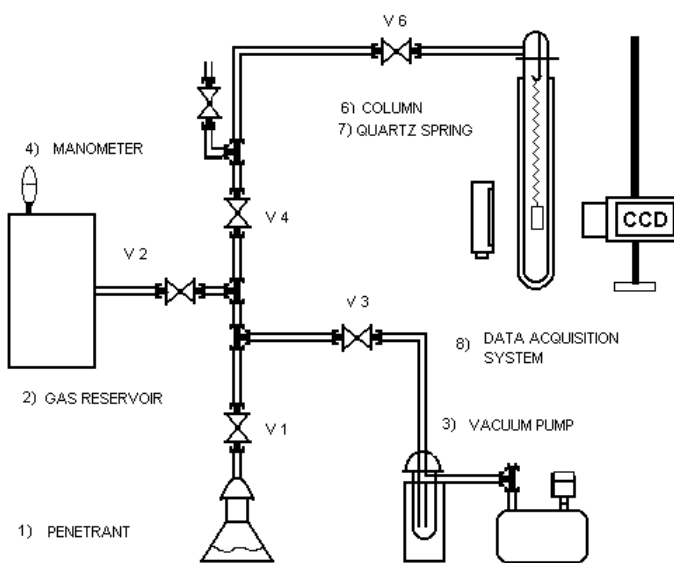
Fig. 4.4   Layout of the Quartz Spring Apparatus

The sorption experiments performed with the Quartz Spring Apparatus are usually differential sorption experiments, in which the vapor activity is raised, step by step, collecting the mass uptake and thus the solubility data at each of the activity value. Before increasing the vapor activity enough time is waited to ensure that equilibrium or pseudo equilibrium conditions have been reached.

4.3.   *Quartz Crystal Microbalance*

The Quartz Crystal Microbalance[94] is another kind of gravimetric vapor sorption measurement device in which the mass uptake during the sorption step is retrieved by means of the change in the natural frequency of oscillation of an electric resonator that is coated with the polymer. In fact, the change of the weight of the polymer will affect the oscillation properties of the resonator, according to the so called Sauerbrey law. The polymer is coated on the electrode of the quartz crystal, shown in Fig. 4.5, by means of a spin coater, in order to have a really thin and homogeneous film.
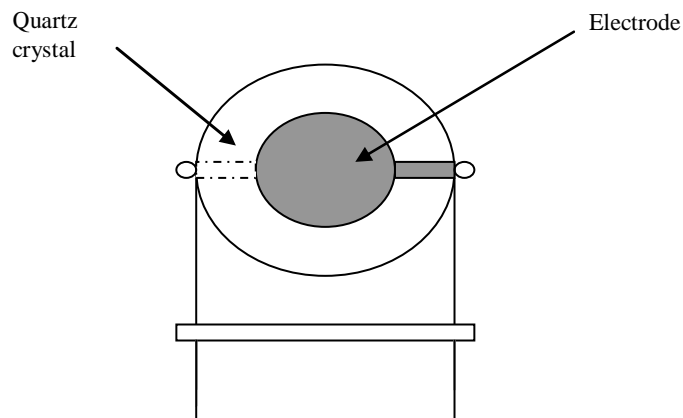
Fig. 4.5   The resonator used in the Quartz Crystal Microbalance.

The Quartz Crystal is hosted in a metallic vessel and is provided with piping and ancillary vessels similarly to those of the Quartz Spring Apparatus, in order to control the activity of the vapor to which the sample is exposed. Temperature control is achieved keeping the entire apparatus immersed in a thermostatic bath that allows to operate at temperature comprised between ambient temperature and 50°C. Also this apparatus is used f or running differential sorption experiments.

4.4.   *Pressure Decay Apparatus*

The Pressure Decay Apparatus[95] is used for performing gas and vapor sorption measurements on the base of the principle that the sample is kept in a calibrated volume comportment and exposed to an initially known vapor pressure. The compartment is sealed and the change in pressure that is measured in the compartment during the sorption step can be used to estimate the residual number of moles in the gas phase, by means of a suitable equation of state for the gas, and ultimately to evaluate the sample mass uptake. The scheme of the Pressure Decay Apparatus is shown in Fig. 4.6. The entire apparatus is hosted inside an incubator, that proved temperature control from

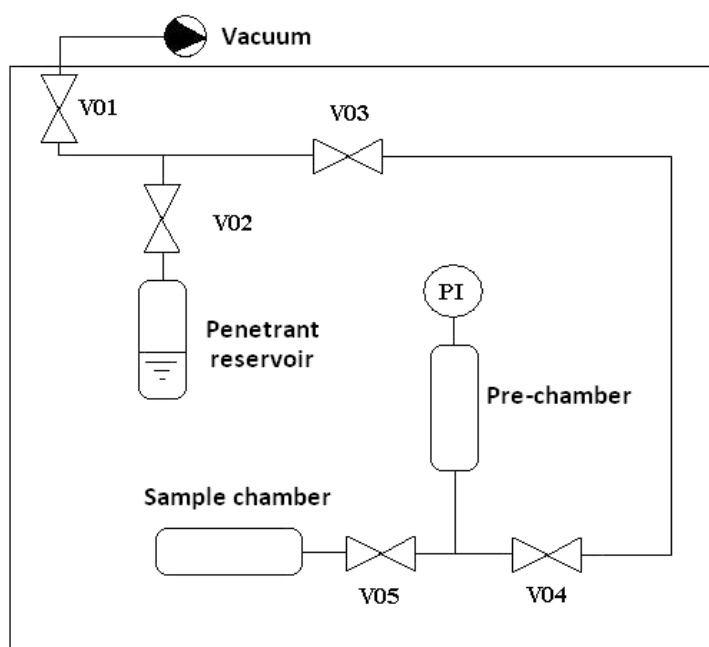25℃ to 65℃. Again differential sorption experiment s are performed also in this apparatus.

Fig. 4.6   The lay out of the Pressure Decay Apparatus.

Measurement of vapor sorption isotherms perfomed with Quartz Spring, Quartz Crystal Microbalance and Pressure Decay apparatus proved to be in good agreement with each others and with the data available in literature for the same polymer penetrant pairs. It has been estimated that the maximum deviation between Quartz Spring and Pressure Decay measurements is well below 10%.

4.5.   Gravimetric Measurament of Pure and Mixed Liquids Sorption

The measurement of liquid solubility in polymers was done gravimetrically, directly measuring the mass uptake with a Sartorious analytical balance model CPA225D-O-CE, that provides a precision of 10^{-5} g or with a Mettler Toled

analytical balance model MS105DU that operates with the same precision. The sorption experiments were performed according to a classical blot and weight method: samples were immersed in vials or flasks filled with liquid, placed in a thermostatic oven or in a thermostatic bath and weighted at regular intervals. In order to weight the samples and register the mass uptake, the samples were removed from the liquid, quickly dried with a paper towel, weighted on the analytical balance and then putted back in the liquid. In this way the mass uptake as a function of time was obtained. Trials in order to understand if cooling the sample with liquid nitrogen in order to reduce the evaporation could improve the measurement process were exploited, but no effective advantage was recognized. In the case of mixed liquids, only solutions into which one component was really volatile and the other one had negligible vapor pressure were used. After that the measurement of the total mass uptake was done according to the previously described procedure, the samples were left under hood to let evaporate the volatile component, till constant weight was obtained. In same case the samples were put in a vacuum chamber for a while and then weighted again, to check if the removal of the volatile component was complete. Mass balance calculations provided the separate mass uptake of the volatile and of the non volatile component.

There are many source of experimental errors in the gravimetric measurement, for instance the viscosity of the liquid and its surface tension could affect the wiping procedure, while with species with really high vapor pressures could be difficult to measure the mass uptake before that desorption start to take place. Repetition of the measurements, on the same sample and on different samples, could provide a means to reduce the error. Generally speaking the error depends significantly on magnitude of the mass uptake. In all the measurement that were performed the dry mass of the sample was in the range 0.25 ÷ 1 g and it was found that for polymer penetrant systems in which the solubility of the liquid is in the 0.1 ÷ 6 g/gpol the relative error is always less then 5.5% and usually lower than 2.5%. In the case of liquids with solubility lower than 0.1 g/gpol, errors as high as 10% have been estimated.

4.6. An example of Glassy Polymer: Matrimid 5218

Matrimid 5218[29, 72, 73, 87, 96] is a material that is gaining increasing attention for its properties and for applications in gas separation and organic solvent nanofiltration, moreover it is characterized by some peculiar properties, such as a really high glass transition temperature and was used here as an example of glassy polymer. Matrimid 5218 used in the sorption experiments was kindly provided by Huntsman Advanced Materials, has an average molecular weight of 80000 g/mol and its polydisperisty index is 4.5. Matrimid 5218 is a polyimide based on 5(6)-amino-1-(4' aminophenyl)-1,3,-trimethylindane, fully imidized, and its molecular structure is shown in Fig. 4.7. Glass transition temperature is around 320℃ and at ambient pressure present itself as a tough yellow polymer. It is known to exhibit good resistance to many organic liquids and it is soluble only in a limited number of specialty solvents, such as THF, DMF, dichlorometane and cyclohexanone. For the sorption experiments dense films were prepared from solution casting, starting from 1% weight (for the samples used for vapor sorption) and 5% weight (for the samples used for liquid sorption) solutions in dichloromethane. After drying, the samples were removed from the Petri disks used for solution casting and were put under vacuum in a oven for a thermal annealing treatment. Generally speaking the samples were annealed at 200℃ for 24h, but other temperatures w ere used for limited testing and the effect of the treatment temperature will be discussed in the following.
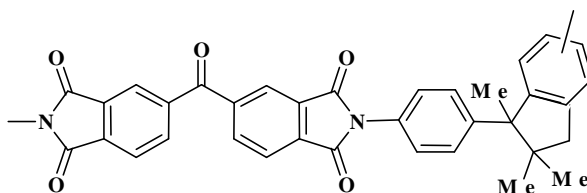

Fig. 4.7   Molecular structure of Matrimid 5218.

4.7.   An example of Rubbery Polymer: PDMS

Crosslinked Polydimethylsiloxane[97-99] was used as an example of rubbery polymer and was selected for its wide use in applications, especially in membrane separation processes and for its resistance to solvents. The PDMS samples were prepared by means of reactive solution casting starting from a filler free commercial uncrosslinked PDMS, commercialized by Wacker Silicones Corp. under the name of Dehesive 944. The PDMS was crosslinked by means of a platinum based, proprietary catalyzer-crosslinker system, sold by the same Wacker Silicones Corp.. In order to promote the formation of the crosslinks, after drying of the solvents the films were placed into a oven, set at 110°C, for 30 minutes. After that, a series of three extractions cycles with hexane or heptane were performed in order to remove the catalyst, the residual unreacted oligomers and any other species that could be still present inside the gelled network. It was found that after three extractions the weight of the samples was not anymore changing. Before starting actual sorption experiments, the samples were put for some hours under vacuum. The structure of PDMS and a possible crosslinking mechanism is depicted in Fig. 4.8.
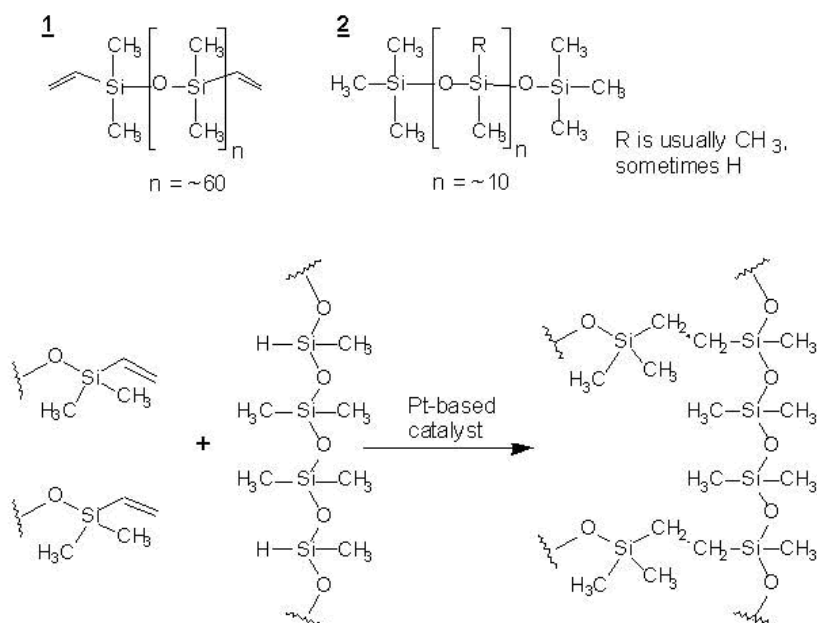
Fig. 4.8   Molecular structure and crosslinking mechanism of PDMS.

4.8.   Sorption in Matrimid 5218

Vapor sorption in Matrimid 5218 was experimentally characterized for the following species: water, methanol and dichloromethane. The solubility of liquid water and liquid methanol has been characterized as well, while no attempt was made to measure liquid dichloromethane solubility since it is a very well known solvent of the polymer itself. The organic solvent were purchased by Aldrich and were all of reagent grade purity, while double distilled deionized water, with conductivity lower than 0.01 µS/cm was used for the vapor and liquid sorption experiments. Solubility isotherms were collected at 35°C with the Quartz Spring Apparatus, while in the case of dichloromethane, solubility measurements were done also at 10°C, 18°C, 32°C and 35°C using both Q uartz Spring Apparatus and Quartz Crystal Microbalance. Among this three species water was found to be the less soluble, with mass uptakes less than 0.03 g/gpol, while solubility of methanol is up to an order of magnitude higher, reaching for unitary activity the value of 0.166 g/gpol. Solubility of dichloromethane exhibits quite the same values at 35°C, but it was found to be much higher at lower temperatures, reaching values as high as 0.6 g/gpol when measured at activities higher than 0.9 at 10°C.

The solubility isotherm of water in Matrimid 5218 is shown in Fig. 4.9. It is possible to note that for mass uptake higher than 0.01 g/gpol, the sorption isotherm seems to have a flex point and its curvature seems to indicate an upward concavity, like that discussed in the case of rubbers or in a sigmoidal shape like the one that is observed in the case of plasticizing penetrants. However, since the mass uptake is so little, there should be little chance that this effect can be related only to a penetrant induced swelling or glass transition effect. Instead it is reasonable to assume that this effect is due to water hydrogen bonding, as suggested by Chen et al.[100] in their 2011 work about water vapor permeation in polyimides and with a mechanism analogous to that described by Davis et al.[101] in their 2012 work on non equilibrium sorption of water in polylactide.
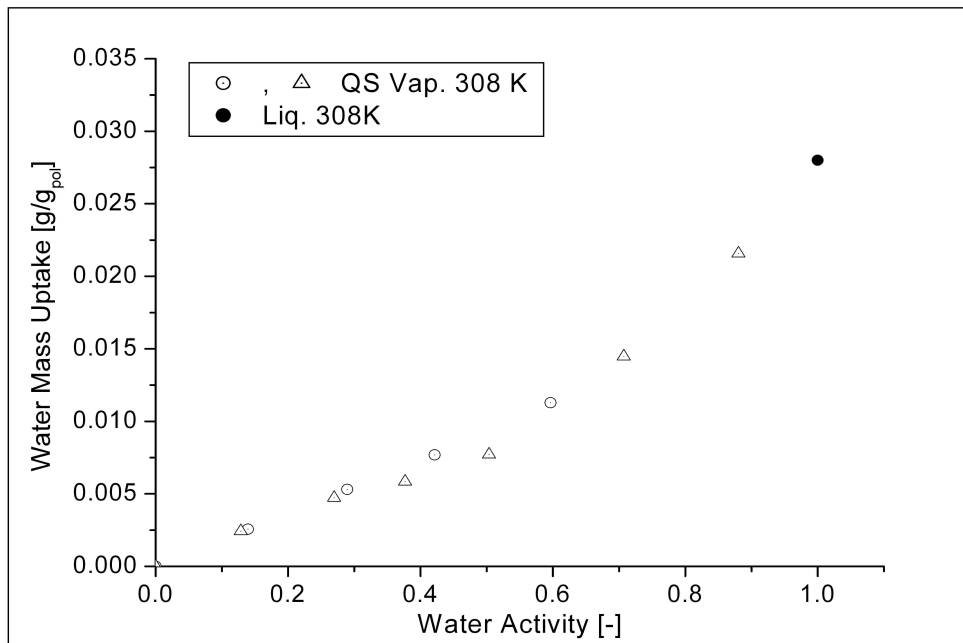
Fig. 4.9   Water sorption isotherm in Matrimid 5218 at 308 K.

The sorption isotherm of methanol in Matrimid 5218 is shown in Fig. 4.10. The solubility follows a slightly depicted sigmoidal shape, but till activity high as 0.6 the usual shape of solubility isotherms in glassy polymers is recognizable. In Fig. 4.11is shown the mass uptake kinetic of the first vapour sorption step, ranging from activity equal to zero, to activity equal to 0.089: it is quite evident that the behaviour adhere to the Fickian's one. It seems reasonable that in the first, low activity step, no swelling and relaxation effects are yet detectable. The third step, shown in Fig. 4.12, has been collected after an activity jump that ranges from activity 0.19 to activity 0.47 and it is easy to recognize that after and initial Fickian behaviour, in which the mass uptake is proportional to $\sqrt{t}$, then relaxation phenomena starts to take place and the mass drifts slowly toward the pseudo equilibrium value. The fourth step, from activity 0.47 to activity 0.62 is shown in Fig. 4.13: in this case the kinetic deviates completely from the Fickan behavior and the mass uptake is proportional to t^{n} with the exponent n that is definitely different from 0.5. Finally in Fig. 4.14 it is shown the

mass uptake kinetic of the liquid sorption experiment, that is an integral sorption experiment in which the activity of the penetrant jumps from 0 to 1.
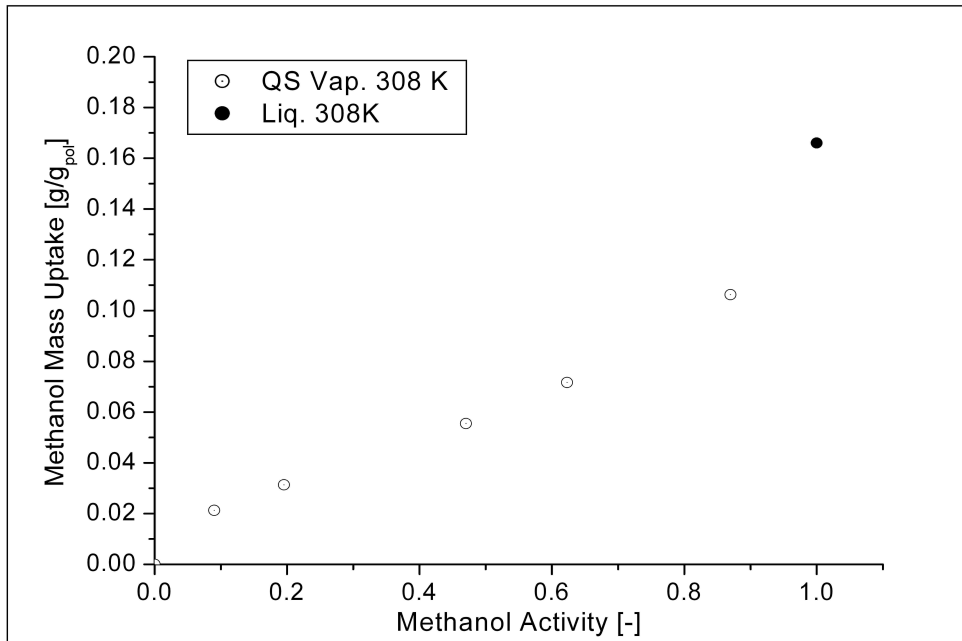

Fig. 4.10   Methanol sorption isotherm in Matrimid 5218 at 308 K.
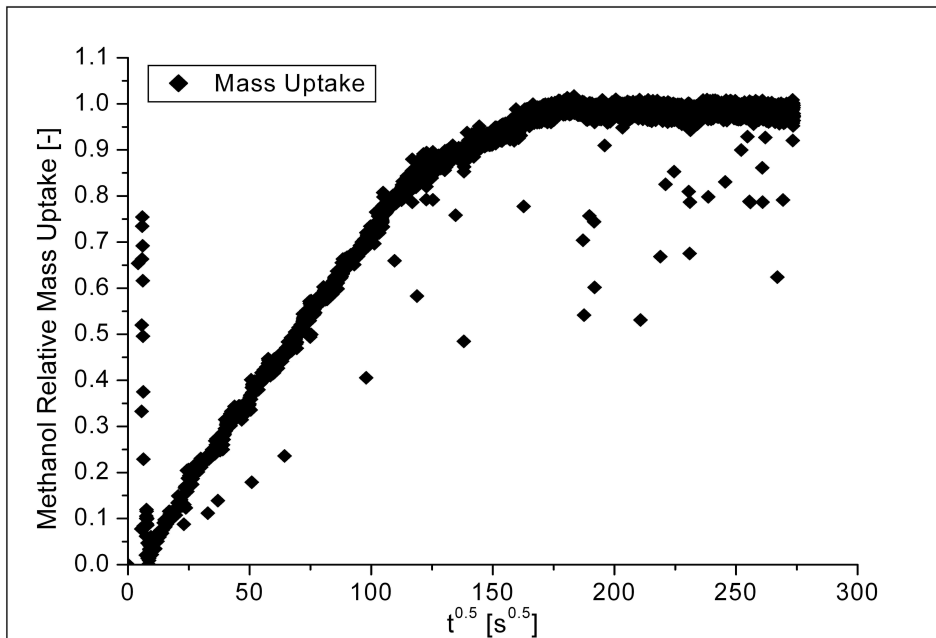

Fig. 4.11   Methanol sorption in Matrimid 5218 at 308 K: first step, from activity 0 to activity 0.089.
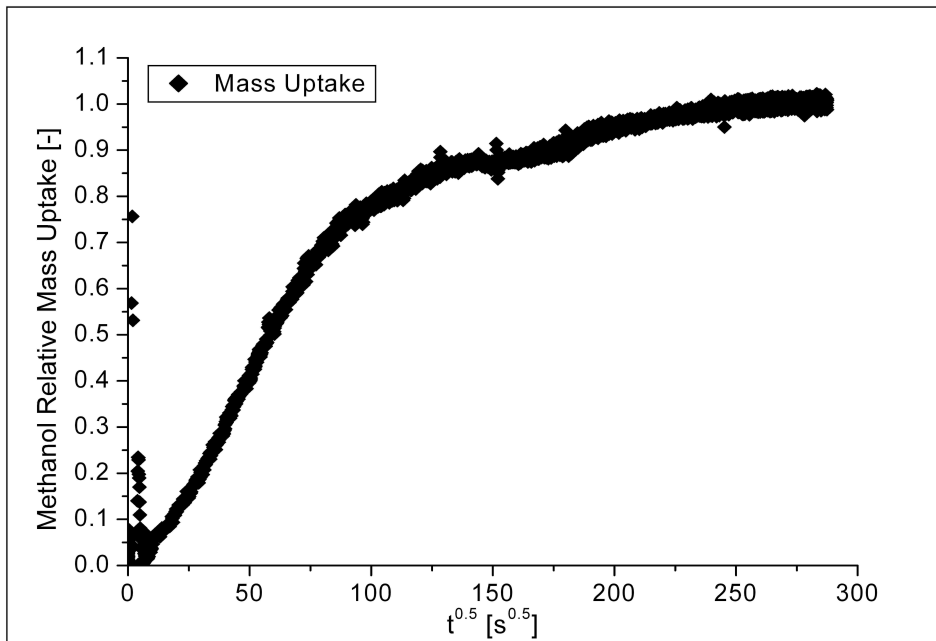
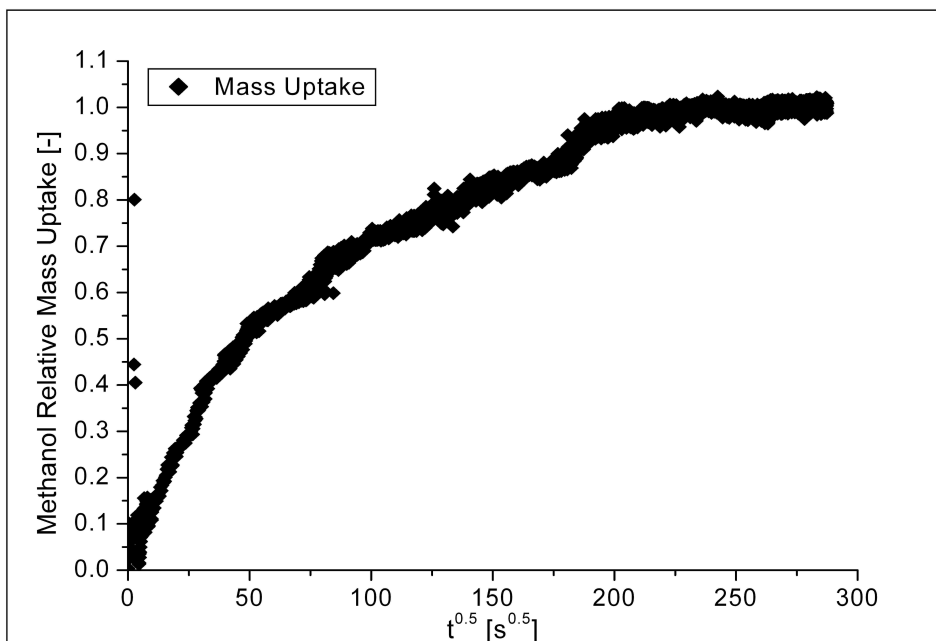Fig. 4.12   Methanol sorption in Matrimid 5218 at 308 K: third step, from activity 0.19 to activity 0.47.

Fig. 4.13   Methanol sorption in Matrimid 5218 at 308 K: fourth step, from activity 0.47 to activity 0.62.
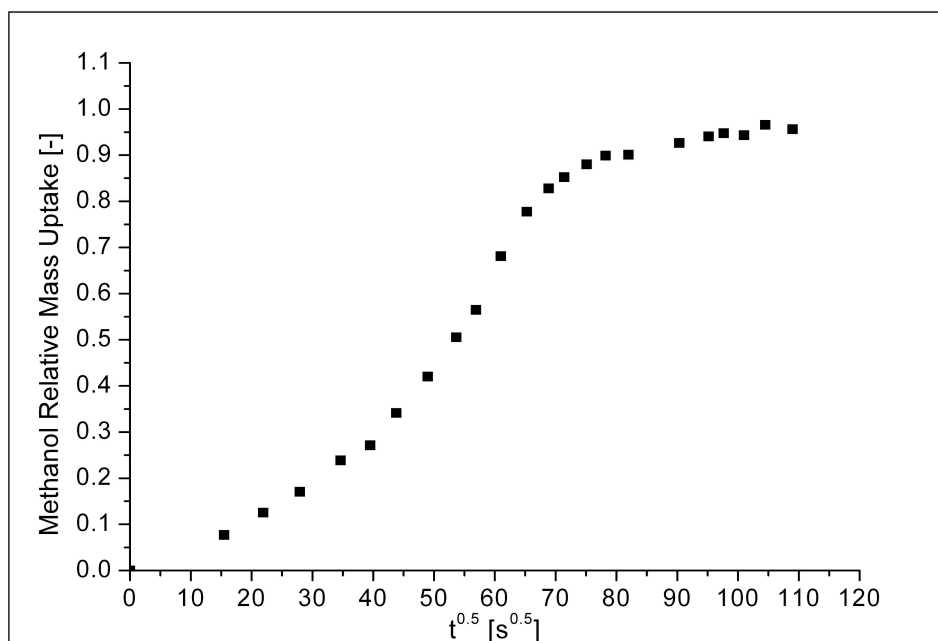
Fig. 4.14   Liquid Methanol sorption in Matrimid 5218 at 308 K.

Also in this case, deviation from the Fickian behavior are recognizable, since there is a S shaped mass uptake curve and maybe a slight drift is recognizable, instead of the steady state plateau that would be expected in the case of Fickian sorption.

The solubility isotherms of Dichloromethane in Matrimid 5218 collected with the Quartz Crystal Microbalance are depicted in Fig. 4.15, while in Fig. 4.16 can be found the ones measured with the Quartz Spring Apparatus. It can be recognized that solubility decreases with temperature, as it should happen if the sorption of Dichloromethane and Matrimid 5218 is exothermic. The enthalpy change upon sorption is made by the sum of the enthalpy of mixing and the enthalpy of condensation of the penetrant. It is relevant that while sorption isotherms collected at the experimentally realizable activities in this two apparatuses, the sorption isotherms collected at 18°C, 32°C and 35°C show the downward concavity that is expected for glasses. Only at 18°C a slight change of curvature could be detected in the last two experimental points, when mass uptake is higher than 0.3 g/g_{pol}. On the contrary, at 10°C, the solubility at the

activities that were explored, is so high that swelling and plasticization effects takes place in such a relevant way that there is a marked and abrupt change in concavity and the portion of the solubility isotherm in which the mass uptake is higher than $0.2 \div 0.3$ g/g$_{pol}$ is definitely like those of the rubbery systems. In the following chapter, in which a rigorous thermodynamic modeling of this sorption isotherms will be performed, it will be shown that equilibrium and not pseudoequilibrium conditions hold in that region and that actually dichloromethane depress the glass transition temperature of the system at a value that is below the temperature at which the experiment is performed.
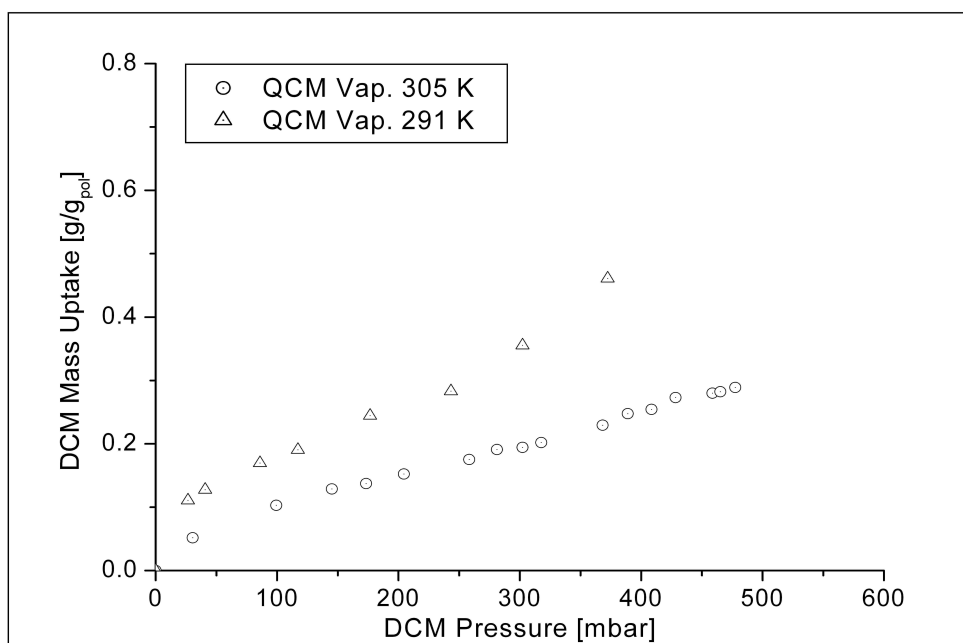

Fig. 4.15   Dichloromethane sorption isotherms in Matrimid 5218 at 291 K and 305 K, measured with the Quartz Crystal Microbalance.
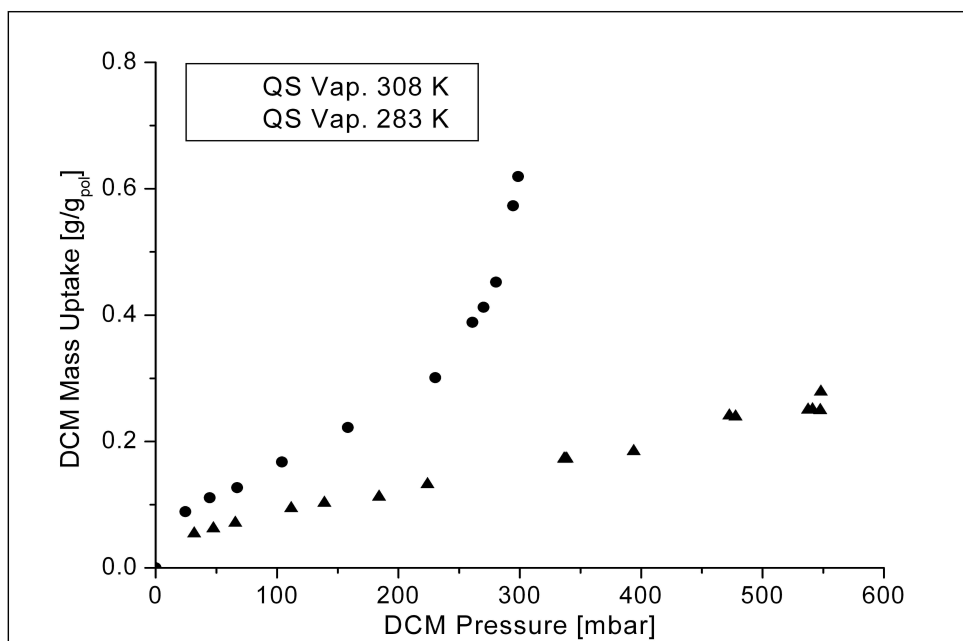
Fig. 4.16 Dichloromethane sorption isotherms in Matrimid 5218 at 283 K and 308 K, measured with the Quartz Spring Apparatus.

Beside this vapor and liquid complete characterization, the solubility of several others organic liquids was measured in Matrimid 5218, at 35℃. Solubility of an homologous series of alcohols was measured, namely methanol, ethanol , 1 propanol, 2 propanol, 1 hexanol and 1 octanol. The results are shown in Fig. 4.17. For comparison Hesse et al.[29] published some liquid sorption data for the ethanol – Matrimid 5218 system, collected at 298.15 K, 313.15 K and 333.15 K. Ethanol solubilities were, respectively, 0.20, 0.22 and 0.21 g/gpol. The samples used by Hesse et al. were casted from DMF solutions and were annealed at 200℃ for 1 week. The measurements performed at 308 K in this work led to an ethanol solubility of 0.21 g/gpol, in really good agreement with the data published by Hesse et al.[29]
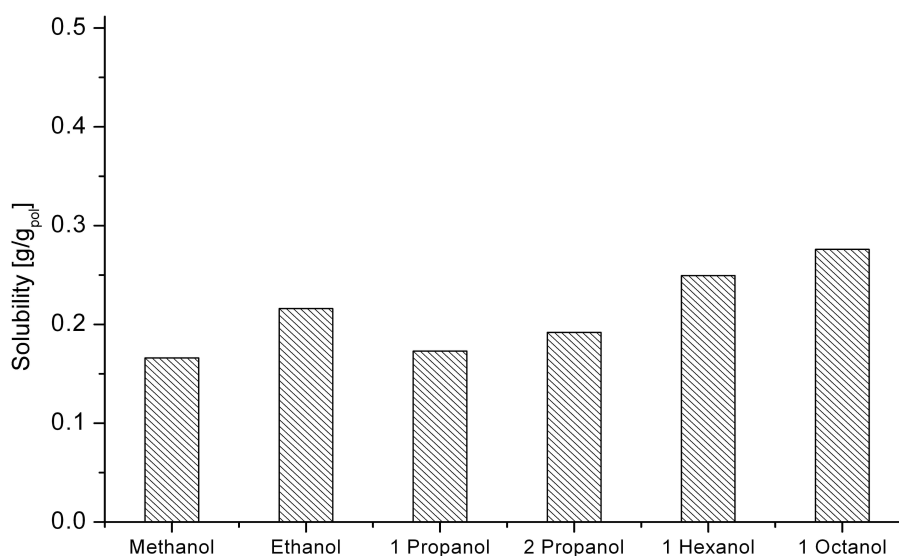
Fig. 4.17   Liquid alcohols sorption in Matrimid 5218 at 308 K.

Liquid Sorption experiments were performed also with acetone, acetic acid and a series of alkyl acetates, namely methyl acetate, ethyl acetate, butyl acetate and hexyl acetate. Results are represented in Fig. 4.18. In all cases the mass uptake was pretty high and during the subsequent desorption crazes and cracks were frequently observed in the samples. The sorption kinetic of Acetone, shown in Fig. 4.18, seemed to be quite adherent to the Fickian one, while in the other cases the S shaped kinetic was frequently observed. For the system Ethyl acetate – Matrimid 5218 Hesse et al. published liquid sorption data collected at 284.15 K, 298.15 K and 328.15 K. Solubility were respectively equal to 0.38, 0.39 and 0.36 g/gpol. The value measured in the present work at 308 K is 0.38 g/gpol, again in really good agreement with the published data.
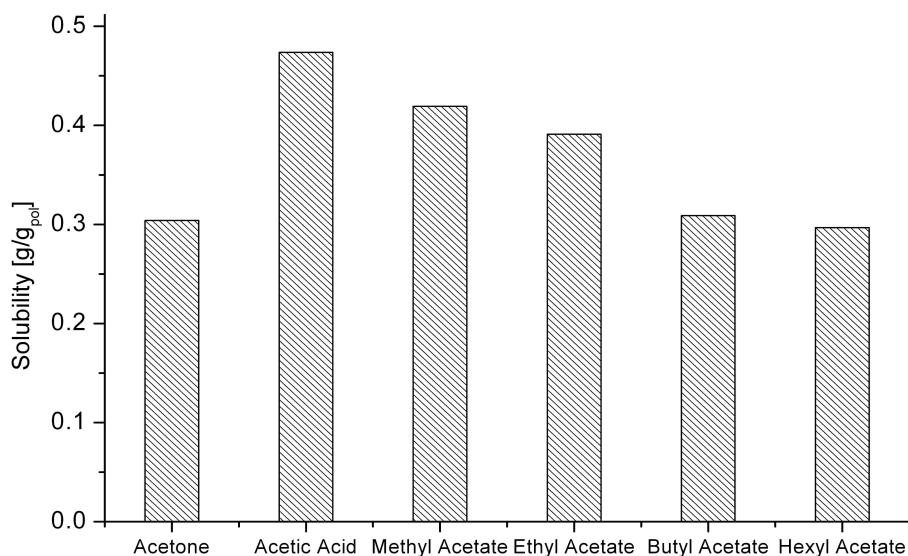
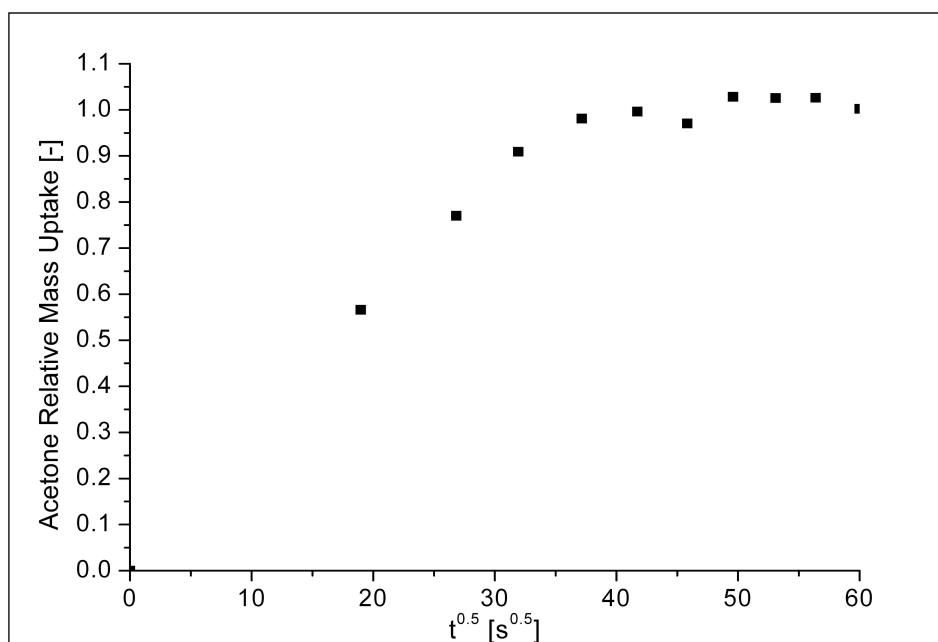Fig. 4.18   Liquid oxygenated solvents sorption in Matrimid 5218 at 308 K.

Fig. 4.19   Liquid acetone mass uptake kinetic in Matrimid 5218 at 308 K.

Finally some word has to be spent about the effect of the annealing treatment on the solubility values that were measured. The above mentioned data are all referred to samples that were annealed for 24 h at 200℃, but some testing was performed also on samples annealed, for 24 h, at lower temperatures, namely 50℃ and 100℃. It must be noted that they are alwa ys greater than the normal

boiling point of the solvent used for the casting procedures, since dichloromethane normal boiling point is close to 40℃ . For instance in Fig. 4.20 are shown the different values of liquid solubility measured after different annealing procedures, while in Fig. 4.21 the vapor and liquid sorption isotherms for methanol are depicted. It is easy recognizable that the sample treated at higher temperature were able to take up more penetrant. Exploratory FTIR ATR tests seems to show that even after the annealing at 50℃ there should be no detectable amount of residual dichloromethane and thus that a mixed solubility effect should be discarded.
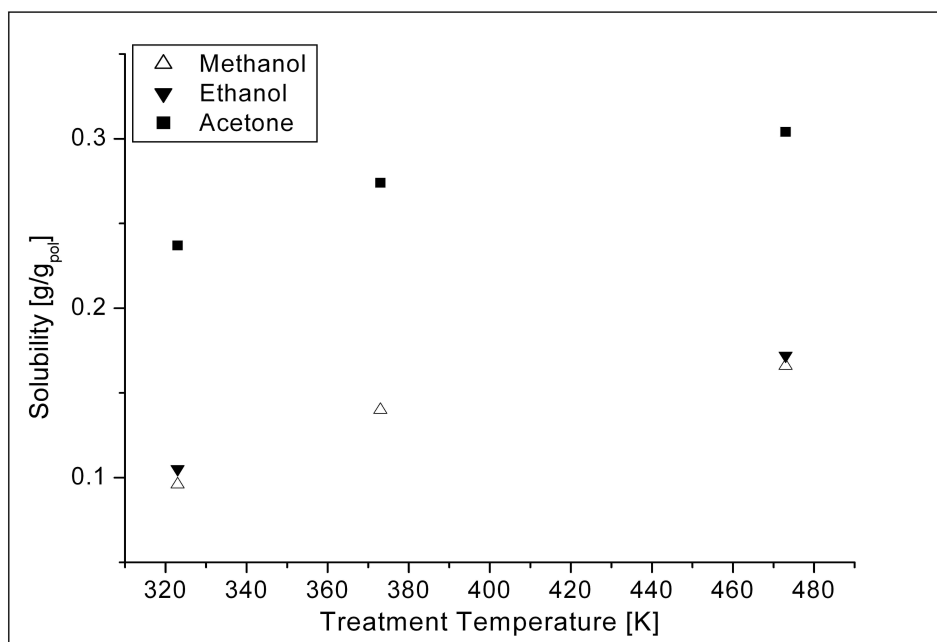

Fig. 4.20   Liquid solvents sorption in Matrimid 5218 at 308 K, effect of the annealing temperature.
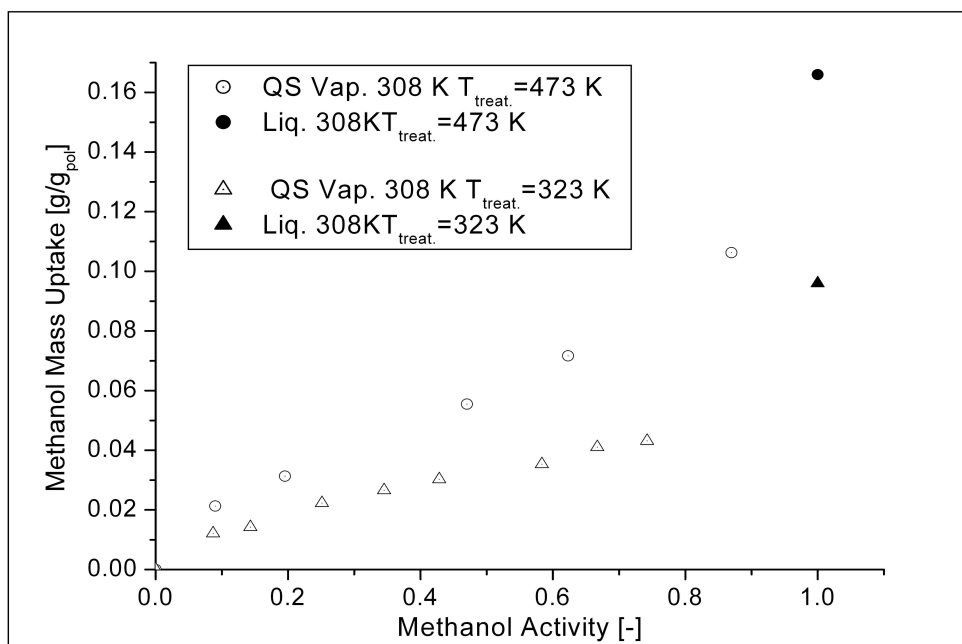
Fig. 4.21   Methanol Sorption isotherms in Matrimid 5218 at 308 K, effect of the annealing temperature.

4.9.   Sorption in PDMS

Mainly pure and mixed liquid sorption experiments were performed in PDMS. Some limited vapor sorption data were collected with Pressure Decay Apparatus and with the Quartz Spring Apparatus for acetone and, only with the last apparatus, for pentane, in order to gain same insight on the shape of the sorption isotherms as a function of the penetrant activity. Since the behavior was always found to be Fickian, for pure liquids, when enough data were available, the mass uptake kinetics were regressed with the equation that results from the solution of the local mass balance and the diffusivity value was retrieved. The following liquid penetrants were used: pentane, hexane, octane, decane, dodecane, tetradecane esadecane, octadecane, eicosane, ciclohexane, water, PEG 400, acetone, ethanol, ethyl acetate, 1 propanol, 1 butanol, iso butanol, tert butanol, 1 pentanol, 1 hexanol, Squalene, limonene, linalool, geraniol, olive oil, groundnut oil, sunflower oil and oleic acid. Oils were

purchased in local shops and were of commercial, food grade. Quite all the liquid organic solvent were purchased by Aldrich and were all of reagent grade purity, while double distilled deionized water, with conductivity lower than 0.01 µS/cm was used for the liquid sorption experiments. The main exceptions were those of squalene, that was supplied by Acros, PEG 400 that was supplied by Merck and oleic acid that was supplied by Aldrich but was of technical grade (90% purity).

Sorption experiments were performed with alkanes ranging from pentane through octadecane, while eicosane was used only for mixed liquid sorption, since at 35°C, while pure, is in solid form. Solubi lity and diffusivity depicts quite a regular trend, when plotted, as it is done in Fig. 4.22 and Fig. 4.23, as a function of the number of carbon atoms that form their chains. Solubility decreases linearly, while diffusivity decreases much more markedly. Actually the sorption of the lowest alkanes is really huge, since it could be as high as 5.23 g/gpol, in the case of pentane. The sample undergoes a massive swelling upon such a mass uptake. It must be remarked that the diffusivity were obtained as values referred to the dry polymer thickness and thus should be regarded as the values that hold in the fixed polymer reference frame.
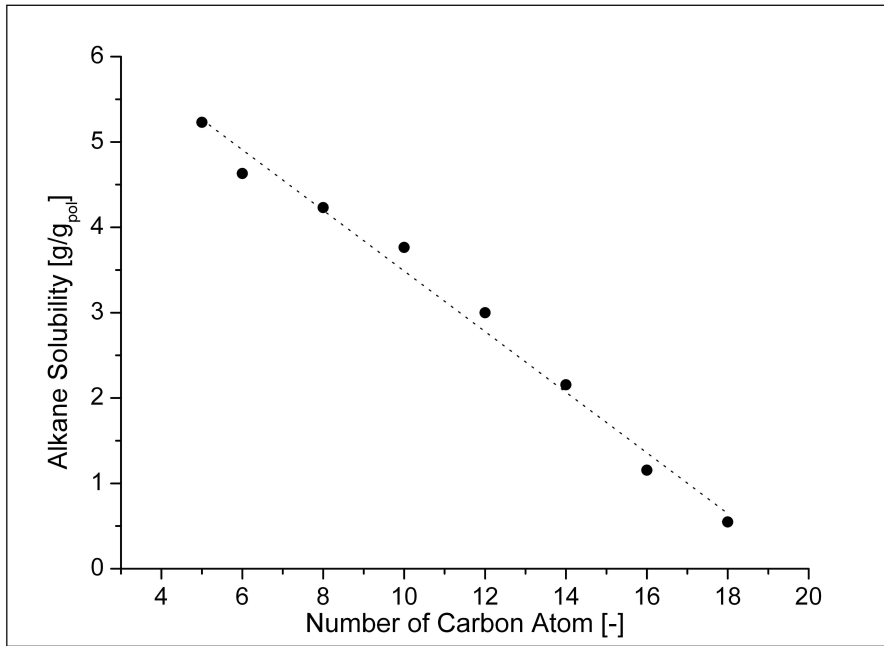
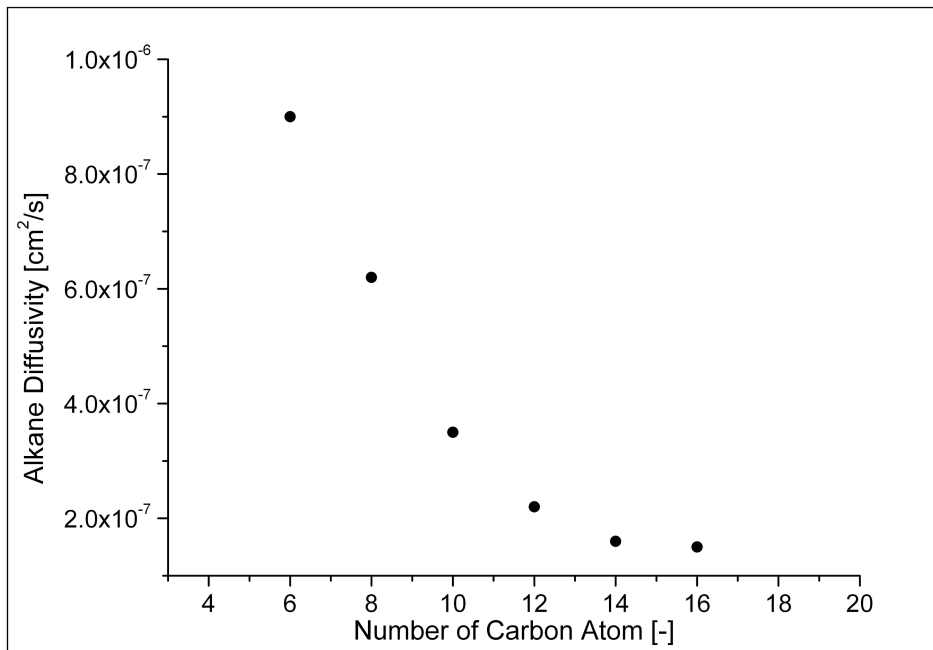Fig. 4.22   Liquid alkanes sorption in PDMS at 308 K.

Fig. 4.23   Liquid alkanes diffusivity in PDMS at 308 K.

Then in Fig. 4.24 and Fig. 4.25 the solubility and the diffusivity for several others liquids in PDMS are represented. It is interesting to observe that the component with the highest solubility is cyclohexane, while polar, hydrogen bonding prone,

species like water and PEG 400, that are known to be mutually miscible, have really low solubility in PDMS. Solubility of many oxygenated species is in the range 0.1 ÷1 g/gpol with the only exception of ethyl acetate. The solubility of linear chain alcohols show a non monotonous behavior, but this can be explained considering the fact that the PDMS has a scarce affinity with the hydroxyl group $-OH$, while it has a much greater one with the alkyl groups, but their solubility decreases with their size, as shown by the behavior of straight chains alkanes. Interestingly, even if the number of carbon atoms of the alkyl group is held fixed, its actual size and shape deeply affects solubility. In fact, as shown in Fig. 4.26, tert butanol is much more soluble then iso butanol, which is more soluble than normal butanol. In tertiary alcohols the alkyl group is able to shield to a larger extent the hydroxyl group, while this effect is less evident, but still present, for secondary alcohols. Diffusivities, shown in Fig. 4.27, follow the opposite trend, since the biggest cross section of the tertiary alcohol and of the secondary one hinders the kinetic of their molecular transport across the polymer.
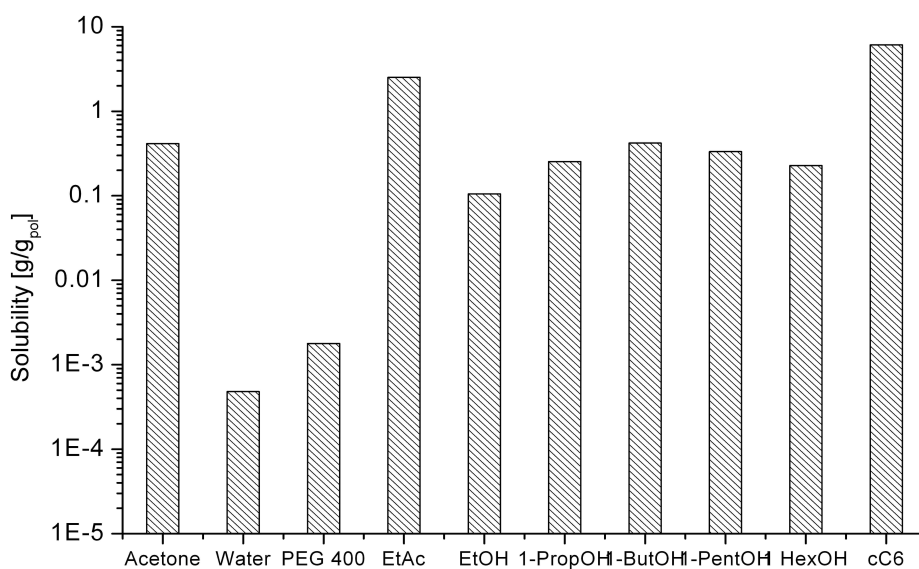

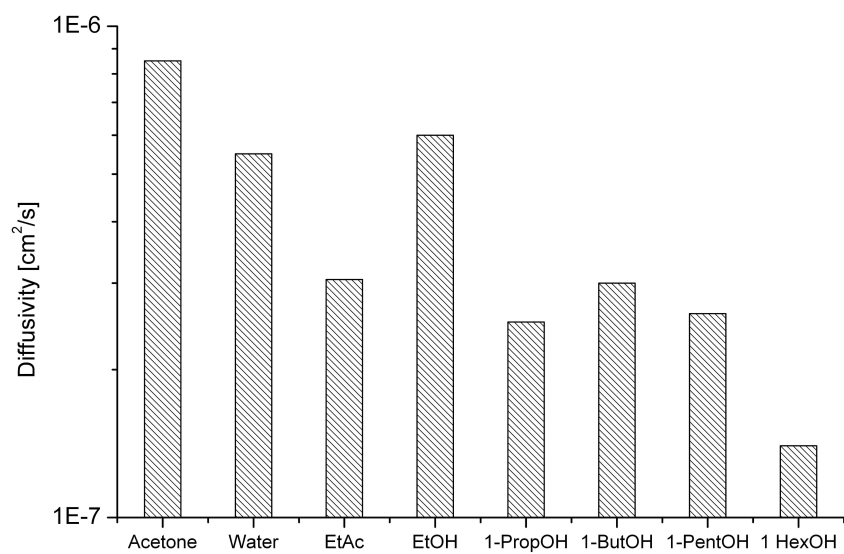Fig. 4.24   Solubility of several liquids in PDMS at 308 K.

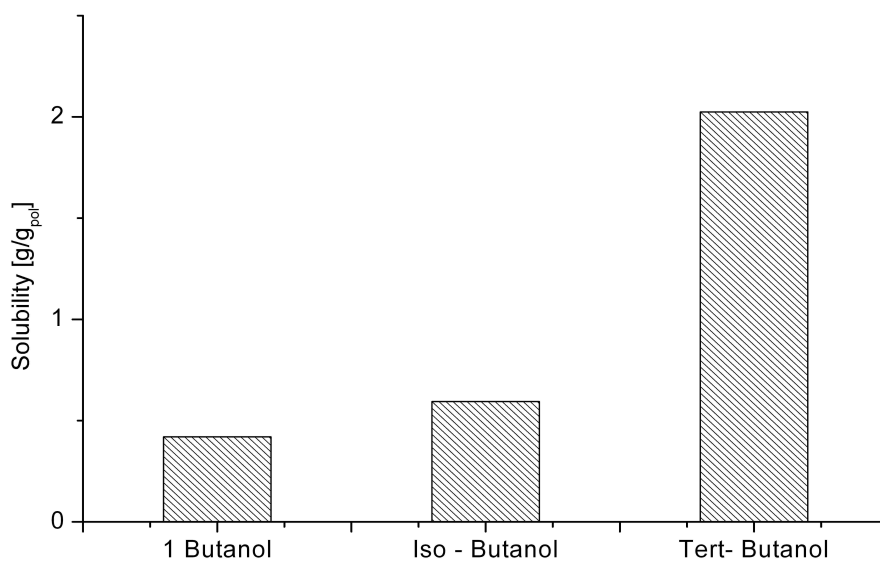Fig. 4.25   Diffusivity of several liquids in PDMS at 308 K.

Fig. 4.26   Solubility of butanols in PDMS at 308 K: effect of the molecular structure.
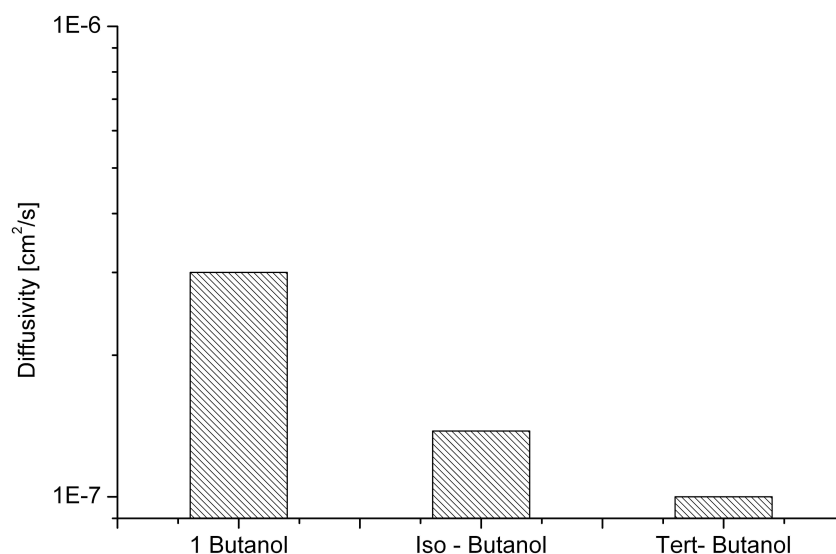
Fig. 4.27   Dffusivity of butanols in PDMS at 308 K: effect of the molecular structure.

Liquids of interest for the pharmaceutical and for the aroma industry, like squalene, limonene, geraniol and linalool have quite different molecular structure, but they all belongs to the class of terpenes. Squalene is a triterpene, analogous to an hydrocarbon with 30 carbon atoms, limonene is a cyclic terpene with a 6 carbon ring, analogous to that of cyclohexane, geraniol is a monoterpenic alcohol and linalool is a terpenic alcohol as well and they share the same number of carbon atoms in chains. Solubility and diffusivities are shown in Fig. 4.28 and Fig. 4.29. It is interesting to note that limonene, due to its strong similarity with cyclohexane, that is the component with the highest solubility, at least among those tested, has a pretty high solubility as well. Geraniol is a primary alcohol, while linalool is a tertiary one and also in this case the solubility of the tertiary alcohol is higher than the solubility of the primary one and the diffusivities behave in the opposite way, like was previously discussed for the case of the butanols.
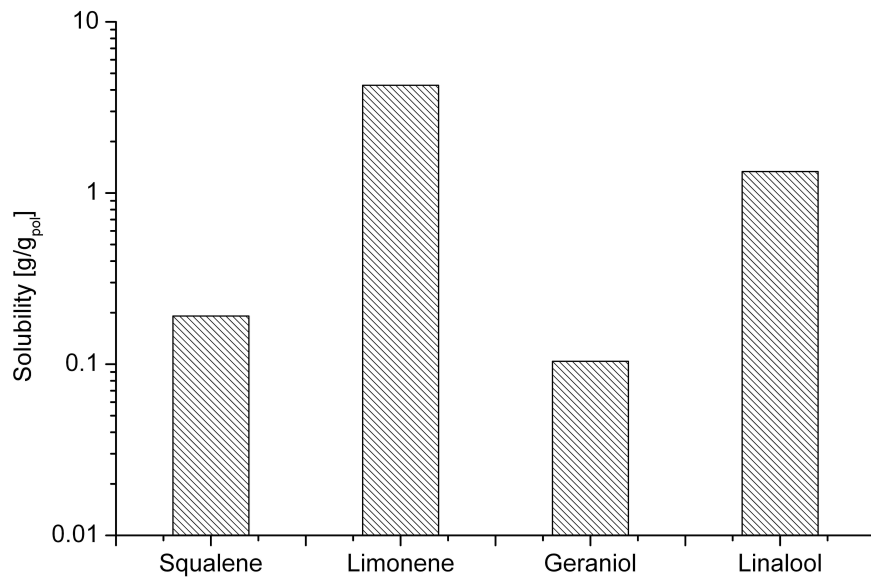
Fig. 4.28   Solubility of terpenes in PDMS at 308 K.
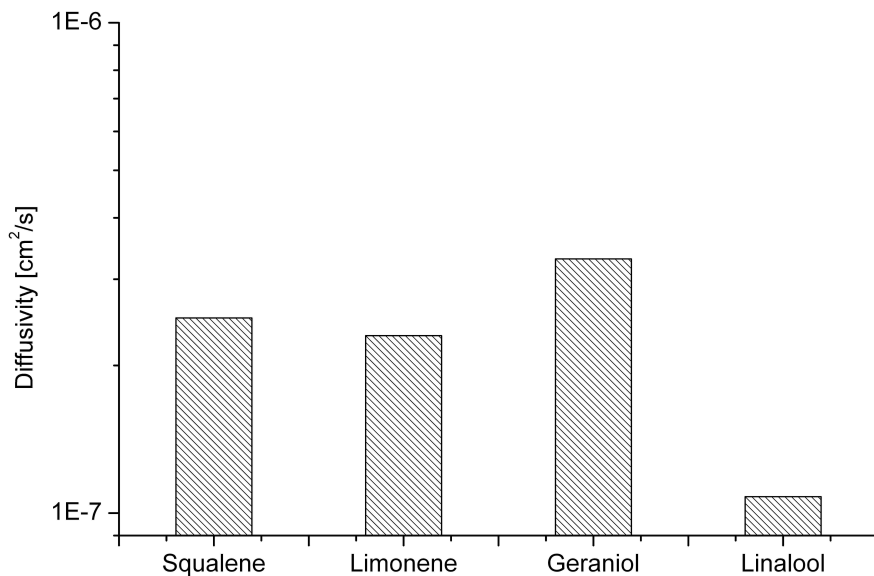
Fig. 4.29   Diffusivity of terpenes in PDMS at 308 K.

Solubility and diffusivities of edible oils, as well as those of oleic acid, are reported in Fig. 4.30 and Fig. 4.31. Since naturally occurring vegetable oils are complex multicomponent mixtures, the diffusivity and solubility values are to be intended as apparent or global values. The olive oil is a low acidity one, with less than 0.3 % of free fatty acids. Solubility of the edible oils are quite the same, while oleic acid is almost one order of magnitude more soluble.

Diffusivities are quite the same for all. In order to understand what was the effect of the oleic acid content on solubility and diffusivity, olive oils samples were added of known amounts of oleic acid and the sorption tests were repeated. The results are reported in Fig. 4.32 and Fig. 4.33: solubility seems to increase linearly with the free fatty acid content, while, as noted before, no systematic effect on diffusivity is recognizable.
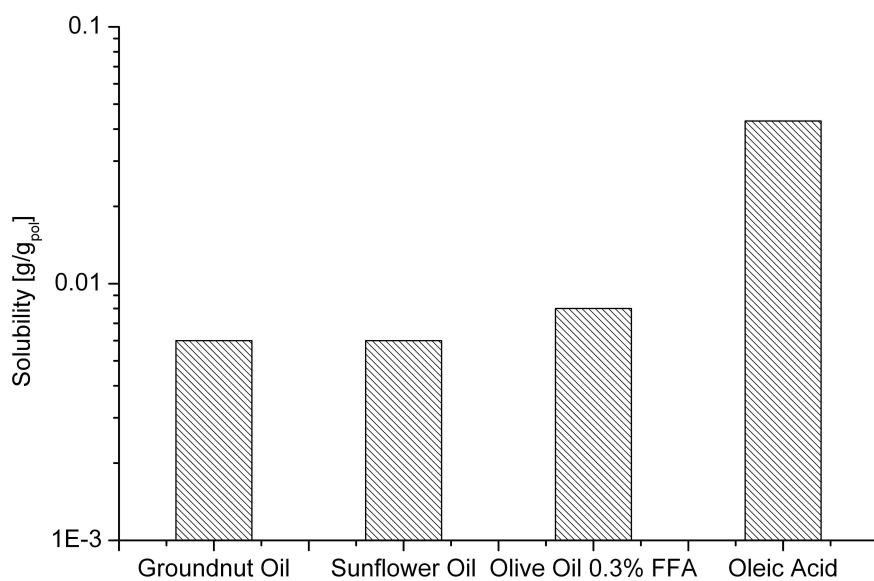
Fig. 4.30   Solubility of edible oils and of technical grade oleic acid in PDMS at 308 K.

Fig. 4.31   Diffusivity of edible oils and of technical grade oleic acid in PDMS at 308 K.
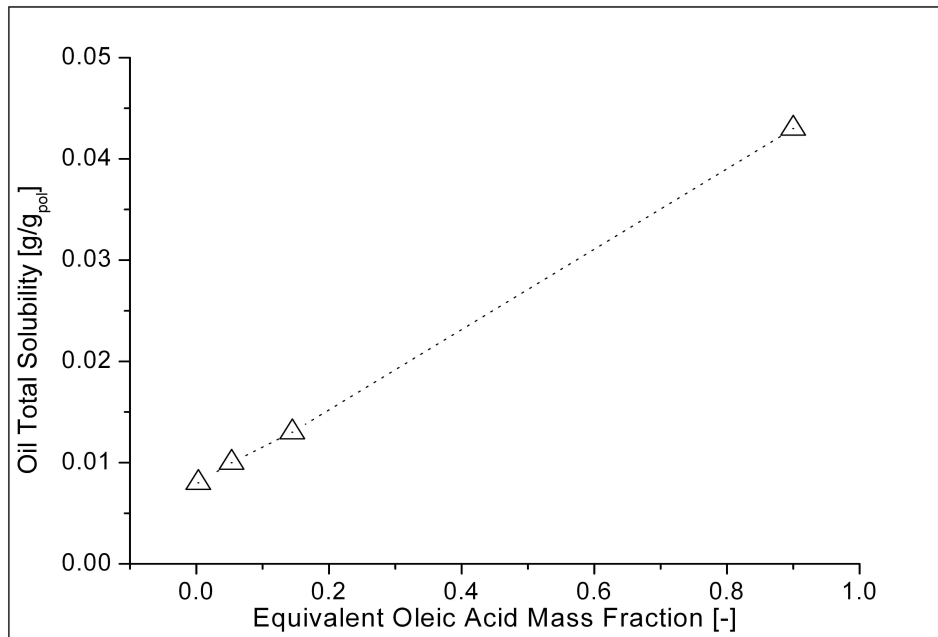
Fig. 4.32   Solubility of edible oils and of technical grade oleic acid in PDMS at 308 K as a function of the free fatty acid contents expressed as equivalent oleic acid.
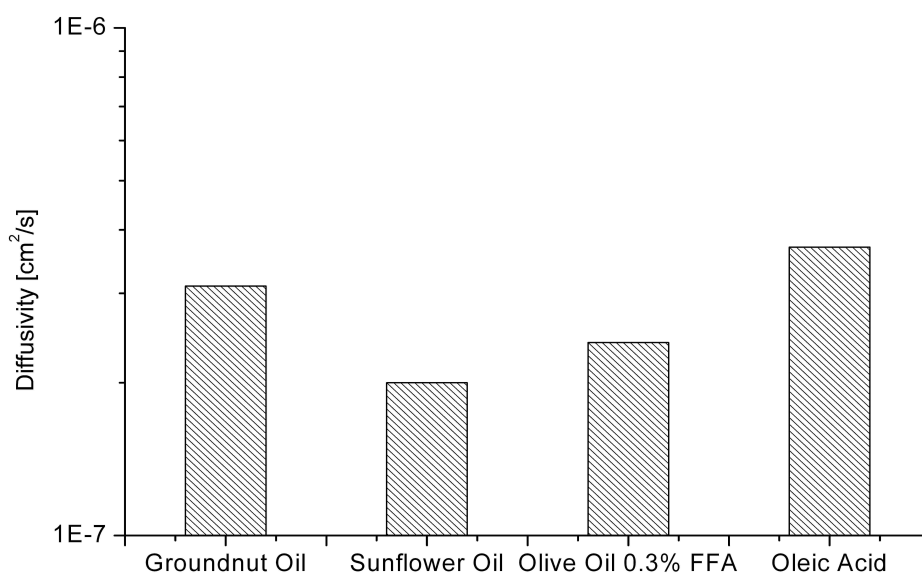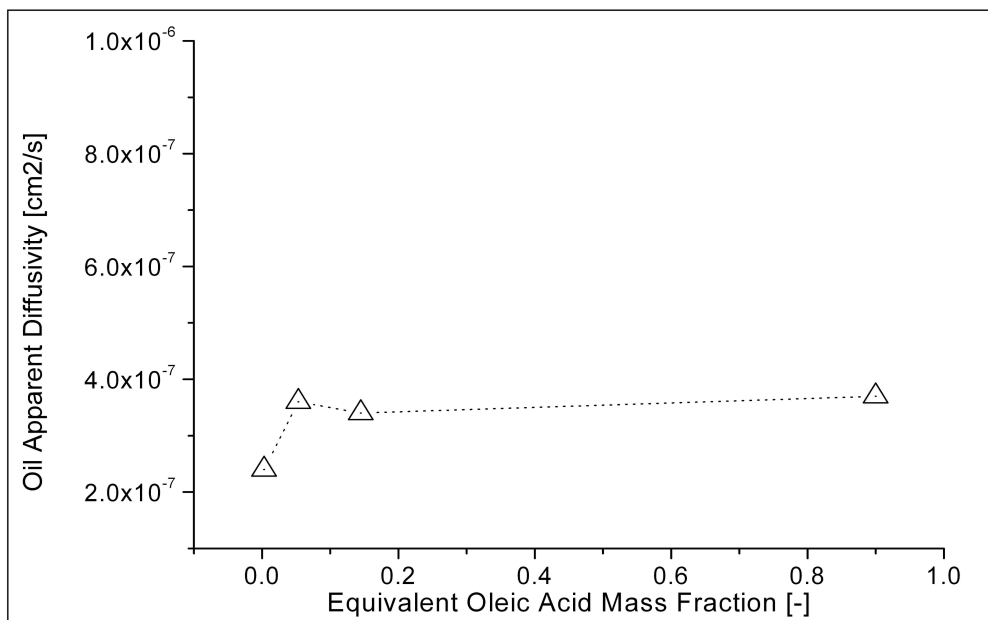

Fig. 4.33   Diffusivity of edible oils and of technical grade oleic acid in PDMS at 308 K as a function of the free fatty acid contents expressed as equivalent oleic acid.

Some liquid mixtures were considered. First of all the sorption of a mixture of pentane and eicosane was measured at 35℃. The resu lts are shown in Fig. 4.34. The solubility of pure eicosane is not available, due to the fact that eicosane is solid at 35℃. It is really interesting to note that the solubility of the component that globally is less soluble, is being enhanced by the other, more soluble components. In fact the huge swelling induced by pentane promotes also the solution process of eicosane. This behavior has been found in all the mixtures that were considered. It is also interesting to note that the pentane solubility curve has the same concavity of the solubility isotherms in rubbers, when plotted against activity.

Fig. 4.34   Pentane and eicosane solubility in PDMS at 308 K as a function of the pentane mass fraction in the external liquid phase.

A mixture made by squalene and acetone was also tested. Results are shown in Fig. 4.35. Since solubility of squalene is rather high, quite of the same order of magnitude of that of acetone, there seem to be a synergic effect, since the solubility of both components in the mixture is found to be greater than the one of the pure species.
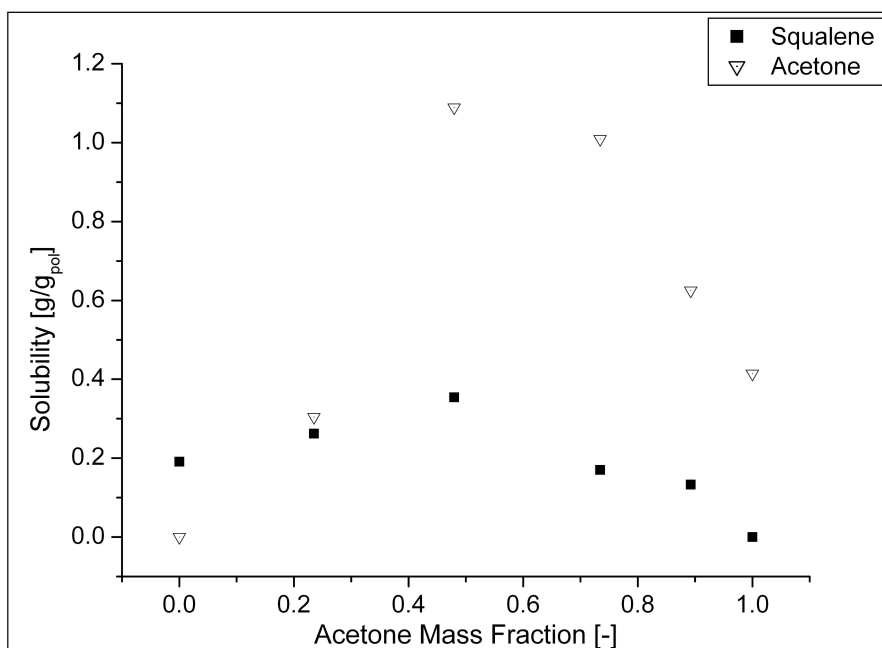
Fig. 4.35   Acetone and Squalene solubility in PDMS at 308 K as a function of the acetone mass fraction in the external liquid phase.

Mixtures of acetone and oleic acid, as well as of acetone and olive oils were considered also and the results are shown in Fig. 4.36 and Fig. 4.37. In this case the less soluble components are the oleic acid and the olive oil and acetone acts promoting their solutions. It is interesting to note that in this case the shape of the acetone solubility curve differs greatly from that of pentane, especially regarding its curvature. On the other hand, the solubility of pentane and oleic acid, shown in Fig. 4.38, are more close to that of pentane and eicosane. Finally Fig. 4.39 depicts the results of the liquid mixture sorption of tertbutanol and PEG 400. That, as previously said, is scarcely soluble in PDMS. Also in this case, the presence of a component that is highly soluble in PDMS promotes the solubility of the other component. All this effects should be taken into account for membrane separation process, since they acts lowering the separation factors from the values that could be estimated by the sole pure liquids data.
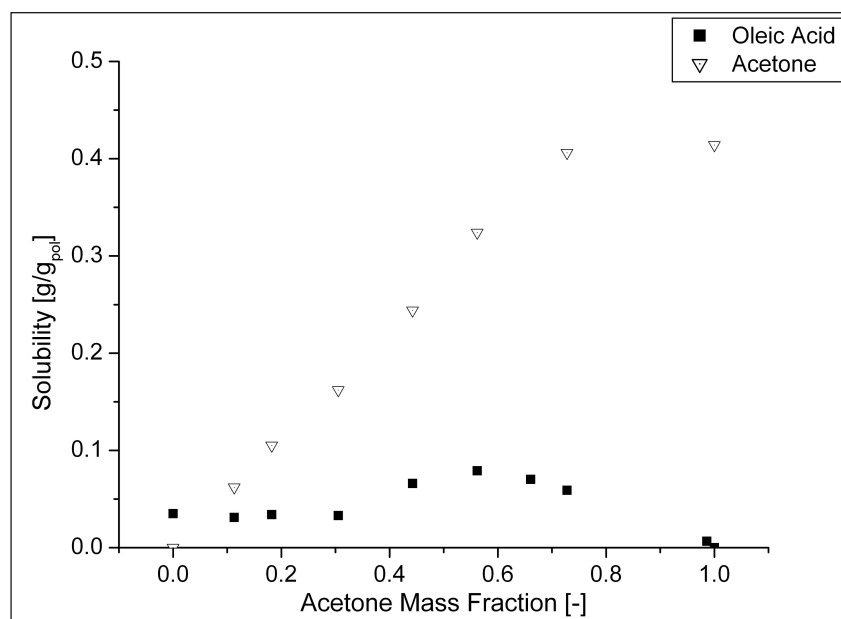
Fig. 4.36 Acetone and oleic acid solubility in PDMS at 308 K as a function of the acetone mass fraction in the external liquid phase.

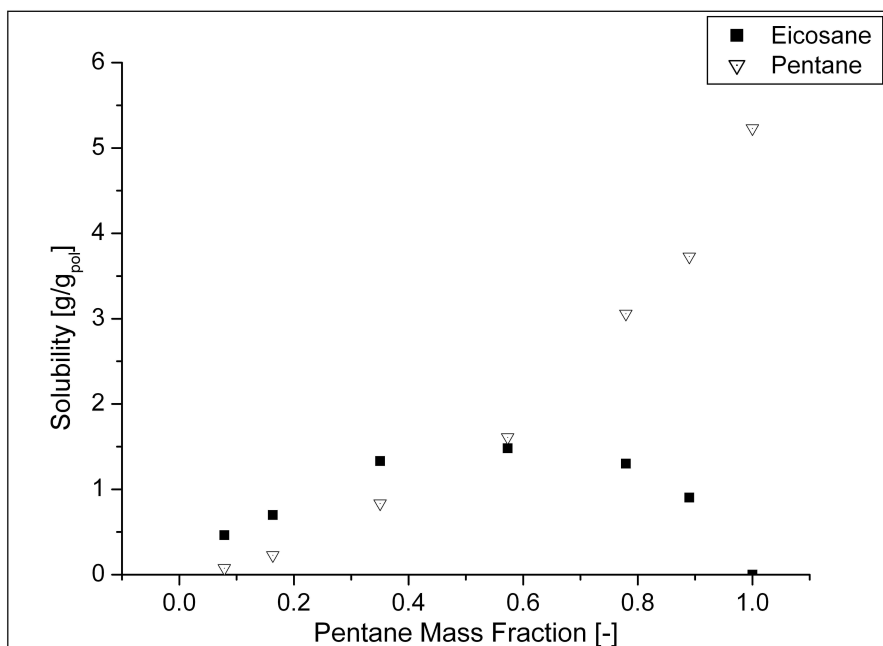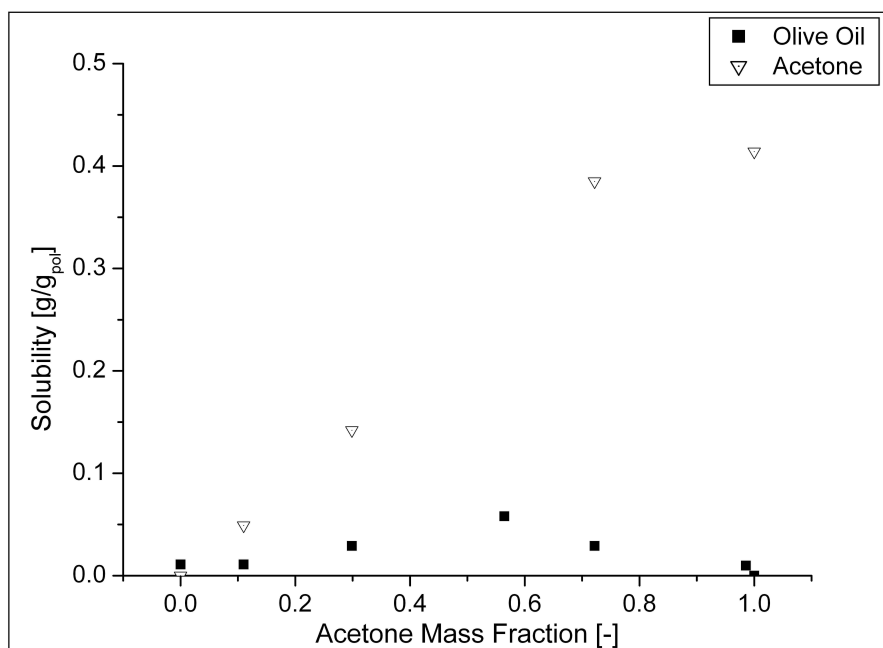Fig. 4.37 Acetone and olive oil solubility in PDMS at 308 K as a function of the acetone mass fraction in the external liquid phase.
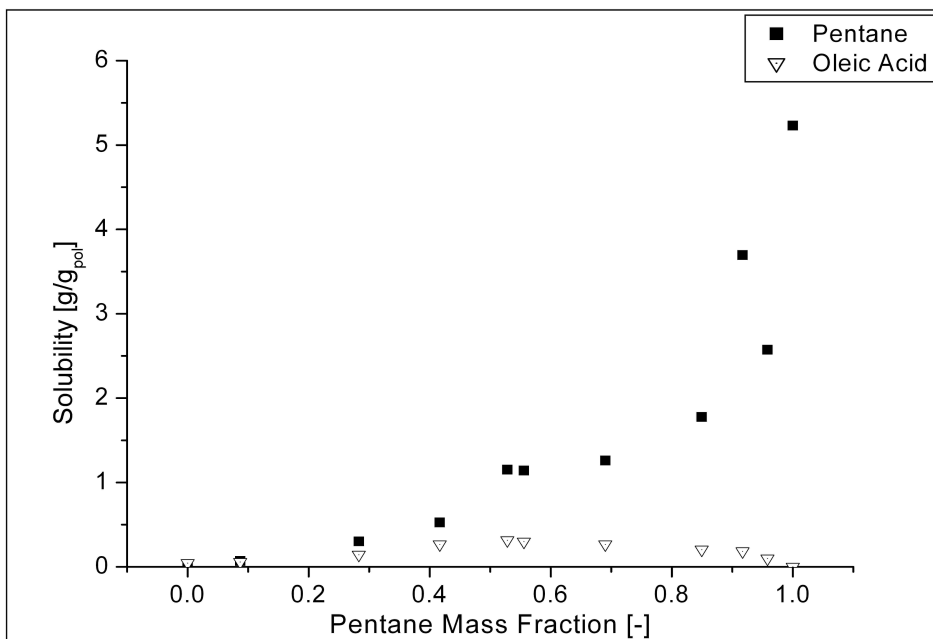
Fig. 4.38   Pentane and oleic acid solubility in PDMS at 308 K as a function of the pentane mass fraction in the external liquid phase.
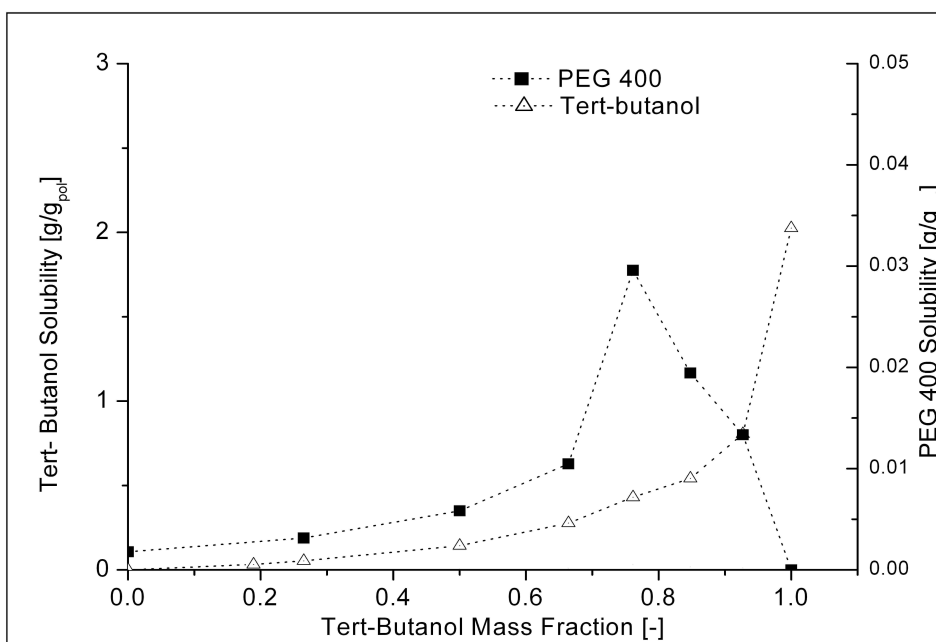
Fig. 4.39   Tert butanol and PEG 400 solubility in PDMS at 308 K as a function of the tert butanol mass fraction in the external liquid phase.

4.10.   Concluding remarks

Vapors and liquids sorption experiments had been performed for many solvent/penetrant – polymer systems, with glassy and rubbery polymers, that gave rise to the peculiar behavior that is expected for that kind of systems. In glassy polymer several relevant features were observed, ranging from swelling and plasticization effects, to relaxation and history dependence. Solubility of pure and mixed liquids in rubbery polymers were measured and it was found that in mixtures the presence of an highly soluble, swelling inducing penetrant, can deeply affect the solubility of those penentrants that, while pure, exhibit really low solubility.

5. Modeling of the Sorption Isotherms of Low Molecular Weight Species in Glassy Matrimid 5218 with the NET-GP Approach

5.1. Introduction

The application of Equation of State approach for modeling complex vapor liquid and liquid liquid phase equilibria has already been shown in the previous chapter about water-1,4 dioxane – polylactides systems. In order to evaluate the chemical potential of the species involved in the phase equilibria calculations, expressions arising from mechanical statistics theory were employed. This expressions depend, among the other state variable, on the density of the phases. Thus solution of the chemical potential equalities require that the corresponding volumetric Equations of State are simultaneously solved for each phases. Equations of State are obtained assuming that equilibrium conditions holds: $G \rightarrow G_{\min}$, $P_{eq} = -\left(\dfrac{\partial A}{\partial V}\right) = f(V,T)$. It can be argued that such approach leads to calculation of the complete equilibrium conditions, in the meaning that not only thermal, mechanical and phase equilibria conditions holds between the species that forms the different phases, but also each phase is assumed to be at the equilibrium conditions pertaining to their pressure, temperature and composition. This can be safely regarded to be the case of quite all the systems that are made by low molecular weight species. Even if

departure from the local equilibrium conditions can be recognized under specific conditions and when the time scale of the observed phenomena is really low, in an engineering perspective, the equilibrium assumption can often be applied, at least as a first guess, usually with good results. It is remarkable that even physical and chemical details of premixed gaseous combustion fronts, detonation phenomena and shock waves, that are indeed really fast processes, have been successfully modeled applying Equation of States[102, 103]. On the other hand, it is a well recognized fact that the equilibration processes of macromolecular species below their glass transition temperature are kinetically hindered and the glassy phase is a non equilibrium phase. In many case, the properties of the glassy phase, for example its density, will change with time, but will remain pretty different from its equilibrium value even if the observation process is continued for really long times. Therefore, if a sample of glassy polymer is exposed to a controlled atmosphere of a given pressure of a vapor or gaseous species, some kind of apparent equilibrium will be reached between the low molecular weight components dissolved in the polymer and the external atmosphere. The gaseous phase outside the polymer can be assumed to be at equilibrium, thus suitable to be modeled with an Equation of State, while the same conclusion cannot be taken for the polymer phase, at least in a general sense. In fact, two cases can be distinguished. If the plasticizing effect of the low molecular weight species is strong enough, the glass transition temperature of the polymer phase could be lowered enough to be equal or lower than the temperature of the sample and thus also the polymer phase could be at equilibrium. In that case, not only the chemical potential of the low molecular weight species inside the polymer will be equal to that of the same species in the external gaseous phase, but also the volumetric behavior of the polymer phase could be described by means of an Equation of State. Then if this is the case, the solubility (and the phase equilibria) of the low molecular weight species in the polymer could be calculated with the already discussed equilibrium methods[94]. On the other hand, if the penentrants are not able to plasticize the polymer, that phase will remain glassy and out of equilibrium. Thus the Equation of State models should be used only to describe the

external, gaseous phase. Moreover, it is known that the initial density of the glassy phase, that is affected by its history, will exert an influence on the solubility of the low molecular weight species and that upon sorption of the penetrant, the glassy phase will swell. Thus the volumetric behavior of the glassy phase, that cannot be modeled with an Equation of State, is really important for the sorption process itself. This features of the sorption phenomena in glass polymers and the lack of classical thermodynamic tools that can deal with them, have hampered the development of theoretically models for the description of glassy polymeric systems and have led to a widespread use of deeply empirical models such as the previously mentioned Dual Mode model[88]. An approach that have to be remarked for its internal coherence and completeness is that of Kirchheim[82, 104-106], which assumes that in order to accommodate solute molecules inside the holes of the glassy polymer's free volume, the holes should somewhat undergo an elastic deformation process. The energetic contribution of the elastic deformation of the holes is taken into account using the tools of the elastic solid thermodynamics. Statistic arguments are then been employed to derive an expression for the sorption isotherms, starting from this simple microscopic picture and taking into account that the actual free volume is made by holes which size obeys a given distribution function. Both the Dual Mode model and the above mentioned Kirchheim approach, are inherently different from the usual tools of chemical engineering thermodynamics and the microscopic pictures onto which are based are not directly compatible with those of the molecular models that have proven their ability to describe equilibrium phases. In 1996 Sarti and Doghieri[14], using the conceptual tools of the thermodynamics of systems endowed with internal state variables, have introduced the Non Equilibrium Theory for Glassy Phase, that offers a general procedure that enables to extend the results of any equilibrium Equation of State model of the polymer penetrant mixtures, to the non equilibrium glassy state.

5.2. Non Equilibrium Theory for Glassy Phase

Glassy polymer phases are assumed to be homogenous, amorphous and isotropic. As previously observed, one of their properties that is more easily related to the distance from equilibrium is the density. This has been recognized long ago and it is a matter of fact that glass transition is commonly discussed in term of volumetric properties. Specifically, one of the diagnostic features of the glass transition, along with the change in heat capacity that is usually detected through calorimetric methods, is the change of the slope respect to the temperature of the isobaric volumetric curves in PVT data . Moreover, since the works of Struik[83] about ageing, it has been recognized that during ageing of the glassy polymer phases, their density drifts toward the equilibrium value, that is quite different from the value observed in the glassy phase. Moreover, when dilation data are available along the sorption isotherms, as in the case of the CO2 – PC data published by Fleming and Koros[107, 108], it is possible to recognize that the effect of conditioning, annealing and history of the samples, that is really evident in the sorption isotherm, it is paralleled by a corresponding effect on the volumetric properties of the polymer. Thus the choice of using the polymer density ρ_P as an order parameter that measures the departure from equilibrium, yet empirical, is quite straightforward and coherent with the actual level of knowledge of the physical picture of the glassy state. Since the evolution of this order parameter depends on the other variables that define the state of the system, it should be regarded as an internal state variable and its rate of change has to be assumed as a function of the temperature, of the pressure, of the penetrant mass fraction and on the polymer density itself:

5.1
$$\frac{d\rho_P}{dt} = f\left(T, P, \omega_1, \rho_P\right)$$

This function describes the volume relaxation processes of the glassy polymer matrix and should be retrieved from a rheological model that is able to identify the effective driving force and to describe the kinetic of the relaxation process

itself. Since the swelling of the glassy polymer matrix that is induced by the sorption of a low molecular weight penetrant has to be regarded as the result of a set of complex phenomena, a relevant amount of empiricism is required in order to choose the appropriate rheological assumptions. On the other hand, the pseudo equilibrium criterion for the phase equilibria between the low molecular penetrant dissolved in the glassy matrix and the one in the external gaseous phase, can be defined without any further attempt to identify a proper choice for the relaxation function. One has only to observe that pseudoequilibrium, that is inherently a kinetic fact, can be assumed to hold when the rate of change of polymer density becames negligible: $\frac{d\rho_P}{dt} = f(T, P, \omega_S, \rho_P) \approx 0$. In other words, pseudoequilibrium is not a condition that holds when same thermodynamic function is maximum or minimum like in true thermodynamic equilibrium, but pseudoequilibrium conditions are achieved when sorption and dilation kinetic slow down to the point that their characteristic times became longer than the characteristic time of the sorption experiment. Clearly, even in that condition, the mobility of the low molecular weight penetrant is not kinetically hindered, thus as shown by in 1998 by Sarti and Doghieri[109], the mass flux at the interface between the polymeric phase and the external gaseous phase can be zero only when the difference between the chemical potentials in the two phases became equal to zero. Therefore when the glassy polymer density is frozen at the non equilibrium value ρ_P, the pseudoequilibrium conditions for the low molecular weight component is:

5.2 $$\mu_S^{Ext}(T, P) = \mu_S^{NE}(T, P, \omega_S, \rho_P)$$

where $\mu_S^{Ext}(T, P)$ is the chemical potential of the penetrant in the external phase, while $\mu_S^{NE}(T, P, \omega_S, \rho_P)$ is the chemical potential of the penetrant in the glassy phase, that since is not an equilibrium phase, it depends also on the

order parameter ρ_P. Chemical potentials on a mass basis, even under non equilibrium conditions, can be calculated by derivation of the Helmholtz Free Energy per unit of volume respect to the mass density of the single species. Thus once an expression for Non Equilibrium Helmholtz Free Energy is available, the equality of the chemical potential in pseudo equilibrium condition can be solved for the penetrant mass fraction and the computations of the solubility isotherms in glassy polymer could be performed. Under non equilibrium conditions, it is assumed that a functional dependence of the following form $A'''^{NE} = A'''^{NE}(T, P, \rho_P, \rho_S)$ holds, with ρ_P acting as an order parameter. The main achievement of the Non Equilibrium Theory for Glassy Phase by Sarti and Doghieri[14, 25, 26, 109, 110] is that proper maps of the non equilibrium thermodynamic functions in term of equilibrium thermodynamic function are given by the simple relations which follow:

5.3 $$A'''^{NE}(T, P, \rho_P, \rho_S) = A'''^{EQ}(T, \rho_P, \rho_S)$$

5.4 $$\mu_S{}^{NE}(T, P, \omega_S, \rho_P) = \mu_S{}^{EQ}(T, \omega_S, \rho_P)$$

Non equilibrium properties are calculated with the same expressions that arise from equilibrium theory, except for the fundamental fact that the polymer density ρ_P is not the value that can be obtained as the root of an Equation of State but should be experimentally known or should be estimated on the basis of the rheology of the swelling process, in order to represent the specific non equilibrium state of a given sample of glassy polymer. For the case of sorption experiments, the density value should be the one at the end of the sorption step, when $\frac{d\rho_P}{dt} = f(T, P, \omega_S, \rho_P) \approx 0$. In the cases in which pressures are really low, and penetrant activities also are low, the mass uptake will be quite limited and swelling of the polymer matrix could be negligible and pseudoequilibrium calculation could be performed assuming that the polymer density is equal to the density of the dry polymer, as measured before sorption. In the other cases the extensive literature available on the application of the Non Equilibrium

Theory for Glassy Polymer show that a simple linear relationship is usually adequate for estimating the swelling of the polymer matrix:

5.5
$$\rho_P = \rho^0{}_P \left(1 - k_{sw} P\right)$$

The coefficient k_{sw}, whose units are that of the reciprocal pressure, is known as the swelling coefficient and represent the swelling of the glassy polymer phase, upon sorption of the penetrant. This expression is an integrated form of the evolution law $\frac{d\rho_P}{dt} = f(T, P, \omega_S, \rho_P)$, but is not able to provide, per se, any guidance on the kinetic of the relaxation processes, since effectively does not bear any explicit link to any rheological model and is commonly used as an adjustable parameter, unless dilation data are directly available. Minelli et al. in 2012[111], have shown that a simple viscoelastic model can be used for predicting the swelling behavior and the onset of solvent induced glass transition. The model is defined assuming that the total specific polymer volume, below glass transition, is made by the sum of two contributions, one for the relaxation modes that have relaxation times shorter than the duration of the sorption experiments, and one for the relaxation modes that can relax on longer times. The short term modes are supposed to owe to a fraction of polymer that is able to equilibrate to the density values that correspond to the true thermodynamic equilibrium, at the actual temperature, pressure and penetrant chemical potential. The short term contribution will be named $\hat{V}_P{}^{EQ}(T, P, \mu^S)$ and should be calculated from an appropriate equilibrium model, such as a Volumetric Equation of State. The long term modes are assumed to represent an absolutely rigid element, that is not affected by the sorption process, and will be indicated as $\hat{V}_{P,g}$.

5.6
$$\hat{V}_P = \frac{1}{\rho_P} = \chi \hat{V}_P{}^{EQ}(T, P, \mu^S) + (1 - \chi)\hat{V}_{P,g}$$

The weight factor χ between the short term and the long term modes has been shown by Carlà et al.[112] and by Minelli et al.[111] to be equal to the ratio between the apparent compressibility of the glassy polymer and the compressibility of the same polymer under rubbery (equilibrium) conditions, evaluated in the vicinity of the glass transition temperature. Once that the parameter χ is known, the specific volume of the long term modes $\hat{V}_{P,g}$ can be estimated from the dry glassy polymer density, that can be regarded as the limit of $\hat{V}_P$ for vanishing pressure. It is interesting to note that at the penetrant pressure at which glass transition is induced by the plasticizing effect of the sorbed molecules, the equilibrium specific volume is equal to the specific volume of the rigid element that represents long term modes:

5.7 $$\hat{V}_P^{EQ}\left(T,P,\mu^S\right)=\hat{V}_{P,g}$$

This simple, yet powerful approach, enable to show that the above mentioned linear swelling relationship is a first order approximation of the dependence of the non equilibrium polymer specific volume respect to the penetrant external pressure. A rigorous application of this approach could have been really interesting in the present case, since several of the collected isotherms range from the glassy region to the rubbery one, passing through the solvent induced glass transition. Unfortunately in order to apply that approach it is necessary to estimate some parameters that are directly related to the volumetric behavior of the polymer under equilibrium condition and presently no such data are available for Matrimid 5218, manly due to the fact that its really high glass transition temperature poses a serious challenge to the ability to perform the PVT measurements above glass transition temperature without interference from pirolysis and other thermal degradation processes. In any way, some comments and estimates about the parameters of that simple viscoelastic model will be discussed along the way of presenting the modeling results for the sorption isotherms.

The conceptual framework of Non Equilibrium Thermodynamics of Glassy Phase is independent from the choice of the thermodynamic model, since it is based on general results on how to map the non equilibrium states respect to a known representation of the equilibrium ones. Originally the thermodynamic model used was the Lattice Fluid Equation of State by Sanchez and Lacombe and the non equilibrium model was known as Non Equilibrium Lattice Fluid or NELF. Since the first paper from Sarti and Doghieri, many others models have been considered for providing a suitable representation of the Helmholtz Free Energy, for example the Statistical Associating Fluid Theory in its various version, known as NE – SAFT, NE-PCSAFT and so on. In the present work, modeling results obtained with the NELF and NE PCSAFT version of the general Non Equilibrium Thermodynamic of Glassy Phases will be shown.

5.3. Non Equilibrium Lattice Fluid

The Sanchez Lacombe characteristic parameters for the low molecular weight penetrants were obtained from the literature and are typically obtained through regression of pure component vapor liquid equilibria and saturated liquid densities. The characteristic parameters of Matrimid 5218 adopted for the calculations are those presented in Minelli et al.[113], to be published in 2013, that have been retrieved by means of an alternate procedure, that is described in the following lines. As previously said, the rigorous way to retrieve the characteristic parameters of volumetric Equations of State for polymeric species is to regress them on the PVT isobars at temperatures above glass transition. Since no such data exists for Matrimid 5218, a different approach had to be used. The alternate procedure have been previously used by the Sarti and Doghieri research group, for those polymers for which no PVT data in the rubbery region exists, like PTMSP and AF2400[114]. The procedure is based on the fact that whenever infinite dilution solubility coefficients of several gases are available, the characteristic parameters of Sanchez Lacombe equation of state

can be obtained with a best fitting procedure of regression of those data. At low pressure the swelling coefficient can be set to zero, so no dilation was taken into account and the dry polymer density values available in the original papers from which the solubility data were taken were used directly. The binary interaction parameters were set equal to zero. This characteristic parameters were then validated against low and high pressure isotherms of selected gases. All the characteristic parameters that have been used are reported in Tab. 5.1.

Substance	T* [K]	P* [MPa]	ρ* [g/cm^3]	Ref.
Matrimid 5218	880	450	1.350	**113**
Water	670	2400	1.050	**113**
Methanol	510	1080	0.900	**113**
Dichloromethane	487	560	1.540	**113**

Tab. 5.1   Sanchez Lacombe EoS Characteristic parameters for the substance of interest, retrieved from several different sources.

Then the Non Equilibrium Lattice Fluid Model has been applied to modeling the experimental sorption isotherms that have been already shown in the previous chapter. The dry glassy polymer density was set equal to $1.239 g / cm^3$, as determined in Minelli et al.[113] for specimens weighted in air and dodecane at 27°C. The binary interaction parameters and the swelling coefficients are considered adjustable parameters that can be used for optimizing the model prediction, in order to regress the actual isotherm. When mass uptake was reasonably high, so that it seemed justifiable to assume that the highest activity points could be close to the true thermodynamic equilibrium, the binary coefficient was checked against them using directly the equilibrium model, while the swelling coefficient was regressed only on the mid activity data points, where the concavity of the sorption isotherm was indeed that of a glassy polymer. The change in concavity and the onset of glass transition was quite obviously recognizable in the case of the 10°C sorp tion isotherm of dichloromethane, that is a good solvent of Matrimid. In other cases, such as for the oxygenated components, the liquid solubility has been found to be

dependent on sample thermal history. This is a well known feature of polymeric glasses. Then it is clear that even if the liquid solubility is perfectly modeled by the equilibrium models, the actual equilibrium nature of that points could be questioned. In fact, since around unit activity the equilibrium solubility curve is rather steep, a slight change of the value of the binary interaction parameter could be enough to predict a very different value of the solubility, ranging in the full span experimentally observed, and without affecting too much the prediction of the non equilibrium portion of the isotherms. It could be argued that in this case the actual value of the binary interaction parameters provide a correction to some of the error that is done when a true equilibrium model is used to regress data obtained for conditions in which some departure from equilibrium is still there.

The first example of solubility isotherm modeling that will be considered is that of water in Matrimid 5218. In order to model the water solubility isotherm at 308 K, it was made the choice to assume that no swelling is taking place and thus the swelling coefficient have been set equal to zero. In fact the mass uptake is so limited, that no swelling or plasticizing effect could be postulated, similarly to what could be observed for gas solubility at low pressure, for the same polymer. The results of the NELF model, shown in Fig. 5.1, are in quite a good agreement with the experimental values up to activity equal to 0.6, where larger deviation and a change in concavity start to appear. This change in concavity cannot be justified in term of plasticization and thus it should be regarded as an effect of the water hydrogen bonding, that is an effect that is well beyond the limits of the physical picture on which the Sanchez Lacombe Equation of State is based. It must be reported that with the parameters available for water substance, its saturated liquid density is poorly predicted, as it is expected for a model that does not take into account hydrogen bonding.
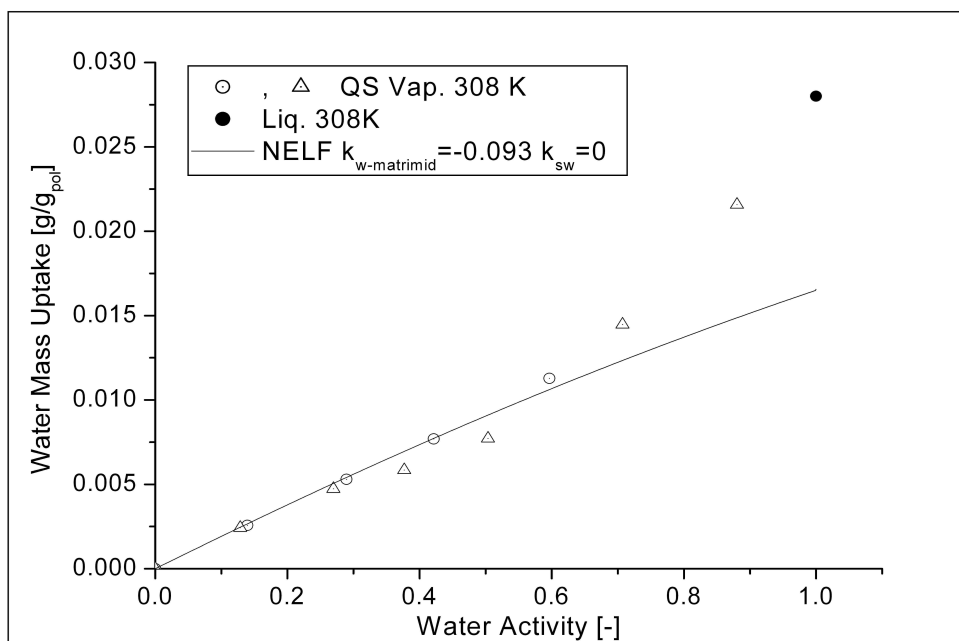
Fig. 5.1   NELF modeling of the sorption isotherm of water in Matrimid 5218 at 308 K, complete with the value measured for liquid water. The swelling coefficient was set equal to zero, under the assumption that at such low mass uptake, the effect of the partial molar volume of water is negligible.

As shown in Fig. 5.2, the methanol sorption isotherm at 35℃ can be modeled quite adequately up to activity 0.6, modeling the swelling of the polymeric matrix through the linear swelling relationship. The solubility of the liquid cannot be directly represented neither through linear swelling, nor through the equilibrium model. In fact, if the equilibrium sorption isotherm is calculated with the binary interaction parameter that has been obtained trough regression of the experimental data at low activity with the non equilibrium model, the results deeply underestimate the liquid methanol solubility. Even if it is known that methanol could give rise to polar or even to hydrogen bonding interactions, the parameters used for the pure methanol are known to provide excellent description of both vapor pressure and saturated liquid density. Moreover the sorption is quite big and thus there is no way to dismiss the possibility that the upward concavity in the higher activity region is to be considered due to swelling phenomena.
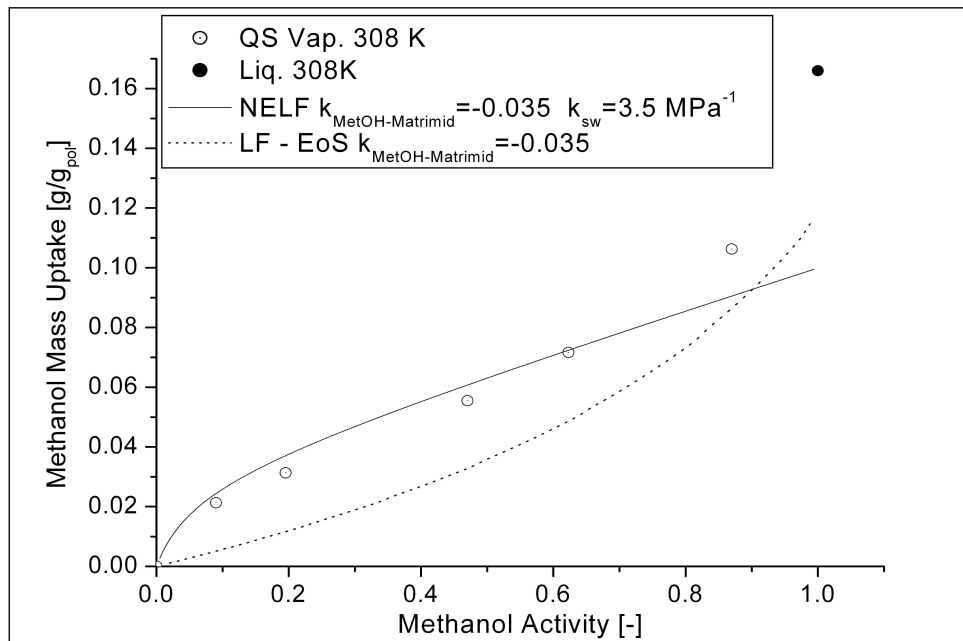
Fig. 5.2   NELF modeling of the sorption isotherm of methanol in Matrimid 5218 at 308 K. The mass uptake is certainly enough to compel the necessity to take into account swelling phenomena. The equilibrium isotherm lies entirely below the complete set of experimental data and not even the data pertaining to the liquid methanol could be considered as a true equilibrium point.

Finally the modeling of the sorption isotherms of dichloromethane in Matrimid 5218 at 283 K and 305 K was attempted. The isotherm at 283 K is quite peculiar and intriguing, since it shows a really evident change of concavity, that clearly suggest the onset of the penetrant induced glass transition. Therefore the binary interaction parameter for the pair dichloromethane – Matrimid 5218 was retrieved fitting directly the higher pressure portion of that isotherm with the true thermodynamic equilibrium Sanchez Lacombe model. Subsequently the values of the swelling coefficients required in order to apply the model to the non equilibrium portion of the same isotherm and to the 305K isotherm were retrieved directly from the comparison with the experimental data. Therefore the modeling of the equilibrium portion of the 283 K isotherm was performed with only one adjustable parameter, namely the binary interaction parameter $k_{DCM-Matrimid}$, while the non equilibrium isotherms were modeled with again only one adjustable parameter, the swelling coefficient k_{sw}. The comparison between

the experimental isotherms and those predicted with the NELF model can be considered excellent, as shown by Fig. 5.3.
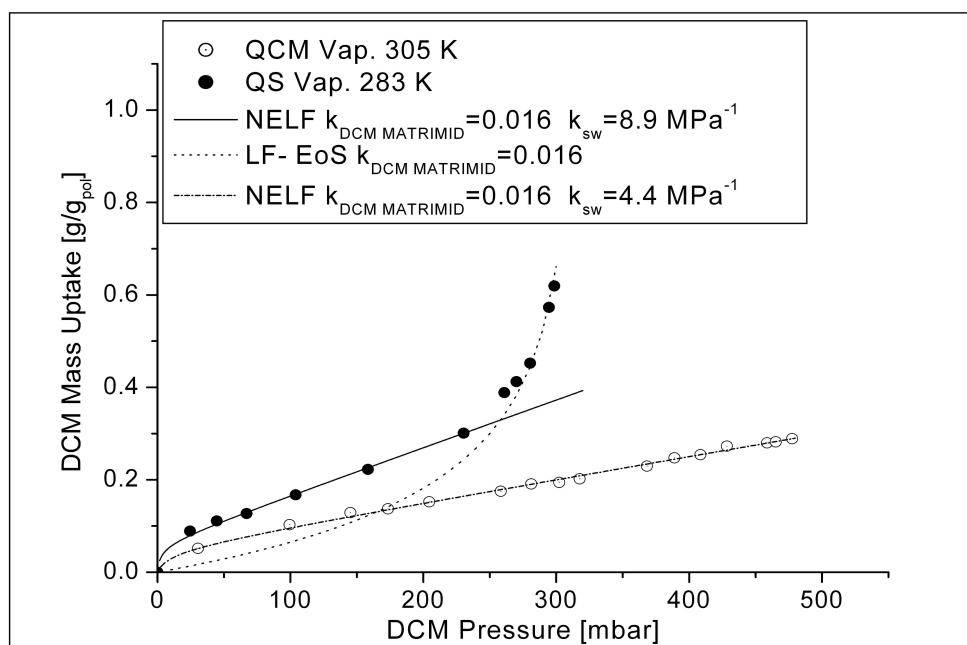
Fig. 5.3   NELF modeling of the sorption isotherms of dichloromethane in Matrimid 5218 at 283K and 308 K.

As previously observed, there are no available equilibrium volumetric data of the pure Matrimid 5218 in order to apply the latest development of the model, that ideally would be capable to predict the swelling behavior upon sorption, up to plasticization. In what follows, a simplified approach will be discussed, in order to show how and to what extent, it could be possible to apply the model. As a starting point, it is possible to observe that the specific volume of the polymer at the glass transition pressure could be estimated by means of finding the specific volume at the pressure corresponding to the point of intersection between the isotherm predicted with the NELF and the isotherm predicted with the Sanchez Lacombe EoS. The polymer specific isotherm volumes at 283K for the dichloromethane sorption had been calculated with the equilibrium Sanchez Lacombe and with the linear swelling hypothesis and are depicted in Fig. 5.4 and the crossing point can be recognized to take place around 270 mbar. The

specific volume of the rigid contribution is $\hat{V}_P^{EQ}(T, P, \mu^S) = \hat{V}_{P,g} = 1.075 \quad cm^3/g$.

Since the dry polymer density is known and the equilibrium density of the pure polymer can be estimated through the Sanchez Lacombe Equation of State, also the weight factor χ now can be estimated. The value that is obtained through this calculation is $\chi = 0.815$, a rather high value, but that it is still among the range of values found with the rigorous procedure by Minelli at al.[111], for many other glassy polymers. Now that both parameters are known, the calculation of the complete isotherms could be performed, but this time only the binary interaction parameter can act as an adjustable parameter, since the swelling coefficient is no longer required. In the case of the dichloromethane sorption isotherm the results are shown in Fig. 5.5. The value of the binary interaction parameter was kept equal to the value that had been previously retrieved from the equilibrium portion of the 283 K isotherm. The results for the DCM Matrimid isotherm at 10℃ is remarkable, while the comparison with a set of sorption data collected at 35℃ on the same Quartz Spring Apparatus show some deviation in the higher pressure region, but the agreement is still good. It was chosen to apply the complete model, with the parameters retrieved according to the previously introduced simplified procedure, only to the results of the Quartz Spring experiments, because similar conditions apply, respect to the thickness and the mechanical constraints acting upon the sample. In fact, in the Quartz Cristal Microbalance, the samples were much thinner (~1 µm in QCM respect to ~50 µm in the case of QS) and are supposed to adhere to a rigid substrate, while in Quartz Spring the film is left free standing. Both parameters could exert some effect on the swelling behavior, that is a relaxation phenomenon taking place in non equilibrium, history dependent material. Comparison with the methanol – Matrimid 5218 dataset, shown in Fig. 5.6, is certainly of interest, because despite some systematic overestimate, the shape of the isotherm is predicted quite well and with a little change of the binary interaction parameter from the value previously used, it is possible to give reason of the liquid solubility. It must be emphasized that the equilibrium model, with the same values of the binary interaction parameters, underestimate the

liquid solubility, as previously shown, while the present model, taking into account the extra free volume of the glassy phase can produce a more reasonable estimate. This results have been obtained with a pretty rough estimate of χ and $\hat{V}_{P,g}$, and using only one adjustable parameter for each polymer penetrant pair. Therefore the resulting predictions of the swelling behavior, at temperature different from the one of the isotherm that was used for estimating $\hat{V}_{P,g}$ and for a different penetrant, are to be considered satisfactorily. Finally it is interesting to note that when the model for swelling is applied to the prediction of the water solubility isotherm, as shown in Fig. 5.7, the results are quite the same of the simpler model that was shown previously and for which $k_{sw} = 0$ was postulated, at least up to activity 0.5. Even if at larger activity the complete model have a slightly better performance, still it is not able to take into account of the change of curvature. Thus the no swelling hypothesis, albeit not completely correct, was quite a good one and the deviations of the experimental data from the model predictions at high activity have to blamed mainly to hydrogen bonding effects.
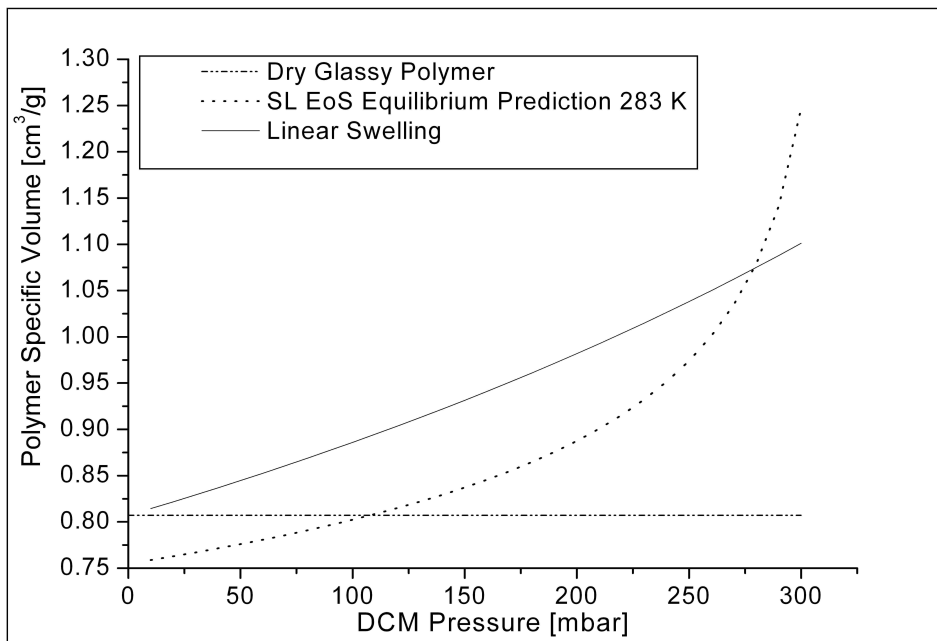
Fig. 5.4   Equilibrium and non equilibrium polymer specific volume as a function of the penetrant pressure.
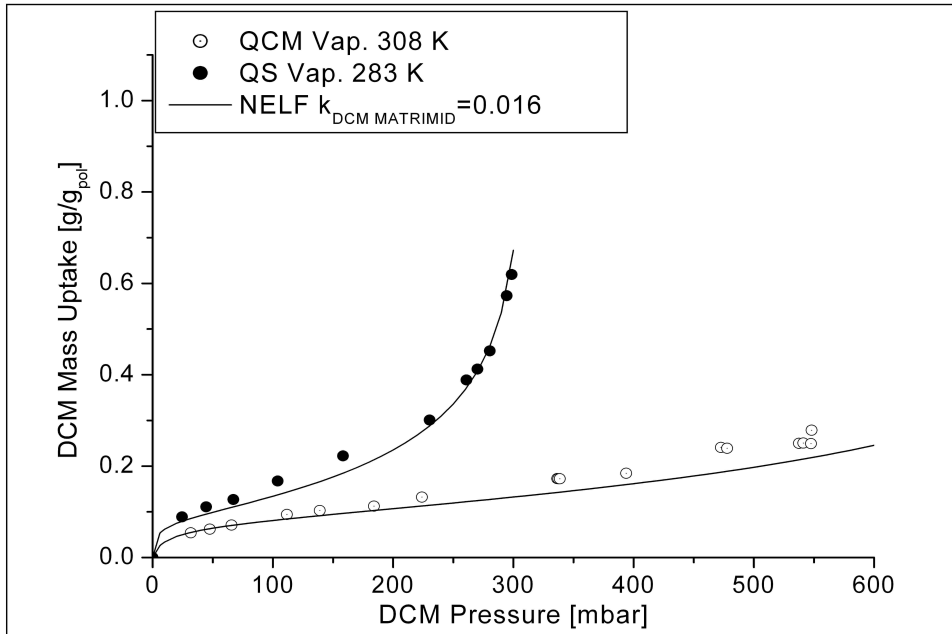
Fig. 5.5   Solubility isotherms of Dichloromethane in Matrimid at 283 K and 308K, with swelling behavior prediction according to the latest version of the Non Equilibrium Thermodynamic for Glassy Phase model.
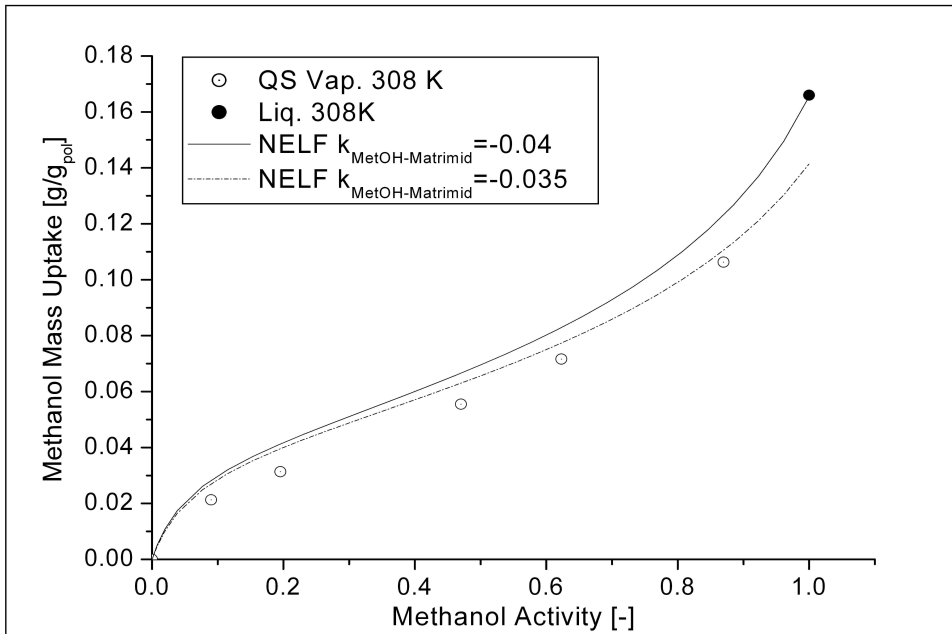
Fig. 5.6   Solubility isotherm of Methanol in Matrimid at 308K, calculated with the swelling behavior prediction according to the latest version of the Non Equilibrium Thermodynamic for Glassy Phase model. The results of calculations shown with two slightly different values of the binary interaction parameters are shown.
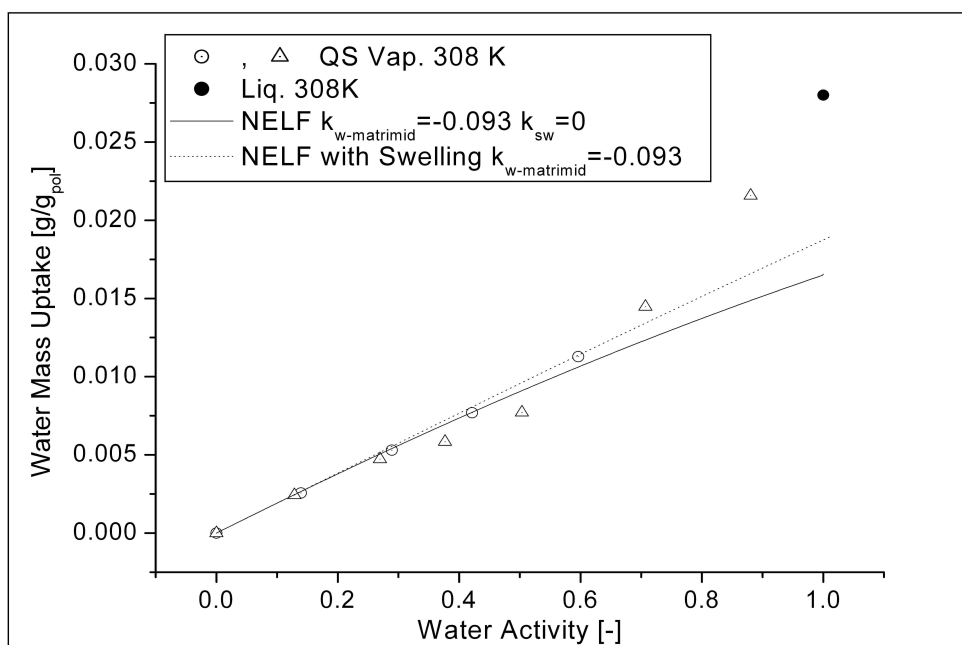
Fig. 5.7   Solubility isotherms of water in Matrimid at 308K, with swelling behavior prediction according to the latest version of the Non Equilibrium Thermodynamic for Glassy Phase model. For comparison the result of the calculation without swelling is shown.

5.4.   Non Equilibrium Perturbed Chain Statistical Associating Fluid Theory

As previously said, the Non Equilibrium Thermodynamic of Glassy Phase approach is general and have been applied to many different equilibrium thermodynamic models[25, 26]. Among them, one of the most interesting is the extension to non equilibrium of the Perturbed Chain Statistical Associating Fluid Theory by Gross and Sadowski[22-24]. The non equilibrium version will be indicated as NEPC-SAFT. The characteristic parameters for the low molecular weight species considered for the modeling of their sorption isotherms in Matrimid 5218 are listed in Table 2 and were available in the literature, from several sources that are indicated in the same table. Also the characteristic parameters for Matrimid 5218 were available in the literature, from a paper by Hesse and Sadowski[29] and were obtained by fitting on a data set made by the solubilities of several liquids in Matrimid 5218 and simultaneously to the PVT

data of a mixture made of Matrimid 5218 and dimethylsulfoxide, a known solvent of the Matrimid 5218 itself. That mixture was really lean in polymer, since the Matrimid 5218 mass fraction was equal to 2.5% and thus also the quality of the dimethylsulfoxide plays a major role in the regression procedure adopted for retrieving Matrimid 5218's parameters. It must be observed that the liquid solubilities are probably referred to a glassy, not yet completely equilibrated state, as observed also for the data discussed in the present work, but had been fitted by Hesse and Sadowski[29] by means of an equilibrium solubility calculation. Moreover, the prediction of PVT of the liquid mixture of Matrimid 5218 and dimethylsulfoxide is characterized by some systematic deviation between the experimental and the calculated values. Therefore the use of this parameter should be regarded as a strictly empirical one, but this is to be blamed only to the fact that when dealing with glassy polymer with such an high glass transition temperature, the measurement or the estimation of any equilibrium thermodynamic properties is impervious.

Substance	m/M [mol/g]	σ [Å]	ε [K]	Ref.
Matrimid 5218	0.0380	3.1	320.0	**29**
Acetone	0.0498	3.2279	247.4	**115**[115]
Methyl Acetate	0.0424	3.1888	235.8	**116**[116]
Dichloromethane	0.0266	3.338	274.2	**116**

Tab. 5.2   Pertubed Chian Statistical Associating Fluid Theory EoS Characteristic parameters for the substance of interest, retrieved from several different sources.

As examples of application of the NEPC-SAFT, it was decided to consider the case of Acetone, Methyl Acetate and Dichloromethane. Since the code available at the University of Bologna does not have the capability to use a validated association contribution term, the modeling of water and methanol, that would have proven to be powerful benchmarks for the NEPC-SAFT model, was not attempted. The solubilities of Acetone and Methyl Acetate in Matrimid 5218 at 308K at activity lower than one are available in Minelli et al.[113]. The modeling results Acetone and MetylAcetate are depicted in Fig. 5.8 and Fig. 5.9. As previously discussed, the solubility of the liquid penetrants was found to

be somewhat history dependent and thus it could be argued that the polymer, even for mass uptakes in the range of 0.3 ÷ 0.4 g/g_{pol} of this two penetrants, retains some kind of the character of the glassy phases. It must be cited that while performing the liquid sorption experiments for characterizing acetone and metylacetate solubility in Matrimid 5218, it was observed the development of cracks and crazes in the samples, both around the edges and in the bulk of the specimens. Therefore it is reasonable to say that an internal stress state developed upon sorption of the penentrant. In literature, such as in the works authored or supervised by Francis, McCormick and Scriven of the University of Minnesota[68-71], there is a wide consensus that stress states in polymer solvent system arise due to frustrated swelling or frustrated shrinkage. In other words, if the specific volume of the sample in the stress free state is different from the actual specific volume, the actual state is a strained one and if the material is capable of elastic answer, stress arise. Eventually, if the material can also behave viscously, the stresses will relax and fade. When this is not possible, due to a lack of viscous answer or due to some constraint, the stress could build up to the point of locally exceeding the strength of the material. Since the films used in this work were free standing, the stress state could not be due to the effect of an external constraint, but are to be blamed to the absence of viscous relaxation, or to a characteristic time of the stress relaxation process far too large respect to the characteristic time of the stress build up (and thus of the sorption process). It is interesting to note that the sorption kinetic for acetone and methyl acetate are really close to the Fickian one and after the knee of the curve, no ongoing relxation was observed. This could indeed be the case of a rubber, but the appearance of stresses and of history dependence for the solubility value are characteristics of the glassy state. Thus no definite decision can be made regarding to considering the solubilities at unitary activity as equilibrium or non equilibrium ones. It appeared that those points were fitted quite naturally with the equilibrium curve. In the case of methyl acetate, shown in Fig. 5.9, it was also quite evident that a change in concavity is taking place for penetrant activities higher that 0.8. Following this discussion, it appears that the most correct point of view is to say that binary interaction parameters and

swelling coefficients were regressed simultaneously on the full isotherm, by comparing the equilibrium and non equilibrium predictions with the experimental data, again simultaneously. In this way some of the ambiguities about the exact nature of the liquid solubility are removed and the good agreement between the liquid solubilities and the values predicted with the equilibrium model is a mere consequence of the good results obtained at lower activities with the non equilibrium model.
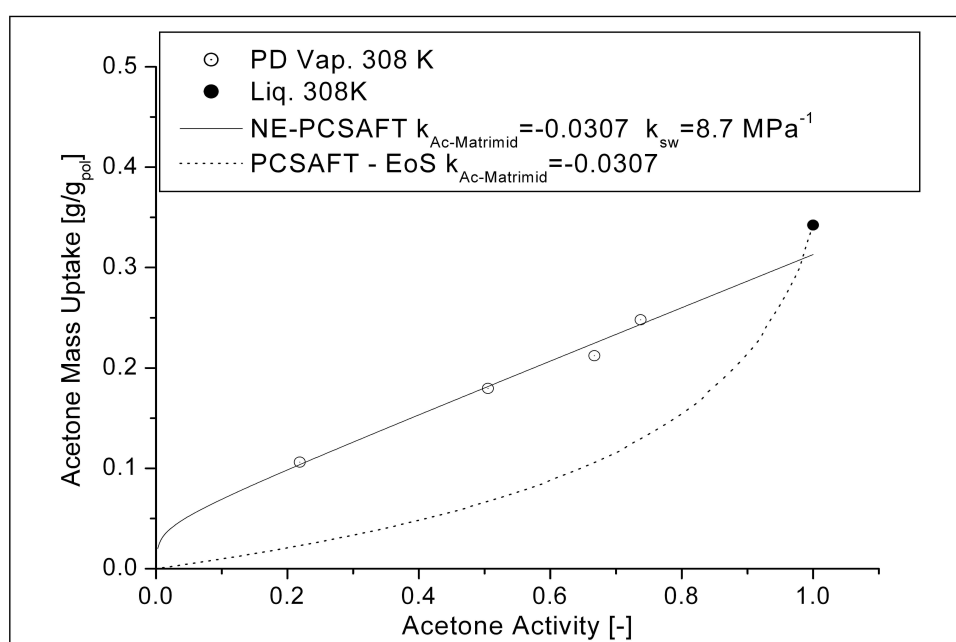
Fig. 5.8   Solubility isotherm of Acetone in Matrimid 5218 at 308K, predicted with NEPC-SAFT and PC-SAFT models.
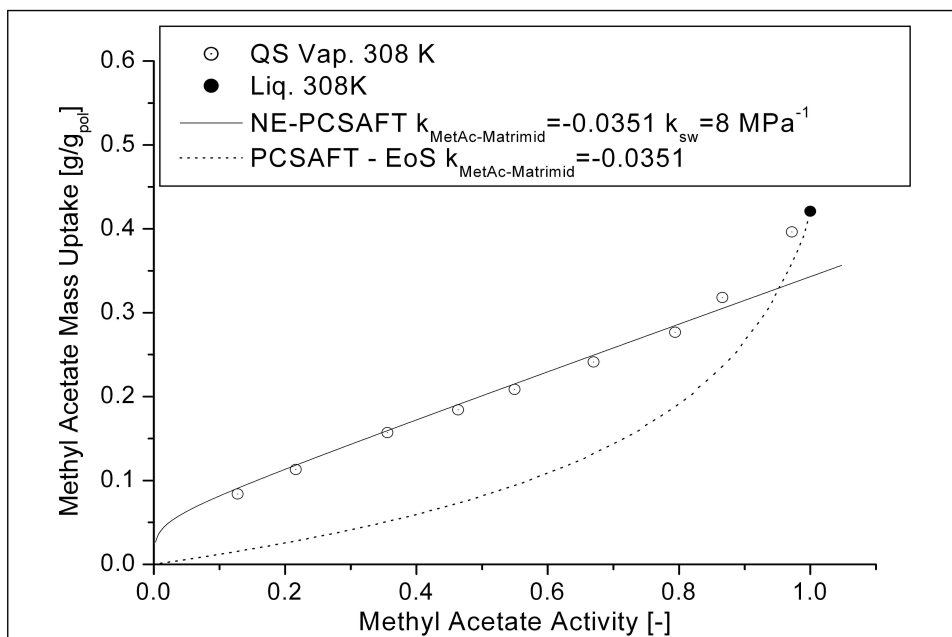
Fig. 5.9   Solubility isotherm of Methyl Acetate in Matrimid 5218 at 308K, predicted with NEPC-SAFT and PC-SAFT models.

Modeling of the solubility isotherms of dichloromethane in Matrimid 5218 was done with the same procedure adopted for NELF, with excellent results, shown in Fig. 5.10. It should be noted that the swelling coefficients required for fitting the non equilibrium portion of the isotherms were found to be lower than that found when applying the NELF model. The same effect is observable for the swelling coefficient for Acetone and methylacetate in Matrimid 5218, when compared to those that can be found in Minelli et al.[113] . This systematic differences could be explained by taking into account that different models could predict different partial molar volumes of the penetrants in the mixture with the polymer and on the fact that since the parameters for the Matrimid 5218 had been retrieved with two different empirical procedure, the close packing state and thus the free volume available in the glassy polymer matrix could be predicted in different way by NELF and NEPC-SAFT. Since this differences, it was retained that application of the latest version of the NET-GP approach in order to predict the swelling behavior of the glassy Matrimid 5218, would have been of limited usefulness.
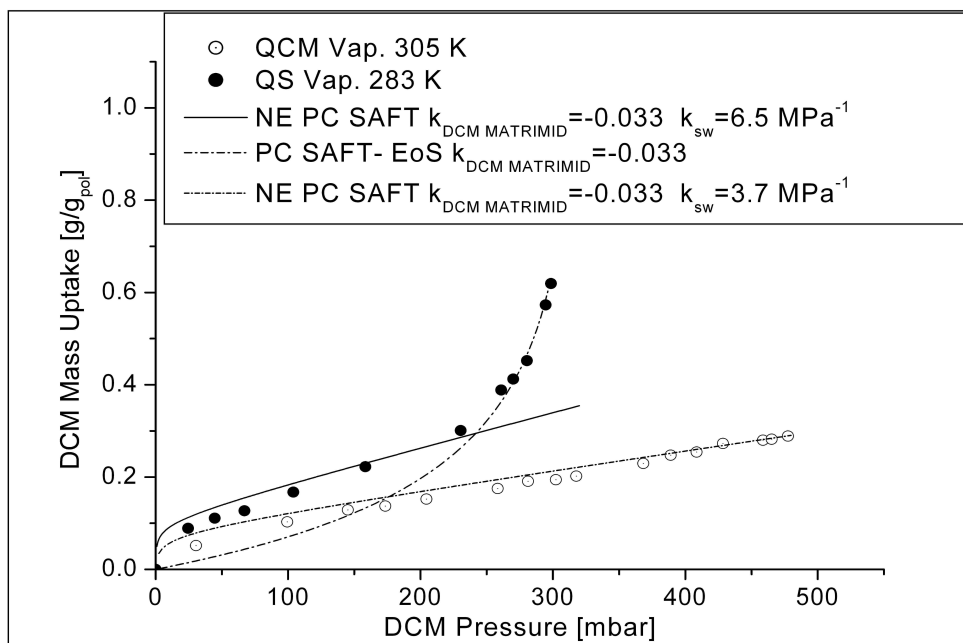
Fig. 5.10   Solubility isotherms of Dichloromethane in Matrimid 5218 at 283 K and 305K, predicted with NEPC-SAFT and PC-SAFT models.

5.5.   Concluding Remarks

In his chapter modeling of the sorption isotherms of low molecular weight species in glassy Matrimid 5218 with the NET-GP approach had been performed, applying the NELF and the NEPC-SAFT versions of the NET-GP. In some cases, when plasticization induced by solvent was reasonable, modeling with equilibrium models was attempted with success. A simplified procedure for applying the latest version of NET-GP/NELF in order to predict the swelling of the polymer matrix was applied, again with good results.

6. Modeling of the Sorption Kinetic of Low Molecular Weight Species in Glassy Matrimid 5218 within the NETGP framework

6.1. Introduction

The kinetic of the sorption (and desorption) of low molecular weight species in glassy polymers is relevant to many industrial processes and applications. In fact, processes like the production of polymeric foams, membrane separation processes, coating deposition and drying, controlled drug release and sensor applications are deeply affected by the kinetic of the mass transfer of low molecular weight in polymers that are quite often used at temperatures below their glass transition temperature. The production of foam from expandable thermoplastics requires that polymer pellets, loaded with a given amount of blowing agents, undergo a sudden temperature jump, along with the exposure to a suitable heat carrier, in order to trigger the start of the expansion process. Upon heating, inside the bulk of the pellet, the solvent starts the nucleation of multitude of bubbles and their internal pressure drives the expansion process. The diffusion of the solvent, along with the viscoelastic answer of the material to the stress state that develops, deeply affect the expansion process, in terms of global kinetic and final morphology of the expanded pellets. The process is run

at a temperature lower than the actual glass transition temperature of the neat thermoplastic, but close to the value of the glass transition temperature of the mixture made by the polymer loaded with the blowing agents. Modeling the kinetic of the sorption and desorption of the blowing agent could be useful for process analysis and optimization. Membrane separation process are usually operated under steady state conditions and in the case of dense films the solution diffusion model applies. The parameters that control the permeation across the membrane and its selectivity are the solubilities and the diffusivities of the low molecular weight species, under steady state conditions. Although apparatus specifically designed for characterizing the gases and vapors permeabilities across membranes exist, they commonly provide a direct measurement only of diffusivity and permeability, while solubility is only estimated from the other two variables. Therefore it is quite common to perform differential and integral sorption experiments in order to characterize directly the solubility of the low molecular weight species in the membranes. As shown by Crank[77], differential sorption experiments enable to observe how the diffusion coefficient is affected by the average concentration of penetrant across the membrane and thus provide information relevant also to the steady state permeation process. The experimental data obtained from sorption experiments can be used to validate a model that, in turn can be used for design and for predicting the performance of a membrane separation device, for instance. The drying of polymer coating is essentially a desorption process: while solvent concentration decreases, the concentration of the macromolecules increases and the mechanical properties shift from the ones of a viscous liquid to the ones of a tough, elastic solid material. If the glass transition temperature of the polymer that is being used in the coating formulation is above the ambient temperature, then when the solvent concentration became lower than the amount required for plasticize the polymer, vetrification takes place and finally the coating would be glassy. The evaporation of the solvent takes place at its free boundary, while commonly the substrate onto which the coating is being applied is quite impermeable respect to the solvent. Thus the drying process takes place along with the diffusion of the solvent across the coating. If the

characteristic time of the drying process is far lower than the characteristic time of the mechanical relaxation processes, the build up of the stresses in the film will finally cause the appearance of cracks, delaminations and other defects. In the case of drug controlled release, the rate of release of the drugs, for example from a pill, into the body, should be tailored respect to the gastrointestinal transit time, the pharmacokinetics, dosage and blood concentration required in order to guarantee the pharmacological activity. A lack of control of the rate of release of the drug will cause an improper concentration in the blood, possibly causing toxic effects in the case of an excessive release, or a concentration too low to exert the desired pharmacological effect, or even causing the elimination of the pill along with the feces before the complete release of the required dosage. Usually the pills, as well as others drug controlled release devices, are made by a polymeric matrix loaded with the drug and the others ancillary components. The rate of release is determined, along with many other factors that acts in the *in vivo* environment, by the rate of diffusion of the drug in the polymeric matrix, as well as by the swelling, the sorption of water and other fluids and, in same case, by the degradation of the polymer itself (i.e. due to hydrolysis). Again a modeling tool capable of dealing with sorption, desorption and swelling of the polymer matrix in glassy state can be useful for the design and optimization of controlled drug release devices. Similar reasoning applies to the cases of sensors made by a polymer film conjugated with an electromechanical transducer. In fact the solubility and diffusivity of the low molecular weight species to which the sensor is exposed and the induced swelling in the polymer film directly affect the sensibility and the response time of the sensor itself.

As previously said in the chapter of the experimental sorption results, a constitutive law is required in order to close the set of mass balance equation in local form. Constitutive laws cannot be derived directly from the conservation principles or from the law of thermodynamics, but they should be based on experimental observation and should never contradicts the Second Law of Thermodynamic, as well as the principle of locality, causality and material objectivity (their form should not depend from the reference frame). For

example, the assumption that the diffusive mass flux of a given component is proportional to the gradient of its chemical potential could be a rather general form of constitutive equation for diffusion. A complete and extensive discussion of this topics can be found in the works of Truesdell[117] and Slattery[6] on continuum thermomechanics and rational thermodynamic, therefore it will not be discussed further here. A more common choice, that can be obtained through application of the chain rule to the gradient of the chemical potential and with some reasonable simplifying assumptions, is that the diffusive mass flux of a component is proportional to its concentration gradient. This constitutive equation is known as Fick's law and has been found to be applicable to a huge number of cases. As previously discussed, sorption of low molecular weight penetrants in glassy polymers is one of the most notorious exceptions. Useful insight in the non Fickian sorption of solvents and low molecular weight penetrants in glassy polymers can be gained considering the characteristic timescales of the diffusion process and of the relaxation processes. Diffusion characteristic time can be readily estimated as $\tau_D = \dfrac{\delta^2}{D}$, where δ is the thickness of the sample along the sorption direction, while D is the diffusion coefficient of the penetrant in the polymer. The characteristic time of the relaxation processes is somewhat undefined, since a truly unified view on the argument is lacking, but a close analogy to rheological (mechanical) relaxation processes, like in creep or in stress relaxation can be surely portrayed and the characteristic time of polymer relaxation can be assumed to be the ratio between viscosity and bulk modulus of the polymer matrix: $\tau_R = \eta / E$. The ratio between polymer relaxation characteristic time and diffusion characteristic time is a dimensionless quantity known as Deborah number and is commonly used for identifying different regimes in the analysis of non Fickian sorption.

6.1 $$De = \frac{\tau_R}{\tau_D}$$

When $De \ll 1$, the polymer will relax much faster than the time required to the low molecular weight penentrant molecules in order to diffuse from the boundary of the sample to its core. Therefore the diffusion process will mainly take place in an already relaxed polymer matrix and the process will be adequately represented by means of the Fick's constitutive law. In the case in which $De \gg 1$, the relaxation process will take longer than the diffusion and separate contribution to the sorption process could be recognized. For example, in low pressure gas sorption in glassy polymers, the penetrant does not plasticize significantly the glassy matrix and thus the relaxation times are much longer than the duration of the sorption experiment itself. For differential sorption experiments for which $De \gg 1$ and the duration of the sorption experiment is longer than the polymer relaxation time itself, the sorption kinetic will present two separate stages. The first one, that exhibits a kinetic close to the Fickian one, is due to the diffusion driven mass uptake, while the second one is due to relaxation. It can be observed that during the relaxation driven sorption stage, the concentration gradient across the sample is negligible. Commonly the two stages appear to be separated by a sort of plateau or of pseudo steady state, that arise from the superposition of the slowing down of the diffusion driven sorption and of the initially slow relaxation rate. In this work, two stages kinetics were observed several times in the case of dichloromethane sorption in Matrimid 5218, especially when dealing with really thin films. When $De \approx 1$, diffusion and relaxation take place in the same timescale and the resulting rate significantly deviates from the Fickian one, leading to *anomalous sorption kinetics.* It must be remarked that even if the diffusion coefficient of the low molecular weight species in a glassy polymer can depend upon to concentration according to an exponential law and even if it is well known that the free volume of the system can exert a deep influence as well, the above mentioned features of the non Fickian processes cannot be simply explained as an effect of the variable diffusion coefficient. Several approaches have been developed in the past for dealing with non Fickian sorption kinetics, ranging

from simplified, phenomenological models, up to models that explicitly take into account, through a suitable rheological model, the effect of polymer volume relaxation[77, 87, 89-92, 112, 118-121]. It is worth mentioning that in order to model some of the most extremely anomalous sorption kinetics, such as those named Case II and Super Case II, in which the mass uptake is found to be proportional to time and even accelerating before reaching the equilibrium value, with rather sharp concentration fronts that propagate inside the sample, hyperbolic formulation of the conservation laws have been proposed and found able to provide results that compare well with the experimental evidence[122, 123].

In order to model the kinetic data collected while performing the experiments aimed to measuring vapor and liquid solubilities in the glassy Matrimid 5218, several approaches had been applied. The most simple one was that based on the application of Berens Hopfenberg Model[87, 119], that should be regarded as a quite versatile correlation tool, but that lacks rigorous foundation and that is mainly phenomenological, despite suggesting some interesting thought about the actual physics of the sorption process. It will be shown that with a simple hypothesis it is possible to use the predictions of NETGP approach in order to reduce the number of adjustable parameters of the Berens Hopfenberg Model. The Long and Richman Model[78, 79] have also been analyzed, providing some insight on the controlling processes in the non Fickian sorption. Finally the model proposed by Carlà and Doghieri[112] on the basis of the simple rheological assumptions that had been found successful in NETGP had been applied to vapor and liquid sorption kinetics.

6.2.   Berens Hopfenberg Model

The model introduced by Berens and Hopfenberg is based on the assumption of linear superposition between diffusion and relaxation processes. The mass uptake during the sorption (or desorption) of a low molecular weight penetrant in

a polymer is calculated by the direct summation of a contribution that is calculated using the integrated form of the partial differential equation that describe the Fickian diffusion process in a non relaxing medium and of a contribution that is calculated with a simple relaxation law, that describes the evolution toward a final value.

6.2
$$\begin{cases} \dfrac{\partial C}{\partial t} = D \dfrac{\partial^2 C}{\partial x^2} \\ C(x,0) = C_0 \quad \forall x \\ C(\delta,t) = C_i \quad \forall t \geq 0 \\ \dfrac{\partial C(0,t)}{\partial x} = 0 \quad \forall t \geq 0 \end{cases}$$

6.3
$$\left(\frac{M(t)}{M_\infty} \right)_D = \left[1 - \sum_{n=0}^{+\infty} \frac{8}{(2n+1)^2 \pi^2} \exp\left(-\frac{(2n+1)^2 \pi^2 t D}{\delta_2} \right) \right]$$

The diffusion problem, here considered in the form that is specific for the geometry of a slab, is formulated assuming that the boundary condition at the surface that is exposed to the external phase is given by the solubility of the penetrant itself, in term of concentration C_i, that is assumed to be constant with time. Therefore the diffusion contribution is calculated assuming that relaxation processes does not influence the mobility of the low molecular weight species, as well as their solubility, that is the parameters that controls the boundary condition. The relaxation process is then completely independent from the penetrant concentration in the film and from its profile: this assumption is clearly a weak one, since it does not take into account the fact that relaxation is promoted by the plasticizing action of the low molecular weight penetrant and thus relaxation rate should be dependent on penetrant concentration. The most important shortcoming of this model is that can predict the mass uptake upon non Fickian sorption, but does not enable to represent correctly the concentration profile inside of the sample.

The mass uptake is then calculated by summing the diffusion contribution $\left(\dfrac{M(t)}{M_\infty}\right)_D$ to the relaxation contribution $\left(\dfrac{M(t)}{M_\infty}\right)_R$, weighted by the coefficient α_D. The simplest form of relaxation law is provided by the exponential decay law $1-\exp\left(-\dfrac{t}{\tau}\right)$, where τ is the characteristic time of relaxation. The relaxation contribution tends to zero when $t \ll \tau$ and reaches monotonously its maximum value when $t \gg \tau$.

6.4
$$\left(\frac{M(t)}{M_\infty}\right) = \alpha_D\left(\frac{M(t)}{M_\infty}\right)_D + \left(1-\alpha_D\right)\left(\frac{M(t)}{M_\infty}\right)_R$$

6.5
$$\left(\frac{M(t)}{M_\infty}\right) = \alpha_D\left(\frac{M(t)}{M_\infty}\right)_D + \left(1-\alpha_D\right)\left[1-\exp\left(-\frac{t}{\tau}\right)\right]$$

The Berens Hopfenberg requires the slab half thickness δ and three adjustable parameters in order to describe the kinetic of the sorption process as $\left(\dfrac{M(t)}{M_\infty}\right)$ and the final mass uptake M_∞ must be supplied too, in order to plot the kinetic in the form of the mass uptake $M(t)$. The adjustable parameters are the diffusivity, the relaxation time τ and the weighting factor α_D. Sometimes the weighting factor between the diffusion and the relaxation contributions is expressed as $\alpha_R = 1-\alpha_D$. In differential sorption experiments all this parameters can be thought to be a function of the activity jump or of the average penetrant concentration and it is not uncommon that the trend of that fitting parameters is not completely regular, as shown, for instance, by Lee et al.[87] in 2009 for the case of Heptane and Toluene sorption in Matrimid 5218 hollow fibers.

It must be noted that, despite its theoretical shortcomings, the Berens Hopfenberg model can be a powerful correlation tool for sorption mass uptake

kinetic and that it is possible to modify the model in order to take into account behaviors that arise when instead of a single relaxation time, the polymer matrix relaxation is characterized by a spectrum of relaxation times. This can be done, for instance, representing the global relaxation contribution as a sum of relaxation contributions with different relaxation times τ_k. If the relaxation spectrum is continuous, the summation can be replaced by an integral, introducing a suitable distribution function for the relaxation times. It is clear that the number of adjustable parameters rises significantly.

6.6
$$\left(\frac{M(t)}{M_\infty}\right) = \alpha_D \left(\frac{M(t)}{M_\infty}\right)_D + (1-\alpha_D)\sum_{k=1}^{N}\alpha_k \left[1-\exp\left(-\frac{t}{\tau_k}\right)\right]$$

Another possibility is to use a single stretched exponential, in the form of a Kohlrausch–Williams–Watts relaxation modulus[124] $1-\exp\left(-\left(\frac{t}{\tau}\right)^\beta\right)$. This form is really versatile, since the use of the exponent β as an adjustable parameter enables to represent a wide range of relaxation behaviors.

6.7
$$\left(\frac{M(t)}{M_\infty}\right) = \alpha_D \left(\frac{M(t)}{M_\infty}\right)_D + (1-\alpha_D)\left[1-\exp\left(-\left(\frac{t}{\tau}\right)^\beta\right)\right]$$

The Berens Hopfenberg Model was applied to the describe the sorption kinetic data of DCM in Matrimid 5218 at 291 K and 305 K that were collected with the QCM apparatus. The films were obtained applying a drop of 5% Matrimid 5218 in DCM solution on one of the crystal resonator electrode. The resonator was placed on a spin coating device and the drop spreading, leveling and drying was obtained operating the spin coater at 2000 rpm for two minutes. The drop of polymer solution was deposited on the resonator during the initial ramp up of the spin coater. Solvent removal was obtained placing the crystal under vacuum at 50°C for one night. The mass of the film of Matr imid 5218 that coated the

electrode of the resonator was estimated by the departure of the crystal frequency, respect to the value measured, for the same crystal, before polymer deposition. The average thickness of the sample was then estimated by the mass of polymer itself, since density of the polymer and area of the electrodes are known. The thickness were around $\approx 1 \mu m$. Since thickness of the samples are only indirect estimates, the characteristic time of diffusion $\tau_D = \dfrac{\delta^2}{D}$ was used directly as the input of the Berens Hopfenberg Model. Some of the results are depicted in the Fig. 6.1 to Fig. 6.5. It was found out that the better fitting of the experimental data was obtained assuming either assuming that two relaxation times existed or using the Kohlrausch–Williams–Watts relaxation modulus. In fact, using only one relaxation time, it was possible to represent only the long time relaxation behavior, while for times only slightly longer than diffusion relaxation time, marked deviation between the experimental data and the model prediction arised. Therefore the two relaxation times were chosen, by comparison with the experimental results, in order to represent a short time relaxation and a long time relaxation. With the Kohlrausch–Williams–Watts relaxation modulus only one relaxation time was required, as by setting the value of the exponent β different to unity some degree of broadening of the relaxation spectrum is achieved. The kinetics that had been modeled are quite variegated, ranging from situation in which after the knee of Fickian behavior starts a slow drift of the mass uptake, to those in which a more evident two stages kinetic is present. In the application of the Berens Hopfenberg model with two relaxation times, it was found out that the weighting factor α_D decreased as the average concentration of the dichloromtehane in the polymer increased, due to an higher and higher contribution of the volume relaxation to the total mass uptake. The weighting factor of the short time relaxation α_{R1} decreased as well, with the increase of dichloromethane concentration. This results are summarized in Fig. 6.6 where the weighting factor of the diffusive contribution is reported as $\alpha_R = 1 - \alpha_D$. The characteristic times of the short time relaxation terms are quite short, ranging from around 500

s in the first steps and decreasing to few seconds for the steps at higher activity, while the characteristic times of the long time relaxation terms seems to increase with the amount of dichloromethane already sorbed in the polymer matrix, ranging from 10000 s up to 35000 s. It must be noted that neither at 291K, nor at 305K was reached the plasticizer induced glass transition and thus this long relaxation times are to be referred to the slow evolution of a glassy matrix. The relaxation times are depicted in Fig. 6.7, in which lines had been drawn for guiding the eye. Some scattering in the parameters required for fitting the experimental sorption curves is evident, but it has already been mentioned that this phenomenon has been reported by other authors.
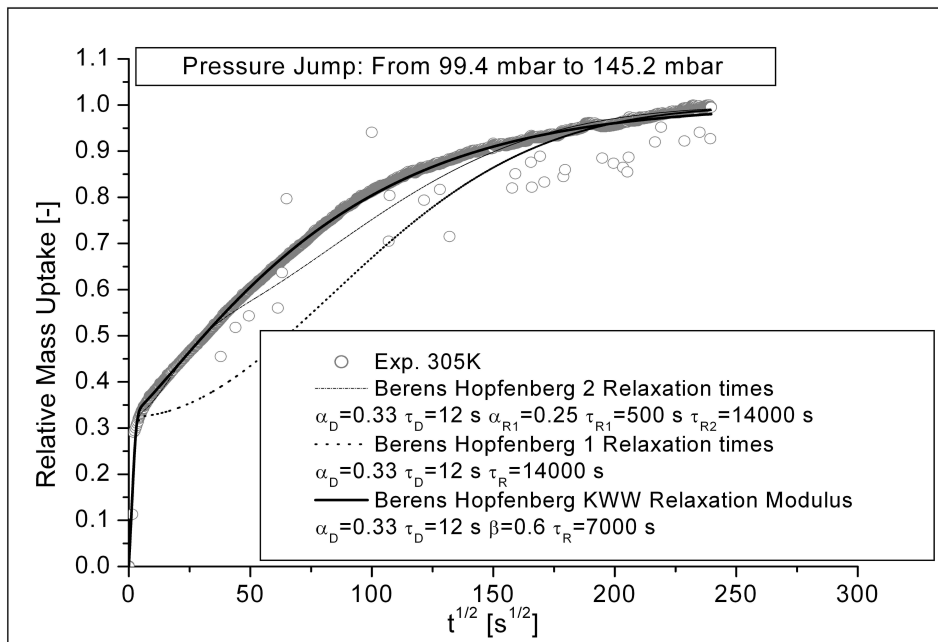

Fig. 6.1   Mass sorption kinetic of Dichloromethane in Matrimid 5218 at 305 K. Initial pressure 99.4 mbar, final pressure 145.2 mbar. Comparison between experimental data and several possible formulation of the Berens Hopfenberg model: one relaxation element, two relaxation elements or the Kohlrausch–Williams–Watts relaxation modulus.

Fig. 6.2   Mass sorption kinetic of Dichloromethane in Matrimid 5218 at 291 K. Initial pressure 26.6 mbar, final pressure 40.8 mbar. Comparison between experimental data and the Berens Hopfenberg model with one relaxation element or two relaxation elements.

Fig. 6.3   Mass sorption kinetic of Dichloromethane in Matrimid 5218 at 291 K. Initial pressure 40.8 mbar, final pressure 85.9 mbar. Comparison between experimental data and the Berens Hopfenberg model with one relaxation element or two relaxation elements.
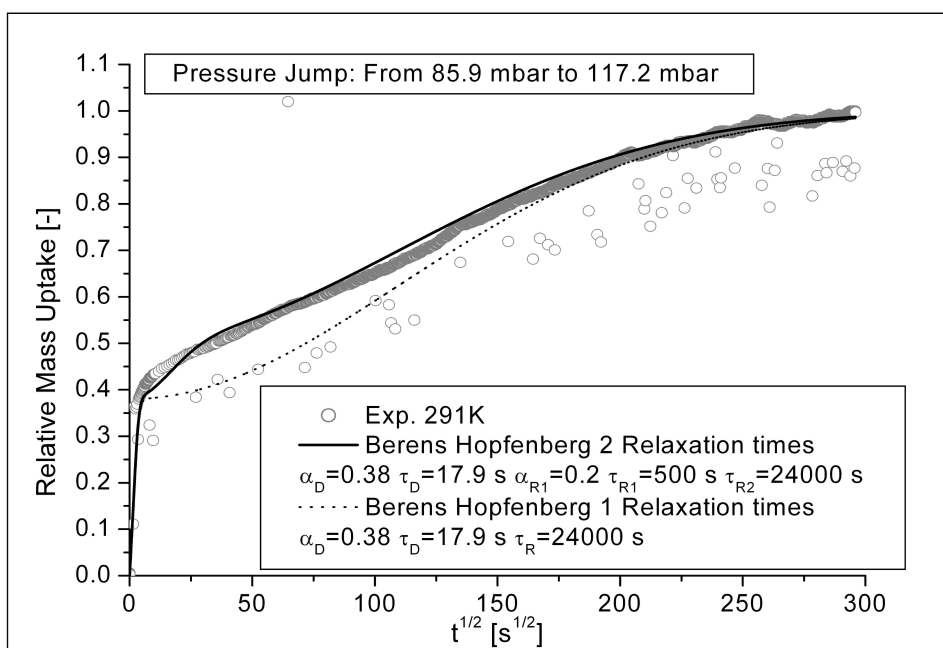
Fig. 6.4   Mass sorption kinetic of Dichloromethane in Matrimid 5218 at 291 K. Initial pressure 85.9 mbar, final pressure 117.2 mbar. Comparison between experimental data and the Berens Hopfenberg model with one relaxation element or two relaxation elements.
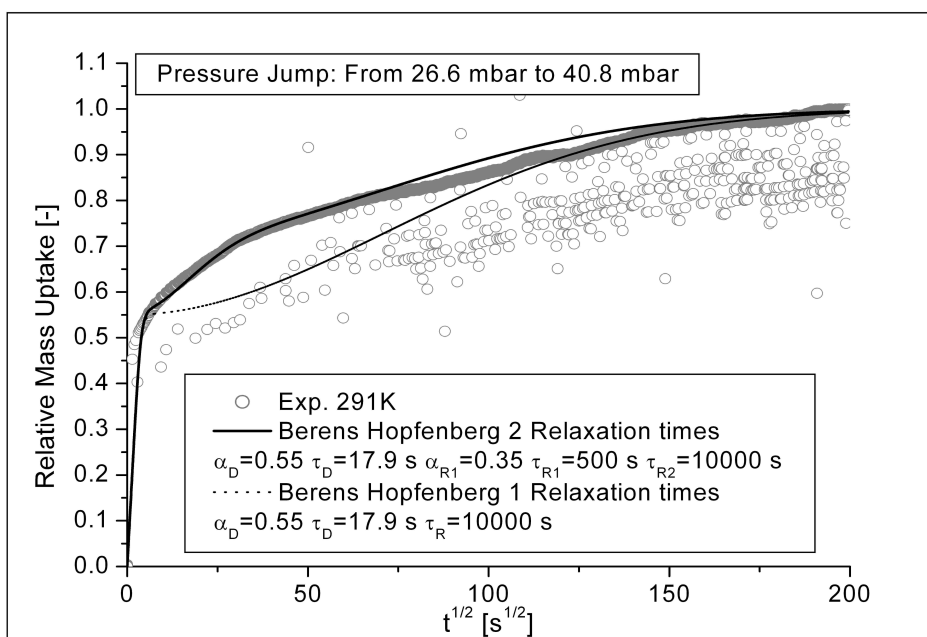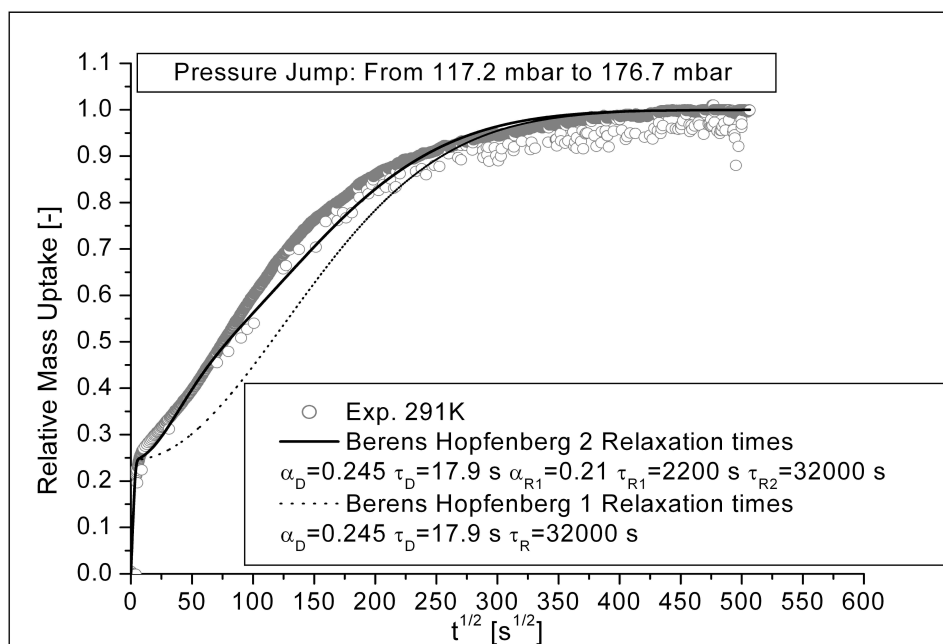

Fig. 6.5   Mass sorption kinetic of Dichloromethane in Matrimid 5218 at 291 K. Initial pressure 117.2 mbar, final pressure 176.7 mbar. Comparison between experimental data and the Berens Hopfenberg model with one relaxation element or two relaxation elements.
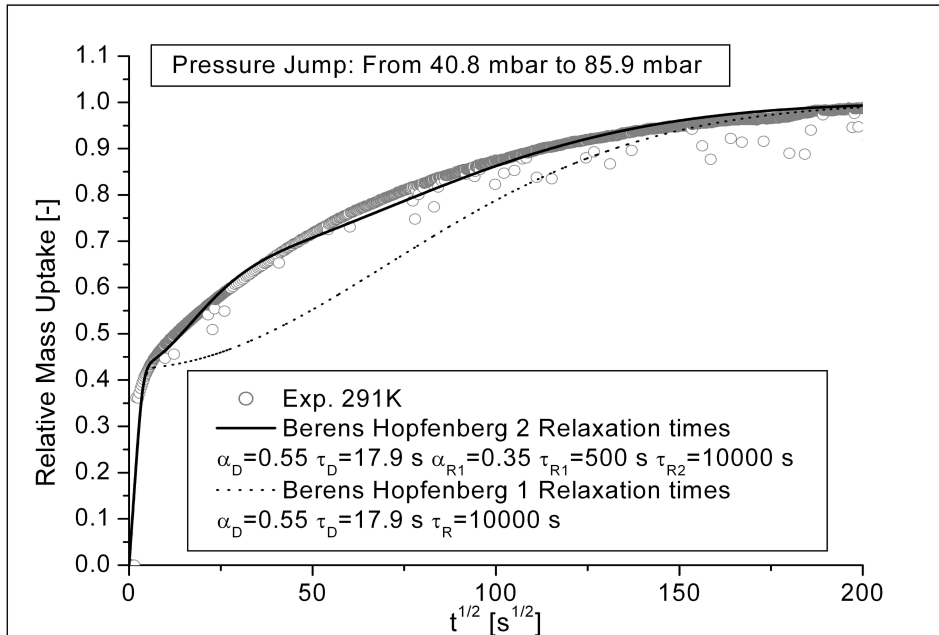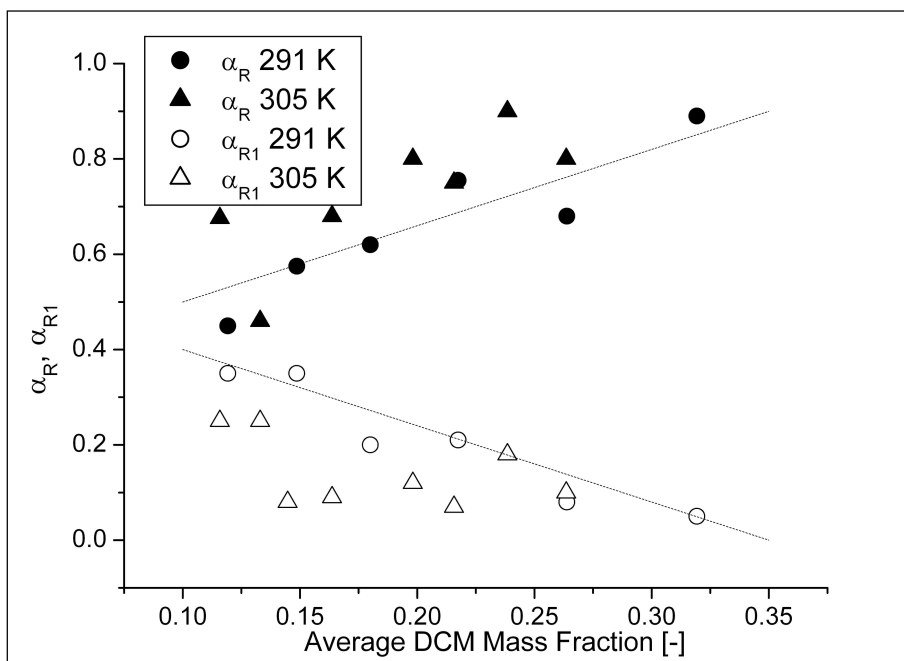
Fig. 6.6   Berens Hopfenberg model of Dichloromethane in Matrimid 5218 at 291 K and 305K:

weighting factors $\alpha_R = 1 - \alpha_D$ and α_{R1}. Lines are drawn only to guide the eyes.
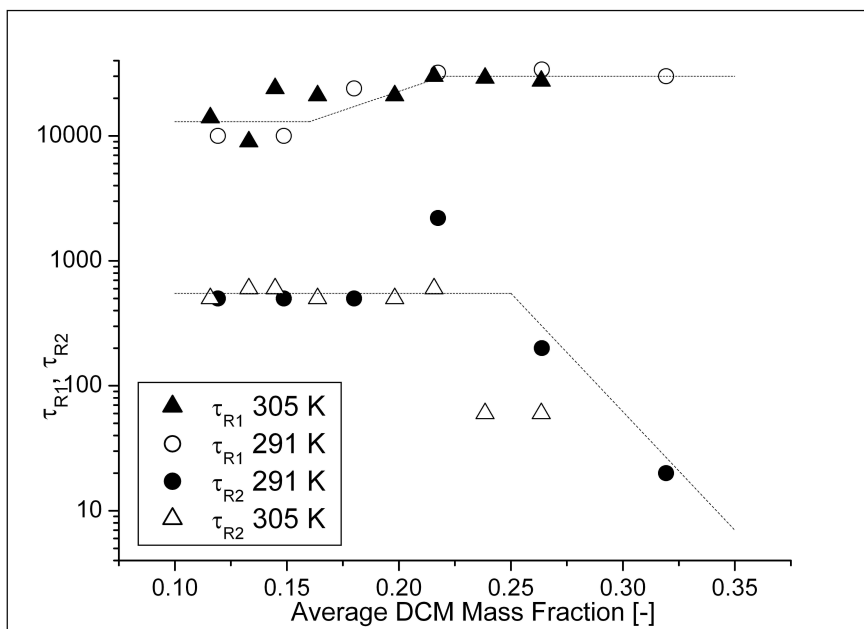
Fig. 6.7   Berens Hopfenberg model of Dichloromethane in Matrimid 5218 at 291 K and 305K:
short time and long time characteristic relaxation times. Lines are drawn only to guide the eyes.

6.3. Berens Hopfenberg Model and NETGP Approach

As previously discussed, the Berens Hopfenberg model requires, among the various adjustable parameters, the value of the weighting factor α_D that dictates how much of the total mass uptake is due to diffusion and how much is due to relaxation of the polymer matrix. The examples of application of the Berens Hopfenberg model to the kinetic of dichloromethane sorption in Matrimid 5218 shown in the previous section, have shown that some separation of diffusion and relaxation timescales was present, to some extent, in quite every steps of the differential sorption experiment. Therefore it is reasonable to assume that diffusion takes place in a polymeric matrix into which relaxation has not yet produced relevant changes, respect to the conditions that were pre existent. Therefore it could be made the hypothesis that diffusion takes place in a polymeric matrix whose density (or specific volume) is equal to the density at the beginning of the sorption step. This hypothesis provide a simple rule for estimating the value of the weighting factor α_D applying the NETGP approach. In fact, the weighting factor α_D is the ratio between the total mass uptake in the sorption step and the mass uptake that is only due to diffusion and the following procedure could be applied:

1. Model the Isotherm with NETGP, retrieving the binary interaction parameter of the polymer-penetrant pair, if not already available from true equilibrium data, and the swelling coefficient.

2. For each sorption step i, that start with the pressure jump from P_{i-1} to the final value P_i, calculate the actual density or specific volume $\hat{V}_{P_i}$ of the polymer at the final pressure P_i. This can be done either by means of the linear swelling approximation or, if the single datapoint departs appreciably from the predicted isotherm, by solving the pseudo equilibrium equation $\mu_S^{Ext}(T, P_i) = \mu_S^{NE}(T, P_i, C_i, \rho_P)$ respect to the polymer density ρ_P.

3. The weighting factor $\alpha_{D,i}$ for the step i is then evaluated according to the following formula:

6.8
$$\alpha_{D,i} = \frac{C\left(T,P_i,\hat{V}_{P_{i-1}}\right) - C\left(T,P_{i-1},\hat{V}_{P_{i-1}}\right)}{C\left(T,P_i,\hat{V}_{P_i}\right) - C\left(T,P_{i-1},\hat{V}_{P_{i-1}}\right)}$$

Fig. 6.8 shows the comparison between the values of α_D required to fit the experimental data collected at 291K and the values calculated according to the above procedure, applying the NELF version of NETGP theory. The NETGP approach provides quite always excellent estimates of the weighting factor α_D, that is being only slightly overestimated. Therefore the present procedure should be considered a suitable tool for predicting α_D and thus removing one adjustable parameters from the model. Moreover this confirms that, at least for the specific conditions in which the data considered in this study were collected, among which it must be considered that the films were just $\approx 1\mu m$ thick, it is quite reasonable that the Fickian mass uptake complete before that significant volume relaxation takes place. In thicker films this timescale separation will be less prominent and the hypothesis that diffusion step is completed in a polymeric matrix whose density (or specific volume) is equal to the density at the beginning of the sorption process will no longer apply.
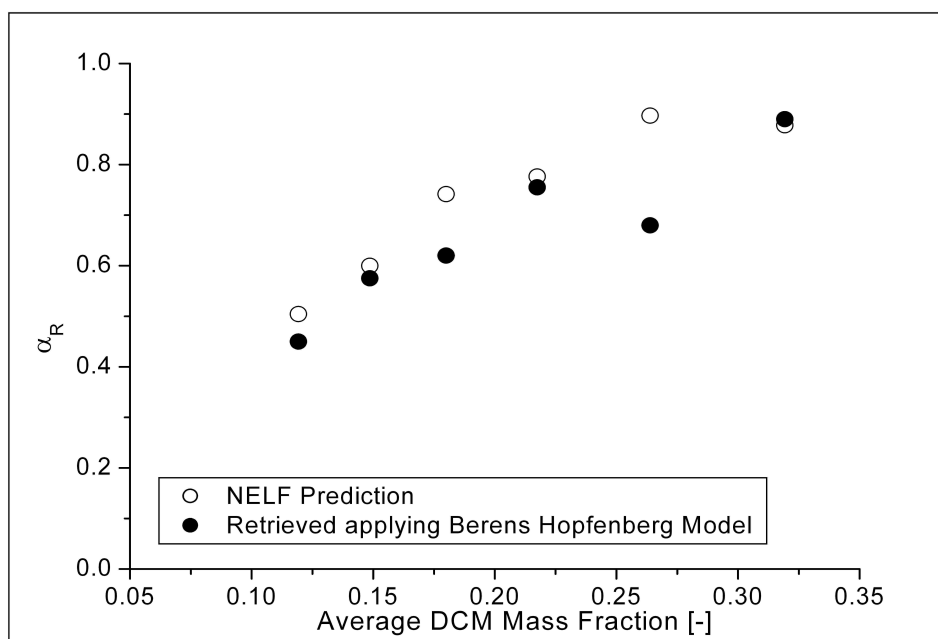
Fig. 6.8 Berens Hopfenberg model of Dichloromethane in Matrimid 5218 at 291 K: comparison between the weighting factor $\alpha_R = 1 - \alpha_D$ retrieved applying the model and the results of the NELF calculations.

6.4. Long Richman Model

In 1960 Long and Richman[78] published two papers dealing with methyl iodide diffusion in PolyVinil Acetate and Cellulose Acetate films at various temperatures, above and below the glass transition temperature of the polymers. The technique adopted made use of a device conceptually similar to the Quartz Spring balance that had been previously described in this thesis. In order to gain some insight on the concentration profile inside the samples, Long and Richmann removed the samples from the sorption cell at predetermined times, quenched them in liquid nitrogen and microtomed the samples itself in a position that was judged to be far enough from the edges. Finally an X ray technique was used for retrieving the methyl iodide concentration profiles. The sorption experiments performed at temperatures above glass transition temperature for PolyVinylAlcetate provided results that are recognizable without

any doubt as Fickian. In the case of methyl iodide sorption in glassy samples, the mass uptake kinetics deviated significantly from the Fickian one, with quite recognizable effects like relaxation, two stage sorption and sigmoid kinetic. The most astonishing result, however, came from the examination of the concentration profile, especially near the surface of the samples, where the boundary conditions apply. In fact, according to the own words of Long and Richman, for the case of methyl iodide in PolyVinylAcetate it was found that *"for the early stages of the sorption the surface concentrations of methyl iodide were well below the equilibrium sorption value and also that the surface concentrations increased with time"*. For the case of methyl iodide in Cellulose Acetate, from the analysis of the concentration profiles they found out that: "*The striking feature … is that the surface concentrations are much lower than the equilibrium value… of methyl iodide and are increasing with time. This result is in sharp contrast to that for diffusion into a non-glassy polymer where the surface concentration is essentially the equilibrium value a t all times.".* Starting from this observations, Long and Richman proposed to model the sorption kinetic in glassy polymers applying a time dependent boundary condition to the classic diffusion problem: transport inside the sample will be still described in term of a mass flux proportional to the gradient of the concentration of the low molecular weight penentrant, while the surface concentration will relax toward the equilibrium or pseudo equilibrium value. Long and Richman found that their approach was quite successful in modeling their kinetic data. In quite general terms, for an infinite slab, the Long Richman model can be formulated in the following way:

6.9
$$
\begin{cases}
\dfrac{\partial C}{\partial t} = D\dfrac{\partial^2 C}{\partial x^2} \\
C(x,0) = C_0 \quad \forall x \\
C(\delta,t) = C_i(t) \quad \forall t \geq 0 \\
\dfrac{\partial C(0,t)}{\partial x} = 0 \quad \forall t \geq 0
\end{cases}
$$

The choice of the function $C_i(t)$ will dictate the main features of the kinetic that is described by the model. Especially it is really relevant the ratio between the characteristic time in which $C_i(t)$ will relax toward the equilibrium value, respect to the characteristic time of diffusion. Long and Richman found that linear dependence of $C_i(t)$ respect to time variable or a relaxation law like those previously introduced in the Berens Hopfenberg model were the two most effective choice, in order to model the results of differential and integral sorption experiments. For example, the sorption kinetics of dichlorometane in Matrimid 5218 that had previously been modeled with the Berens Hopfenberg model could have been fitted also with the output of a Long Richman Model like:

$$6.10 \qquad \begin{cases} \dfrac{\partial C}{\partial t} = D \dfrac{\partial^2 C}{\partial x^2} \\ C(x,0) = C_0 \quad \forall x \\ C(\delta,t) = C_0 + (C_\infty - C_0)\left[1 - \exp\left(-\dfrac{t}{\tau}\right)\right] \quad \forall t \geq 0 \\ \dfrac{\partial C(0,t)}{\partial x} = 0 \quad \forall t \geq 0 \end{cases}$$

Some observations must be formulated, especially taking into account the results of the NETGP approach. In fact, it has been clarified that a strong relationship holds between the solubility of low molecular weight species in glassy polymers and the density of the out of equilibrium glassy matrix. Moreover, it has been shown that a simple rheological model, based on the assumption that the specific volume of the polymer is made by a contribution that will evolve only in times much longer than the sorption experiment itself and by a contribution that will evolve in shorter time, can describe (and even predict!) quite successfully the swelling behavior of the glassy polymer itself. Swelling will take place, if permitted by the local mechanical constraints, in every portion of the sample that is reached by the penetrant, that will act as a plasticizer. Swelling in the bulk of the sample will change the free volume of the system and this could affect the mobility of the low molecular weight penetrant,

as described by the free volume theory by Vrentas and Duda[125], but according to that theory, the driving force of the process will remain the concentration (or chemical potential) gradient. Therefore the assumption of describing the internal mass transport in term of concentration gradient it is still justified, even after that the role of swelling in the bulk of the polymer has been recognized. Swelling of the polymer chains that are immediately below or at the surface, will cause a change of the density of the polymer matrix, locally, that will play no role in terms of diffusivity or mobility of the low molecular weight penetrant, but will definitely cause a change of the solubility. Since relaxation is not instantaneous, but is endowed by kinetic limitations, that are rather typical of the glassy state, the density of the polymer at the interface and thus the solubility of the penentrant will evolve toward the final, equilibrium or pseudoequilibrium value. If the relaxation process is slower than diffusion, its effect will be recognizable and non Fickian kinetics will arise not due to some change of the nature of the bulk transport process itself, but due to the time dependent boundary condition. The model could be re written as:

6.11
$$\begin{cases} \dfrac{\partial C}{\partial t} = D \dfrac{\partial^2 C}{\partial x^2} \\ C(x,0) = C_0 \quad \forall x \\ C(\delta,t) = C_i(\rho_P(t)) \quad \forall t \geq 0 \\ \dfrac{\partial C(0,t)}{\partial x} = 0 \quad \forall t \geq 0 \end{cases}$$

The time dependency of the polymer density $\rho_P(t)$ will then dictate the dependence upon time of the surface concentration. The interface concentration will then be calculated, for a given value of the chemical potential of the penetrant in the external phase, solving the pseudo equilibrium formulation of the phase equilibria problem: $\mu_S{}^{Ext}(T,P) = \mu_S{}^{NE}(T,P,\omega_S,\rho_P)$.

6.5. Long Richman Model and NETGP Approach

A model that encompasses the above formulated observations and that explicitly uses the fact that the density of the polymer, in the NETGP approach, is an internal state variable that obeys to the evolution law $\frac{d\rho_P}{dt} = f(T,P,C_i,\rho_P)$, can be defined in the following way:

6.12

$$
\begin{cases}
\frac{\partial C}{\partial t} = D\frac{\partial^2 C}{\partial x^2} \\
C(x,0) = C_0 \quad \forall x \\
C(\delta,t) = C_i(\rho_P(t)) \quad \forall t \geq 0 \\
\mu_S^{Ext}(T,P) = \mu_S^{NE}(T,P,C_i,\rho_P) \\
\frac{d\rho_P}{dt} = f(T,P,C_i,\rho_P) \\
\frac{\partial C(0,t)}{\partial x} = 0 \quad \forall t \geq 0
\end{cases}
$$

As previously shown, a simple yet effective rheological model suggest that the specific volume of the polymer, and thus its density, can be thought as the sum of two contributions: one that is somewhat rigid and does not evolve during the sorption experiment and one that evolves on short times. The rigid element, say $\hat{V}_L$, will evolve only for really long times. In the previous chapter, it has been shown that the rigid contribution is equal to polymer specific volume at the plasticizer induced glass transition, thus $\hat{V}_L = \hat{V}_{P,g}$. Under pseudoequilibrium conditions, the contribution that evolves on short times, say $\hat{V}_S$, will became equal to the equilibrium value at the same temperature, pressure and penetrant chemical potential. Thus at the end of the sorption step, under pseudoequilibrium conditions, $\hat{V}_S = \hat{V}_P^{EQ}$. In general term, the polymer specific volume will be written as:

6.13
$$
\hat{V}_P = \frac{1}{\rho_P} = \chi\hat{V}_S + (1-\chi)\hat{V}_L
$$

Carlà and Doghieri[112] provided simple evolution laws for $\hat{V}_L$ and for $\hat{V}_S$, assuming that the rheology of the glassy phase can be described by Voigt elements. In this approach the role of the deformation is assumed by $\dfrac{1}{\hat{V}}\dfrac{d\hat{V}}{dt}$ and the driving force is the difference between the pressure at which the specific volume of the element would be of equilibrium, for the given penentrant chemical potential, and the actual pressure of the system. A viscosity η will dictate the "resistance" to the evolution toward the final, equilibrium value. Since the term $\hat{V}_L$ will behave like the volume of a rigid element, whose evolution is not expected to take place during the sorption experiment, its viscosity will be infinite, thus $\eta_g \to +\infty$. On the other hand, the viscosity of the term that evolves in shorter times, $\hat{V}_P^{EQ}$, indeed will assume a finite value.

6.14
$$
\begin{cases}
\dfrac{1}{\hat{V}_L}\dfrac{d\hat{V}_L}{dt} = \dfrac{P^{Eq}\left(T,\hat{V}_{P,g},\mu^S\right)-P}{\eta_g} \\
\eta_g \to +\infty
\end{cases}
$$

6.15
$$
\begin{cases}
\dfrac{1}{\hat{V}_S}\dfrac{d\hat{V}_S}{dt} = \dfrac{P^{Eq}\left(T,\hat{V}^{EQ}_P,\mu^S\right)-P}{\eta} \\
\eta \in \Re^+
\end{cases}
$$

Since $\hat{V}_L$ is rigid, it is always equal to $\hat{V}_{P,g}$ and thus the polymer specific volume can be always written as $\hat{V}_P = \dfrac{1}{\rho_P} = \chi\hat{V}_S + (1-\chi)\hat{V}_{P,g}$, while only under pseuodequilibrium: $\hat{V}_P = \dfrac{1}{\rho_P} = \chi\hat{V}_P^{EQ} + (1-\chi)\hat{V}_{P,g}$.

The following set of equations bears the complete formulation of the problem, with the relevant boundary and initial conditions. The model is actually formulated in a polymer fixed reference frame. It is assumed that diffusivity of the low molecular weight penetrant and the viscosity of the polymer matrix are

161

constants. This assumption is somewhat weak and can withstand only for the purpose of modeling differential sorption steps in which composition and free volume changes are limited and thus average values of the above mentioned kinetic parameters can be used. The model therefore is an hybrid between the Long and Richman model[78] and the model defined by Doghieri and Carlà[112] for CO2 sorption in PMMA, because the formulation by Doghieri and Carlà explicitly accounted for free volume effects and the driving force of the diffusive process was assumed to be the chemical potential gradient and not simply the penetrant concentration gradient. It must be emphasized that this approach requires that a good fitting of the sorption isotherm with the NETGP approach is obtained, since the initial and the final composition of the sample are then simply predicted. From isotherm modeling the values of k_{i_j}, χ and $\hat{V}_{P,g}$ will be already known and the only adjustable parameters for kinetic modeling will be the diffusivity and the viscosity. Therefore it is possible to say that the kinetic model has only two adjustable parameters.

$$
\begin{cases}
\dfrac{\partial C}{\partial t} = D\dfrac{\partial^2 C}{\partial x^2} \\[2mm]
\hat{V}_P = \dfrac{1}{\rho_P} = \chi\hat{V}_S + (1-\chi)\hat{V}_{P,g} \\[2mm]
\dfrac{1}{\hat{V}_S}\dfrac{d\hat{V}_S}{dt} = \dfrac{P^{Eq}\left(T,\hat{V}^{EQ}{}_P,\mu^S\right) - P}{\eta} \\[2mm]
I.C. \\
C(x,0) = C_0\left(\hat{V}_P\left(T,P_{in},\mu^S{}_{in}\right)\right) \quad \forall x \\[2mm]
\hat{V}_P(x,0) = \hat{V}_P\left(T,P_{in},\mu^S{}_{in}\right) \quad \forall x \\[2mm]
B.C. \\
\quad C(\delta,t) = C_i\left(\hat{V}_P(t)\right) \quad \forall t \geq 0 \\[2mm]
\quad \dfrac{\partial \hat{V}_P(\delta,t)}{\partial x} = 0 \quad \forall t \geq 0 \\[2mm]
\quad \dfrac{\partial C(0,t)}{\partial x} = 0 \quad \forall t \geq 0 \\[2mm]
\quad \dfrac{\partial \hat{V}_P(0,t)}{\partial x} = 0 \quad \forall t \geq 0
\end{cases}
$$

6.16

This set of differential equations, along with the calculation required for estimating the required pseudoequilibrium and equilibrium properties with the Lattice Fluid Equation of State and with the NELF model, has been implemented in a Matlab® code. The partial differential equations are solved with a finite element scheme that is available among the internal functions of Matlab®. The above formulated model has then been applied to predict and/or to fit the kinetic of vapor and liquid sorprtion of Methanol in Matrimid 5218 at 308K and the sorption kinetic of liquid 1-propanol in the same polymer and at the same temperature. As a thermodynamic model the usual Lattice Fluid Model by Sanchez and Lacombe was applied.

6.6. Methanol Sorption Kinetic

The vapor sorption data have been collected by means of the Quartz Spring apparatus, on a sample prepared by solution casting from a 1% Matrimid 5218 solution in Dichloromethane, that gave a film with thickness equal to 69.6 μm. The sorption experiment with liquid methanol was performed on a sample prepared by solution casting from a 5% Matrimid 5218 solution in Dichloromethane, and a film 119.5 μm thick was obtained. Even if a tentative modeling effort of the sorption isotherm of Methanol in Matrimid 5218 at 308 k have already been shown in the dedicated chapter, since the kinetic model is quite sensitive to the quality of the isotherm fit, it was decided to redo the fitting, trying to obtain results that, despite the already good qualitative agreement, provided better quantitative agreement with the data. In order to do so, the value of the parameter χ, previously estimated from the sorption isotherm of Dichloromethane in Matrimid 5218, was slightly changed and set equal to 0.872, while the binary interaction parameter was set equal to -0.04 and the specific volume at the plasticization induced glass transition $\hat{V}_{P,g}$ was left equal to the previously estimated value. As shown in Fig. 6.9 the agreement between the NELF model and the experimental data is really good, especially for the first

four points. The liquid solubility remains slightly underestimated, while the fifth vapor point, the one collected at activity close to 0.9, is slightly overestimated. Better results for this latter two points could be obtained only at relevant expenses of the quality of fitting for the other data. Since vapor sorption experiments were conducted as differential sorption experiment while liquid sorption is inherently an integral sorption experiments, the modeling of their sorption kinetic will be discussed separately. In the case of vapor sorption, at first, viscosity of the short term volumetric contribution was set equal to infinity, in order to study what was the effect, if any, of relaxation on the first steps, that most closely resembled the Fickian behavior, as well as for understanding to what extent the diffusion in the unrelaxed polymer matrix contributed to sorption in the last steps, in which relaxation played a more relevant role. Results are shown in Fig. 6.10 and show that even for the first two steps a contribution of the polymer swelling is required to represent the correct final value of the sorption steps. Conversely, in the last three steps, that are undoubtedly dominated by volume relaxation, the contribution of diffusion alone is still of some relevance. The diffusivity values have been retrieved by a manual best fit procedure and are reported in Fig. 6.11 as a function of the average methanol concentration, calculated considering, for each step, the concentration at which the step was started and the final concentration at which the steady state was obtained, without relaxation of the polymer matrix. It is then a value that should be referred to the density of the polymer that was reached before the sorption step was started. In two stage kinetics, this diffusivity value is the one relevant for the first stage. Except for a single outlier, the diffusivity show a recognizable exponential dependence from the average concentration of the methanol in the polymeric matrix, as it is possible to see from the fit shown in Fig. 6.11 (Since the plot is logarithmic, the exponential fit appears like a straight line).

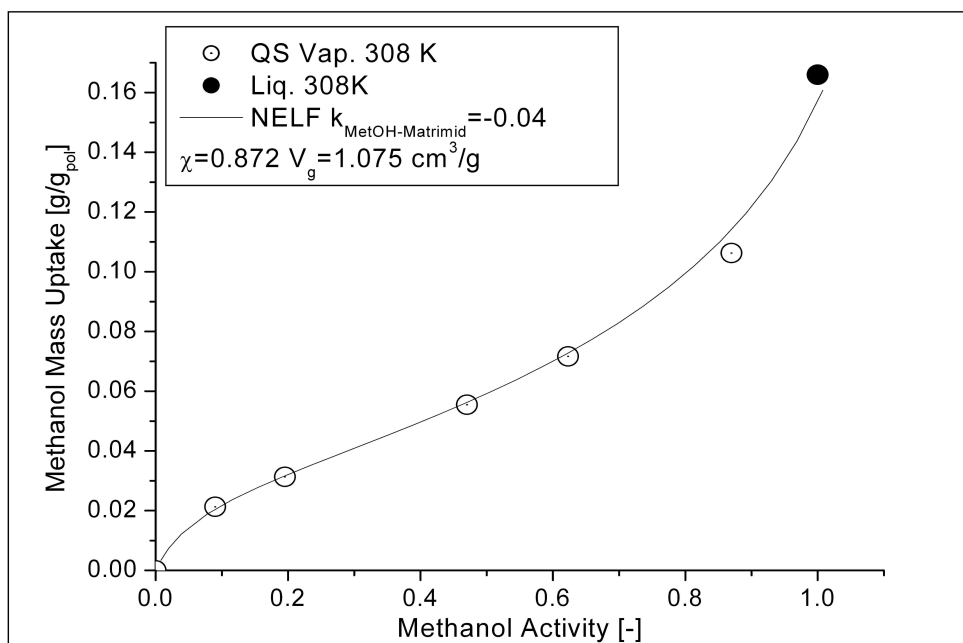Fig. 6.9   Best fit of the sorption isotherm of Methanol in Matrimid 5218 at 308 K with the most recent development of NELF model, that enables to predict the swelling of the glassy polymeric matrix.
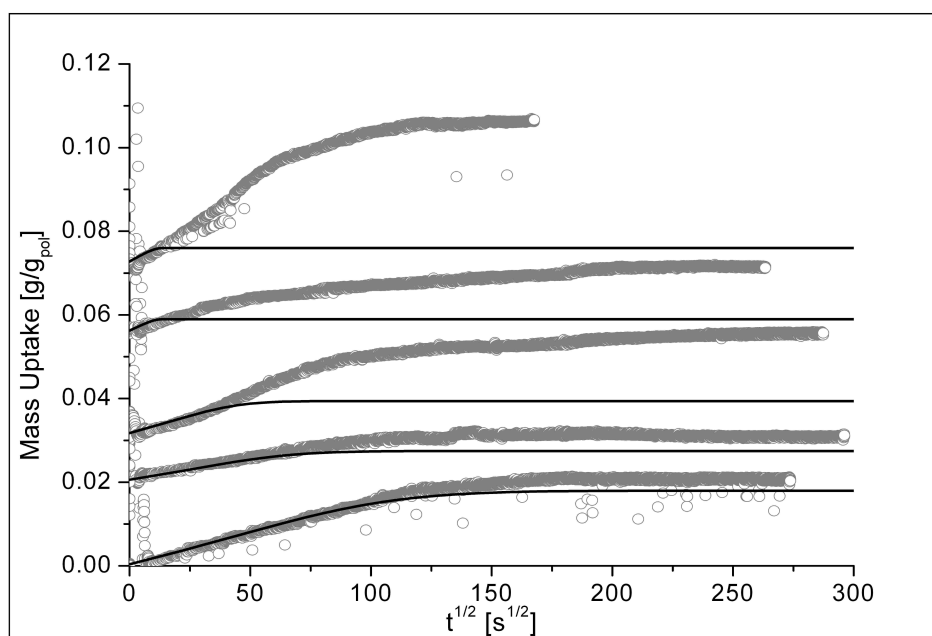

Fig. 6.10   Comparison between the experimental sorption kinetics of vapor Methanol in Matrimid 5218 at 308 K with the prediction of the model derived from the model proposed by Doghieri and Carlà, assuming the viscosity is infinite.
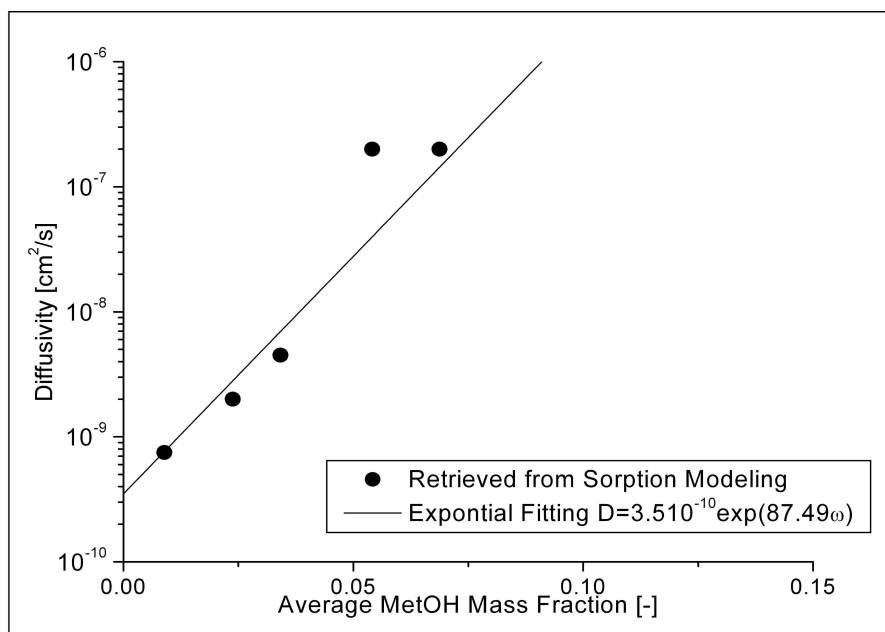
Fig. 6.11   Methanol diffusivity in Matrimid 5218 as a function of the average Methanol concentration, calculated considering, for each step, the concentration at which the step was started and the final concentration at which the steady state was obtained, without relaxation of the polymer matrix.

After this preliminary calculations performed neglecting the description of the relaxation of the polymeric matrix, calculations were redone varying the value of the viscosity, in order to obtain the best fit that was possible of the complete sorption kinetic curves. The results are shown in Fig. 6.12. The largest deviations between the predicted and the experimental results are those of the last two steps. In fact, the predicted kinetic of the fourth step exhibit a quite evident two stage behavior that is not found in the experimental data. This could arise since the diffusivity characteristic time is too short respect to the relaxation characteristic time (this could be tracked back to the choice of a diffusivity coefficient value too high, as suggest also by the fact that this value is the outlier of the plot reported in Fig. 6.11). At the same time it must be observed that, when applying the Berens Hopfenberg model, similar behavior arose when only one relaxation time was used and disappeared when using a broader distribution of the relaxation time itself. The present model use only one relaxation time, therefore if significant separation exist between this relaxation

time and the characteristic diffusion time, two stage behavior will be predicted. The fifth step is represented quite well, from the qualitative point of view, since the shape of the predicted mass uptake curve parallels pretty well the one of the experimental data, but from a quantitative point of view the model overestimates the mass uptake itself. This is not unexpected, since this problem has already been noticed when discussing the quality of the prediction of the sorption isotherm.
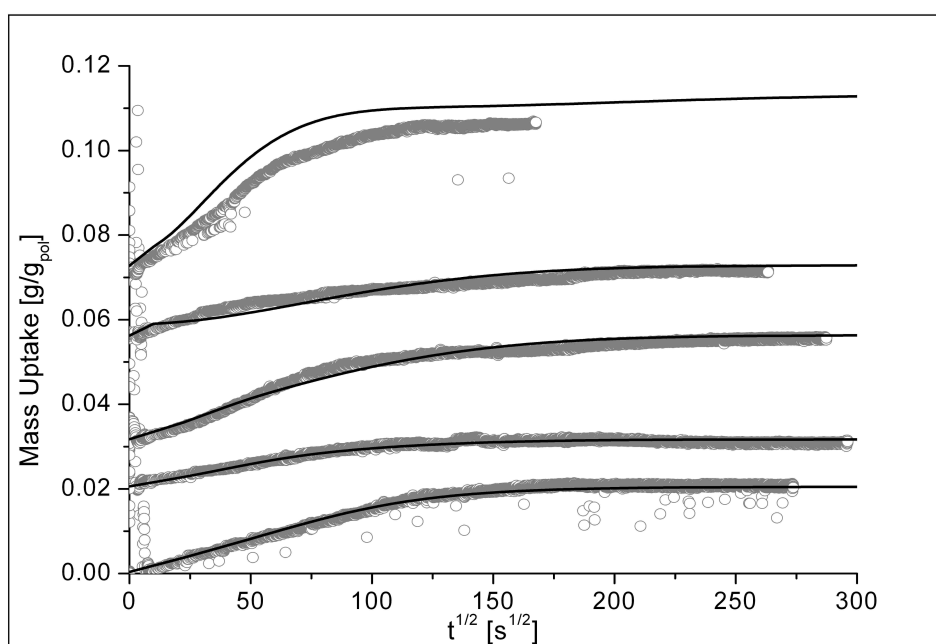
Fig. 6.12   Comparison between the experimental sorption kinetics of vapor Methanol in Matrimid 5218 at 308 K with the prediction of the model derived from the model proposed by Doghieri and Carlà, using the viscosity as an adjustable parameter.

The viscosity values retrieved from the fitting of the vapor sorption kinetics are reported in Fig. 6.13 as a function of the average Methanol concentration, calculated as the average between the composition at which ended the purely diffusive contribution previously calculated and the final concentration of the step. The viscosities decays exponentially as the methanol concentration in the polymer matrix increases, as shown by the exponential fitting of Fig. 6.13. This is certainly expected, since reflects the plasticizing action of the penentrant on polymeric matrix and several authors, like Hesse and Sadowski[126] have applied

such kind of dependence in their effort of modeling non Fickian integral sorption kinetics in glassy polymer. In the present case the viscosity was assumed to be constant during each step, but there are no doubt that such assumption can hold only for differential sorption data, in which the change in concentration is limited during each step. In case of modeling integral sorption kinetic the composition dependence of the viscosity shall be explicitly accounted for.
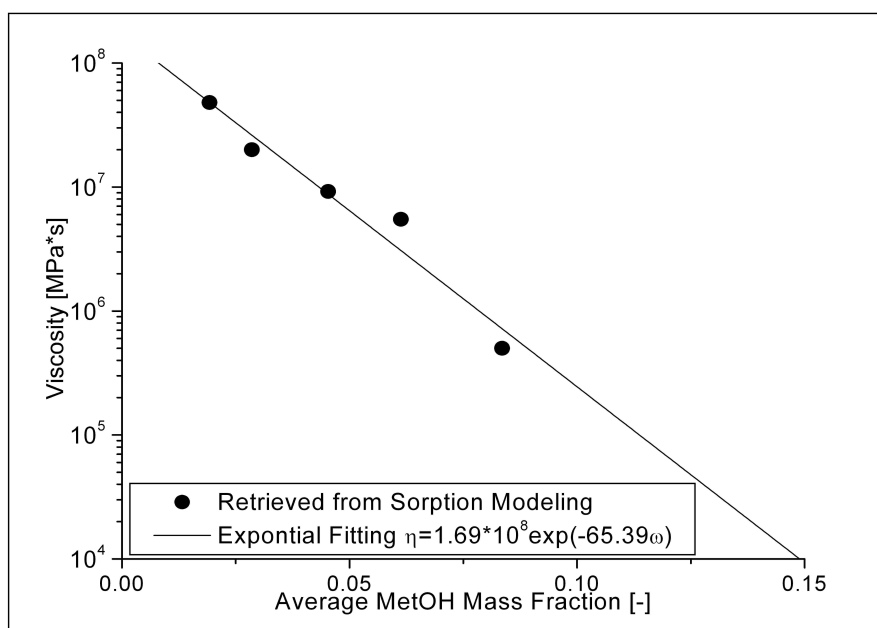
Fig. 6.13   Viscosity of the Matrimid 5218 matrix as a function of the average Methanol concentration, calculated as the average between the composition at which ended the purely diffusive contribution previously calculated and the final concentration of the step.

Modeling of the liquid methanol sorption step requires some specific caution, since it is an integral sorption step in which the polymer undergoes the widest possible activity jump. Thus the driving force is going to be the maximum possible and it is expected that concentration gradient be quite steep inside of the sample. It is then questionable that kinetic properties such as penetrant diffusivity and the viscosity of the polymeric matrix could be assumed to remain constant. In fact, the data collected with the differential sorption experiment suggest that diffusivity of methanol in Matrimid 5218 could increase up to three order of magnitude, as well as viscosity decreases up to three order of

magnitude, in the concentration span that range from zero (dry polymer conditions) to 0.16 g/g$_{pol}$, that is the solubility of the liquid methanol at 35℃. The same results suggest that an exponential dependence from the methanol mass fraction could be appropriate for describing the plasticizing effect of methanol on the glassy Matrimid 5218 matrix. Therefore the equation of the model should be modified as follow:

6.17
$$\begin{cases} \dfrac{\partial C}{\partial t} = -\dfrac{\partial}{\partial x}\left[-D_0 \exp(\beta C)\dfrac{\partial C}{\partial x}\right] \\[2ex] \hat{V}_P = \dfrac{1}{\rho_P} = \chi \hat{V}_S + (1-\chi)\hat{V}_{P,g} \\[2ex] \dfrac{1}{\hat{V}_S}\dfrac{d\hat{V}_S}{dt} = \dfrac{P^{Eq}\left(T,\hat{V}^{EQ}{}_P,\mu^S\right)-P}{\eta_0 \exp(-\gamma C)} \end{cases}$$

The introduction of concentration dependent kinetic parameters increase the non linearity of the model and its computational cost, but it is needed in order to provide a plausible description of the physical picture of the sorption process. At first it was attempted to use the exponential dependence of diffusivity and viscosity that had been obtained applying the model in order to model the vapor sorption kinetics. The result, depicted in Fig. 6.14 with a dotted line, departs significantly from the experimental data, nevertheless it is really relevant the fact that the kinetic predicted by the model has the proper curvature and reproduce many of the qualitative features of the experimental sorption curve, without introducing artifacts such as two stage behavior, that would have meant a completely erroneous representation of the ratio between the diffusion characteristic time and the relaxation characteristic time. In Fig. 6.14 is reported with a continuous black line also the results of calculations performed assuming that the law that describe the dependence of viscosity upon methanol concentration is $\eta = 10^8 \exp(-75\omega)$, that compares more favorable with the experimental data. The law that describe the dependence of the diffusivity on the methanol concentration has been modified as well as

$D = 3.5 * 10^{-10} \exp(110\omega)$. In the same Fig. 6.14 it is reported, in fine dots, the results of the calculations of the sorption kinetic with the modified viscosity dependence and the diffusivity law that has been estimated from the differential sorption experiments: the only difference is recognizable in the initial portion of the curve.
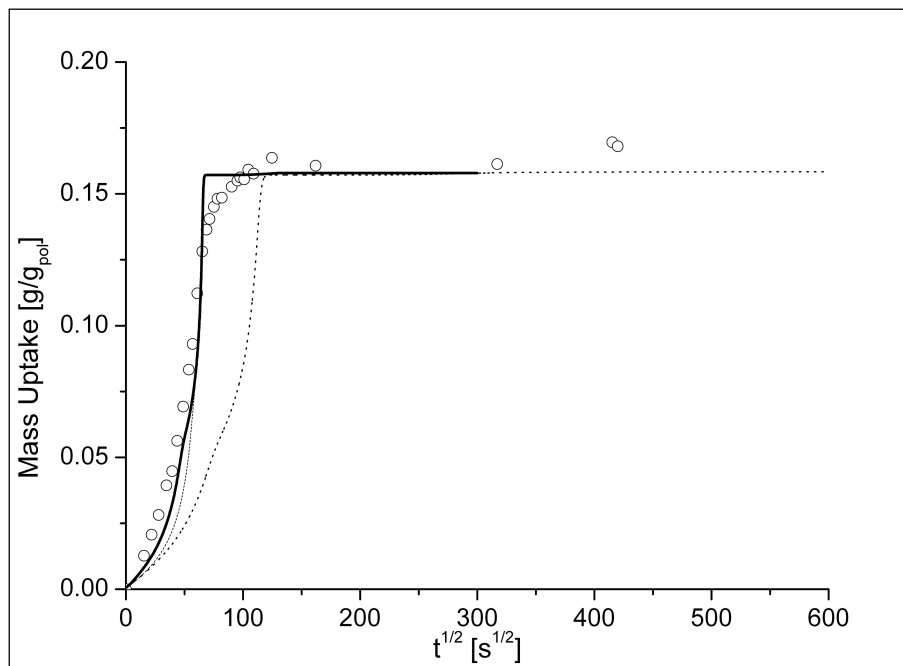
Fig. 6.14   Comparison between the experimental sorption kinetics of liquid Methanol in Matrimid 5218 at 308 K with the prediction of the model derived from the model proposed by Doghieri and Carlà, assuming that diffusivity and viscosity depends exponentially from the methanol concentration.

In Fig. 6.15 are depicted some of the calculated concentration profile for the liquid methanol sorption: it is quite evident that the time evolution of the concentration at the boundary drive the sorption process and that at the beginning of the sorption process the concentration profile is characterized by the presence of some kind of intruding front, that is smoothed by the effect of diffusion. In any way, diffusion and relaxation process appear to be coupled and their characteristic timescales are not separated, because even at long times there are still recognizable concentration gradient across the sample.

Fig. 6.15   Concentration profiles predicted for liquid Methanol sorption in Matrimid 5218 at 308 K, assuming that diffusivity and viscosity depends exponentially from the methanol concentration. The spatial variable is represented in non dimensional term and is normalized respect to the half thickness of the sample.
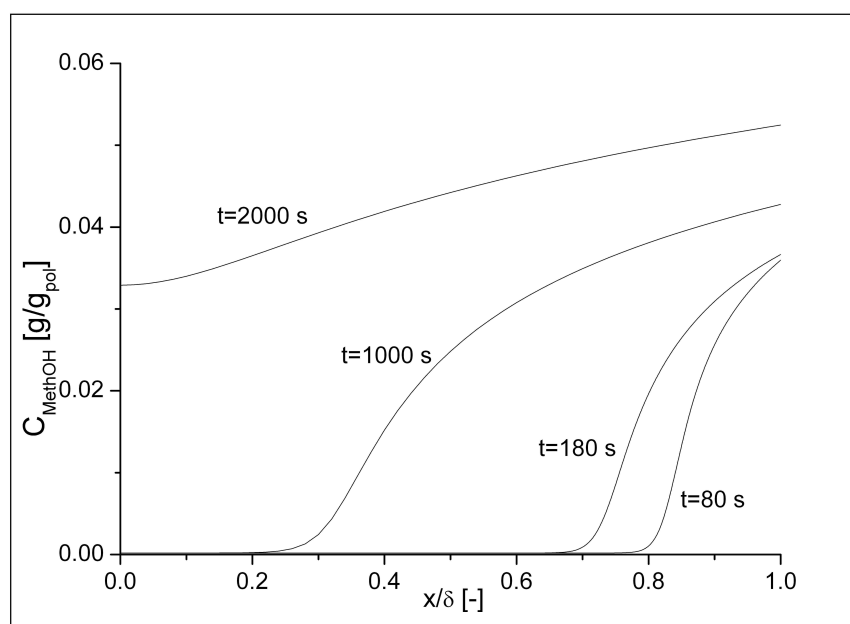
6.7.   1-Propanol Sorption Kinetic

The sorption experiment with liquid 1 propanol was performed on a sample prepared   by solution casting from a 5% Matrimid 5218 solution in Dichloromethane, that gave a film 68.8 μm thick. The sorption experiment was characterized by a really slow kinetic and lasted more than one month and the steady state mass uptake is equal to 0.172 g/gpol. Since no vapor sorption data are available, there is only one pseuodoequilibrium solubility datum that can be used for the purpose of tuning the thermodynamic model that is used for estimating the surface concentration and the driving force of the volume relaxation process. Therefore it was made the decision to retain the values of χ and $\hat{V}_{P,g}$ that had been estimated directly from the sorption isotherms of dichloromethane in Matrimid 5218, in which the plasticizer induced glass transition has been detected. With this choice the binary interaction parameter

$k_{1\Pr opOH-Matrimid}$ remains the only adjustable parameter of the thermodynamic model and it was found that it has to be set equal to 0.0397 in order to predicted the correct value of the solubility of liquid 1 Propanol in Matrimid 5218. The coefficients of the laws $D = D_0 \exp(\beta C)$ and $\eta = \eta_0 \exp(-\gamma C)$ that describe the dependence of diffusivity and viscosity upon penetrant concentration have been retrieved by fitting the integral sorption curve of the liquid 1 propanol in Matrimid 5218 at 308K. The best fit of the experimental kinetic data is obtained with $D = 2*10^{-10} \exp(10\omega)$ and $\eta = 10^8 \exp(-15\omega)$, it is then evident as suggested also by the longer duration of the experiment, that the plasticizing action that the 1 Propanol molecules can exert on the Matrimid 5218 chains is less marked than that of Methanol. The result of the model calculations is the solid line in Fig. 6.16.
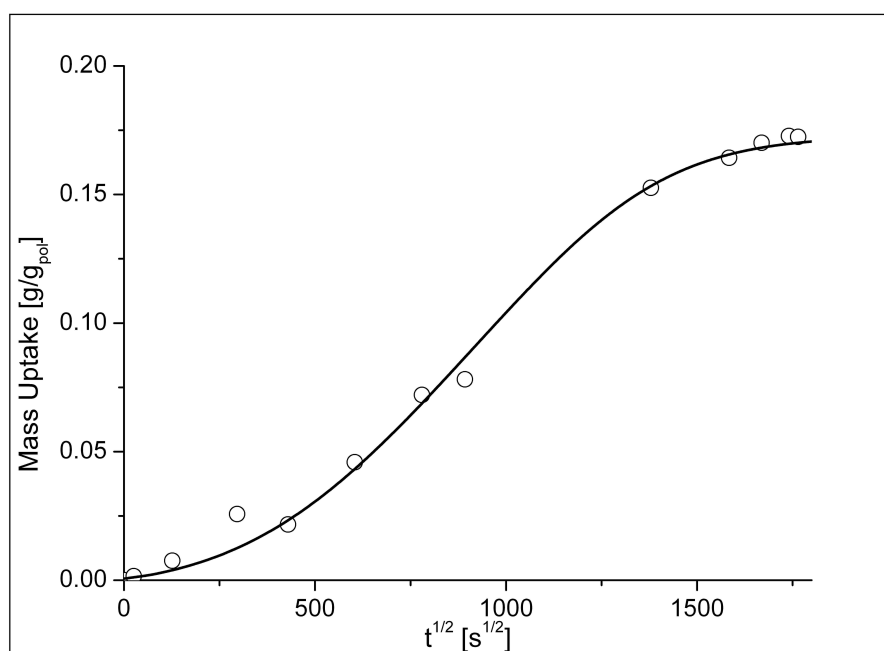

Fig. 6.16 Comparison between the experimental sorption kinetics of liquid 1 Propanol in Matrimid 5218 at 308 K with the prediction of the model derived from the model proposed by Doghieri and Carlà, assuming that diffusivity and viscosity depends exponentially from the 1 Propanol concentration.

Finally in Fig. 6.17 are depicted some of the concentration profiles predicted by the model, from which it is possible to observe that even in such a long lasting sorption process diffusion and relaxation are deeply coupled. The initial concentration profiles appear to be smoother than those obtained for the much faster methanol sorption.
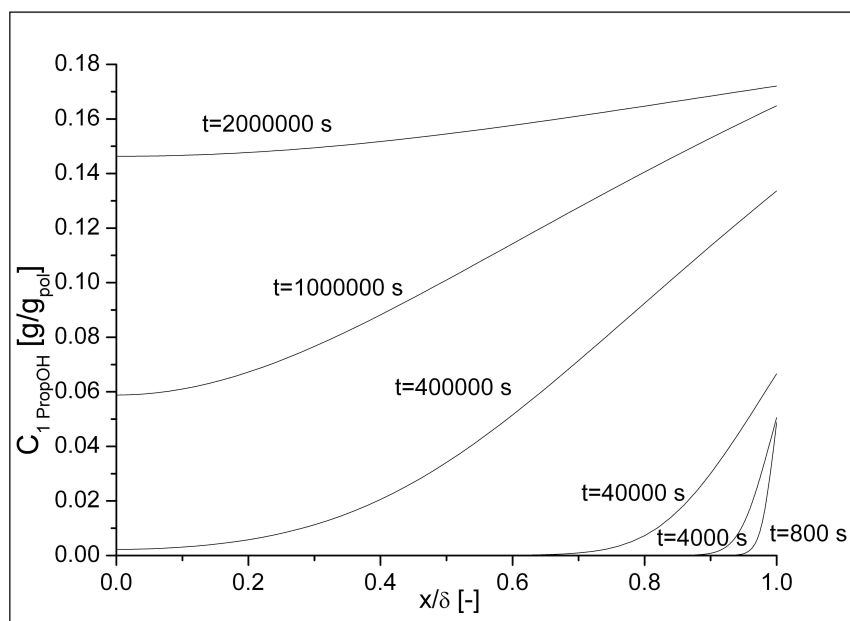
Fig. 6.17 Concentration profiles predicted for liquid 1 Propanol sorption in Matrimid 5218 at 308 K, assuming that diffusivity and viscosity depends exponentially from the 1 Propanol concentration. The spatial variable is represented in non dimensional term and is normalized respect to the half thickness of the sample.

6.8. Concluding remarks

The Berens Hopfenberg Model is a phenomenological tool suitable for modeling and correlating experimental data regarding the kinetic of the sorption of low molecular weight species in glassy polymers. In the present work it was applied in order to model the data about the sorption kinetic of dichloromethane in Matrimid 5218 that had been collected with the Quartz Crystal Microbalance. It has been found out that the best modeling results are obtained using two

separate contribution with different relaxation characteristic times for representing the relaxation global contribution to sorption. The use of the stretched exponential, known as the Kohlrausch–Williams–Watts relaxation modulus, provide another successful option for modeling the same data. Since the Berens Hopfenberg model require the use of a relevant number of adjustable parameters, the development of procedures that enable to estimate some of the parameters, effectively reducing the degree of freedom of the model, can be useful. It has been shown that, when enough timescale separation exists between the diffusion characteristic time and the relaxation characteristic time, the weighting factor α_D can be estimated applying the NETGP approach in order to estimate the mass uptake due to diffusion only in absence of relaxation of the glassy matrix. Comparison with the empirical values of α_D is favorable. The fundamental hypothesis of the Long and Richman Model have then been discussed, especially taking into account the relationship that can be exploited between the surface concentration, that is assumed to evolve during the sorption experiment, and the polymer density, as described by NETGP approach. Finally a model, that is hybrid between the Long and Richman model and the model proposed by Doghieri and Carlà has been introduced and applied to liquid and vapor sorption of Methanol in Matrimid 5218 and to the sorption of liquid 1 Propanol in the same polymer.

7. Gas Permeation in Electron Beam Cured Trifunctional Acrylate Films

7.1.   Introduction

Polymerization reactions of the radical chain type require that, along with monomers and, if required, a solvent, the mixture contains a substance capable to act as an initiator. The initiator is a substance that upon a stimulus, such as UV radiation or heat, will be promptly homolyzed, producing one or more radical species, that will start the chain of reactions that lead to polymerization of the monomers. Thermal stimulus or UV radiation usually does delivery enough energy, at a molecular level, in order to break up the monomer molecules, so the introduction in the mixture of a specific initiator molecule is not avoidable. This may be a problem for several reasons. In fact, initiator have an high price, are really reactive and are frequently species dangerous to health and that pose environmental problems. Moreover it is really difficult to assure that all the initiator molecules are reacted and thus the finished product could contain traces of the initiator: this should be avoided in food applications, as well as for products that are to be used inside the human body. Finally, if the strength of the initiating stimulus is not uniform across the sample, for example due to optical absorption of the UV radiation, will cause a non uniform reaction rate and conversion, potentially leading to stress build up that can cause loss of dimensional control and the generation of defects like crazes and cracks[127].

Instead application of ionizing radiations, such as an electron beam, to a mixture of liquid monomers will produce enough radical species to start the chain reactions, without the need of any substance that act as an initiator[128]. This technology have many applications, for instance the manufacturing of hot water pipes in crosslinked polyethylene or the production of insulated cables for aeronautical applications, in which a good resistance to oil and grease contamination is required[129-131]. Another field of application, in substitution to the more traditional UV curing, is the curing of polymeric protective coatings. For this last application, the most interesting monomers are those of the family of the multifunctional acrylates and among them the trimethylolpropantriacrylate (TMPTA) is one of the most studied and characterized. Its molecular structure is shown in Fig. 7.1 In this work, this trifunctional monomer have been used for producing free standing films by means of electron beam curing of the liquid monomer. Several values of the radiation doses have been used, in order to study the effect that the dose of radiation delivered to the sample could exert on its final properties. In any case the monomers where polymerized and formed a glassy polymer in a matter of seconds: this process is characterized by an abrupt change of phase, along with the sudden onset of the kinetic constraints that hold in glassy phases. The samples were prepared at the 3M research laboratories of Saint. Paul (Minnesota). Conversion characterization through FTIR analysis was conducted at the Characterization Facility of the University of Minnesota, while gas permeation characterization of the previously prepared samples have been exploited at the University of Bologna. Several gases had been tested, in order to develop an understanding of the effect of radiation dose on the gas transport parameters and in order to evaluate if changing the radiation dose it was possible to tailor the properties of TMPTA glassy membranes for applications like hydrogen separation, air fractionation and carbon dioxide capture.
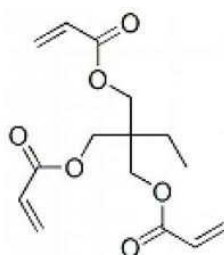
Fig. 7.1   TMPTA molecular structure.

7.2.   Interaction of ionizing radiation with organic materials

Ionizing radiation are charged particles, nucleons or photons that possess enough energy to cause the ionization of neutral molecules onto which they may collide. Ionizing radiations are emitted by particle accelerator devices, by nuclear reactions and by the interaction between ionizing radiation beams and by solid targets of some specific materials[132]. The more common forms of ionizing radiations are, in order of increasing energy and penetration depth in common materials, the α particles, the β particles and γ rays. The α particles are nuclei of the helium atoms, β particles are accelerated electrons or positrons (thus it should be made a distinction between β^+ and β^- radiation) and γ rays are photons of very very high frequency. Other accelerated particles, like neutrons, are further example of ionizing radiations. Interactions between ionizing radiation and solid or liquid matter are extremely complex, since they involve phenomena that takes place at different lengthscales and timescales, affecting the electrons of the atoms, their nuclei, the intramolecular bonds and so on, up to the supramolecular level, when the ions and the radicals that are being generated by the radiation react with each other and with other molecules, initially neutral. This field of study is very complex and intriguing and has deserved a lot of attention, especially for what concern the interaction between ionizing radiation and living cells, in order to understand the relationship between exposure to radiation and health hazard and

consequences. This studies have led to the understanding that two kinds of effects exists, known as *deterministic effects* and *stochastic effects*. The first kind of effects are characterized by a recognizable dose – effect relationship and typically takes place at high exposures, such those that lead to acute radiation sickness. The second kind of effects are related to the development of ailments such as cancer and damage to fetuses of exposed pregnant mothers. The relationship between exposure doses and this effects is lacking, but it is known that this effects are related to the damage that the radiation inflicts on the DNA molecules of the target tissue. Many of the molecular details of this interactions are still uncharacterized. The other field concerning interactions between radiation and solid and liquid matter that has developed substantially after 1940's, is the study of the radiation damage on the materials commonly used in the nuclear energy field. The study of the damage that the long time exposure causes to steel and other metallic alloys, as well as to ceramics and concrete, is relevant for the safety and reliability of nuclear reactor pressure vessel, biologic shields and nuclear combustible rods. Radiolysis of the moderator fluid or of the thermovector fluid employed in nuclear reactors is another field of considerable interest. Since the vast majority of civil, military and research reactors use water as moderator and/or thermovector fluid, an extensive literature exist on the topic of water radiolysis. The literature that deals with the radiolysis of organic liquids is really limited, probably because the use of that materials, as well as the use of rubbers and polymeric materials, is not common in the area of nuclear power plant where radiation fields are more intense. In any case, some general features can be outlined as follows, especially regarding the fact that the ions and the radicals formed due to the effect of radiation on an organic mediums can trigger polymerization and crosslinking reactions or can cause chain scission effects. It has been recognized that there exists different kind of interaction events between an incoming radiation beam and a material media (known in the radiation chemistry literature as *spur*) with significantly different yield of chemical species formed. It is then useful to distinguish between single ionization and multiple ionization events, as their different chemical yield lead to different effects. In the present

case the irradiation is always performed with an electron beam, but the electrons of the beam itself do not play any important role in the chemical reaction that develops immediately after the interaction event. The phenomena of energy transfer explain the possible different results of the interaction of the interaction between the beam and the polymer chains. According to several estimates the ratio between the average energy loss of the incoming electrons due to the collision with atomic or molecular electrons and the average energy loss due to interactions with nucleus for an organic, carbon based media, is[132]:

7.1
$$\frac{\langle \delta E \rangle_n}{\langle \delta E \rangle_e} \propto \frac{m}{M_2} Z_2 \approx \frac{6*10^{-31}}{12*10^{-27}} \approx 0.5*10^{-4}$$

Therefore it is possible to assume that in the present case all the relevant interactions take place with the molecular electrons and that the primary event following the collision is the detachment of electrons from the molecule. In ion irradiation, were $m \approx M_2$, it has been reported that also interaction with nuclei plays a relevant role. The primary detached electrons can have very different energies and can travel different ways and undergo different fates, more frequently being trapped in a diversity of modes. In single ionization spurs the most frequent results of the evolution of the detached electron and of the positive charged site in the polymer/oligomer chain or in the monomer molecule is an initial pair recombination followed by transfer of the excitation energy between different molecules modes and finally the formation of an unpaired electron in the polymer, a reactive macro radical, due to homolysis of one of the bond of the pendant side group of the chain, such as in the case of hydrogen detachment or of the chain itself[129, 131]. The fate of the detached electron can be different and it can react with other positive charged sites, different from the original one or with cationic species, but even solvation of the free electron with a previously neutral molecule is a possibility. Crosslinking then happens when the radicals produced react producing chemical bonds between adjacent chains. Multi ionization spurs contain more energy than single ionization spurs

and cause chain scissioning and production of low molecular weight debris. Further development of the reaction in the aftermath of a multi ionization event depends on the type of polymer as the loose end of the broken chain can react with neighboring chains, giving raise to crosslinked structures, but the general result can be a reduction of the average molecular weight. Both types of spurs contribute in a different way to the final effects and property modification of irradiation on polymers. The radical site on the chains can attach reactive compounds, such as molecular oxygen. This effect will limit the reaction between polymer chains or oligomers and monomers, therefore in polymer modification or curing it is required to operate under nitrogen blanket. In the present case the polymer itself was obtained by radiation initiated crosslinking of monomer (TMPTA). It is then obvious that the crosslinking plays a major role in the structure build up, especially the concentration of the activated species and the possibility that an already inert chain is again made reactive due to the formation of a radical site. It is not possible to exclude that some of the final properties of the sample are influenced by the relative relevance of the crosslinking effect and of the chain scission effect as once that the macromolecular structure had already been formed the radiation effects should be equal to those previously explained in the case of polymer irradiation.

7.3. Material Preparation

The sample preparation has been carried on at 3M corporate research laboratories in Saint Paul, Minnesota, US.

The sample preparation procedure can be summarized in the following step:

1. Monomer deposition on a suitable substrate
2. Irradiation under nitrogen atmosphere
3. Film removal from the substrate

As a substrate a commercial flexible film of polyester provided by 3M has been used and the monomer has been coated on it by means of a slit device. The

coating thickness was set to be 50 μm, but the final thicknesses of the samples were systematically higher and not homogenous. This could be relayed due to errors in the deposition step and to dewetting of the substrate that was observed to occur in the timeframe between deposition and irradiation. Electron Beam Irradiation then has been performed with a commercial apparatus for irradiation on a web line. The operating parameters that could be controlled were the web speed, the beam voltage (or the electron's kinetic energy) and the beam current. It was then possible to choose different irradiation dose and dose rate. The values of the operating parameters used for each protocol are summarized in Tab. 7.1. The volume surrounding the irradiation window was shielded with lead and steel and in the irradiation chamber the samples were kept under nitrogen blanket, in order to prevent radical scavenging by oxygen. Radiation dose measurements were performed with a physical detector embedded in the irradiation apparatus and with a commercial radiochromic device that was introduced along with a sample. The irradiation protocols that were used are listed in Tab. 7.1 and Tab. 7.2. Due to the quick volumetric shrinkage frustrated by the substrate adhesion and the simultaneous onset of high elastic modulus and brittle behavior the glassy film made by TMPTA cracked and delaminated during the curing process and were directly recovered from the substrate as stand alone specimens.

TMPTA				
Protocol	Voltage [kV]	Current [mA]	Web Speed [m/s]	Dose [kGy]
A	170	1	0.15	8
B	170	2	0.07	32
C	170	4	0.07	64
D	170	8	0.07	128

Tab. 7.1   TMPTA samples irradiation protocol.

7.4. Conversion Measurement with FTIR-ATR

The Attenuated Total Reflection Fourier Transform Infrared Spectroscopy is a method suitable for measuring the degree of conversion of multifunctional acrylates monomer or oligomers in electron beam cured films. The drop in the double bond C=C absorbance peaks, at 1635 1/cm and 1619 1/cm, respect to the peaks measured for the uncured monomer, is a measure of the extent of the polymerization reaction. In order to take into account the density differences between monomer and polymer and any eventual effect introduced by the adhesion to the ATR crystal, it is necessary to normalize the area under the changing C=C peaks respect to the area of the peaks of C=O, at 1722 1/cm, from the same spectra, that are assumed to be not affected by the reaction. According to this the expression for conversion is: $\chi = 1 - \left(\dfrac{Area_{C=C}}{Area_{C=O}}\right)_{cured} \left(\dfrac{Area_{C=O}}{Area_{C=C}}\right)_{uncured}$ In the case of TMPTA the conversion of the double bonds of the monomer were obtained by numerical integration of the absorbance curve and show a characteristic increase with the irradiation dose. The absorbance spectra of uncured monomer and of the TMPTA films are shown in Fig. 7.2.
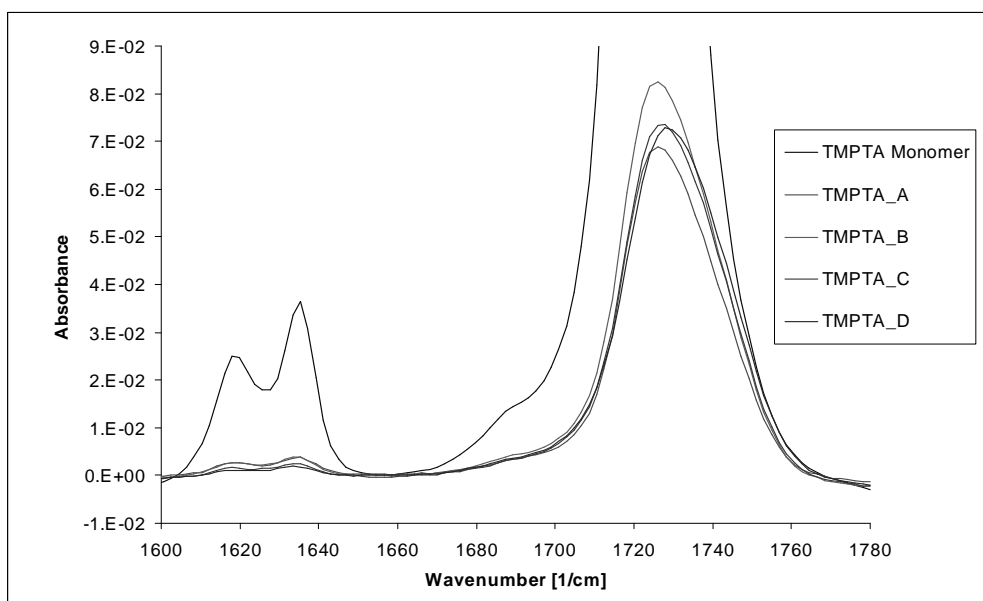
Fig. 7.2   TMPTA FT – IR ATR absorbance spectra.

The measured conversions of the double bonds for each preparation protocols are reported in Tab. 7.2 and are shown, as a function of the radiation dose, in Fig. 7.3. Quite reasonably conversion increase with the dose of radiation delivered to the monomer films. It should be noted that even with the lowest irradiation the conversion is pretty high: the interaction between electron beam and the monomers quickly generate a huge pool of radical, that initiate and speed up the chain reactions that lead to formation of the macromolecular structure.

TMPTA	Conversion
Protocol	
A	56
B	66
C	81
D	85

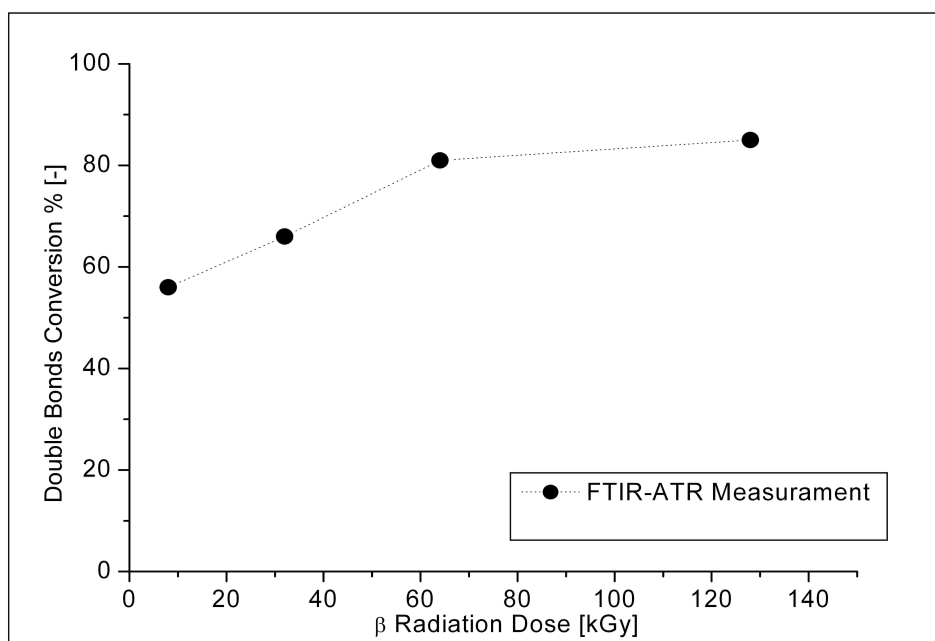Tab. 7.2   TMPTA samples measured conversion.

Fig. 7.3   TMPTA's double bonds conversion as a function of the radiation dose delivered to the monomer films.

7.5.   Permeability Measurement

Pure gas transport properties of the TMPTA e-beam cured films were investigated by means of a closed volume barometric device[133]. The permeability, the diffusivity and the solubility of Helium, Oxygen, Nitrogen, Carbon Dioxide, Argon and R134a where measured. Appropriate samples of the film were posed in a leak proof sample holder, in such a way that one side of the film can be connected to a pressurized reservoir of the pure penetrant gas, namely the upstream section of the device, while the other side of the film is exposed to a little chamber of which pressure is constantly monitored. The apparatus is embedded in an incubator with PID temperature controller, in order to ensure isothermal test conditions. The lay out of the permeation apparatus is shown in Fig. 7.4. Before the test starts both sides of the sample and the downstream section are kept under vacuum for at least 12 h, in order to remove any previously absorbed gases or vapors. At the beginning of the test, when the upstream reservoir is connected to the gas holder, the downstream chamber is

still under vacuum and the difference of pressure between the sides of the film will act as the driving force for the permeation process. Under steady state conditions the relationship between the flux and the driving force is: $J_{ss} = \dfrac{P}{l}(p_{upside} - p_{downside})$. The permeability P is defined as the product between the average diffusivity and the average solubility coefficients across the film: $P = S * D$. The flux across the film will be monitored by means of continuous measurements of the pressure in the downstream chamber. The sensibility of the apparatus is then related to the lower chamber volume, as according to the ideal gas law the relationship between the steady state flux and the pressure increase in that vessel is: $J_{ss} = \left(\dfrac{dp_{downside}}{dt}\right)_{ss} \dfrac{V}{RT} \dfrac{1}{A}$

It is usually assumed that the slight increase of the downstream pressure will not affect the driving force of the permeation process. The test is usually run until a steady state condition is reached. Under the assumption that the solution –diffusion model applies and that the diffusion process is well modeled by means of the Fick law it is then possible to apply well known results from the theory of the unsteady diffusion across a slab and estimate the diffusivity from the time lag value. The time lag is the value of time that can be extrapolated from the plot of the time integral of the downstream flux respect the time variable itself, when a straight line tangent to the steady state curve is drawn, as shown in Fig. 7.5, that is plot of the downstream pressure as a function of time, in a permeation test.

$$7.2 \qquad\qquad \tau_{lag} = \frac{l^2}{6D}$$

From the permeability and the diffusivity values it is then possible to estimate the solubility coefficient of the penetrant in the polymer. As long as with this method there is no direct measurement of this parameter it is affected by more relevant uncertainties. In order to compare the permeation of different gases in

a polymeric matrix it is often useful to define the ideal selectivity for each couple

of gases: $\alpha_{ij} = \dfrac{P_i}{P_j}$ as the ratio of the pure gases permeability.

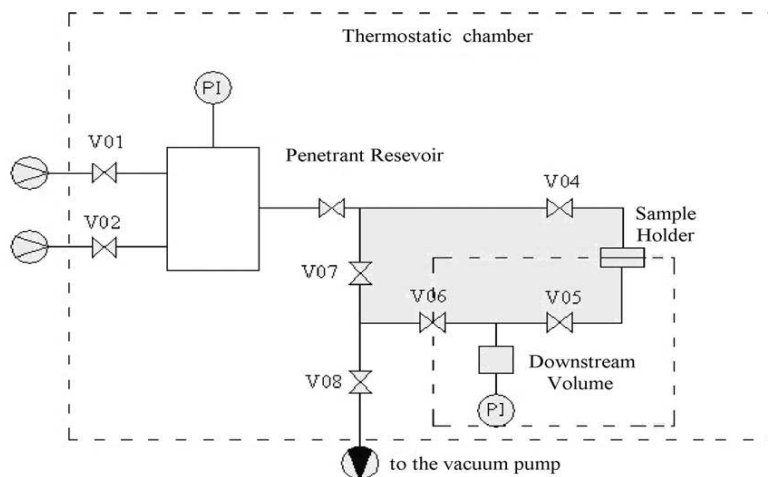

Fig. 7.4   Lay out of the permeation apparatus.
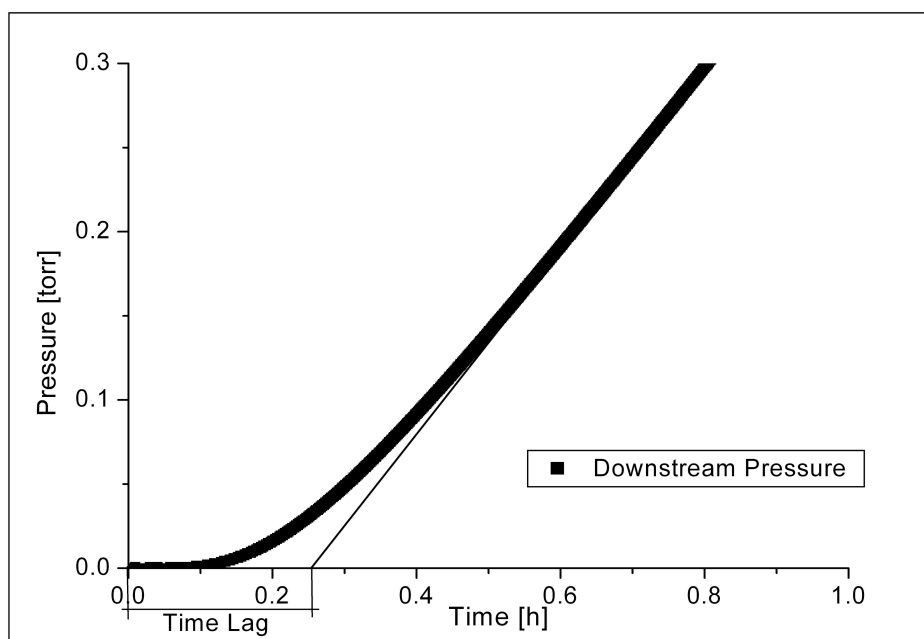

Fig. 7.5   Characteristic result of a permeation test. Here is depicted the one performed with
CO_2 at 308 K on the TMPTA prepared according to protocol A.

At least two samples for each preparation protocol (A, B, C, D) were tested and
the permeation experiment, for each polymer-gas pair, was repeated three

times. Film thicknesses were measured for each sample by means of a micrometer device, as previously stated some inhomogenities were found and each fragment that was used in the characterization process was measured several times and in several position and the average of their specific measured values was used in the data analysis. In Tab. 7.3 are listed the average thickness for the TMPTA film obtained taking into account all the measurement made on all the sample tested, for each tested sample the standard deviation of the thickness measurement is much less than the global value listed in the table.

TMPTA		
Protocol	Thickness [mm]	%Standard Deviation
A	0.093	18
B	0.077	4
C	0.072	9
D	0.095	18

Tab. 7.3   TMPTA samples thickness measurements.

The apparatus was operated at 35℃ and the upstream pressures were generally kept at around 1 atm. The results of the measurements of pure gas permeability and diffusivity are represented in Fig. 7.6 and Fig. 7.7 and show that the irradiation dose directly affects the gas transport properties of the glassy TMPTA. All the values were obtained at 35 ℃ . The experimental data show that there is a recognizable trend of decreasing permeability and diffusivity with the increase of the exposition dose. Solubility coefficients that are indirectly obtained from the permeation experiments are represented in Fig. 7.8. Although the solubility coefficients are affected by larger uncertainties it seems that this parameter is only a weak increasing function the dose. Finally in Fig. 7.9 the same permeability results are plotted as a function of the measured conversion of the double bonds of the TMPTA monomers: this two properties, each one function of the radiation dose, are found to be completely correlated. Permeability depends on the degree of conversion of the double bonds

according to an exponential law of the type: $P = P_0 \exp(-\beta\chi)$, where P_0 is the permeability in a fictive glassy TMPTA in which no double bonds have reacted.
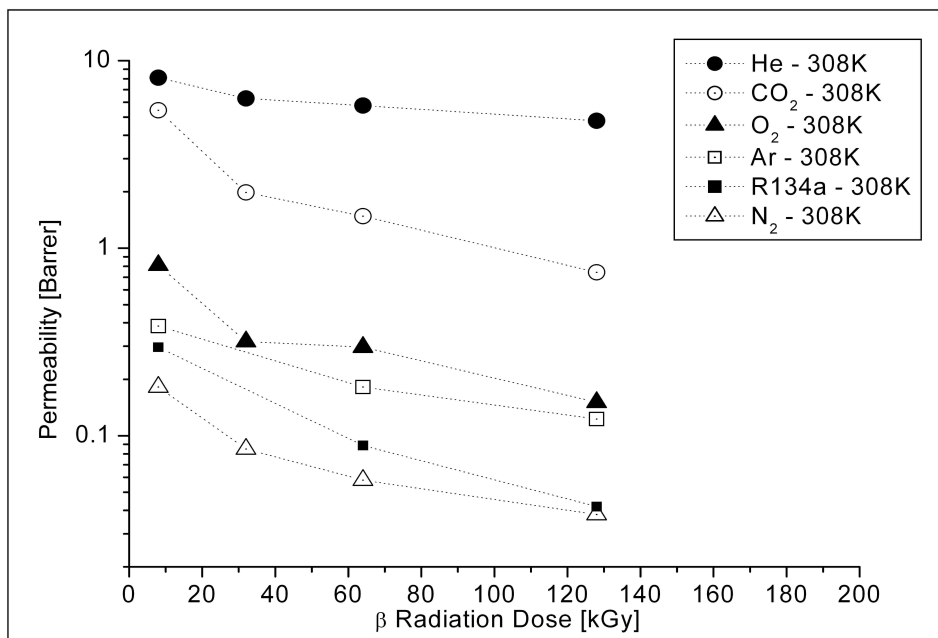
Fig. 7.6 Pure gas permeability as a function of the radiation dose.
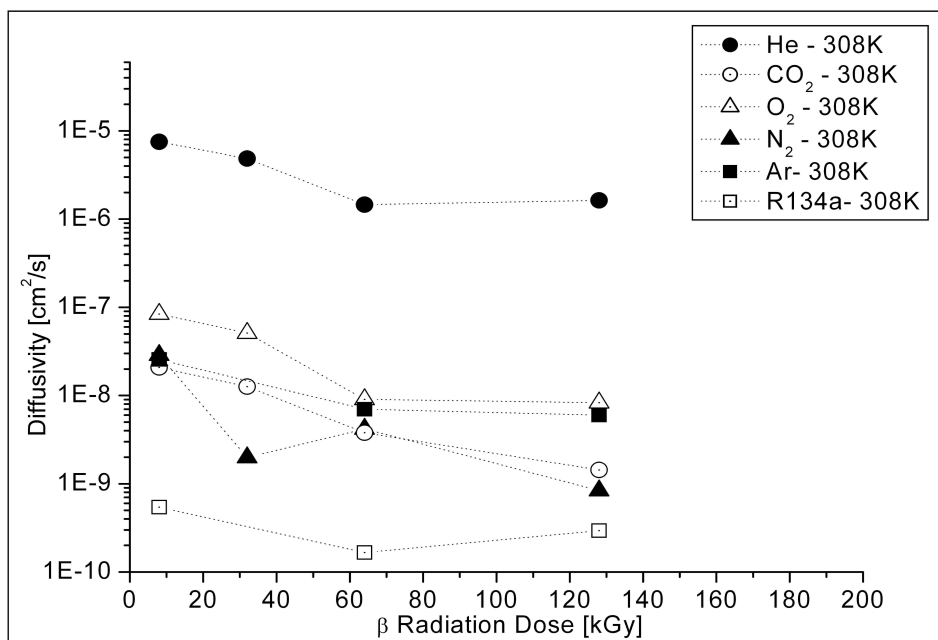

Fig. 7.7 Pure gas permeability diffusivities as a function of the radiation dose, as calculated from the thickness and time lag measurements.
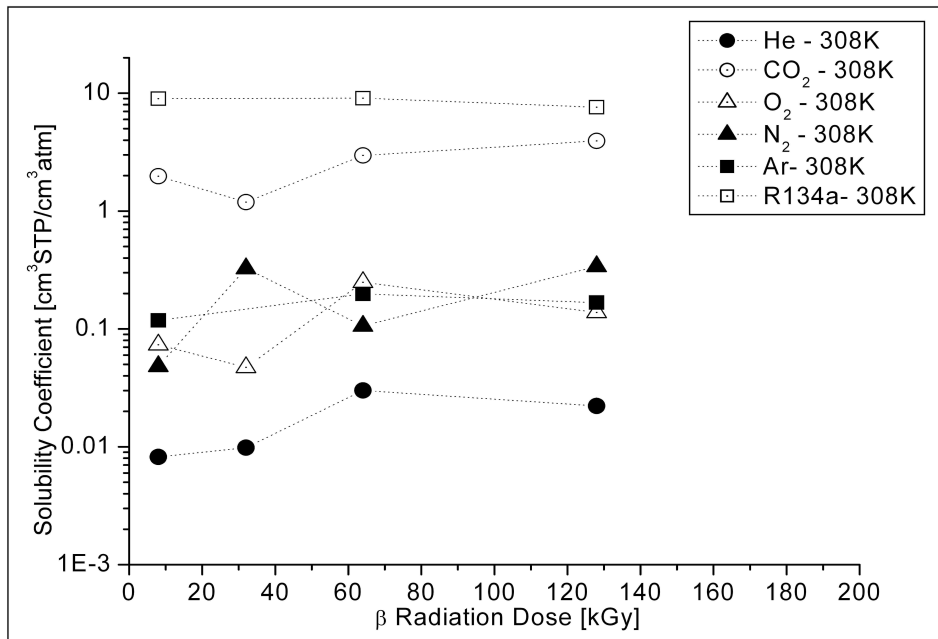
Fig. 7.8 Pure gas solubility coefficients a function of the radiation dose, as calculated from permeability and diffusivity.
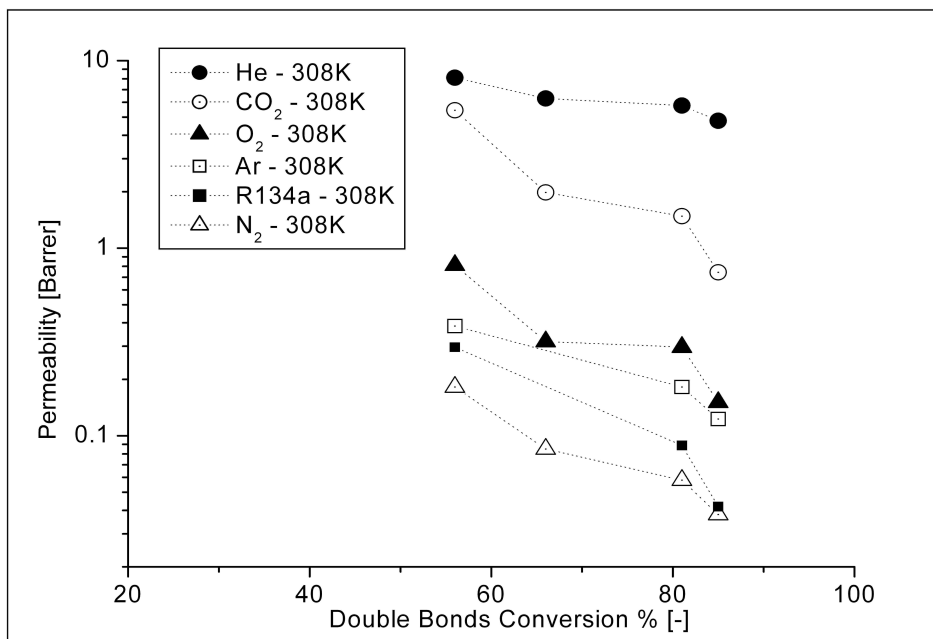
Fig. 7.9 Pure gas permeability a function of the conversion of the double bonds of the monomer.

Besides the general trend of permeability decrease with the dose, according to Fig. 7.10 the diffusivity is a decreasing function of the kinetic diameter of the gaseous penetrant, that are summarized in Tab. 7.4. This trend is expected and has been documented for many other polymeric glasses. Fig. 7.11 show that despite their scatter the solubility increase with critical temperature of the penetrant according to an empirical relations such $\ln S \propto T_c$, also this behavior is well recognized in the polymer literature[134] and it is related to the gas condensability. The critical temperature of the gaseous penetrants used in this study are reported in Tab. 7.5.
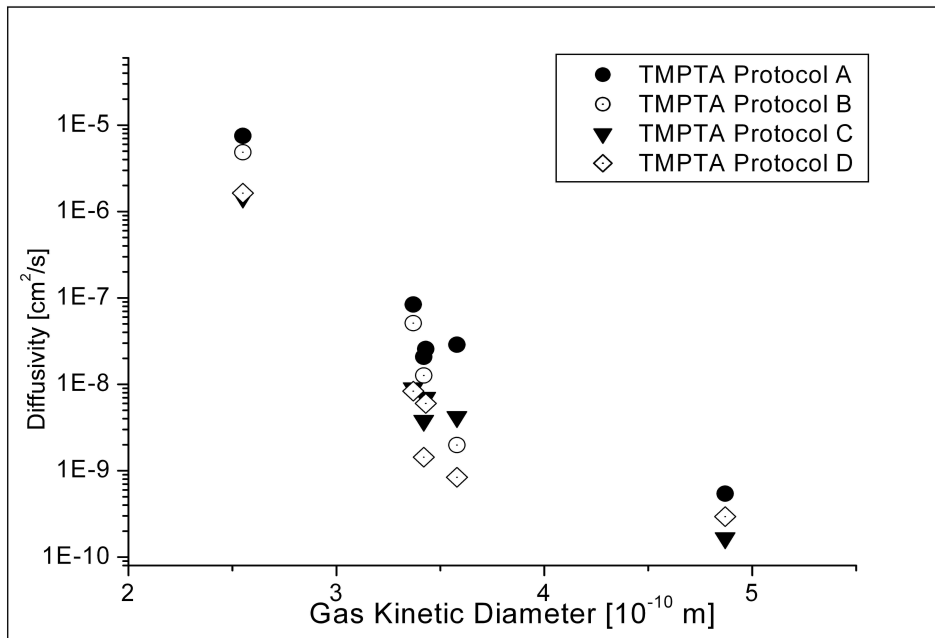
Fig. 7.10   TMPTA Pure gases diffusivity versus penetrant kinetic diameter.

He	2.55
O2	3.37
CO2	3.42
Ar	3.43
N2	3.58
R134a	4.87

Tab. 7.4   Gas kinetic diameters in Å.

Gas	T_c [K]
He	5.2
N2	126.2
O2	154.6
Ar	151.0
CO2	304.1
R134a	474.2

Tab. 7.5   Critical temperature of the gaseous penetrants
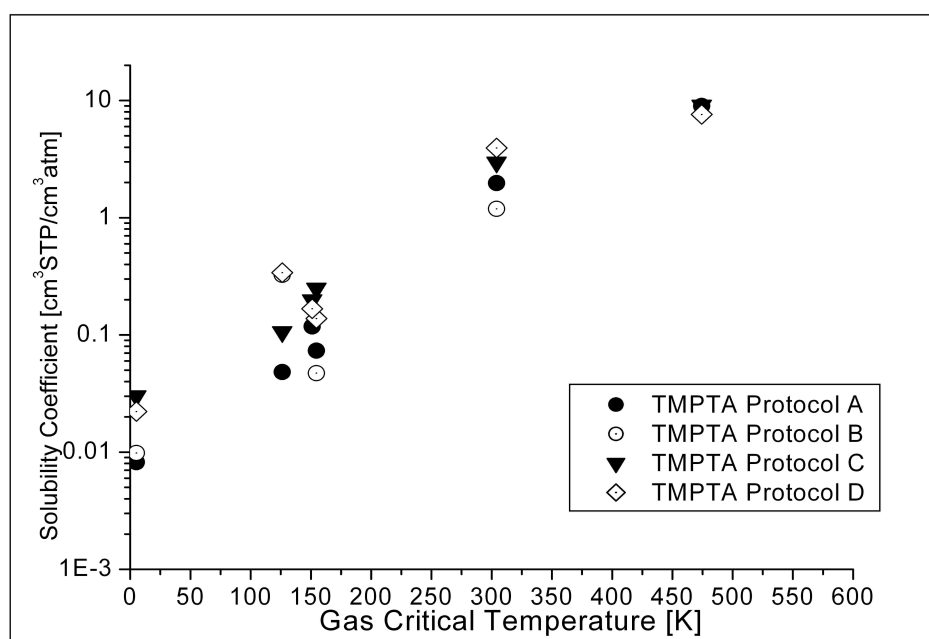
Fig. 7.11   TMPTA Pure gases solubility versus penetrant critical temperature.

Beside the raw effect that the curing dose exerts on the gas permeability values there is also an interesting effect on the ideal selectivity values, as the decrease in permeability with dose can be different for each gas. According to the data shown in Fig. 7.12 there is a marked increase in the ideal selectivity of Helium versus Nitrogen and in a less marked way also in the ideal selectivity of Helium respect to Oxygen. This can be explained considering that the permeability of Helium decreases with dose in a less significant way than the permeability of other gases of higher molecular weight. Also the ideal selectivity of Helium versus Carbon Dioxide is deeply affected by the radiation dose.
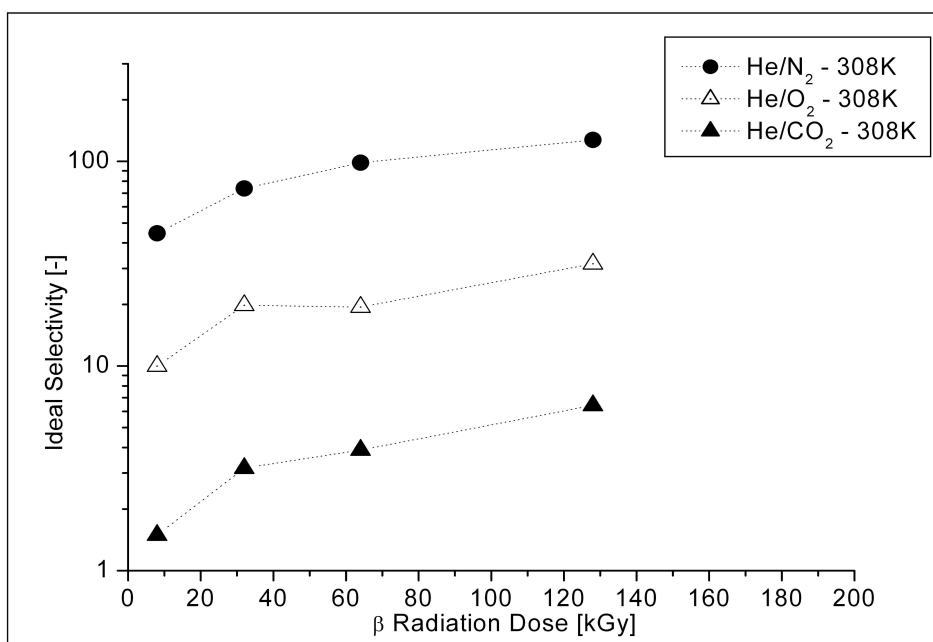
Fig. 7.12   TMPTA Ideal selectivities of helium versus other gases as a function of the dose.

The ideal selectivity of oxygen respect to Nitrogen, shown in Fig. 7.13, is almost dose independent, while the ideal selectivity of carbon dioxide versus nitrogen, depicted in the same plot, decrease slightly with the dose. A similar trend is observed for the ideal selectivity of carbon dioxide respect to oxygen.

Fig. 7.13   TMPTA Ideal selectivities of several gases versus nitrogen as a function of the dose.

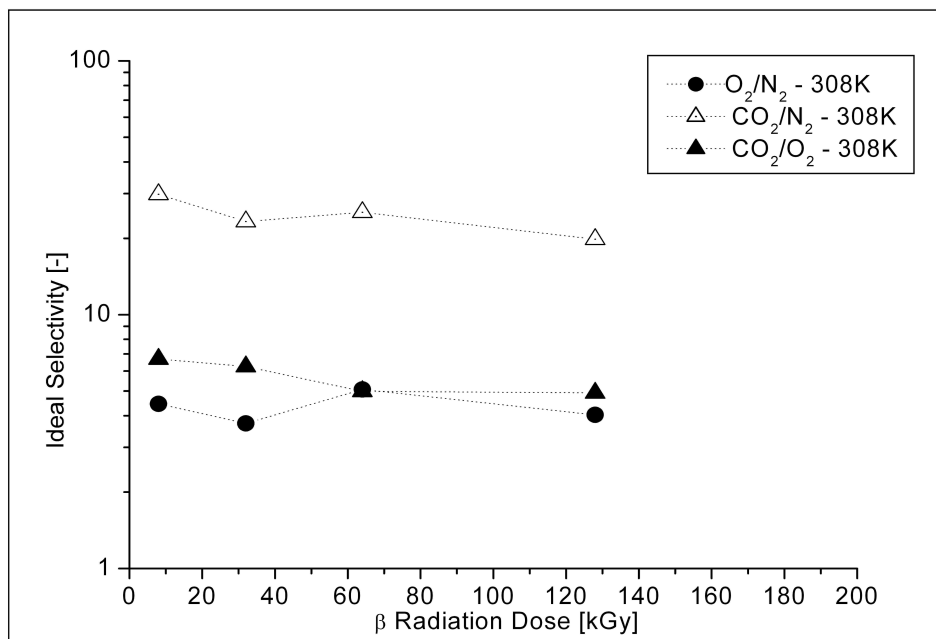Due to their inherent volume each penetrant molecule can access only to the polymer holes that are bigger than a given threshold value. The little effect of the dose on the ideal selectivity of the pairs O2/N2, CO2/N2 and CO2/O2, as well as the decrease in permeability of the same species suggest that although the free volume accessible to these penetrants is decreasing with the dose, the shape of the size distribution of the holes with radius higher than the threshold radius of these gases is not affected. Analogous consideration respect to the ideal selectivity of the helium respect to the same gases suggest that the accessible volume to the small molecule of helium is really reducing with the increase of the dose, therefore the shape of the size distribution of the holes with radius higher than the threshold radius of helium is affected by the irradiation dose.

The ideal selectivities of Helium respect to the heavier gases suggest that also hydrogen separation could attempted with these membranes, eventually tailoring the tradeoff between permeability and selectivity by means of a proper choice of the irradiation dose. The gas permeation tests have shown that the curing dose of electrons delivered to the sample affects the transport properties of the gas in the glassy TMPTA. Specifically the permeability decrease markedly with the dose, as well as the diffusivity, on the other side the solubility seems to be only a weak function of the dose. Comparison of the transport properties of gaseous penetrant with different molecular size and shape has shown that the permeability follow the order: $He > CO_2 > N_2 > Ar > R134a > O_2$.

7.6.   Comparison with Permeability in Polymers Exposed to Ionizing Radiation

Comparison with the gas permeability and other transport properties of low molecular weight penetrants in other glassy or rubbery polymers obtained through direct radiation curing of the monomers would have been beneficial, but

to knowledge of the author, such kind of data are lacking in the open literature. Some limited data are available concerning the permeability of polymers irradiated with β radiation, such as those published in 1987 by Kita et al.[135] In their work samples of polybutadiene, polycarbonate, polydimethylsiloxane, polypropylene, polyethylenterephtalate and polymethylpentene were irradiated with different radiation doses and tested for permeability of helium, nitrogen, carbon dioxide, sulfur hexafluoride, oxygen and methane. Kita et al. found out that three possible behavior existed: permeability remained quite unchanged upon irradiation, permeability decreased upon irradiation and permeability increased with irradiation. Doses up to 800 kGray were applied. Permeability through polypropylene films increased with dose: this effect is probably due to chain scission effects. Permeability through polybutadiene decreased with radiation dose. Permeabilities in the other polymers were substantially unchanged. Kita et al., through analysis of liquid toluene sorption experiments, have shown that the degree of crosslinking of polybutadiene chains was dose dependent and increased with the dose. It is really interesting to note that, like in the case of electron beam cured TMPTA, helium permeability is the less affected, while more pronounced decreases are observed with bigger penetrants like carbon dioxide. Also solubility coefficients were found to be only weak function of the radiation dose, similar to what observed with TMPTA in this work.

7.7. Concluding Remarks

In this chapter the preparation of electron beam cured TMPTA and the characterization with conversion measurements and permeability experiments conducted with a set of molecular probes of different sizes and condensability have been described. Since radiation dose influence the ideal selectivity of gas pairs like helium and carbon dioxide, helium and nitrogen and helium and oxygen, it is possible to speculate that glassy membrane prepared through

radiation curing could be used for hydrogen separation, since helium is a simulant of hydrogen. Ideal gas selectivity of the gas pairs relevant for carbon dioxide capture and air fractionation are not relevantly influenced by the dose and the separation factor seems to be too low to be acceptable for that applications.

8. Characterization of Rheological Properties of Pentane Loaded Polystyrene

8.1.   Introduction

Polystyrene pellets can be processed in order to form expanded beads, essentially made by a closed cell solid foam, that have outstanding thermal properties and quite interesting mechanical properties. The expanded polystyrene beads can be sintered to form slabs, blocks and other geometries, even complex. Due to their ability to absorb and dissipate mechanical shocks expanded polystyrene sheets and slabs are commonly used in packaging and shipping applications. Expanded polystyrene is used for the manufacturing items of common use, such as disposable cups and dishes used for serving hot food and beverages. The very low thermal conductivity and density of the materials formed through sintering of the expanded polystyrene beads make them suitable for insulation applications in house building. Expanded polystyrene sheets are commonly applied in basements, roofing and in composite walls, in the form of sheets that are inserted between layers of concrete, bricks and gypsum boards, in order to reduce the flow of heat between the room of the house and the external environment. This is beneficial both in summer, reducing the need or the time of operation of the energy consuming air conditioning units, as well as in winter, reducing the gas and electricity consumption required to keep the house warm. In non structural

applications concrete formulations in which part of the inert fraction (typically made by stones) is substituted by expanded polystyrene beads can be used. The expanded polystyrene concrete has better thermal and sound insulation properties, respect to the ordinary concrete, with reduced weight, thus helping to reduce the load on the structures. The use of expanded polystyrene in the building industry is increasing year by year. In Fig. 8.1 are shown yearly consumption of expanded polystyrene products in the Italian construction industry, as provided by A.I.P.E., that is an association between expanded polystyrene producers. It is quite evident that the consumption and thus the demand of expanded polystyrene products has increased in the last decade.
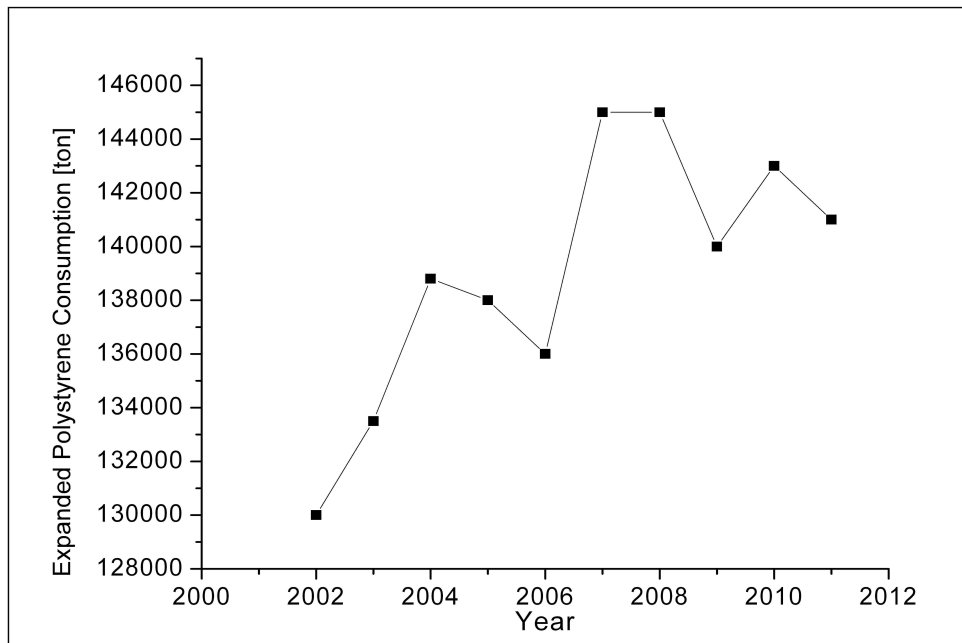
Fig. 8.1   Yearly consumption of Expanded Polystyrene products in the Italian construction industry.

Production of expanded polystyrene beads is a complex process and the final properties of the product, that are required for the above mentioned applications, are deeply affected by many variables, among which the nature and concentration of the expansion agent, its ability to depress the value of the glass transition temperature of the polymer and the influence exerted on the

rheological properties. It can be argued that this process is one of those in which the coupling between thermodynamic, mechanical and mass transport properties is more deep and fundamental. The expansion is usually performed by applying a thermal stimulus to polystyrene pellets loaded with around 5% by weight of pentane or of its isomers, that act as the blowing agent. The thermal stimulus is delivered exposing the pellets to a stream of water vapor, that acts as a heat carrier. In laboratory characterizations nitrogen can be used as the heat carrier. Since pentane solubility in polystyrene will decrease upon heating, pentane bubbles will start to nucleate inside the bulk of the pellet and the internal pressure of the bubbles will drive the expansion process. Optimization of the expansion process should be pursued with a systematic approach based on both experimental characterization and modeling.

The expansion process is characterized by a sequence of four different stages that takes place after that the polystyrene pellet is thermally equilibrated with the heat carrier agent. These four stages can be recognized looking at the change with time of the pellet radius. An example of what is commonly observed in the expansion experiments is shown in the following Fig. 8.2, in which the origin of the time axis is set at the end of the thermal equilibration.
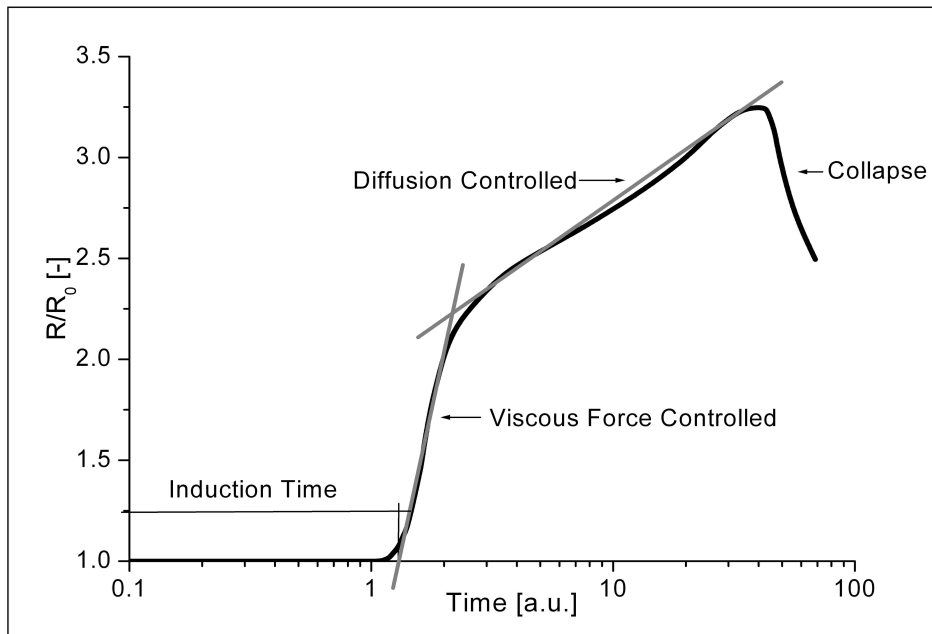
Fig. 8.2   Characteristic time evolution of the radius of a spherical pellet of pentane loaded polystyrene that undergoes the expansion process.

The first thing that can be observed is the presence of an induction period, that range from the end of the thermal equilibration to the point at which the radius starts to increase. This is the first stage of the process. The duration of the induction period, known as the induction time t_{ind}, has been found to depend on the temperature according to an Arrhenius-like law:

8.1 $$t_{ind} = A \exp\left(-\frac{E}{RT}\right)$$

It should be observed that experiments conducted seeding the polystyrene with particles, in order to promote heterogenous nucleation, have shown a reduction of the duration of the induction time , but not its complete elimination. Therefore it should be considered that the induction time is not only a consequence of the kinetic of bubble nucleation, but there should be some other concurring cause. At the end of the induction period, the pellet starts to expand pretty quickly and it is commonly assumed that the rate of expansion in this second stage is due to the balance between the pressure inside the bubbles and the viscous forces

that slow the extension of the surface of the bubble walls. After this second stage, the rate of expansion slow down, as shown by the change of the slope of the radius versus time curve. This third stage is thought to be diffusion controlled, in the sense that the further increase of the inner pressure of the bubbles that is required for the prosecution of the expansion process is due to the flux of pentane that diffuse toward the bubbles from the polymer layers that are far from the bubble walls. At the very end, the walls of the bubble burst and the expanded bead start to collapse. The Diffusion In Polymer research group of the University of Bologna and by Polimeri Europa S.p.A. (now Versalis S.p.A.) developed a model that is quite successful in describing the process, at least qualitatively, since it reasonably predicts the slopes of the second and third stages, but systematically overpredicts the induction time and its activation energy as well as wrongly predict the effect exerted by the initial pentane concentration.

It must be said that the thermodynamic properties of the polystyrene – pentane system are quite well characterized, both in glassy and rubbery conditions, as well as the diffusion kinetics. Empirical or semiempirical correlations for estimating the glass transition temperature depression induced by the plasticizing effects of pentane are known as well. The mechanical and rheological properties of neat polystyrene are also well known, while the effect of pentane concentration on mechanical properties is not well characterized. This lack of knowledge hampers the modeling efforts that had been previously developed by the Diffusion In Polymer research group of the University of Bologna and by Polimeri Europa S.p.A. (now Versalis S.p.A.). The following Fig. 8.3 and Fig. 8.4, obtained from the re-elaboration of data provided by Polimeri Europa S.p.A. that will not be further disclosed, show the deep sensitivity of the length of induction period respect to temperature and initial pentane concentration. The effect of the initial concentration of the blowing agent is really astonishing, since moving from 4% to 5% will almost double the induction time. The effect of the polystyrene molecular weight is less evident.
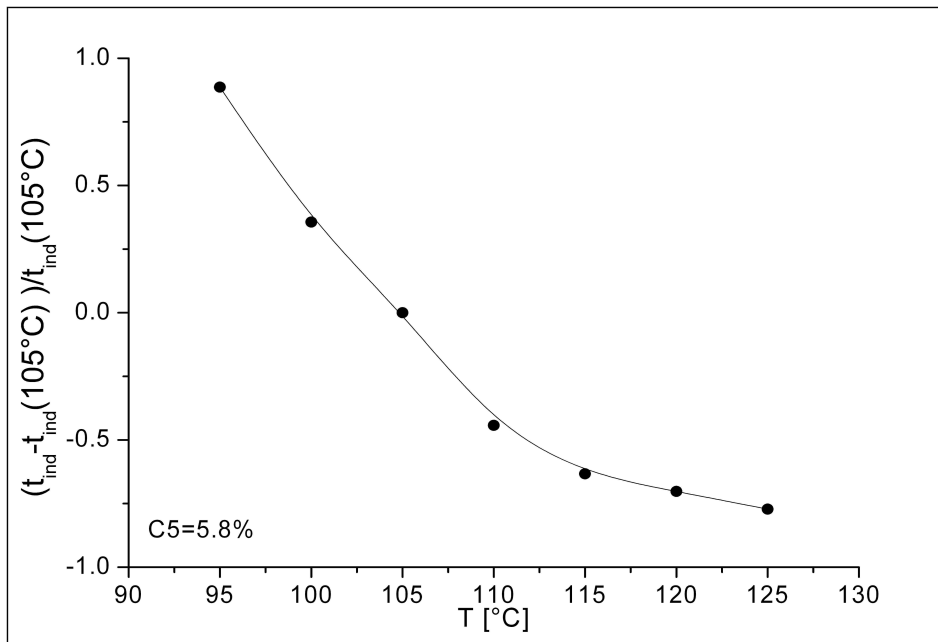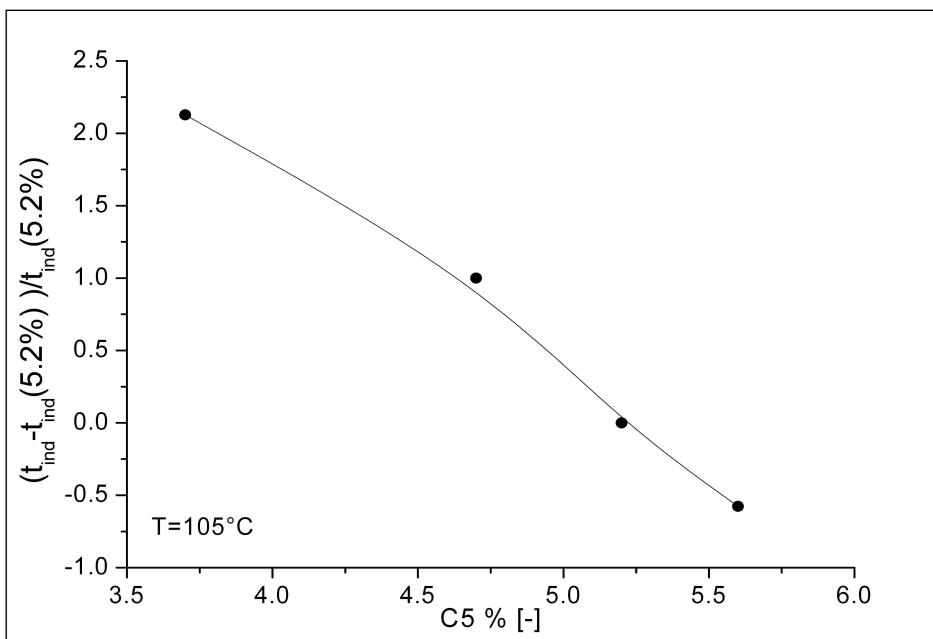
Fig. 8.3   Temperature effect on induction time.

Fig. 8.4   Initial pentane effect on induction time.

It is clear that experiments should be done in order to asses the effect of temperature, pentane concentration and polymer molecular weight on the mechanical properties of pentane loaded polystyrene. Therefore the aim of the

experimental activities that I performed at the Chair of Thermodynamics of Technical University of Dortmund was to run creep experiments on samples of polystyrene loaded with a controlled amount of n-pentane, according to the protocol described by Mueller et al.[136], in order to fill the above mentioned knowledge gap.

8.2.   Materials

Supply of polystyrene in pellet form was kindly provided by Polimeri Europa S.p.A. and n-Pentane, empirical formula C_5H_{12}, of analytical grade was purchased from Merck&Co. Inc. as well as the toluene required for the film casting procedure. Two different kind of polystyrene of industrial use, differing for their molecular weight, known as N2982 and N2380, were tested in the present work. The molecular weight of the former is 127948 kg/kmol, with polydispersity index equal to 2,09, while the latter's molecular weight is 270349 kg/kmol with polydispersity index equal to 2,19.   The glass transition temperature of these polymers is 105°C and their de nsity at ambient temperature is around to 1,033 kg/L.

8.3.   Pentane Solubility and Diffusivity in Polystyrene

Measurement of the solubility of vapors of n-pentane in the polystyrenes of interests were performed at DICMA-University of Bologna by Dr. Michele Galizia with gravimetric techniques, using the quartz spring balance, the quartz crystal microbalance and with the pressure decay apparatus that have already been described in previous chapters. Data had been collected at 60°C, for vapor activities ranging from 0,1 to 0,7. According to Chow's theory[94] glass transition temperature, at 60°C, should take place at a pentane concentration that can be reached equilibrating the sample an activity of pure pentane around

0,5. This has been proved, at least indirectly, by inspection of the kinetic of the mass uptake in sorption experiments. Sorption steps taking place at activities lower than 0,5 are characterized by Non –Fickian behavior, such as those that could be modeled with the Berens Hopfenberg model or with the Long and Richman model, while above this activity the kinetic perfectly agrees with predictions of the Fickian model, as shown in the Fig. 8.5 and Fig. 8.6, that reproduce data previously obtained by Dr. Michele Galizia under the supervision of Professor Ferruccio Doghieri.
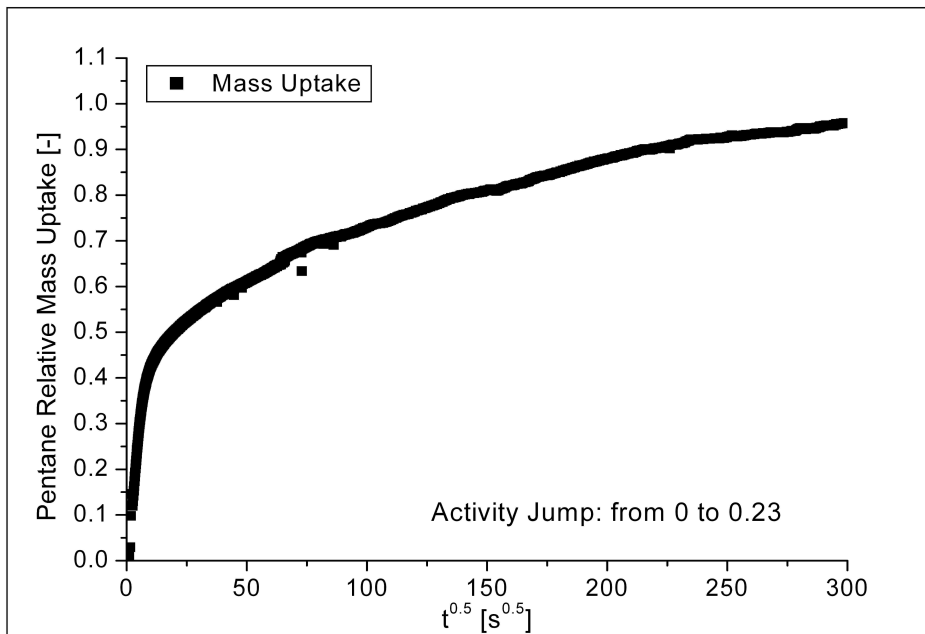
Fig. 8.5   Relative mass uptake kinetic of pentane in polystyrene at 333K, measured with the QCM apparatus, below penetrant induced glass transition.
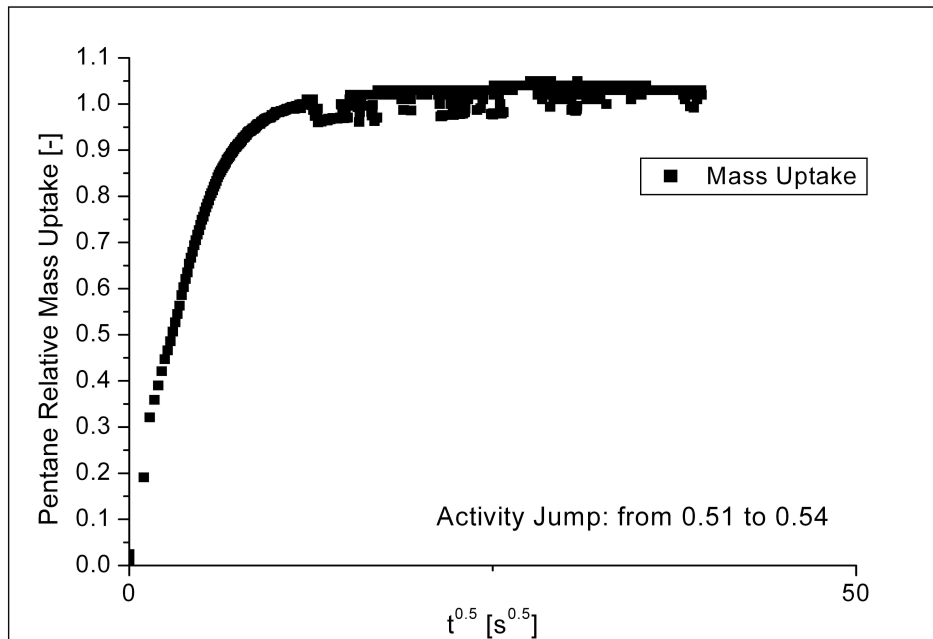
Fig. 8.6   Relative mass uptake kinetic of pentane in polystyrene at 333K, measured with the QCM apparatus, above penetrant induced glass transition.

The value of the diffusivity of n-pentane in the polystyrenes of interest can be retrieved by application of the fickian model to the mass uptake data, as previously discussed. When the behavior is markedly non-fickian it is still possible to estimate that value by trying to fit the initial slope of the curve of mass uptake in the plot M/M_∞ $vs \sqrt{t}$, under the assumption that the initial kinetic is dominated by diffusion, while the influence of relaxation phenomena is much more pronounced at late times. This assumption as been shown to be quite adequate in the kinetic modeling chapter and it is equivalent to the result that were obtained, for the case of Matrimid 5218, setting the viscosity equal to infinite. This analysis have been previously performed by Dr. Michele Galizia and the results are shown in Fig. 8.7.
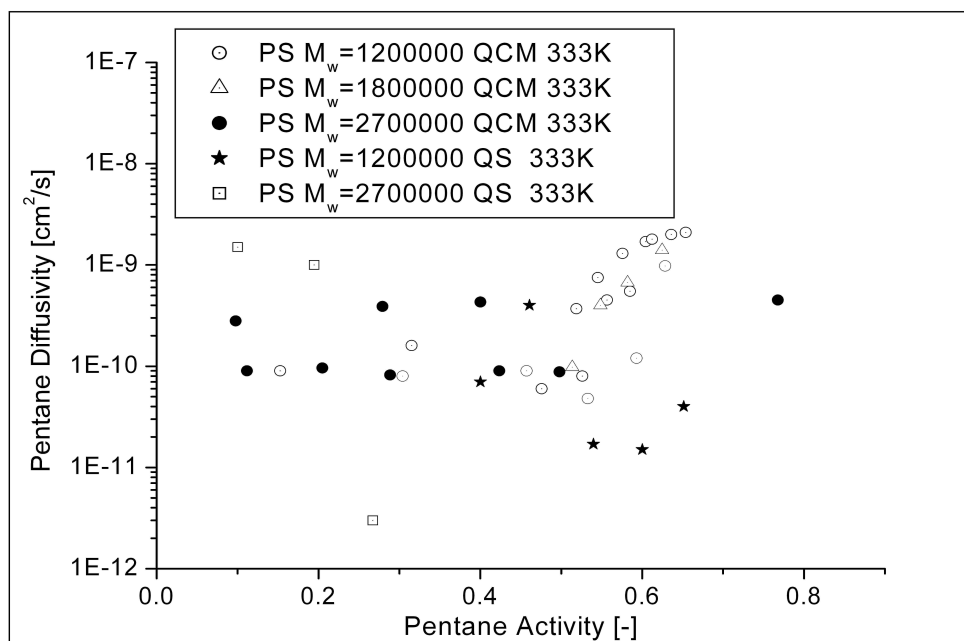
Fig. 8.7   Diffusivity of pentane in polystyrene at 333K, measured with the QCM and the QS apparatus, for a wide range of activities and for different polysterene molecular weights.

Despite the not negligible scatter in the dataset, it is still evident that diffusivity is only a weak function of the penetrant activity and that there is no recognizable influence of the polymer's molecular weight.

From the mass uptakes of (pseudo-)equilibrium measured in the sorption experiments it has been obtained a sorption isotherm, that represents the amount of n-pentane that these polystyrenes can take up under isotherm conditions. The sorption isotherm is shown in Fig. 8.8.
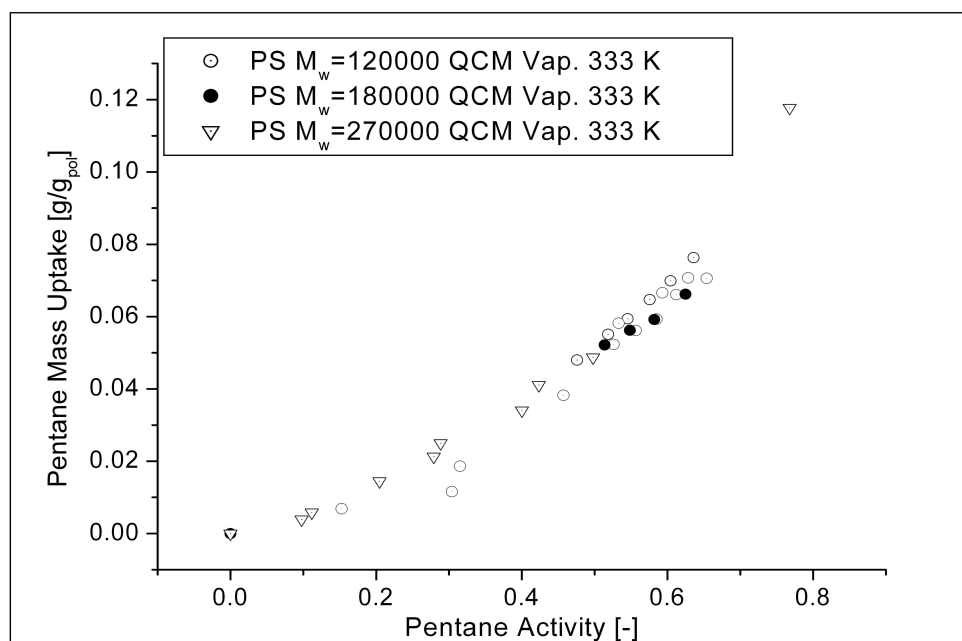
Fig. 8.8   Solubility of pentane in polystyrene at 333K, measured with the QCM and the QS apparatus, for a wide range of activities and for different polysterene molecular weights.

Again no effect of the molecular weight have been detected. Modeling of the sorption isotherms has been attempted with NELF model and has been successful only for the low activity region, while at activities higher than 0,5 it is certainly correct to use an equilibrium approach based on the Lattice Fluid EOS, consistently with the abovementioned consideration on glass transition depression induced by n-pentane sorption. The results of the modeling are depicted in the following Fig. 8.9.
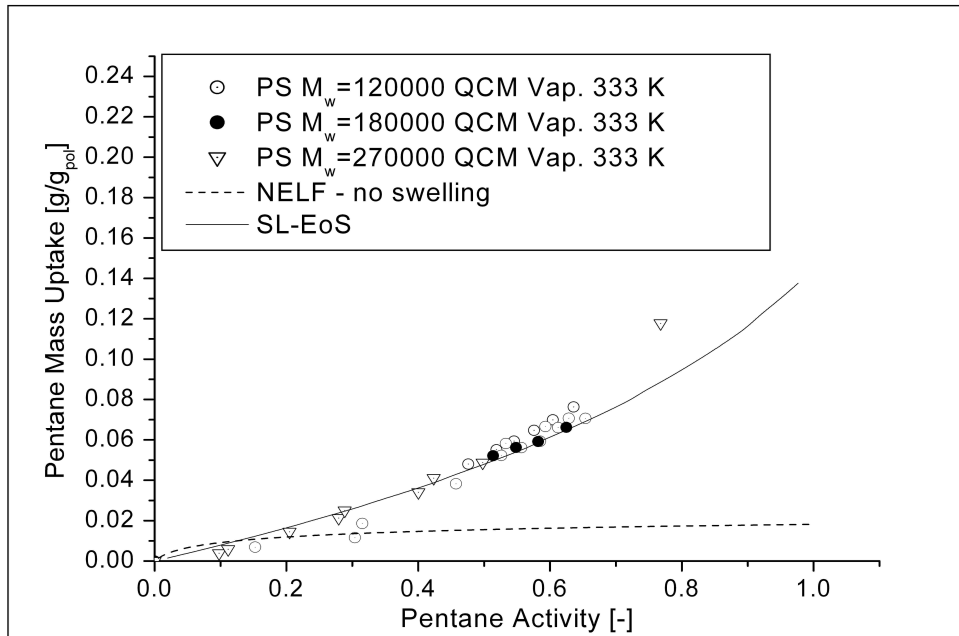
Fig. 8.9   Solubility of pentane in polystyrene at 333K, modeled with NELF and Sanchez Lacombe Equation of State.

The characteristic parameters of polystyrene are $T^* = 750K$ $T^* = 750\,K$, $P^* = 360MPa$ $P^* = 360\,MPa$ and $\rho^* = 1.099kg/L$ $\rho^* = 1.099\,kg/L$ and those of n-pentane are $T^* = 451\,K$, $P^* = 305\,MPa$ and $\rho^* = 0.749\,kg/L$. Interaction parameter required to model the data is set equal to $k_{ij} = 0.03$. The data are very well fitted by the equilibrium sorption isotherm even for quite low activities.

8.4.   Experimental Procedure

The measurement were performed in the setup for creep measurement described in 2010 by Mueller et al.[136]. that is available at the Chair of Thermodynamics of the Chemical Engineering Faculty of Technical University of Dortmund. The device is built in such a way that enable to apply a controlled force up to 20N to a polymer film that is clamped between a VOC resistant force transducer and a linear drive that can perform linear steps greater than 100 nm and up to 50 mm. The linear drive is controlled by a LabView program that

enables to impose to the sample, with the proper choice of the PID controller parameters, a given force history. The sample and its holding clamps are put inside a measuring chamber that is surrounded by an air thermostat that ensures isothermal conditions and that can be operated from 20 to 85°C, with a control better than 0,03°C. The present experiments were run at 70°C and 80°C.The measuring chamber is designed to withstand vacuum and in order to control the sorption of VOC components inside the polymer its internal atmosphere is imposed by a continuous vapor flow, at a pressure that can range from 0.1 mbar to 1330 mbar and that in the operating conditions used (P>1000 mbar) was never fluctuating more than 5 mbar. The polymer films were casted from toluene/polystyrene solutions on a glass surface, flattened with a slit of defined height and stored under vacuum for at least five days in order to promote toluene removal. Pentane was degassed by means of the freezing-evacuation-melting procedure, that was repeated at least three times for each amount of pentane that had to be introduced in the apparatus. After loading the sample inside of the measuring chamber vacuum was pulled for 24h in order to promote degassing and desorption of any possible VOC still present inside the film, meanwhile the temperature of the thermostat was ramped up to the operating value. Then the pentane's vapor flow was established through the chamber and the pressure controller was turned on. The thickness of the sample was never higher than 50 μm and according to the previously shown estimate of the diffusivity coefficient, it was assumed that one week was enough to obtain an homogeneous profile of the pentane concentration inside the samples. The operating conditions, as well as the predicted pentane loading are summarized in Tab. 8.1. As mentioned above, it was decided to run the experiments at 70°C and 80°C, at a vapor pressure h igh enough to have pentane equilibrium concentration around 0.04 g/g_pol. For N2982 were run three experiments, two at 80°C and two different pr essure, and one at 70°C but at a pressure value that was chosen in order to have, according to model predictions, the same amount of pentane's uptake of one of the steps at 80°C. Finally with N2380 was run only one experiment in order to replicate one of the 80°C's step, to try to address the effect of the po lymer molecular weight.

P[mbar]	T [°C]	gC5/gpol
1057	70	0.043
1150	80	0.0365
1320	80	0.043

Tab. 8.1   Operating conditions.

After one week of equilibration at given temperature and pentane pressure the creep experiment was performed. At the beginning of each test a small tension was applied to the sample, then as soon as a stable force value was measured, a larger strain was applied in order to reach the final force's setpoint. Once that a steady value of the force was obtained, the linear drive kept imposing a steadily increasing elongation strain to the sample, in order to compensate the stress relaxation and impose constant stress creep. The experiment was terminated once enough data were collected and when the elongation was so large that it was thought that the change in the sectional area could give rise to a big discrepancy between engineering stress and true stress.

8.5.   Data Analysis

Stress was obtained directly from the measured force, as $\sigma(t) = F(t)/A$, while elongation was recovered from the position of

the linear drive, as $\varepsilon(t) = \dfrac{L(t) - L(t=0)}{L(t=0)}$.   The area A is calculated from the thickness of the films, measured after the solvent removal procedure, and from their width, measured before clamping it inside the measuring chamber. The stress will be calculated using the initial value of the area A, thus rigorously this stress is not the real stress but should be regarded as the so called engineering stress. For small strains the two value should overlap, while for large strains the discrepancies could be relevant, especially if

local effects like necking take place. The following Fig. 8.10 to Fig. 8.15 show some of the elongation history and of the imposed stress that were collected in the experimental activity.

Fig. 8.10 Polystyrene N2982 – Elongation history at 1320 mbar of pentane and 80℃.
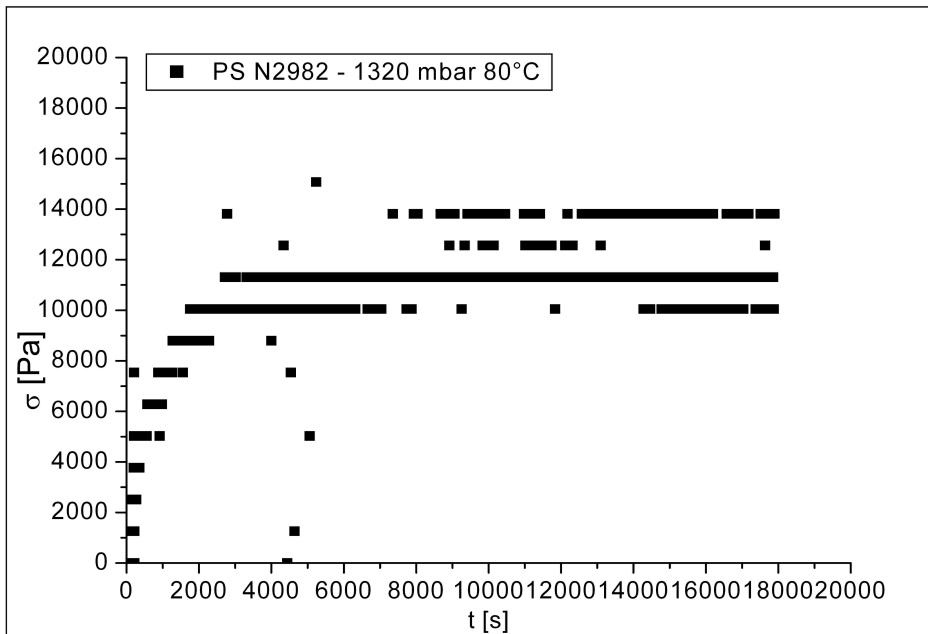
Fig. 8.11 Polystyrene N2982 – Imposed stress at 1320 mbar of pentane and 80℃.

Fig. 8.12   Polystyrene N2982 – Elongation history at 1150 mbar of pentane and 80℃.

Fig. 8.13   Polystyrene N2982 – Imposed stress at 1150 mbar of pentane and 80℃.

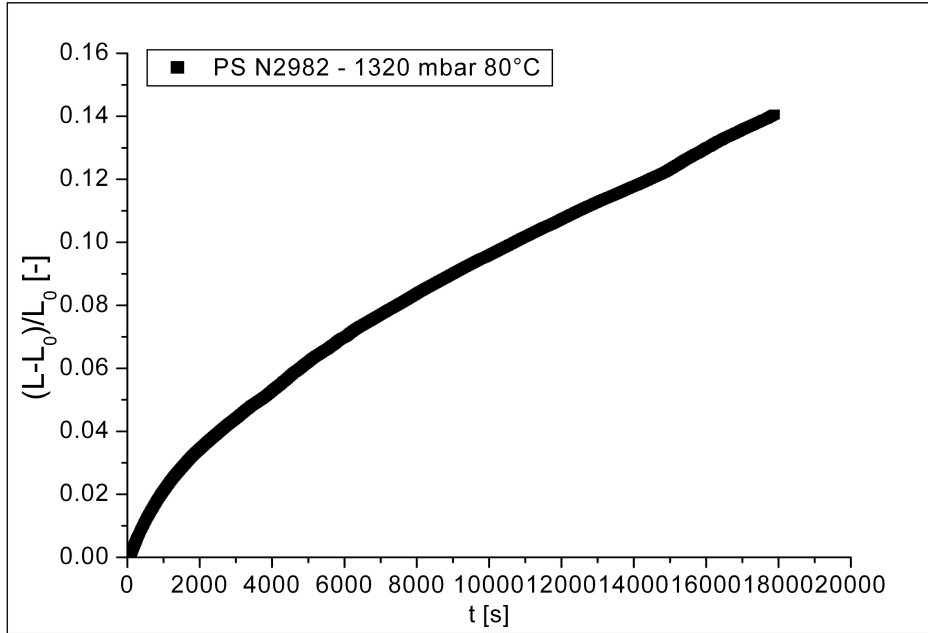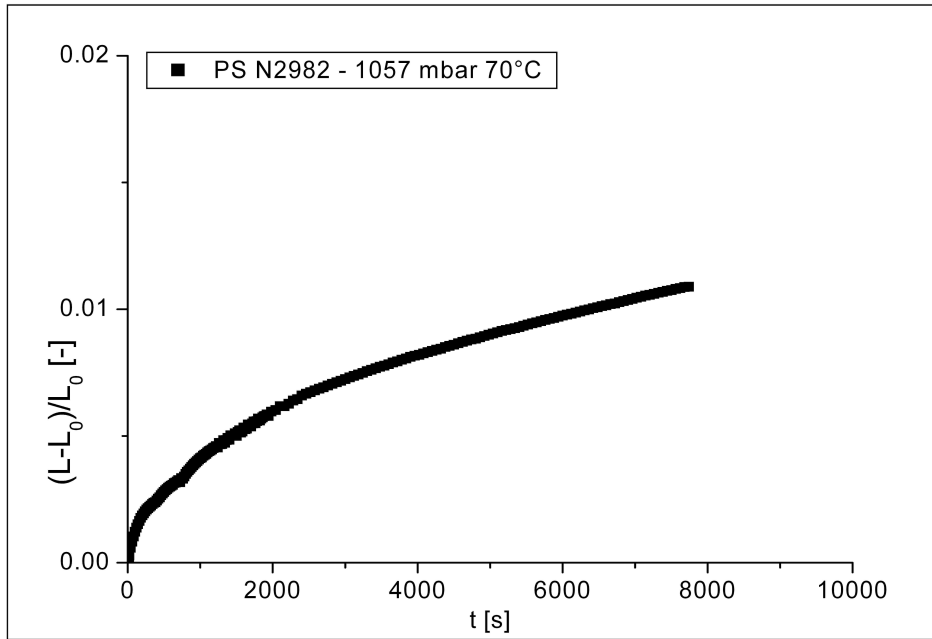Fig. 8.14   Polystyrene N2982 – Elongation history at 1057 mbar of pentane and 70℃.
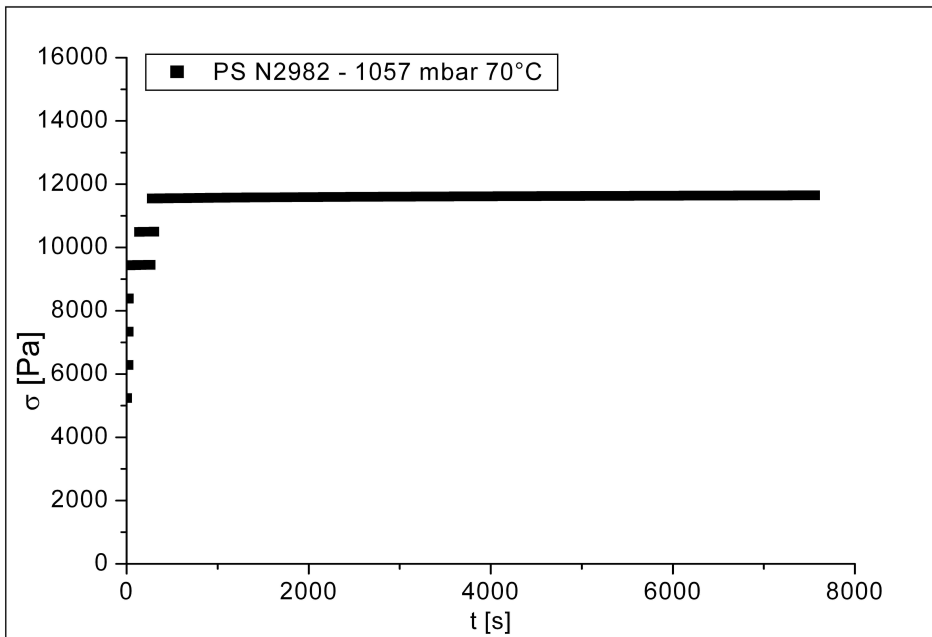
Fig. 8.15   Polystyrene N2982 – Imposed stress at 1057 mbar of pentane and 70℃.

The creep compliance is defined respect to the steady value of the stress, say σ_∞ σ_∞, as $J(t) = \dfrac{\varepsilon(t)}{\sigma_\infty}$ $J(t) = \dfrac{\varepsilon(t)}{\sigma_\infty}$. Shear modulus is related to creep

compliance according to: $G(t) = \dfrac{1}{3J(t)}$. For a linear viscoelastic

material that follows the simple spring dashpot Maxwell fluid model the creep compliance can be expressed in term of the spring modulus E_0 and of the dashpot viscosity η_0 as:

$$J(t) = \frac{1}{E_0} + \frac{t}{\eta_0}.$$

If the response of the viscoelastic material can be idealized as a spring, a dashpot and a series of N Voigt models, such as in Mueller et al.[121, 136], the creep compliance is:

$$J(t) = \frac{1}{E_0} + \frac{t}{\eta_0} + \sum_{i=1}^{N} \frac{1}{E_i} \left[1 - \exp\left(-t \frac{E_i}{\eta_i} \right) \right]$$

Under the hypothesis of linear viscoelasticity and of small deformation, it is possible to assume that superposition holds between stress (and strain) induced by the small pretension step and the stress (and strain) induced by the effective creep measurement. Therefore these values have been subtracted by the data and the test is assumed to start effectively at the end of pretension step.

The above mentioned expression for calculating creep compliance in (generalized) Maxwell model holds true rigorously only when the stress history can be idealized as a step function:

$$\begin{cases} t < 0 & \sigma(t) = 0 \\ t \geq 0 & \sigma(t) = \sigma_\infty \end{cases}$$

In the actual experiments the force was not applied instantly, but was ramped up by the controller that actuated the linear drive, as shown by the data reported in Fig. 8.11, Fig. 8.13 and Fig. 8.15. Thus the application of the abovementioned relationship in order to retrieve the characteristic moduli and viscosities can be considered only approximate. In particular, it must be considered that, since the set point value of the stress was reached after a not

negligible amount of time, in the order of $10^3 s$, the value of the modulus E_0 that should have represented the instantaneous answer of the material, is certainly ill defined and possibly affected by large errors. Anyway, it sounds reasonable to assume that η_0, that is evaluated at later times, when $\sigma(t) \approx \sigma_\infty$, retains the same physical meaning of the parameter evaluated under the above defined ideal stress history.

Fig. 8.16   Polystyrene N2982 – Creep compliance at 1320mbar of pentane and 80℃.
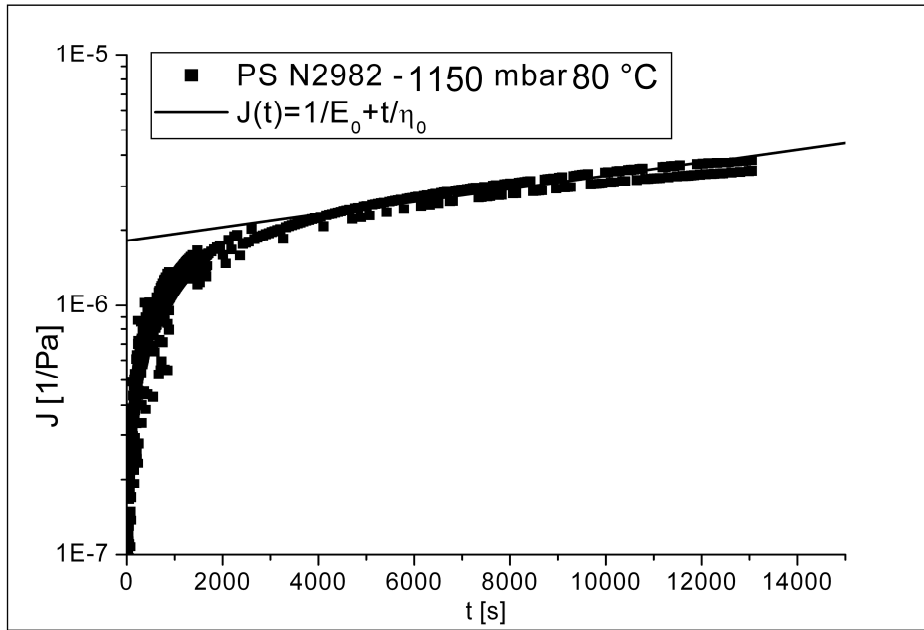
Fig. 8.17   Polystyrene N2982 – Creep compliance at 1150 mbar of pentane and 80℃.

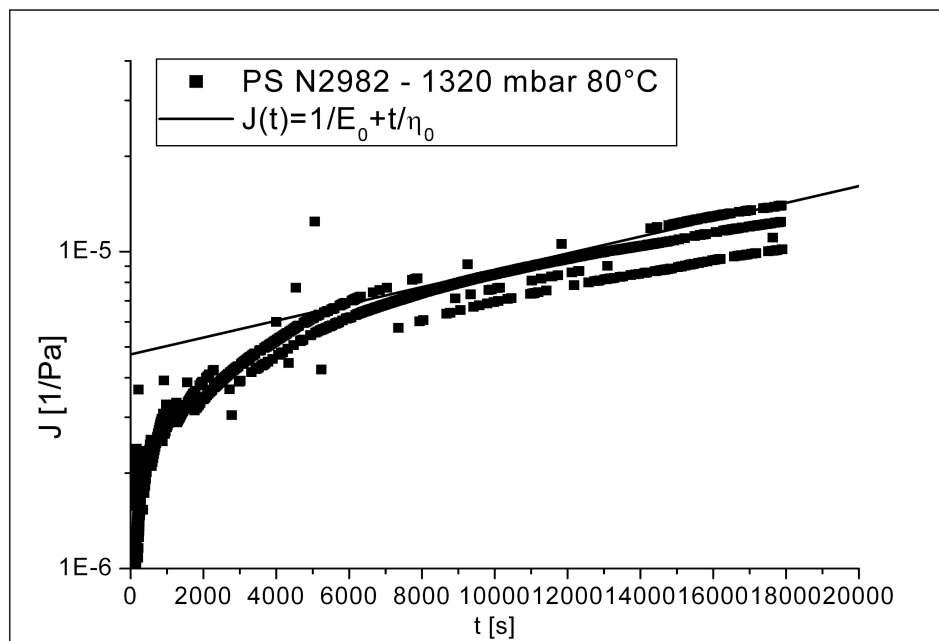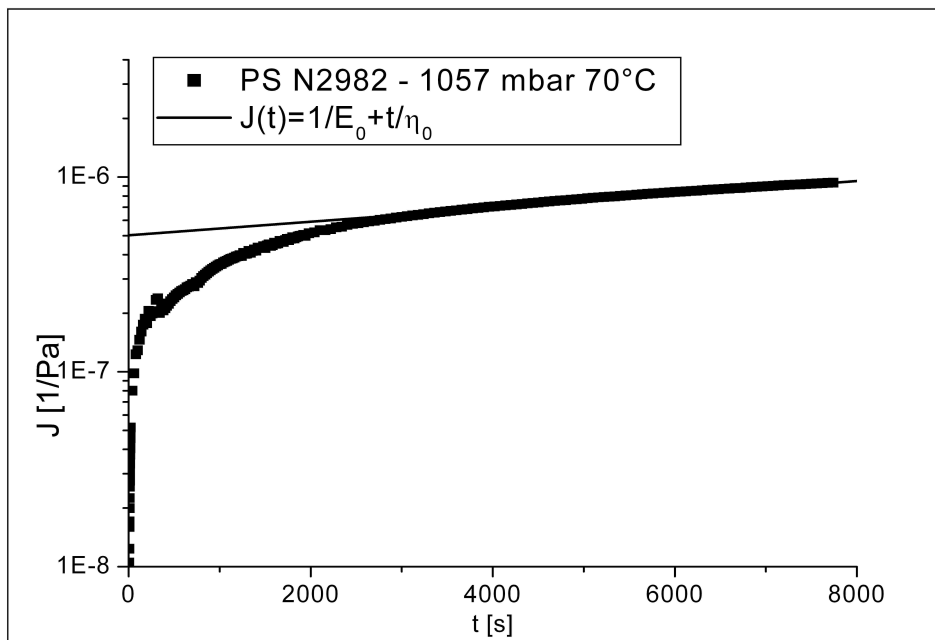Fig. 8.18   Polystyrene N2982 – Creep compliance at 1057 mbar of pentane and 70℃.

P [mbar]	T [°C]	gC5/gpol	η_0 [Pa*s]	E_0 [Pa]	Polymer
1057	70	0.0430	7.75E+9	1.99E+06	N2982
1150	80	0.0365	4E+09	5.5E+05	N2982
1320	80	0.0430	1.46E+09	2.11E+05	N2982
1320	80	0.0430	8.76E+09	3.08E+05	N2380

Tab. 8.2 Moduli and viscosities retrieved through the regression of the Maxwell model to the experimental compliance data.

The Tab. 8.2 and the Fig. 8.16, Fig. 8.17 and Fig. 8.18 summarize the values of the modulus and of the viscosities obtained by means of application of the Maxwell model $J(t) = \dfrac{1}{E_0} + \dfrac{t}{\eta_0}$. Inspection of the results show that modulus and viscosities are affected by all the parameters that were allowed to change in a systematic way in the experiments. For a given equilibrium pentane concentration and for an assigned temperature the molecular weight of the polymer influences the rheological properties, that seems to be increasing function of that parameter. It must be noted that this behavior should be expected mainly for rubbery states or for very long time load applications, where the viscous behavior became relevant. In the present case it is not clear enough if the observed behavior has to be ascribed to the depression of glass transition temperature induced by pentane or to the effect of the stress history. On the other side increasing the amount of sorbed pentane lowers viscosity, while lowering the temperature lead to an increase of the value of that property. It is possible to observe that the apparent energy of activation that can be estimated from the viscosity of the pentane loaded polystyrenes is around half the value of apparent energy of activation that can be estimated from the final relaxation times of polystyrene reported by Rault[137] in 2003, with appropriate correction for the effect of pentane on the actual glass transition temperature. At the same time, the apparent activation energy retrieved from viscosity data is around twice the apparent activation energy of the induction time that is measured in the expansion experiments. Lastly, the sensitivity of viscosity to pentane concentrations happens to be five times higher than the sensitivity of induction time respect to the same variable. Therefore it is possible to conclude that the

mechanical behavior of pentane loaded polystyrene deviate from the predictions that can be made using the data of neat polystyrene alone, but further analysis is required for identifying and describing the phenomena that govern the duration of the induction period of the expansion process.

8.6. *Some speculations on the effect of strain rate on solubility*

It is commonly accepted that Helmholtz free energy can be written as a sum of terms that represent the contribution of different effects and physical processes. The structure of the Statistical Associating Fluid Theories is an example of this, but several other successful examples are the introduction of an elastic term in the Flory Huggins Theory or in Compressible Lattice Fluid Theories for describing the swelling behavior of crosslinked polymer such as the hydrogels or the organogels. In the previous discussions of the solubility calculation of low molecular weight species in glassy or rubbery polymers, it was always assumed that the Helmholtz free energy of the mixture and the chemical potential of the single species were not affected, even in out of equilibrium conditions like those addressed through the NET-GP approach, by the strain rate of the volume relaxation process. Under out of equilibrium condition the polymer density is the order parameter/internal state variable that, at fixed temperature, pressure and penetrant chemical potential, measures the departure from equilibrium and enable us to calculate the actual Helmholtz free energy of the system. The ratio between the actual polymer density and the equilibrium polymer density is a measure of the strain of system, that actually is directly linked to deformation tensor $\underline{F}$, being equal to its determinant. Therefore it is possible to argue that the mechanical strain that comes along with the out of equilibrium nature of the glassy state and with the volume relaxation process that characterize sorption in glasses is accounted for in NET-GP approach through the choice of the polymer density as the order parameter. Do isochoric mechanical process like

creep, uniaxial elongation, stress relaxation and so on, in which the strain is not volumetric, affect Helmholtz free energy of a polymeric system? The answer is yes. The seminal work of Marrucci et al.[138], published in 1983, has provided a way to calculate, in the framework of reptation theory and under the Indipendent Alignment Approximation, the contribution to Helmholtz Free Energy that is due to strain rate in shear flow and in uniaxial elongation. Coppola et al.[139] have shown that it is possible to express that contribution as a function of the mechanical Deborah number of the flow, defined as $De = \dot{\varepsilon}\tau_{DE}$, where $\dot{\varepsilon}$ is the deformation rate and τ_{DE} is the disentanglement time of the polymer chains. The free energy change from the no flow situation can be estimated as:

$$\Delta A = 3cRT \int_0^{+\infty} \dot{\mu}(z)F(Dez)dz$$

Where c is the entanglement density, defined starting from the polymer density ρ, the molecular weight between entanglement M_e and the Avogadro number, and as $c = \dfrac{\rho N}{M_e}$. The function $\mu(z)$ is the Doi Edwards memory function and F is an integral function of the deformation history that is calculated according to the procedure depicted by Marrucci et al. in 1983. Coppola et al. have shown that in the limit of little Debora number, the function ΔA can be simplified, for example for an uniaxial extension flow, as:

$$\Delta A = 3cRT \frac{\pi^4}{200} De^2$$

Coppola et al.[139] have shown that using that contribution it is possible to successfully model and predict flow induced crystallization in polyethylene and polypropylene. The flow regime that could describe the expansion process is, at a first level of approximation, a non isochoric elongation, since pentane desorption will certainly induce a volumetric change in the polystyrene, while at the same time the internal pressure of the bubbles will cause the elongation of the polymer that forms the wall of the bubble itself. Developing an expression for the contribution to Helmholtz free energy that is due to that flow is indeed a relevant task, due to the complex kinematic that has to be described, but some

approximate estimate could be obtained assuming that the volumetric change upon pentane desorption is negligible and thus using the above reported results for isochoric flow. The Helmholtz free energy contribution have then been added to the residual Helmholtz free energy calculated according to the Sanchez Lacombe Theory and some solubility calculation, have been performed and the results are shown in Fig. 8.19.
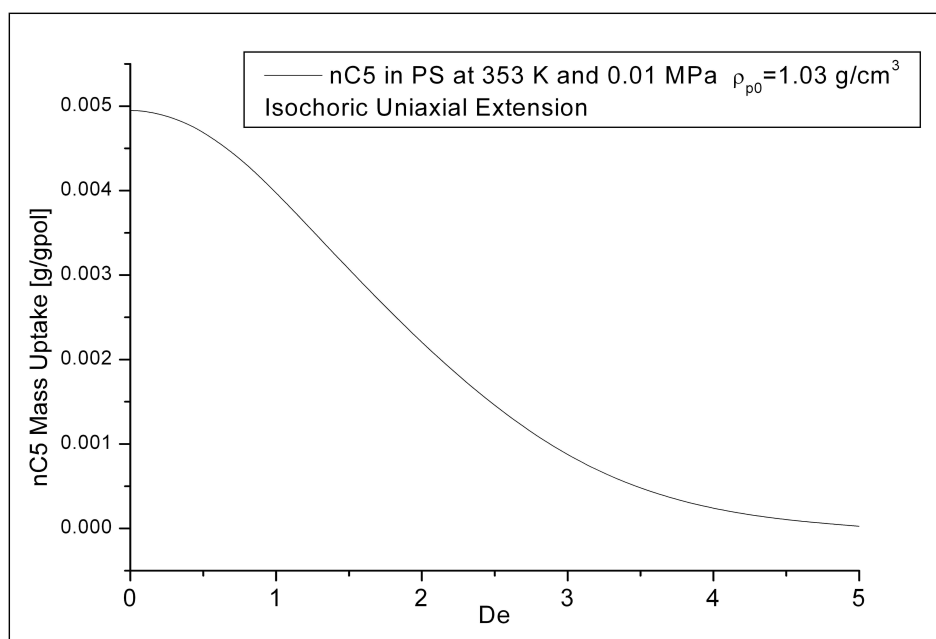
Fig. 8.19   Pentane Solubility in Polystyrene N2982: effect of uniaxial extension.

The results show that at high mechanical strain rates solubility is indeed affected by the flow. Actually solubility will decrease as much as the polymer elongation rate increase. Since the desorption rate ultimately will determine the pressure rise inside the bubbles and since the internal pressure is the driving force of the elongation process, the expansion process could be somewhat self accelerating.

8.7. Concluding remarks

An experimental characterization of mechanical properties in pentane loaded polystyrenes have been conducted by means of creep experiments. The results have been discussed in term of compliance modulus and by means of the application of the Maxwell model.

Concluding remarks

In this work several theoretical and experimental methods had been applied to the characterization of thermodynamic, mechanical and transport properties of system made by solvent, or other low molecular weight species, in polymers. Various specific problems had been addressed, ranging form phase equilibria measurement and modeling to sorption kinetic measurement and modeling. Whenever it was possible, the coupling between thermodynamic and mechanical (often rheological) properties and effects has been recognized and discussed. In same cases the relationship between mechanical and thermodynamic properties was made clear by the experimental method itself, such as in the case presented in Chapter 7, while other times it was the modeling effort that called for the adoption of a rheological point of view, such as in Chapters 4 and 5.

The following results have been obtained in this work:

- It was shown that Equations of State, that successfully represent the volumetric behavior of the polymer species, can be applied to modeling challenging systems such as those ternary system involving a macromolecular component in which the low molecular weight species behave as a solvent-non –solvent pair ;
- Vapor and liquid solubility in glassy and rubbery polymers have been measured, along with their mass uptake kinetics, and it was possible to

identify several aspect of the relationship between size, shape and chemistry of the low molecular weight penetrants and their solubility and mass transport properties. Moreover solvent induced glass transition was observed for the dichloromethane –Matrimid 5218 system, while for the sorption of other species, like alcohols, alkylacetates and acetone, that had huge solubility in the same polymer, effects of the thermal history of the polymer were detected, suggesting that those polymer penetrant systems, albeit largely swollen, were still somewhat out of equilibrium;

- Sorption isotherms had been successfully modeled with the Non Equilibrium Thermodynamic of Glassy Phase approach. It was also found a way to overcame the lack of experimental PVT data of rubbery Matrimid 5218 and to apply the latest version of the NETGP approach, that through the adoption of a simple rheological model enables to predict the swelling behavior of the polymer penetrant system, even in glassy region;

- Mass uptake kinetics of dichloromethane in Matrimid 5218 have been modeled with the Berens Hopfenberg model and it was find a procedure that enables to reduce the number of adjustable parameters of the model, through application of the NETGP approach;

- Modeling of differential and integral sorption kinetics for methanol in Matrimid 5218 and of an integral sorption step for 1 propanol in the same polymer had been performed with a model that is based on an appropriate description of the diffusion of the low molecular weight species in the polymer and of its volumetric relaxation behavior; The model used is based on the NETGP theory and on a simple rheological assumption about the short and long time behavior of the glassy phases, that is described by means of a series of Voigt models;

- Conversion and gas permeability measurements had been performed on electron beam cured acrylate monomers and the effect of the radiation dose had been characterized. It must be remarked that the only data that can be found in literature are about gas permeability in irradiated

polymers. No data exist about gas permeability in radiation cured polymers.

- Creep experiments had been performed on pentane loaded polystyrenes and through the application of the Maxwell model for creep compliance, moduli and viscosities had been retrieved.

All the above mentioned results open to future research work.

For what concerns the PC-SAFT modeling of the liquid liquid ternary equilibria of the PLAs-water-1,4 dioxane systems, the validation of the model against the equilibrium data, that are those of the binodal curves, opens up to the possibility of modeling also the spinodal curves and to couple the thermodynamic model to a kinetic model that can be used for describing the actual thermal induced phase separation process. This is a required step for developing a working knowledge of the phenomena that control the final scaffold morphology. This will be really important for the future clinical applications.

The solubility data collected for pure edible oils and oleic acid and for some of their mixtures with solvents in PDMS suggest some effects that could be beneficial in membrane based deacidification process: further work is in progress at the laboratories of the Diffusion in Polymers research group of the University of Bologna.

Liquid and vapor sorption in Matrimid 521 can provide some insight in processes, such as the so called Organic Solvent Nanofiltration, for which hollow fibers modules made by that polymer are being introduced in the market. Solubility and diffusivity modeling of low molecular weight species in glassy polymers will be a fundamental part of the process design and analysis. The huge plasticization effects that had been observed and modeled pose some intriguing challenges to the durability of glassy membrane modules.

Gas transport properties of radiation cured polymers can be tailored acting on the irradiation dose. It could be possible to prepare nanocomposite membrane by directly curing a monomer solution in which nanoparticles had been dispersed. Membrane separation or barrier material applications could be imagined, but are yet to be proven.

Future modeling efforts for thermoplastic expansion process will be supported by the data measured on pentane loaded polystyrenes.

Bibliography

1.   Sandler, S. I.; Lewin, D. R., *Chemical and engineering thermodynamics*. Wiley New York: 1989; Vol. 3.

2.   Zemansky, M. W.; Abbott, M. M.; Van Ness, H. C., Basic engineering thermodynamics. McGraw-Hill. *New York* 1975.

3.   Callen, H. B., Thermodynamics and an Introduction to Thermostatistics. *Thermodynamics and an Introduction to Thermostatistics, 2nd Edition, by Herbert B. Callen, pp. 512. ISBN 0-471-86256-8. Wiley-VCH, August 1985.* 1985, 1.

4.   Astarita, G., *Thermodynamics*. Springer: 1989.

5.   Müller, I., *A history of thermodynamics: The doctrine of energy and entropy*. Springer: 2007.

6.   Slattery, J. C., *Advanced transport phenomena*. Cambridge University Press: 1999.

7.   Prausnitz, J. M.; Lichtenthaler, R. N.; de Azevedo, E. G., *Molecular thermodynamics of fluid-phase equilibria*. Prentice Hall: 1998.

8.   Peng, D.-Y.; Robinson, D. B., A new two-constant equation of state. *Industrial & Engineering Chemistry Fundamentals* 1976, 15, 59-64.

9.   Soave, G., Equilibrium constants from a modified Redlich-Kwong equation of state. *Chemical Engineering Science* 1972, 27, 1197-1203.

10.   Sanchez, I. C.; Lacombe, R. H., An elementary molecular theory of classical fluids. Pure fluids. *The Journal of Physical Chemistry* 1976, 80, 2352-2362.

11.   Flory, P. J., Thermodynamics of high polymer solutions. *The Journal of Chemical Physics* 1941, 9, 660.

12.   Huggins, M. L., Solutions of long chain compounds. *The Journal of Chemical Physics* 1941, 9, 440-440.

13.   Huggins, M. L., Thermodynamic Properties of Solutions of Long - chain Compounds. *Annals of the New York Academy of Sciences* 1942, 43, 1-32.

14.   Doghieri, F.; Sarti, G. C., Nonequilibrium lattice fluids: a predictive model for the solubility in glassy polymers. *Macromolecules* 1996, 29, 7885-7896.

15.   Sanchez, I. C.; Lacombe, R. H., Statistical thermodynamics of polymer solutions. *Macromolecules* 1978, 11, 1145-1156.

16.   Chapman, W. G.; Gubbins, K. E.; Jackson, G.; Radosz, M., SAFT: equation-of-state solution model for associating fluids. *Fluid Phase Equilibria* 1989, 52, 31-38.

17.   Chapman, W. G.; Gubbins, K. E.; Jackson, G.; Radosz, M., New reference equation of state for associating liquids. *Industrial & engineering chemistry research* 1990, 29, 1709-1721.

18.   Huang, S. H.; Radosz, M., Equation of state for small, large, polydisperse, and associating molecules. *Industrial & Engineering Chemistry Research* 1990, 29, 2284-2294.

19.   Huang, S. H.; Radosz, M., Equation of state for small, large, polydisperse, and associating molecules: extension to fluid mixtures. *Industrial & Engineering Chemistry Research* 1991, 30, 1994-2005.

20.   Aslam, N.; Sunol, A. K., Reliable computation of all the density roots of the statistical associating fluid theory equation of state through global fixed-point homotopy. *Industrial & engineering chemistry research* 2006, 45, 3303-3310.

21.   Koak, N.; de Loos, T. W.; Heidemann, R. A., Effect of the power series dispersion term on the pressure-volume behavior of statistical associating fluid theory. *Industrial & engineering chemistry research* 1999, 38, 1718-1722.

22. Gross, J.; Sadowski, G., Perturbed-chain SAFT: An equation of state based on a perturbation theory for chain molecules. *Industrial & engineering chemistry research* 2001, 40, 1244-1260.

23. Gross, J.; Sadowski, G., Application of the perturbed-chain SAFT equation of state to associating systems. *Industrial & engineering chemistry research* 2002, 41, 5510-5515.

24. Gross, J.; Sadowski, G., Modeling polymer systems using the perturbed-chain statistical associating fluid theory equation of state. *Industrial & engineering chemistry research* 2002, 41, 1084-1093.

25. Doghieri, F.; Quinzi, M.; Rethwisch, D. G.; Sarti, G. C. In *Predicting Gas Solubility in Glassy Polymers through Nonequilibrium EOS*, ACS Symposium Series, ACS Publications: 2004; pp 74-90.

26. Doghieri, F.; Quinzi, M.; Rethwisch, D. G.; Sarti, G. C., Predicting Gas Solubility in Membranes through Non-Equilibrium Thermodynamics for Glassy Polymers. *Materials Science of Membranes for Gas and Vapor Separation* 2006, 137-158.

27. Valderrama, J. O., The state of the cubic equations of state. *Industrial & engineering chemistry research* 2003, 42, 1603-1618.

28. Gauter, K.; Heidemann, R. A., A proposal for parametrizing the Sanchez-Lacombe equation of state. *Industrial & engineering chemistry research* 2000, 39, 1115-1117.

29. Hesse, L.; Sadowski, G., Modeling Liquid–Liquid Equilibria of Polyimide Solutions. *Industrial & Engineering Chemistry Research* 2011, 51, 539-546.

30. Belloni, F.; Fermeglia, M.; Pricl, S., From molecular to process simulation: novel approaches to the prediction of phase equilibria and PVT behavior based on molecular/quantum mechanics and molecular dynamics simulations. *Molecular Simulation* 2000, 25, 53-71.

31. Fermeglia, M.; Pricl, S., Equation - of - state parameters for pure polymers by molecular dynamics simulations. *AIChE journal* 1999, 45, 2619-2627.

32. Minelli, M.; Cane, V. G.; Angelis, M. G. D.; Hofmann, D., A novel multiscale method for the prediction of the volumetric and gas solubility behavior of high-T_g polyimides. *Fluid Phase Equilibria* 2012.

33.   Neau, E., A consistent method for phase equilibrium calculation using the Sanchez–Lacombe lattice–fluid equation-of-state. *Fluid phase equilibria* 2002, 203, 133-140.

34.   Panagiotopoulos, A. Z.; Reid, R. C. In *New mixing rule for cubic equations of state for highly polar, asymmetric systems*, ACS Symp. Ser, ACS Publications: 1986; pp 571-582.

35.   Adachi, Y.; Sugie, H., A new mixing rule—modified conventional mixing rule. *Fluid Phase Equilibria* 1986, 28, 103-118.

36.   Michelsen, M. L., A modified Huron-Vidal mixing rule for cubic equations of state. *Fluid Phase Equilibria* 1990, 60, 213-219.

37.   Wong, D. S. H.; Sandler, S. I., A theoretically correct mixing rule for cubic equations of state. *AIChE Journal* 1992, 38, 671-680.

38.   Schwartzentruber, J.; Renon, H., Equations of state: how to reconcile flexible mixing rules, the virial coefficient constraint and the "michelsen-Kistenmacher syndrome" for multicomponent systems. *Fluid phase equilibria* 1991, 67, 99-110.

39.   Huron, M.-J.; Vidal, J., New mixing rules in simple equations of state for representing vapour-liquid equilibria of strongly non-ideal mixtures. *Fluid Phase Equilibria* 1979, 3, 255-271.

40.   Wong, D. S. H.; Orbey, H.; Sandler, S. I., Equation of state mixing rule for nonideal mixtures using available activity coefficient model parameters and that allows extrapolation over large ranges of temperature and pressure. *Industrial & engineering chemistry research* 1992, 31, 2033-2039.

41.   Altena, F. W.; Smolders, C. A., Calculation of liquid-liquid phase separation in a ternary system of a polymer in a mixture of a solvent and a nonsolvent. *Macromolecules* 1982, 15, 1491-1497.

42.   Hsu, C. C.; Prausnitz, J. M., Thermodynamics of polymer compatibility in ternary systems. *Macromolecules* 1974, 7, 320-324.

43.   Hollister, S. J., Porous scaffold design for tissue engineering. *Nature materials* 2005, 4, 518-524.

44.   Drury, J. L.; Mooney, D. J., Hydrogels for tissue engineering: scaffold design variables and applications. *Biomaterials* 2003, 24, 4337-4351.

45.   Schugens, C.; Maquet, V.; Grandfils, C.; Jérôme, R.; Teyssie, P., Biodegradable and macroporous polylactide implants for cell transplantation: 1. Preparation of macroporous polylactide supports by solid-liquid phase separation. *Polymer* 1996, 37, 1027-1038.

46.   Schugens, C.; Maquet, V.; Grandfils, C.; Jérôme, R.; Teyssie, P., Polylactide macroporous biodegradable implants for cell transplantation. II. Preparation of polylactide foams by liquid - liquid phase separation. *Journal of Biomedical Materials Research* 1998, 30, 449-461.

47.   Witte, P. v. d.; Esselbrugge, H.; Dijkstra, P. J.; Berg, J. W. A. v. d.; Feijen, J., A morphological study of membranes obtained from the systems polylactide-dioxane-methanol, polylactide-dioxane-water and polylactide-N-methyl pyrrolidone-water. *Journal of Polymer Science, Part B: Polymer physics* 1996, 34, 2569-2578.

48.   Goates, J. R.; Sullivan, R. J., Thermodynamic properties of the system water-p-dioxane. *The Journal of Physical Chemistry* 1958, 62, 188-190.

49.   Gmehling, J.; Onken, U., *Dechema chemistry data series*. Dechema: 1982; Vol. 1.

50.   Vinson Jr, C. G.; Martin, J. J., Heat of Vaporization and Vapor Pressure of 1, 4-Dioxane. *Journal of Chemical and Engineering Data* 1963, 8, 74-75.

51.   Nayak, J. N.; Aralaguppi, M. I.; Aminabhavi, T. M., Density, viscosity, refractive index, and speed of sound in the binary mixtures of 1, 4-dioxane+ ethanediol,+ hexane,+ tributylamine, or+ triethylamine at (298.15, 303.15, and 308.15) K. *Journal of Chemical & Engineering Data* 2003, 48, 1152-1156.

52.   Papanastasiou, G. E.; Papoutsis, A. D.; Kokkinidis, G. I., Physical behavior of some reaction media. Density, viscosity, dielectric constant, and refractive index changes of ethanol-dioxane mixtures at several temperatures. *Journal of Chemical and Engineering Data* 1987, 32, 377-381.

53.   Mannella, G. A.; La Carrubba, V.; Brucato, V., On the calculation of free energy of mixing for aqueous polymer solutions with group-contribution models. *Fluid Phase Equilibria* 2010, 299, 222-228.

54.   Witte, P. v. d.; Dijkstra, P. J.; Berg, J. W. A. v. d.; Feijen, J., Phase behavior of polylactides in solvent-nonsolvent mixtures. *Journal of Polymer Science, Part B: Polymer physics* 1996, 34, 2553-2568.

55.   Takamuku, T.; Yamaguchi, A.; Tabata, M.; Nishi, N.; Yoshida, K.; Wakita, H.; Yamaguchi, T., Structure and dynamics of 1, 4-dioxane-water binary solutions studied by X-ray diffraction, mass spectrometry, and NMR relaxation. *Journal of molecular liquids* 1999, 83, 163-177.

56.   Li, G.; Li, H.; Turng, L. S.; Gong, S.; Zhang, C., Measurement of gas solubility and diffusivity in polylactide. *Fluid phase equilibria* 2006, 246, 158-166.

57.   Sato, Y.; Inohara, K.; Takishima, S.; Masuoka, H.; Imaizumi, M.; Yamamoto, H.; Takasugi, M., Pressure - volume - temperature behavior of polylactide, poly (butylene succinate), and poly (butylene succinate - co - adipate). *Polymer Engineering & Science* 2000, 40, 2602-2609.

58.   Zoller, P., PVT relationships and equations of state of polymers. *Polymer Handbook* 1989, 475-483.

59.   De Angelis, M. G.; Sarti, G. C.; Doghieri, F., NELF model prediction of the infinite dilution gas solubility in glassy polymers. *Journal of membrane science* 2007, 289, 106-122.

60.   Colussi, S.; Elvassore, N.; Kikic, I., A comparison between semi-empirical and molecular-based equations of state for describing the thermodynamic of supercritical micronization processes. *The Journal of supercritical fluids* 2006, 39, 118-126.

61.   Cameretti, L. F.; Sadowski, G.; Mollerup, J. M., Modeling of aqueous electrolyte solutions with perturbed-chain statistical associated fluid theory. *Industrial & engineering chemistry research* 2005, 44, 3355-3362.

62.   Cameretti, L. F.; Sadowski, G., Modeling of aqueous amino acid and polypeptide solutions with PC-SAFT. *Chemical Engineering and Processing: Process Intensification* 2008, 47, 1018-1025.

63.   Kleiner, M.; Sadowski, G., Modeling of polar systems using PCP-SAFT: An approach to account for induced-association interactions. *The Journal of Physical Chemistry C* 2007, 111, 15544-15553.

64.   Davis, E. M.; Theryo, G.; Hillmyer, M. A.; Cairncross, R. A.; Elabd, Y. A., Liquid Water Transport in Polylactide Homo and Graft Copolymers. *ACS Applied Materials & Interfaces* 2011, 3, 3997-4006.

65.   Tanaka, T.; Lloyd, D. R., Formation of poly (L-lactic acid) microfiltration membranes via thermally induced phase separation. *Journal of membrane science* 2004, 238, 65-73.

66.   Baker, R., *Membrane technology and applications.* Wiley: 2012.

67.   Uhrich, K. E.; Cannizzaro, S. M.; Langer, R. S.; Shakesheff, K. M., Polymeric systems for controlled drug release. *Chemical Reviews-Columbus* 1999, 99, 3181-3198.

68.   Basu, S. K.; Scriven, L. E.; Francis, L. F.; McCormick, A. V., Mechanism of wrinkle formation in curing coatings. *Progress in organic coatings* 2005, 53, 1-16.

69.   Lei, H.; Francis, L. F.; Gerberich, W. W.; Scriven, L. E., Stress development in drying coatings after solidification. *AIChE journal* 2002, 48, 437-451.

70.   Lei, H.; Payne, J. A.; McCormick, A. V.; Francis, L. F.; Gerberich, W. W.; Scriven, L. E., Stress development in drying coatings. *Journal of applied polymer science* 2001, 81, 1000-1013.

71.   Basu, S. K.; Scriven, L. E.; Francis, L. F.; McCormick, A. V.; Reichert, V. R., Wrinkling of epoxy powder coatings. *Journal of applied polymer science* 2005, 98, 116-129.

72.   Hesse, L.; Mićović, J.; Schmidt, P.; Górak, A.; Sadowski, G., Modelling of organic solvent flux through a polyimide membrane. *Journal of Membrane Science* 2012.

73.   Cocchi, G.; Troiano, C.; De Angelis, M. G.; Doghieri, F.; Sarti, G. C., Solubility and Diffusivity of Liquids in Polymers Suitable for Membrane Separation Processes: The Cases of Matrimid< sup>®</sup> and PDMS. *Procedia Engineering* 2012, 44, 1241-1242.

74.   Subramanian, R.; Raghavarao, K.; Nakajima, M.; Nabetani, H.; Yamaguchi, T.; Kimura, T., Application of dense membrane theory for differential permeation of vegetable oil constituents. *Journal of food engineering* 2003, 60, 249-256.

75.   Subramanian, R.; Raghavarao, K.; Nabetani, H.; Nakajima, M.; Kimura, T.; Maekawa, T., Differential permeation of oil constituents in nonporous denser polymeric membranes. *Journal of Membrane Science* 2001, 187, 57-69.

76.   Subramanian, R.; Nakajima, M.; Kawakatsu, T., Processing of vegetable oils using polymeric composite membranes. *Journal of food engineering* 1998, 38, 41-56.

77.   Crank, J., The mathematics of diffusion, Clarendon. Oxford: 1975.

78.   Long, F. A.; Richman, D., Concentration Gradients for Diffusion of Vapors in Glassy Polymers and their Relation to Time Dependent Diffusion Phenomena1, 2. *Journal of the American Chemical Society* 1960, 82, 513-519.

79.   Richman, D.; Long, F. A., Measurement of Concentration Gradients for Diffusion of Vapors in Polymers1, 2. *Journal of the American Chemical Society* 1960, 82, 509-513.

80.   Chow, T.-S., *Mesoscopic physics of complex materials.* Springer Verlag: 2000.

81.   Pfromm, P. H.; Koros, W. J., Accelerated physical ageing of thin glassy polymer films: evidence from gas transport measurements. *Polymer* 1995, 36, 2379-2387.

82.   Pekarski, P.; Hampe, J.; Böhm, I.; Brion, H. G.; Kirchheim, R., Effect of aging and conditioning on diffusion and sorption of small molecules in polymer glasses. *Macromolecules* 2000, 33, 2192-2199.

83.   Struik, L. C. E., *Physical aging in amorphous polymers and other materials.* Elsevier Amsterdam: 1978; Vol. 106.

84.   Hutchinson, J. M., Physical aging of polymers. *Progress in Polymer Science* 1995, 20, 703-760.

85.   Huang, Y.; Paul, D. R., Physical aging of thin glassy polymer films monitored by gas permeability. *Polymer* 2004, 45, 8377-8393.

86.   Doghieri, F.; Biavati, D.; Sarti, G. C., Solubility and diffusivity of ethanol in PTMSP: Effects of activity and of polymer aging. *Industrial & engineering chemistry research* 1996, 35, 2420-2430.

87.   Lee, J. S.; Adams, R. T.; Madden, W.; Koros, W. J., Toluene and< i> n</i>-heptane sorption in Matrimid< sup>®</sup> asymmetric hollow fiber membranes. *Polymer* 2009, 50, 6049-6056.

88.   Kanehashi, S.; Nagai, K., Analysis of dual-mode model parameters for gas sorption in glassy polymers. *Journal of membrane science* 2005, 253, 117-138.

89.   Sanopoulou, M.; Roussis, P. P.; Petropoulos, J. H., A detailed study of the viscoelastic nature of vapor sorption and transport in a cellulosic polymer. I. Origin and physical implications of deviations from Fickian sorption kinetics. *Journal of Polymer Science Part B: Polymer Physics* 1995, 33, 993-1005.

90.   Sanopoulou, M.; Petropoulos, J. H., Sorption and longitudinal swelling kinetic behaviour in the system cellulose acetate-methanol. *Polymer* 1997, 38, 5761-5768.

91.   Sanopoulou, M.; Petropoulos, J. H., Systematic analysis and model interpretation of micromolecular non-Fickian sorption kinetics in polymer films. *Macromolecules* 2001, 34, 1400-1410.

92.   Petropoulos, J. H., Interpretation of anomalous sorption kinetics in polymer‐penetrant systems in terms of a time‐dependent solubility coefficient. *Journal of Polymer Science: Polymer Physics Edition* 2003, 22, 1885-1900.

93.   Piccinini, E.; Giacinti Baschetti, M.; Sarti, G. C., Use of an automated spring balance for the simultaneous measurement of sorption and swelling in polymeric films. *Journal of membrane science* 2004, 234, 95-100.

94.   Carla, V.; Wang, K.; Hussain, Y.; Efimenko, K.; Genzer, J.; Grant, C.; Sarti, G. C.; Carbonell, R. G.; Doghieri, F., Nonequilibrium model for sorption and swelling of bulk glassy polymer films with supercritical carbon dioxide. *Macromolecules* 2005, 38, 10299-10313.

95.   De Angelis, M. G.; Lodge, S.; Giacinti Baschetti, M.; Sarti, G. C.; Doghieri, F.; Sanguineti, A.; Fossati, P., Water sorption and diffusion in a short-side-chain perfluorosulfonic acid ionomer membrane for PEMFCS: effect of temperature and pre-treatment. *Desalination* 2006, 193, 398-404.

96.   Comer, A. C.; Kalika, D. S.; Rowe, B. W.; Freeman, B. D.; Paul, D. R., Dynamic relaxation characteristics of Matrimid< sup>®</sup> polyimide. *Polymer* 2009, 50, 891-897.

97.   De Angelis, M. G.; Merkel, T. C.; Bondar, V. I.; Freeman, B. D.; Doghieri, F.; Sarti, G. C., Hydrocarbon and fluorocarbon solubility and dilation in poly (dimethylsiloxane): Comparison of experimental data with predictions of the

Sanchez–Lacombe equation of state. *Journal of Polymer Science Part B: Polymer Physics* 1999, 37, 3011-3026.

98.   Merkel, T. C.; Bondar, V.; Nagai, K.; Freeman, B. D., Hydrocarbon and Perfluorocarbon Gas Sorption in Poly (dimethylsiloxane), Poly (1-trimethylsilyl-1-propyne), and Copolymers of Tetrafluoroethylene and 2, 2-Bis (trifluoromethyl)-4, 5-difluoro-1, 3-dioxole. *Macromolecules* 1999, 32, 370-374.

99.   Singh, A.; Freeman, B. D.; Pinnau, I., Pure and mixed gas acetone/nitrogen permeation properties of polydimethylsiloxane [PDMS]. *Journal of Polymer Science Part B: Polymer Physics* 1998, 36, 289-301.

100.   Chen, G. Q.; Scholes, C. A.; Qiao, G. G.; Kentish, S. E., Water vapor permeation in polyimide membranes. *Journal of Membrane Science* 2011, 379, 479-487.

101.   Davis, E. M.; Minelli, M.; Baschetti, M. G.; Sarti, G. C.; Elabd, Y. A., Nonequilibrium Sorption of Water in Polylactide. *Macromolecules* 2012.

102.   Glassman, I., *Combustion*. Academic press: 1996.

103.   Zeldovich, I. A.; Barenblatt, G. I.; Librovich, V. B.; Makhviladze, G. M., Mathematical Theory of Combustion and Explosions. 1985.

104.   Grüger, A.; Gotthardt, P.; Pönitsch, M.; Brion, H. G.; Kirchheim, R., Sorption of small molecules in various polycarbonates and Kapton - H. *Journal of Polymer Science Part B: Polymer Physics* 1998, 36, 483-494.

105.   Kirchheim, R., Partial molar volume of small molecules in glassy polymers. *Journal of Polymer Science Part B: Polymer Physics* 2003, 31, 1373-1382.

106.   Pekarski, P.; Kirchheim, R., On the sorption of gas mixtures by polymer glasses. *Journal of membrane science* 1999, 152, 251-262.

107.   Fleming, G. K.; Koros, W. J., Dilation of polymers by sorption of carbon dioxide at elevated pressures. 1. Silicone rubber and unconditioned polycarbonate. *Macromolecules* 1986, 19, 2285-2291.

108.   Fleming, G. K.; Koros, W. J., Carbon dioxide conditioning effects on sorption and volume dilation behavior for bisphenol A-polycarbonate. *Macromolecules* 1990, 23, 1353-1360.

109.   Sarti, G. C.; Doghieri, F., Predictions of the solubility of gases in glassy polymers based on the NELF model. *Chemical engineering science* 1998, 53, 3435-3447.

110.   Doghieri, F.; Canova, M.; Sarti, G. C. In *Solubility of gaseous mixtures in glassy polymers: NELF predictions*, ACS Symposium Series, ACS Publications: 1999; pp 179-193.

111.   Minelli, M.; Doghieri, F., A Predictive Model for Vapor Solubility and Volume Dilation in Glassy Polymers. *Industrial & Engineering Chemistry Research* 2012, 51, 16505-16516.

112.   Carlà, V.; Hussain, Y.; Grant, C.; Sarti, G. C.; Carbonell, R. G.; Doghieri, F., Modeling Sorption Kinetics of Carbon Dioxide in Glassy Polymeric Films Using the Nonequilibrium Thermodynamics Approach. *Industrial & Engineering Chemistry Research* 2009, 48, 3844-3854.

113.   Minelli, M.; Cocchi, G.; Ansaloni, L.; Giacinti Baschetti, M.; De Angelis, M. G.; Doghieri, F., Vapor and liquid sorption in Matrimid polyimide: experimental characterization and modeling. *Industrial & Engineering Chemistry Research*.

114.   Ferrari, M. C.; Galizia, M.; De Angelis, M. G.; Sarti, G. C., Gas and vapor transport in mixed matrix membranes based on amorphous Teflon AF1600 and AF2400 and fumed silica. *Industrial & Engineering Chemistry Research* 2010, 49, 11920-11935.

115.   Tumakaka, F.; Sadowski, G., Application of the Perturbed-Chain SAFT equation of state to polar systems. *Fluid phase equilibria* 2004, 217, 233-239.

116.   Grenner, A.; Tsivintzelis, I.; Economou, I. G.; Panayiotou, C.; Kontogeorgis, G. M., Evaluation of the Nonrandom Hydrogen Bonding (NRHB) Theory and the Simplified Perturbed-Chain– Statistical Associating Fluid Theory (sPC-SAFT). 1. Vapor– Liquid Equilibria. *Industrial & Engineering Chemistry Research* 2008, 47, 5636-5650.

117.   Truesdell, C.; Noll, W., *The non-linear field theories of mechanics.* Springer: 2004; Vol. 3.

118.   Chandra, P.; Koros, W. J., Sorption and transport of methanol in poly (ethylene terephthalate). *Polymer* 2009, 50, 236-244.

119.   Berens, A. R.; Hopfenberg, H. B., Diffusion and relaxation in glassy polymer powders: 2. Separation of diffusion and relaxation parameters. *Polymer* 1978, 19, 489-496.

120.   Davis, E. M.; Minelli, M.; Giacinti Baschetti, M.; Elabd, Y. A., Non-Fickian Diffusion of Water in Polylactide. *Industrial & Engineering Chemistry Research* 2012.

121.   Mueller, F.; Krueger, K.-M.; Sadowski, G., Non-Fickian Diffusion of Toluene in Polystyrene in the Vicinity of the Glass-Transition Temperature. *Macromolecules* 2012, 45, 926-932.

122.   Carella, A. R.; Dorao, C. A., Solution of a Cattaneo-Maxwell diffusion model using a Spectral element least-squares method. *Journal of Natural Gas Science and Engineering* 2010, 2, 253-258.

123.   Doghieri, F.; Roda, G. C.; Sarti, G. C., Rate type equations for the diffusion in polymers: thermodynamic constraints. *AIChE journal* 1993, 39, 1847-1858.

124.   Anderssen, R. S.; Husain, S. A.; Loy, R. J., The Kohlrausch function: properties and applications. *Anziam Journal* 2004, 45, C800--C816.

125.   Vrentas, J. S.; Duda, J. L., Molecular diffusion in polymer solutions. *AIChE Journal* 1979, 25, 1-24.

126.   Hesse, L.; Naeem, S.; Sadowski, G., VOC Sorption in Glassy Polyimides–Measurements and Modeling. *Journal of Membrane Science* 2012.

127.   O'Neal, D. J. Cure Induced Stress Generation and Viscoelasticity in Polymer Coatings. university of minnesota, 2010.

128.   Richter, K. B., *Pulsed electron beam curing of polymer coatings*. ProQuest: 2007.

129.   Clough, R. L.; Shalaby, S. W., *Radiation effects on polymers*. ACS Publications: 1991; Vol. 475.

130.   Clough, R. L., High-energy radiation and polymers: A review of commercial processes and emerging applications. *Nuclear Instruments and Methods in Physics Research Section B: Beam Interactions with Materials and Atoms* 2001, 185, 8-33.

131.   Zagórski, Z. P., Modification, degradation and stabilization of polymers in view of the classification of radiation spurs. *Radiation Physics and Chemistry* 2002, 63, 9-19.

132.   Sigmund, P., *Particle penetration and radiation effects: general aspects and stopping of swift point charges.* Springer: 2006; Vol. 151.

133.   Minelli, M.; De Angelis, M. G.; Doghieri, F.; Marini, M.; Toselli, M.; Pilati, F., Oxygen permeability of novel organic–inorganic coatings: I. Effects of organic–inorganic ratio and molecular weight of the organic component. *European Polymer Journal* 2008, 44, 2581-2588.

134.   Freeman, B. D.; Pinnau, I. In *Polymeric materials for gas separations*, ACS Symposium Series, ACS Publications: 1999; pp 1-27.

135.   Kita, H.; Muraoka, M.; Tanaka, K.; Okamoto, K.-i., Permeation of gases through electron-beam-irradiated polymer films. *Polymer journal* 1988, 20, 485-491.

136.   Mueller, F.; Heuwers, B.; Katzenberg, F.; Tiller, J. C.; Sadowski, G., Tensile Creep Measurements of Glassy VOC-Loaded Polymers. *Macromolecules* 2010, 43, 8997-9003.

137.   Rault, J., Ageing of glass: role of the Vogel–Fulcher–Tamman law. *Journal of Physics: Condensed Matter* 2003, 15, S1193.

138.   Marrucci, G.; Grizzuti, N., The Free Energy Function of the Doi - Edwards Theory: Analysis of the Instabilities in Stress Relaxation. *Journal of Rheology* 1983, 27, 433-450.

139.   Coppola, S.; Grizzuti, N.; Maffettone, P. L., Microrheological modeling of flow-induced crystallization. *Macromolecules* 2001, 34, 5030-5036.